A.P.OLIVA

THE DESIGN AND ANALYSIS OF A RECONFIGURABLE FLIGHT CONTROL SYSTEM FOR ADVANCED CIVIL AIRCRAFT

CRANFIELD INSTITUTE OF TECHNOLOGY

COLLEGE OF AERONAUTICS

Ph.D THESIS

CRANFIELD INSTITUTE OF TECHNOLOGY

COLLEGE OF AERONAUTICS

Ph.D. THESIS

APRIL 1994

A.P.OLIVA

The Design and Analysis of a Reconfigurable Flight Control System for Advanced Civil Aircraft

Supervisor : M.V. Cook

This thesis is submitted in fulfilment of the requirements for the degree of Ph.D.

ABSTRACT

This work is concerned with the design of a pitch-rate-command-attitude-hold Command and Stability Augmentation System in order that the augmented aircraft meets the Gibson dropback criterion, the Gibson phase-rate criterion and MIL-F-8785C requirements. The work shows two methods of design, pole-placement and optimal control, and discusses the design procedures, the advantages and disadvantages of each method. The work is also concerned with the redundancy aspect of the control law design, and so not only a sensor based design but also an observer-based design are investigated. In order to design the observer-based control law, a Doyle-Stein observer was implemented. Two methods showing how to design the observer are discussed and presented, and the special characteristics of this kind of observer are also considered. The performance of the observer-based control law was compared with that of the sensor-based control law. The failure transients and characteristics of the control law are also studied and presented. Finally an evaluation of the control law was carried out with a non-linear model of the B-747 aircraft, and a simple altitude-hold autopilot was designed to work together with the stability augmentation control law.

ACKNOWLEDGMENTS

I want to say many thanks for my supervisor for his help during the development of this work.

I acknowledge the financial suport of CNPq for this work.

Alvaro P Oliva

DEDICATION

I dedicate this work for God's kindness and for my son Leonardo and my wife Suely.

Alvaro P Oliva

CONTENTS

3 CONTROL LAW DESIGN TO SATISFY THE GIBSON DROPBACK CRITERION AND THE MIL-F-8785C FLYING QUALITIES REQUIREMENTS

3.1 - Introduction
3.2 - Control law structure
3.3 - The Pole-Placement method
3.4 - The Optimal Control law method
3.5 - The Influence of an actuator on control law performance
  3.5.1 - Introduction
  3.5.2 - The results of assessment
3.6 - Assessment of the control laws with the full aircraft model
  3.6.1 - Introduction
  3.6.2 - Summary of aircraft characteristics with both control law designs.
3.7 - The performance of both control law designs with the complete model of the aircraft and the actuator
3.8 - Closed loop pole locations comparison for each case
  3.8.1 - Introduction
  3.8.2 - The pole placement control law design
  3.8.3 - Optimal control law design

4 CONTROL LAW DEVELOPMENT TO SATISFY GIBSON DROPBACK AND PHASE-RATE CRITERIA.

4.1 - Introduction
4.2 - The adjustment of both designs in order to satisfy the dropback criterion and CAP requirement
    4.2.1 - The Pole-Placement control law design
    4.2.2 - The Optimal Control law design
    4.2.3 - Conclusions and Observations
4.3 - Further Development of the control laws to meet the phase-rate criterion
    4.3.1 - Introduction
    4.3.2 - Evaluation of both control laws relative to the phase rate criterion

LIST OF FIGURES

NOTATION

A	aircraft state matrix
A_{RO}	aircraft state matrix of the reduced short period longitudinal model
A_{LM}	aircraft state matrix of the complete longitudinal model.
A_d	disturbance model state matrix
A_r	reference model state matrix
A_0	exogenous inputs model state matrix
A_c	closed loop system state matrix
A_A	State matrix of the actuator state space model.
A_{11}	Sub-matrix of the state matrix of the aircraft.
A_{12}	Sub-matrix of the state matrix of the aircraft.
A_{21}	Sub-matrix of the state matrix of the aircraft.
A_{22}	Sub-matrix of the state-matrix of the aircraft.
a_{LF}	Parameter of the state-space model of the lead filter.
A_{AP}	State matrix of the augmented aircraft with autopilot
a_z	aircraft normal acceleration parallel to the z body axis
a	aircraft lift curve slope
a	parameter of the transfer function of a general phase lead controller.
a_1	horizontal tail lift curve slope
B	Control matrix of the aircraft.
B_{RO}	Control matrix of the aircraft short period reduced order longitudinal model.
B_{LM}	Control matrix of the aircraft complete longitudinal model.
$B^{\#}$	matrix related to the feedforward gain of the pole placement design method.
B^*	matrix related to the feedforward gain of the optimal control law design method.
B_A	Control matrix of the actuator.
B_1	Sub-matrix of the control matrix of the aircraft
B_2	Sub-matrix of the control matrix of the aircraft
b_{LF}	Parameter of the state-space model of the lead filter.

B_{AP}	Control matrix of the augmented aircraft with autopilot
BIBO	bounded input bounded output system
$\bar{c}$	mean aerodynamic chord
C	Output matrix of the aircraft.
C_d	Output matrix of the disturbance model
C_e	Output matrix of the error
C_r	Output matrix of the reference model
CAP	Control anticipation parameter.
C_1	Output matrix of the aircraft relative to the sensed state x_1.
c_{LF}	Parameter of the state-space model of the lead filter.
CL_SB	Sensor-based control law, that means, Control Law_Sensor Based.
CL_OB_w	Observer-based control law with alpha sensor, that means, Control Law_Observer Based_w
CL_OB_q	Observer-based control law with q sensor, that means, Control Law_Observer Based_q.
CL_OB_θ	Observer-based control law with θ sensor, that means, Control Law_Observer Based_θ.
DB	Dropback parameter.
d_{LF}	Parameter of the state-space model of the lead filter.
dB	decibels.
deg	degrees.
e	error with respect to the demanded reference state.
e_1	error relative to the sensed state x_1
e_2	error relative to the observed state x_2
E	matrix of the state-space model of the aircraft when there is a reference input
E_1	input to a general phase lead controller
E_2	output to a general phase lead controller

F	State matrix of the observer.
F	aircraft control matrix relative to the disturbance vector
ft	feet.
FC #	Flight condition.
g	acceleration due to gravity
G	vector of the feedback gains of the control law.
$\bar{G}$	Optimal control law gain obtained by the LQR method
$\bar{G}$	matrix used in the Observer state space model relative to the system output
G_f	vector of the feedback gains of the control law with some feedback chanel failed.
G_0	feedforward gain of the control law, or feedforward gain vector relative to the exogenous inputs
G_r	feedforward gain vector relative to the reference input
G_d	feedforward gain vector relative to the disturbance input
G_1	sub-vector of the vector of feedback gains relative to the measured states.
G_2	sub-vector of the vector of feedback gains relative to the estimated states.
G_{AP}	vector of the feedback gains of the autopilot.
G_u	feedback gain of the u feedback path of the autopilot
G_w	feedback gain of the w feedback path of the autopilot
G_q	feedback gain of the q feedback path of the autopilot
G_θ	feedback gain of the θ feedback path of the autopilot
G_h	feedback gain of the h feedback path of the autopilot
G_{ε_h}	feedback gain of the ε_h feedback path of the autopilot
GW_1	auxiliary matrix used in the autopilot mathematical model
GW_2	auxiliary matrix used in the autopilot mathematical model

G_{AP_1}	sub-vector of the vector of feedback gains of the autopilot relative to the measured states.
G_{AP_2}	sub-vector of the vector of feedback gains of the autopilot relative to the estimated states.
G_M	Gain margin.
H	matrix used in the observer state space model relative to the control input
Hz	Hertz (cycles per second).
h	altitude above the earth.
h_{ref}	reference altitude.
H_m	longitudinal manoeuvre margin controls fixed
$H_0(s)$	closed loop transfer function with full state feedback
I	Identity matrix
I_x	Moment of inertia referred to x body axis
I_y	Moment of inertia referred to y body axis
I_z	Moment of inertia referred to z body axis
I_{xz}	Product of inertia referred to body axis
K_w	feedback gain of the w feedback path of the control law
K_q	feedback gain of the q feedback path of the control law
K_{ε_q}	feedback gain of the ε_q feedback path of the control law
K_{ss}	constant used in the pole placement control law design to recover the zero steady state pitch rate error with respect to the reference pitch rate
K	observer gain vector for a full order observer
k_i	$i = 1$ to 7, inertial parameters used in the non linear aircraft model
k_{lat}	inertial parameter used in the non linear aircraft model
K_1	observer gain vector for a reduced order observer
K_2	observer gain vector for a reduced order observer

k_q gain constant of the transfer function (q/η) obtained from the reduced order short period model

k_η longitudinal static stability margin

L Gain matrix of the observer.

L aerodynamic force (lift) perpendicular to the total velocity vector in the aircraft's plane of simetry

l_T distance between the aircraft centre of gravity and the aerodynamic centre of the horizontal tail

L'_β derivative of the rolling moment in x body axis with respect to sideslip

L'_r derivative of the rolling moment in x body axis with respect to yaw rate in z body axis

L'_p derivative of the rolling moment in x body axis with respect to roll rate in x body axis

$L'_{\delta a}$ derivative of the rolling moment in x body axis with respect to aileron deflection

$L'_{\delta r}$ derivative of the rolling moment in x body axis with respect to rudder deflection

M Riccati matrix obtained from the solution of the Riccati diferential equation in the solution of the LQR problem.

$\bar{M}$ Algebraic Riccati matrix obtained from the solution of the algebraic Riccati equation in the LQR problem

M_1 submatrix of M

M_2 submatrix of M

M_3 submatrix of M

$\bar{M}_1$ submatrix of $\bar{M}$

$\bar{M}_2$ submatrix of $\bar{M}$

$\bar{M}_3$ submatrix of $\bar{M}$

M^*_u derivative of the pitch moment in y body axis with respect to longitudinal velocity in x body axis

M_w derivative of pitch moment in y body axis with respect to normal velocity in z body axis

$M_{\dot{w}}$ derivative of pitch moment in y body axis with respect to normal velocity acceleration in z body axis.

M_q derivative of pitch moment in y body axis with respect to pitch rate in y body axis

$M_{\delta e}$ derivative of pitch moment in y body axis with respect to elevator deflection

M Gain matrix of the observer, obtained as a submatrix of the P^{-1} matrix in the observer design.

m aircraft mass

mach mach number

M_P resonant peak.

m_η non dimensional $M_{\delta e}$ derivative

m_q non dimensional M_q derivative

MIMO multiple input multiple output system

N Gain matrix of the observer, obtained as a submatrix of the matrix P^{-1} in the observer design.

N'_β derivative of yaw moment in z body axis with respect to sideslip

N'_r derivative of yaw moment in z body axis with respect to yaw rate in z body axis

N'_p derivative of yaw moment in z body axis with respect to roll rate in x body axis

$N'_{\delta a}$ derivative of yaw moment in z body axis with respect to ailerion deflection

$N'_{\delta r}$ derivative of yaw moment in z body axis with respect to rudder deflection

N_3 Coefficient relative to s^3 in the numerator of the transfer function of (q / q_{dp})

N_2 Coefficient relative to s^2 in the numerator of the transfer function of (q/q_{dp})

N_1 Coefficient relative to s in the numerator of the transfer function of (q/q_{dp})

N_0 Coefficient relative to s^0 in the numerator of the transfer function of (q/q_{dp})

N_z , n_z normal load factor along the z-body axis

OS overshoot

OCL optimal control law

OwOq_w failure mode from the observer based control law with w output to the observer based control law with q output after a failure of w sensor.

OwOθ_w failure mode from the observer based control law with w output to the observer based control law with θ output after a failure of w sensor.

OqOw_q failure mode from the observer based control law with q output to the observer based control law with w output after a failure of q sensor.

OqOθ_q failure mode from the observer based control law with q output to the observer based control law with θ output after a failure of q sensor.

OθOw_θ failure mode from the observer based control law with θ output to the observer based control law with w output after a failure of θ sensor.

OθOq_θ failure mode from the observer based control law with θ output to the observer based control law with q output after a failure of θ sensor.

P Transformation matrix used in the observer design.

P_M phase-margin.

P.R. pitch-attitude phase-rate.

PIO pilot induced oscillation.

PLF	phase lead filter
PPCL	pole placement control law
p	perturbed roll rate
Q	Weight matrix of the states in the performance index.
q	perturbed pitch-rate.
$\hat{q}$	estimated perturbed pitch-rate
q_{dp}	commanded pitch-rate.
q_{d}	commanded pitch-rate after the lead pre filter, or output of the lead pre filter.
q_{ss}	steady-state pitch-rate.
q_{m}	first peak of the pitch-rate response.
q_{max}	positive end stop of the pitch rate sensor considered in the hardover failure simulations
q_{min}	negative end stop of the pitch rate sensor considered in the hardover failure simulations
R	Weight matrix of the controls in the performance index.
r	perturbed yaw rate
rad	radians.
S	wing area
s	Laplace operator.
sec	seconds.
SBOw_q	failure mode from the sensor based control law to the observer based control law with w output after a failure of q sensor.
SBOw_θ	failure mode from the sensor based control law to the observer based control law with w output after a failure of θ sensor.
SBOq_θ	failure mode from the sensor based control law to the observer based control law with q output after a failure of θ sensor.

SBOq_w	failure mode from the sensor based control law to the observer based control law with q output after a failure of w sensor.
SBOθ_q	failure mode from the sensor based control law to the observer based control law with θ output after a failure of q sensor.
SBOθ_w	failure mode from the sensor based control law to the observer based control law with θ output after a failure of w sensor.
SISO	single input single output system
SIMO	single input multiple output system
T	matrix obtained from the solution of the Lyapunov equation in the second observer design method.
T	parameter of the transfer function of a general phase lead controller.
T_2	time to double the amplitude of the phugoid oscillation
$T_{\theta 2}$	numerator time constant of the open loop transfer function of (q/η) obtained from the reduced order short period model
t_m	time in the pitch-rate response at which the first peak occurs.
t	time.
T	transponse of a matrix.
TDH	threshold time.
U_T , U_1	total forward (longitudinal) velocity in x body axis of the aircraft
U_0	steady-state forward (longitudinal) velocity in x body axis of the aircraft
u	forward (longitudinal) perturbed velocity in x body axis of the aircraft.
$\hat{u}$	estimated forward (longitudinal) perturbed velocity in x body axis of the aircraft

u	control input to the aircraft
u_0	reference control input
$\bar{u}$	total control input
V	aircraft velocity
V_e	steady-state trim velocity.
v_η	control rate effort.
V	performance index used in the design of the inner loop optimal control law design
V_{AP}	performance index used in the design of the autopilot
$\bar{V}_T$	horizontal tail volume ratio
V_T	total lateral velocity in y body axis of the aircraft
V_0	steady state lateral velocity in y body axis of the aircraft
v	perturbed lateral velocity in y body axis of the aircraft
V_{sound}	velocity of the sound
w	normal perturbed velocity of the aircraft
$\hat{w}$	estimated normal perturbed velocity in z body axis of the aircraft
X_0	aircraft weight component in x body axis is steady state flight
X^*_u	derivative of the longitudinal force in the x body axis with respect to the longitudinal velocity in the x body axis.
X_w	derivative of the longitudinal force in the x body axis with respect to the normal velocity in the z body axis
X_q	derivative of the longitudinal force in the x body axis with respect to pitch rate
$X_{\delta e}$	derivative of the longitudinal force in the x body axis with respect to elevator deflection
x	state vector of the aircraft.

x_{RO} state vector of the short period longitudinal reduced order model

x_{LM} state vector of the complete longitudinal model.

$\hat{x}$ estimated state vector

x_d disturbances state vector

x_0 state vector of the exogenous inputs

x_r reference state vector

x_A state vector of the actuator state space model.

x_1 state vector of the aircraft that is sensed.

x_2 state vector of the aircraft that is not sensed.

x_{AP} state vector of the aircraft augmented with autopilot

$\hat{x}_1$ estimate of the sensed state vector of the aircraft

$\hat{x}_2$ estimate of the non sensed state vector of the aircraft

x_{LF} state of the lead filter.

Y_0 aircraft weight component in y body axis in steady state flight

Y_v derivative of lateral force in y body axis with repect to lateral velocity in y body axis

Y_r derivative of lateral force in y body axis with respect to yaw rate in z body axis

Y_p derivative of lateral force in y body axis with respect to roll rate in x body axis

$Y^*_{\delta a}$ derivative of lateral force in y body axis with respect to aileron deflection

$Y^*_{\delta r}$ derivative of lateral force in y body axis with respect to rudder deflection

y output of the aircraft.

$\hat{y}$ estimated output of the aircraft

Z_0	aircraft weight component in z body axis in steady state flight
ZERO	mode of failure in which the sensor output fails to zero.
Z12	matrix (1 x 2) with all elements equal to zero
Z13	matrix (1 x 3) with all elements equal to zero
Z14	matrix (1 x 4) with all elements equal to zero
Z21	matrix (2 x 1) with all elements equal to zero
Z31	matrix (3 x 1) with all elements equal to zero
Z33	matrix (3 x 3) with all elements equal to zero
Z41	matrix (4 x 1) with all elements equal to zero
z	state vector of the observer.
Z_w	derivative of normal force in z body axis with respect to normal velocity in z body axis
z_w	non dimensional Z_w derivative
$Z_{\dot{w}}$	derivative of normal force in z body axis with respect to normal acceleration in z body axis
Z^*_u	derivative of normal force in z body axis with respect to longitudinal velocity in x body axis
Z_q	derivative of normal force in z body axis with respect to pitch rate in y body axis
$Z_{\delta e}$	derivative of normal force in z body axis with respect to elevator deflection
$z_{\dot{w}}$	non dimensional $Z_{\dot{w}}$ derivative
W_0	normal steady state aircraft velocity in z body axis
W_T	normal total velocity of the aircraft in z body axis
w	normal perturbed velocity of the aircarft in z body axis
α	perturbed angle of attack.
α_T	total angle of attack.
α_0	trim angle of attack or steady state angle of attack

α_{max} positive end stop of the angle of attack sensor considered in the hardover failure simulations

α_{min} negative end stop of the angle of attack sensor considered in the hardover failure simulations

β sideslip angle

θ perturbed pitch-attitude.

$\hat{\theta}$ estimated perturbed pitch-attitude

θ_0 steady state pitch attitude

θ_T total pitch-attitude.

θ_{max} positive end stop of the pitch attitude sensor considered in the hardover failure simulations

θ_{min} negative end stop of the pitch attitude sensor considered in the hardover failure simulations

θ_d integral of the q_d state, or demanded pitch attitude

θ_c demanded pitch attitude

ε_q integral of the pitch rate error

ε_h integral of the altitude error

η control effort or elevator deflection

η_c input to the actuator.

$\eta_{c_{nom}}$ designed control law

η_{AP} control effort of the autopilot.

η_{max} maximum control effort.

η_{min} minimum control effort.

$\dot{\eta}_{max}$ maximun control rate effort.

$\dot{\eta}_{min}$ minimun control rate effort.

ρ air mass desity

ζ_{sp} damping ratio of the short-period mode.

ζ_{ph} damping ratio of the phugoid mode.

ω_{sp} natural frequency of the short-period mode.

ω_{ph} natural frequency of the phugoid mode

ω_b bandwidth.

ω_{PR} frequency at -180° phase in the closed loop attitude frequency response

ω_1 frequency of the closed loop attitude frequency response which corresponds to the phase ϕ_1.

ω_2 frequency of the closed loop attitude frequency response which corresponds to the phase ϕ_2.

ω_m frequency at which occurs the maximun phase lead in the phase lead controller.

$\Delta\phi_{LD}$ phase shift necessary to bring the point in which the frequency is 1 Hz to -180° phase.

$\Delta\phi$ increment necessary to add in ϕ_1 or ϕ_2 to obtain the P.R. attitude parameter to the phase rate criterion.

Δ_0 Coefficient of the denominator of the transfer function (q/q_{dp}) relative to s^0.

Δ_1 Coefficient of the denominator of the transfer function (q/q_{dp}) relative to s^1.

Δ_2 Coefficient of the denominator of the transfer function (q/q_{dp}) relative to s^2.

Δ_3 Coefficient of the denominator of the transfer function (q/q_{dp}) relative to s^3.

Δ_4 Coefficient of the denominator of the transfer function (q/q_{dp}) relative to s^4.

Δ_h increment in the steady-state altitude.

$\Delta(s)$ longitudinal characteristic equation

μ_1 longitudinal relative density factor

γ flight path angle.

$\phi(s)$	resolvent of the system
ϕ_m	maximun phase lead given by the phase lead controller
ϕ_1	phase of the closed loop attitude frequency response
ϕ_2	phase of the closed loop attitude frequency response
ϕ	perturbed bank angle
δ_e	elevator deflection
$\delta_{e_{max}}$	positive end stop of elevator deflection
$\delta_{e_{min}}$	negative end stop of elevator deflection
$\dot{\delta}_{e_{max}}$	positive end stop of elevator rate deflection
$\dot{\delta}_{e_{min}}$	negative end stop of elevator rate deflection
δ_a	aileron deflection
δ_r	rudder deflection
ψ	perturbed yaw angle

1 INTRODUCTION

1.1 PROBLEM DEFINITION AND OBJECTIVE OF THE RESEARCH

The problem studied is how redundancy with respect to sensor failures can be obtained in a flight control system without introducing changes in the stability level of the augmented aircraft or changes in its level of flying qualities. The main objective of this work is to explore the use of observers in flight control systems. Specifically, the study was directed to investigate the use of observers in redundant flight control system design with respect to sensor failures. The research was seeking to design observers that don't affect the flying qualities and stability of the augmented aircraft. Although a flight control system designed specifically to meet the Gibson dropback criterion[1] and phase-rate criterion[2] was used, the research can also be applied to a flight control system designed to meet other criteria. Since the main objective of this work is not an evaluation of the criteria themselves, the Gibson[1,2] criteria were used as an example because they correlate very closely with features found in other advanced dynamic handling criteria. Also referring to a recent study performed by Blagg[3] they have been considered as acceptable criteria for guidance in flight control system design.

It is also an objective of this research to use methods that are not only applicable to SISO systems but also to MIMO systems. So, although a SISO system has been studied in this work, the methods used in the flight control system design and observer design are also applicable to a MIMO system. In this research the aircraft model used is the Boeing 747 since at the time of the work this was the only aircraft for which a reasonable aerodynamic data bank was available. It also must be taken into account that this fact does not invalidate the findings of this research program when applied to a more advanced civil aircraft.

1.2 POSSIBLE PROBLEMS AND SOLUTIONS

In general in the design of a redundant flight control system the designer uses two, three or even four sensors. For example, the same for actuators, computers and other systems, in a parallel redundant configuration. This fact causes many problems, like for example, adding extra weight to the system, location problems with respect to the sensors and redundancy management. Figure 1.1 is an example of a duplex redundant configuration showing the system lanes. Figure 1.1. shows a system that uses three sensors, that is, an angle of attack sensor (α), a pitch-rate (q) sensor, and a pitch-attitude sensor (θ).

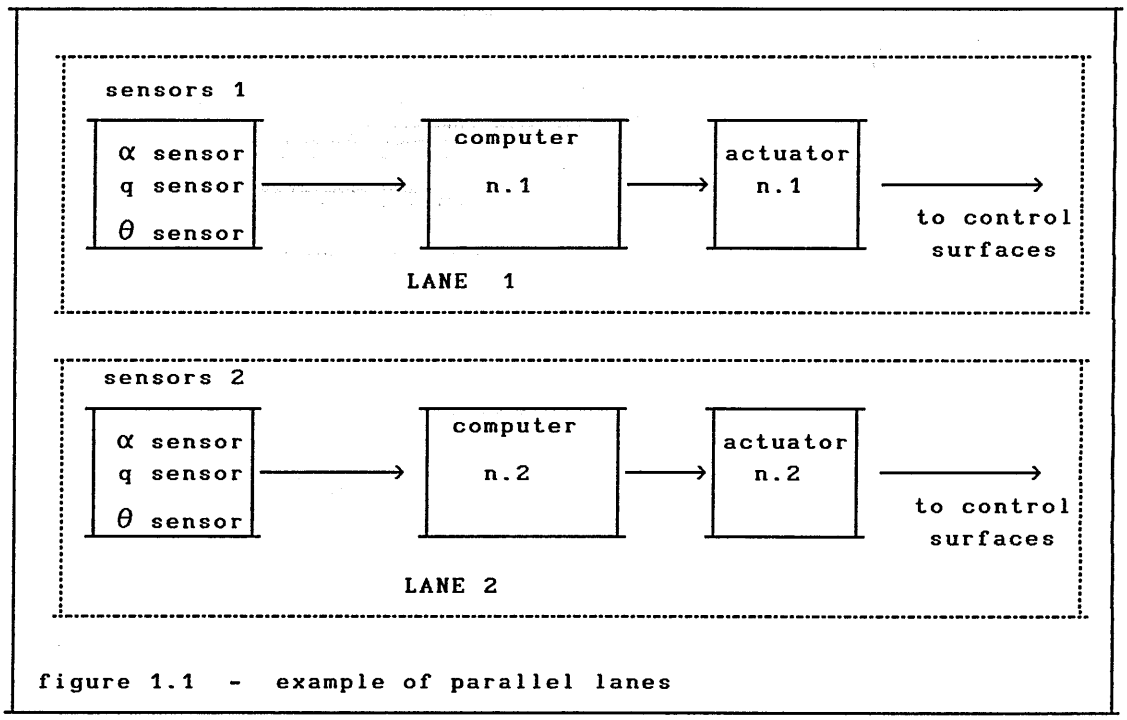

figure 1.1 - example of parallel lanes

To maintain the highest possible system integrity these parallel lanes should ideally be physically and electrically isolated from one another in every respect, which is another problem to deal with in the

design. It is desirable to obtain total lane independence because in this way fault propagation across the lanes is avoided. This research is focussed only on the redundancy aspect of the sensors, not actuators or computers. In military applications the sensors must be distributed in the airframe to reduce the risk of physical damage and as mentioned this is an extra problem. It must also be pointed out that the use of two different computing algorithms for the observers was used in the design, a fact that also contributes to the redundancy if the computer aspect is considered. In addition, redundant sensors need to sense the same signal and their outputs should idealy be identical. It is therefore usualy necessary that they be placed together in close physical proximity thus increasing the possibility for a common mode physical fault.

1.3 INTENDED APPROACH

The approach to the problem in this work is to use observers in order to obtain redundancy with respect to sensors. So the necessity to use two, three or four sensors will be eliminated. The design is carried out by using observers that maintain the flying qualities of the augmented aircraft. Here, observers are investigated for the purpose of estimating state variables in cases where the appropriate sensor has failed. The observer uses inputs from the "healthy" sensors and control surface demands and also means fewer sensors in the flight control system. Figure 1.2 is an example of the intended approach with respect to figure 1.1.

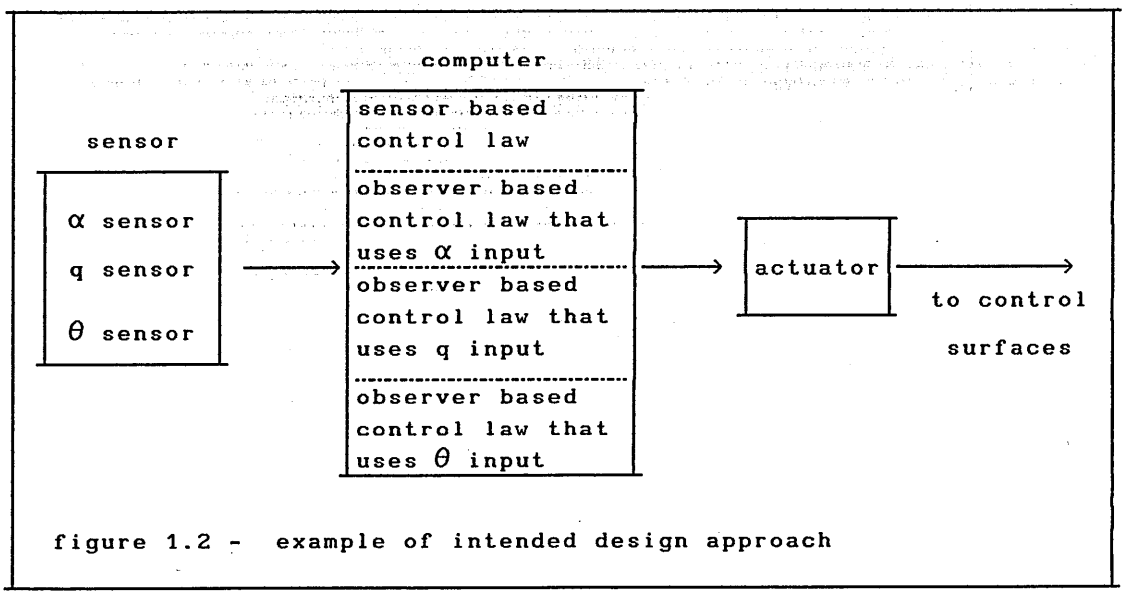

figure 1.2 - example of intended design approach

As can be seen in figure 1.2, redundancy with respect to sensor failures is introduced analytically in the flight control system computer.

The work will be directed to design a flight control system that satisfies the Gibson criteria,[1,2] MIL-F-8785C[4], and also to obtain redundancy with respect to sensor failures. The observers must not destroy the good flying qualities and stability level obtained for the augmented aircraft. The observers must also be able to work not only with the stability agmentation system but with other systems like, for example, an autopilot. Different algorithms to implement the observers are also investigated in order that redundancy in this aspect can also be introduced. The approach will also focus on the failure aspects, that is, how the designed system responds to a failure condition. The work is not concerned with faulty element identification, isolation and replacement. Also, redundancy management is not considered, since it is not the objective of this work. As the control law would be implemented in a digital computer it is very difficult to recognise all potential failure modes and so only the sensor failure modes are analyzed.

1.4 AN OVERVIEW OF THE PERFORMED WORK

In order to obtain good flying qualities and stability a pitch-rate command attitude-hold system was designed by two methods, the pole-placement method and an optimal control method. Modern ideas concerning the flying and handling qualities of high performance aircraft have shown that a controller with this structure can give an aircraft excellent handling qualities The design was tailored to satisfy the requirements of MIL-F-8785C[4], the requirements of the Gibson dropback criterion[1], and also the requirements of the Gibson phase-rate criterion[2]. With the design completed, to implement the control law it is necessary to have the required complement of motion sensors available. If for some reason the aircraft loses one ,or more of the necessary sensors, the flying and handling qualities, and also the level of stability may be seriously degraded. In order to obtain a degree of redundancy observer-based control laws have been designed to operate on a single output variable in order to achieve the same level of stability and flying qualities as obtained with the full sensor-based control law design. To perform this design task the method proposed by Rynaski[5] has been followed, and the theory of robust observers as developed by J.C.Doyle and G.Stein[6] has been applied. The observer-based control law designed in this way is able to maintain the same phase and gain margins as the sensor-based control law, and it preserves the original robustness of the system in the event of a sensor failure. The principal beneffit of the Doyle-Stein observer design is that it does not introduce phase lags that degrade flying qualities as most observers in general do. Another adavantage of the Doyle-Stein observer is that it is not necessary, in some cases, to measure the control surface deflections. With this design, it is possible to introduce analytical redundancy into the flight control system.

This work has also evaluated two methods of design for the control law, the pole placement method and an optimal control method, in order to assess which is most flexible with respect to subsequent modification whilst still satisfying the stability requirements and the handling criteria. The observer control law was designed using

two methods and the advantages and disadvantages of each are compared and discussed. The problems that occur in the design of observers with a pitch-rate sensor or a pitch-attitude sensor are studied and the results reported. Finally, the aircraft was evaluated with a sensor-based control law and three observer-based control laws, and the best order of control law reconfiguration in the event of sensor failures is suggested. The method used to design the observer-based control law can be called *ecletic control*, as suggested by Powell[7] because it uses the best features of classical control and of modern control. The work also considers some aspects of control law implementation, such as numbers of gain parameters to be scheduled.

In the execution of this work the following computer software packages have been used, CODAS[8] , MATLAB[9], and ACSL[10]. The aircraft example used to evaluate the control law designs was the B-747 and the aerodynamic data used was obtained from Heffley[11]. The ACSL computer simulation used in this work is fully described in the report by Oliva and Cook[12]. In the development of this work each control law design starts with the reduced order short period longitudinal model of the aircraft. Subsequent developments make use of the complete aircraft model and actuators. Finally the observer and the autopilot are included in the model for total system evaluations.

2 CRITERIA AND DESIGN TECHNIQUES USED

2.1 BACKGROUND MATERIAL AND LITERATURE SURVEY

2.1.1 BACKGROUND MATERIAL

The foundations of this research are based on the work of Rynaski[5] concerning the use of observers to obtain redundancy in the flight control system. It should be noted that the work of Rynaski was basically founded on the observer theory developed by Doyle-Stein[6] which has developed a robust observer. With respect to flying qualities the work refers to the Gibson dropback criterion[1] and the Gibson phase-rate criterion[2]. Concerning stability requirements the principal reference used was MIL-F-8785C[4]. The control law design was based, on the use of pole-placement methods, described by Friedland[13],Powell[7] ,Chen[14],Patton[15],Shapiro[16] and many other references and also was based on Optimal control methods found in Friedland[13],Anderson and Moore[17], Lewis-Stevens[18],and Lewis[19]. The observer design method was based on Chen[14],Friedland[13],Doyle-Stein[6] ,and Powell-Franklin-Naeini[7] .

2.1.2 LITERATURE SURVEY

Some useful references related to the subjects treated in this work will be given although they have not necessarily been used directly in this work. With respect to a similar design, Monahemi-Barlow-O'Leary[20] describes a very useful procedure, that is, it uses reduced-order observers to obtain precise loop transfer recovery. Now, with respect to observers Phillips-Wilson-Graf-Starks[21] show the observer as a noise filter, also discussed in Chen[14]. Sobel-Banda[22] and Andry-Chung-Shapiro[23] both discuss the design of modal observers, also mentioned by Chen[14], and both applied to flight control system design. Another interesting application is given by Panossian[24] with respect to servoactuator states and parameter estimation. An application to systems with

uncertainties is given by Walcott-Zak[25]. Examples of observers applied to disturbance estimation are given by Bossi-Bryson[26] and Levin-Kreindler[27]. The problem of errors in realization are studied by Stefani[28]. The case when the input is not available is studied by Wang-Davidson-Dorato[29] and Yang-Wilde[30]. Comparison of algorithms are given in Tsui[31] and Tsui[32]. The problem of observer design for time varying linear systems is studied in Carroll-Shafai[33] and Nguyen-Lee[34].

With respect to control law synthesis, in particular with optimal control methods the works of Blight-Gangsaas-Richardson[35] and Gangsaas-Bruce-Blight-Ly[36] are very illustrative. Again, with respect to pole-placement the work of Sobel-Yu[37] is also very useful. Classical references with respect to flying qualities include, for example McRuer-Graham[38], Ashkenas[39], Phillips[40], and Harper-Cooper[41]. With respect to the application of criteria the works of Stengel[42] and Mooij-Gool[43] are important. Examples of flight control systems design can also be obtained from Govindaraj-Rynaski[44], which compares two design methods based on optimal control theory, Cunningham-Pope[45], which discusses modern control analysis and synthesis techniques and in particular Stevens-Lewis-Al Sunni[46],which develops an approach to design control laws for shaping the closed loop step response that uses linear quadratic output feedback techniques. Robustness is considered in Franklin-Ackermann[47], Horowitz-Golubev-Kopelman[48], Ashkenazi-Bryson[49], Schaechter[50],Yanushevsky[51],Okada-Kihara-Ikeda[52], and Burrows-Patton[15]. In particular the work of Chalk[53] is related to the flight control system structure used in this research. Also, alternative methods, such as the low order approach is studied in the works of Mitchell-Hoh[54],Bischoff[55], and Shafer[56]. With respect to the selection of weighting matrices for use in optimal control studies the work of Harvey-Stein[57] can be aplied to more complex problems. Finally ,with respect to stability and control the work of Roskam[58] is very interesting and relevant.

2.2 CONTROL ANTICIPATION PARAMETER (CAP)

2.2.1 INTRODUCTION

The CAP is implicit in the Flying Qualities Requirements MIL-F-8785C[4] and defines the upper and lower frequency limit requirements on the short-period pitching oscillation. The CAP is much more specific than damping ratio or frequency in the description of what it is that a pilot is particularly aware of in the short period motion parameters implicit in the handling characteristics of an aircraft.

2.2.2 DEFINITION

When a pilot applies a pitch command to the aircraft there is a finite time lapse before the steady state condition is reached and during the finite time lapse the transient short period response dynamics are seen. To have good handling the pilot needs some earlier indication of the likely steady state response. Speaking more generally, it is possible to say that the initial transient response and the final steady state response must not be too sensitive to or too insensitive to the commanded flight path change. So CAP is defined as

$$\text{CAP} = \frac{\text{transient peak pitch acceleration}}{\text{steady state normal acceleration}} \qquad (2.1)$$

In terms of the usual aircraft response parameters CAP is defined in the flying qualities requirements documents as the ratio of the initial pitch acceleration to the final steady normal load factor in response to controls. Using the reduced order pitch-rate transfer function

$$\frac{q(s)}{\eta(s)} = \frac{k_q(1+sT_{\theta 2})}{\Delta(s)} \qquad (2.2)$$

where ,
$$k_q = \frac{m_\eta}{T_{\theta 2}\ \omega_{sp}^2} \qquad (2.3)$$

The pitch-acceleration response to a unit step input of elevator angle is,

$$\dot{q}(s) = \frac{k_q(1+sT_{\theta 2})}{\Delta(s)} \qquad (2.4)$$

Applying the initial value theorem

$$\dot{q}(0) = k_q\ T_{\theta 2}\ \omega_{sp}^2 = m_\eta \qquad (2.5)$$

The normal load factor is derived from normal acceleration referred to the C.G. of the aircraft as follows,

$$n_z = -\left[\frac{a_z}{g}\right]_{c.g.} \qquad (2.6)$$

and it is possible to show that

$$n_z(s) = -\frac{m_\eta\ z_w\ V_e\ \eta(s)}{g\ \omega_{sp}^2\ \Delta(s)} \qquad (2.7)$$

Applying the final value theorem, assuming a unit step input

$$n_z(\infty) = -\frac{m_\eta\ z_w\ V_e}{g\ \omega_{sp}^2} \qquad (2.8)$$

Hence,

$$CAP = \frac{\dot{q}(0)}{n_z(\infty)} = \frac{g\ \omega_{sp}^2\ T_{\theta 2}}{V_e} \qquad (2.9)$$

since, $$\frac{n_z}{\alpha} = \frac{V_e}{g\,T_{\theta 2}} \qquad (2.10)$$

it is possible to obtain an alternative expression for CAP as

$$CAP = \frac{\omega_{sp}^2}{\left[\frac{n_z}{\alpha}\right]} \qquad (2.11)$$

2.2.3 INTERPRETATION

CAP can be interpreted in terms of the classical description of static and manoeuvre stability margins. In manoeuvering flight the lift of an aircraft is given by,

$$L = \frac{\rho V^2 S a \alpha}{2} \qquad (2.12)$$

and $$n_z = \frac{L}{m g} = \frac{0.5 \rho V^2 S a \alpha}{m g} \qquad (2.13)$$

So it can be written

$$\frac{n_z}{\alpha} = \frac{0.5 \rho V^2 S a}{m g} \qquad (2.13.a)$$

Allowing perturbations to be small, in limit it is possible to write that $V \simeq V_e$ and from the reduced order longitudinal model is possible to use,

$$\omega_{sp}^2 = \left[\frac{Z_w M_q}{m I_y} - \frac{V_e M_w}{I_y}\right] \qquad (2.14)$$

with Z_w, M_q and M_w dimensional stability derivatives given approximately by,

$$Z_w = -\frac{1}{2}\ \rho\ V_e\ S\ a \qquad (2.15)$$

$$M_q = -\frac{1}{2}\ \rho\ V_e\ S\ \bar{c}^2\ a_1\ \bar{V}_T\ \frac{l_T}{\bar{c}} \qquad (2.16)$$

$$M_w = -\frac{1}{2}\ \rho\ V_e\ S\ \bar{c}\ a\ K_\eta \qquad (2.17)$$

where, k_η is the longitudinal static stability margin.
Then it is possible to write:

$$\omega_{sp}^2 = a\ \bar{c}\ (0.5\ \rho\ V_e\ S)^2 \left[\frac{a_1 \bar{V}_T\ l_T}{m\ I_y} + \frac{k_\eta}{0.5\ \rho\ S\ I_y} \right] \qquad (2.18)$$

Subtituting equation (2.13.a) and (2.18) into equation (2.11) it is possible to write :

$$CAP = \frac{m\ g\ \bar{c}}{I_y} \left[k_\eta - \frac{\bar{c}\ \rho\ S\ m_q}{2\ m} \right] \qquad (2.19)$$

Defining the longitunidal relative density factor as

$$\mu_1 = \frac{m}{\rho\ S\ \bar{c}} \qquad (2.20)$$

it is possible to write

$$CAP = \frac{m\ g\ \bar{c}}{I_y} \left[k_\eta - \frac{m_q}{2\ \mu_1} \right] \qquad (2.21)$$

where

$$H_m = k_\eta - \frac{m_q}{2\,\mu_1} \qquad (2.22)$$

is the longitudinal manoeuvre margin controls fixed.

2.2.4 REQUIREMENTS ON CAP

In MIL-F-8785C[4] a requirement for acceptable values of CAP is not quoted explicitly but it is implicit in the limiting requirements for short period mode frequency. The limits on short period frequency are quoted as a function of n_z/α for each of the flight phase categories. Since the values of CAP are given in MIL-F-8785C[4] these may be read off and used as a constraint in the flight control system design. For level 1 flying qualities the limiting values of CAP may be summarised as follows,

CAT A	0.28	$\leq$	CAP	$\leq$ 3.6
CAT B	0.085	$\leq$	CAP	$\leq$ 3.6
CAT C	0.16	$\leq$	CAP	$\leq$ 3.6

2.3 GIBSON CRITERIA

2.3.1 INTRODUCTION

Although the mission of a civil aircraft differs from that of an advanced fighter, there are tasks, or flight phases, where the handling qualities requirements may be equivalent and where the military criteria can be applied to the civil case. With this is mind this work has used the Gibson criteria. The criterion comes from the necessity to know what kind of approach must be taken when designing a

stability augmentation system in order that the resulting augmented aircraft presents good flying and handling qualities. The basis for the criterion comes from a very extensive analytical study of the longitudinal response characteristics of many aircraft whose flying and handling qualities were known. Gibson was able to identify the parameters which are important in determining the handling characteristics to which pilots are most sensitive. With the determination of limits on the system parameters it is then possible to design flight control systems with an improved probability of providing acceptable flying and handling qualities. Some of the features found within the Gibson criterion correlate very closely with features found in other advanced dynamic handling criteria.

2.3.2 INITIAL CONSIDERATIONS

In common with several other criteria the Gibson criterion is primarily concerned with the longitudinal tracking response of the aircraft since this is an aspect of handling qualities associated with some of the more critical piloting tasks. Traditional measures of flying and handling qualities are based on the assumption that the short term response behaviour of the aircraft is basically second order and so mainly governed by the short period dynamics. In such aircraft the provision of correct short period mode damping and frequency characteristics effectively guarantees acceptable normal acceleration n_z ,pitching acceleration $\dot{q}$ and pitch rate q responses which are, in general sufficient to ensure good handling qualities. As a result it follows that the pitch attitude θ and flight path angle γ responses are also well behaved due to the second order behaviour of the aircraft. Consequently little direct attention has been paid to the role of θ and γ in the determination of handling qualities, but it is known that both pitch attitude θ and flight path angle γ are very important responses with respect to the perception of handling qualities by the pilot. With the increasing complexity of the aircraft and its flight control system the dynamic behaviour is today more and more less second order like and, even if its basic short period mode stability characteristics may be correctly designed it is

quite possible for its pitch attitude and flight path angle behaviour to be unsatisfactory. The main reasons for this are :

- Flight control system dynamics may introduce additional modes with frequencies close to the short period mode.
- It is easy to inadvertently modify attitude response characteristics since in the design of the stability augmentation system to meet the traditional requirements no emphasis is placed on attitude response directly.

From the aircraft model it is possible to establish some simple, but important, response parameters as might apply to the pitch tracking task, these are illustrated on figure (2.1).

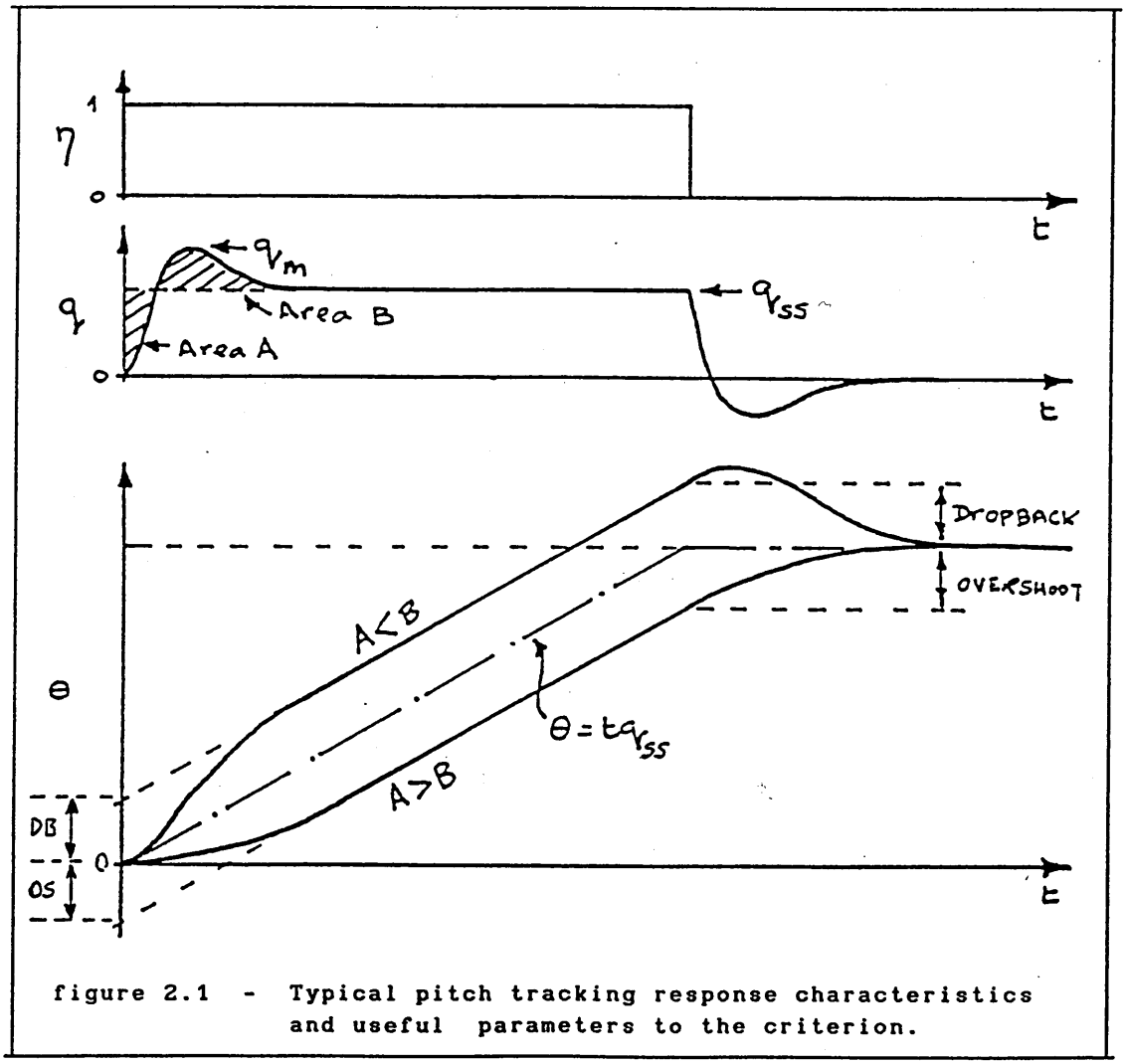

figure 2.1 - Typical pitch tracking response characteristics and useful parameters to the criterion.

With respect to figure (2.1) the input to the aircraft is a unit step of elevator angle which is held for a few seconds and then returned to zero, which corresponds to the trim datum value. The pitch rate and pitch attitude responses that follow are shown and the parameters related with handling qualities important to the pilot are identified as follows,

- pitch rate overshoot ratio $\frac{q_m}{q_{ss}}$
- pitch attitude dropback or overshoot

If, as usual, B > A (in figure 2.1), the pitch attitude drops back to a final value which is less than the value at the time when the pitch demand was removed. If, A > B (in figure 2.1), then the reverse behaviour is seen and this is referred to as overshoot. In general dropback is most common in typical aircraft pitch attitude responses. It is possible to see from figure (2.1) that the value of pitch attitude dropback, or overshoot, is given by the intercept of the projection of the response plot on to the θ axis at t = 0, or it is obtained by the displacement of the linear part of the response plot from the line defined by the equation $\theta = t\ q_{ss}$, as shown on figure 2.1.

2.3.3 THE DROPBACK CRITERION

The dropback criterion, Gibson[1] , was originaly defined in terms of limiting values on pitch rate overshoot ratio and on the ratio of attitude dropback (overshoot) to steady state pitch rate, (DB/q_{ss}) the requirements on these parameters are shown on figure (2.2). A recent study performed by Blagg[3] has concluded that the criterion

could be used as a handling qualities criterion for transport aircraft, if the upper limit of $(DB/q_{ss}) = 0.3$ sec in figure (2.2) is increased to allow lower values of $T_{\theta 2}$ necessary for quick flight path response. However, this modification has not been validated or tested.

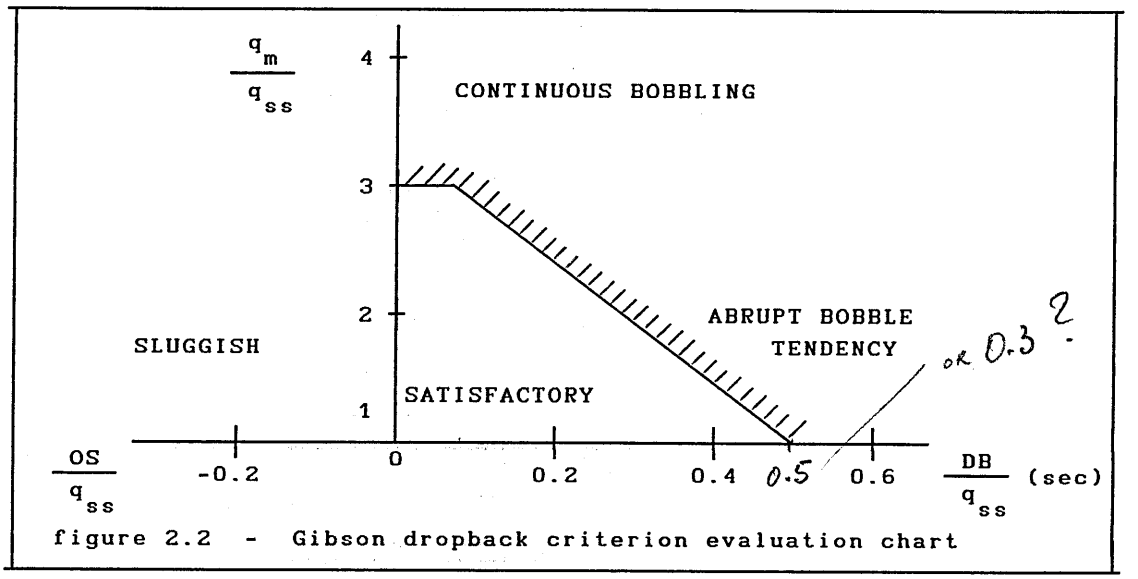

figure 2.2 - Gibson dropback criterion evaluation chart

It is necessary to say that:

- If the pitch rate overshoot ratio $(q_m/q_{ss}) \leq 1$ then dropback is not possible and the lower part of the satisfactory region cannot be attained.
- Subsequently Gibson redefined the criterion such that zero dropback only is acceptable. The satisfactory region then collapses to the (q_m/q_{ss}) axis and in the event that this cannot be obtained then it is better to lie on the side of attitude dropback rather than overshoot.
- The acceptable value of pitch rate overshoot lies in the range $1.0 \leq (q_m/q_{ss}) \leq 3.0$.

2.3.4 THE PHASE-RATE CRITERION

Even when the flying and handling qualities of a high order aircraft are acceptable it is possible that the closed loop gain and phase characteristics may be such that the addition of the pilot in the loop

leads to the propagation of pilot induced oscillation (PIO) at certain conditions. The phase-rate criterion may be applied at the design point after the feedback loop has been developed, in order to reduce the likelihood of PIO ocurrence, that is, after the basic stability characteristics satisfy completely the MIL-F-8785C requirements. The probability of PIO ocurrence is determined by the degree of gain and phase compensation instinctively introduced by the pilot when controlling the aircraft. The required compensation, in general, is determined by the closed loop gain and phase characteristics of the aircraft at frequencies close to the resonant frequency of the human pilot. Gibson[2] studied the problem of PIO occurrence in satisfactory aircraft and identified the desirable gain and phase characteristics for the closed loop high order aircraft if PIO is to be avoided. The Gibson phase-rate criterion has an advantage with respect to other PIO criteria, in that a pilot model is not necessary. The criterion is basically concerned with the closed loop attitude frequency response in the region of -180° phase and is evaluated from a plot of the closed loop attitude frequency response on the Nichols chart as shown in figure (2.3).

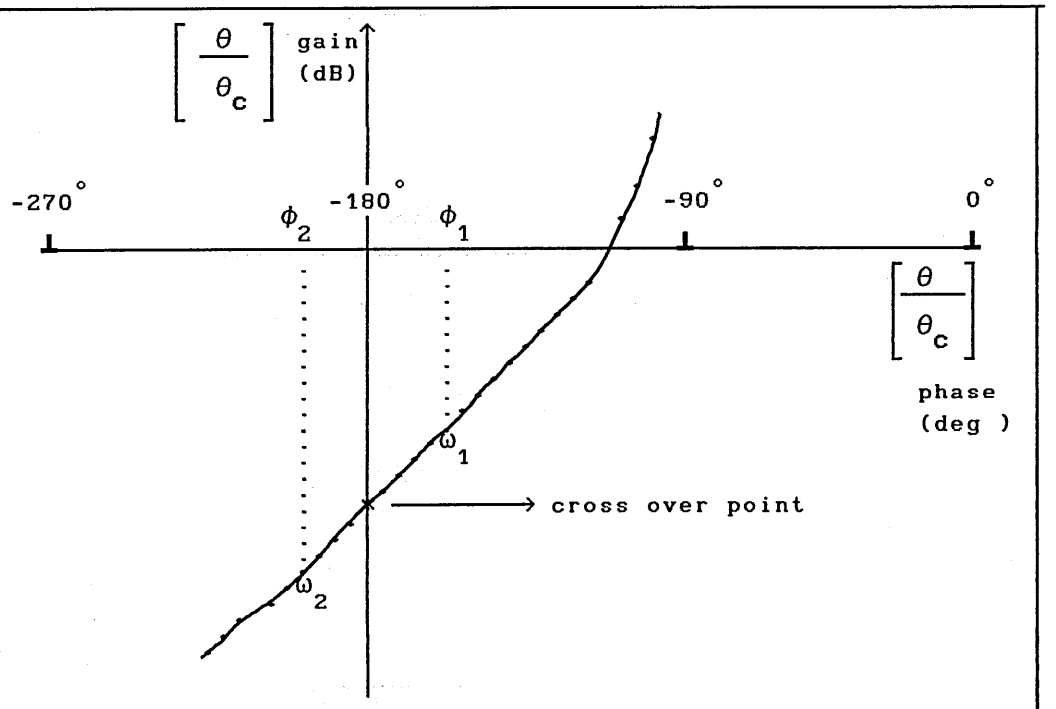

figure 2.3 - Closed loop attitude frequency response on Nichols chart as required by Gibson criterion

Referring to figure (2.3), the point of interest is the cross over point, where the phase first passes through -180° ,the frequency corresponding with this point and the rate of change of phase with frequency at cross over. Again with reference to figure (2.3) the phase-rate is simply defined as :

$$\text{phase-rate} = \text{P.R.} = \frac{\phi_2 - \phi_1}{\omega_2 - \omega_1} \qquad (2.23)$$

and, ideally, Gibson has established that,

$$\text{P.R.} \leq 100^{\circ} / \text{Hz} \qquad (2.24)$$

is desirable in order to avoid PIO with a reasonable safe margin. The criterion can be simply summarised on figure (2.4).

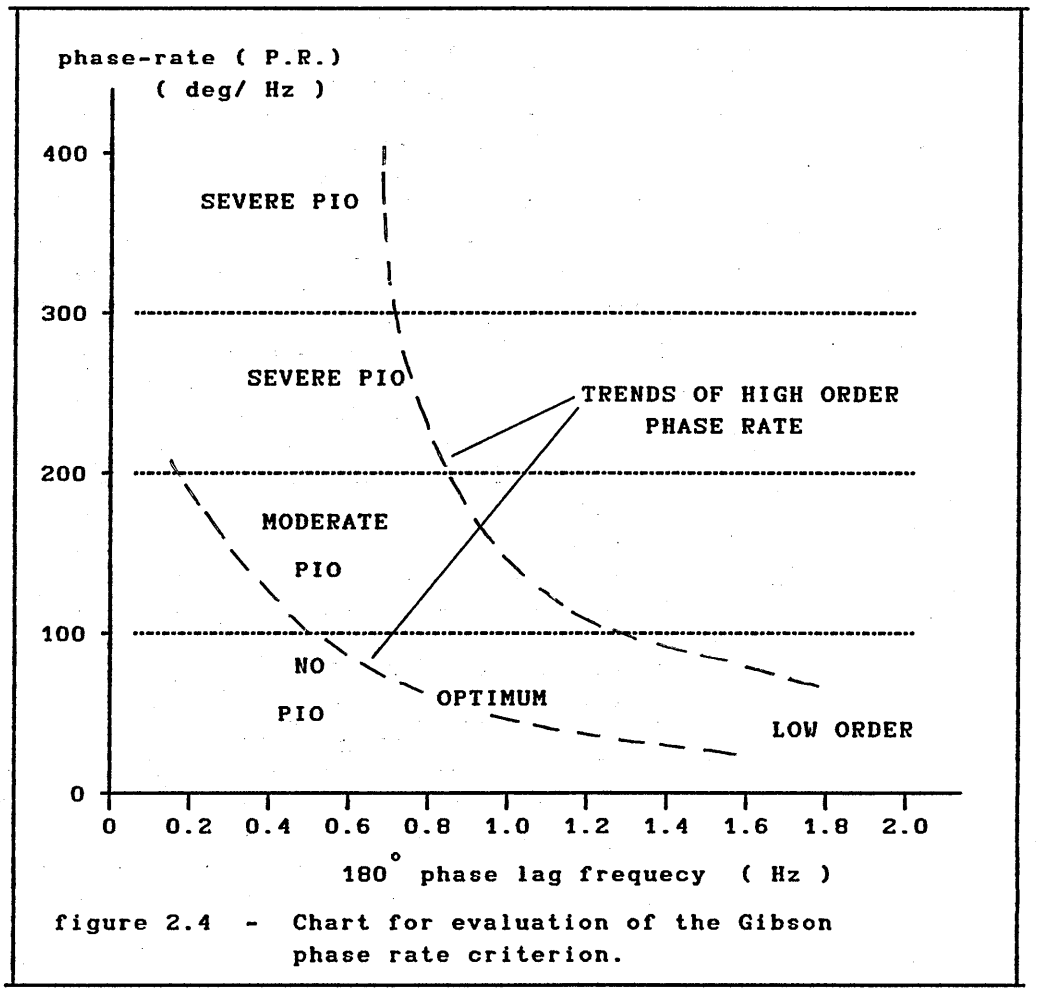

figure 2.4 - Chart for evaluation of the Gibson phase rate criterion.

In general, it is required that the cross-over point should occur at a frequency of 1 Hz and that the phase-rate should be less than 100° per Hz. If an aircraft does not meet the criterion, then a suitable gain and phase compensation can be introduced into the command path with the help of a suitable pre filter resulting in a flight control system structure shown on figure (2.5).

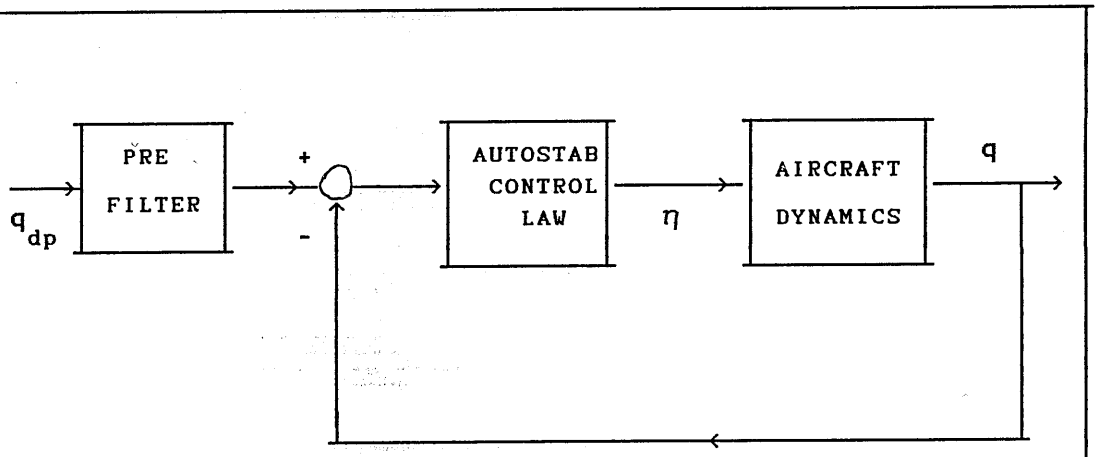

figure 2.5 - Flight control system with pre-filter

When command path compensation is required it is also necessary to include some high frequency gain compensation in order to maintain the slope of the closed loop attitude frequency response plot to a reasonable value at cross over.

2.4 THE POLE-PLACEMENT TECHNIQUE

2.4.1 INTRODUCTION

In the control law design the pole-placement technique will be used as the first method. There are so many references in the literature about pole-placement that is impossible to refer to all here. However, it is possible to refer to some useful design techniques as presented in Patton[13,15], D'Azzo[59], Shapiro[16], and Friedland[13] for example. Obviously the pole-placement technique is a state-space method. In a controllable system, with all the state variables

accessible for measurement and feedback, it is possible to place the closed loop poles anywhere in the complex s-plane. This means that in principle it is possible to completely specify the closed loop dynamic performance of the system, as for example MIL-F-8785C[4] requirements (CAP), and Gibson[1] dropback criterion. So in principle it is possible to satisfy any criteria, but in pratice it is also necessary to ensure that large control signals are not required. If so ,signal limiting as a result of saturation on the actuator might be possible, that is, the actuator will not be able to deliver large control signals. So it is necessary to not only focus on satisfactory handling criterion and stability criterion but also on feasible feedback gains. The first step in the pole-placement design approach is to decide the desired closed-loop pole locations. When selecting pole locations, it is necessary to keep in mind that the control effort required is related to how far the open loop poles are moved by feedback. Furthermore, open-loop zeros attract poles, so considerable control effort is required to move a pole away from a nearby zero. Therefore a pole-placement philosophy that aims to fix only the undesirable aspects of the open-loop response will typically allow smaller control actuators than one that arbitrarily picks all the poles in some location without regard to the original open-loop poles. In aircraft flying qualities specifications, such as MIL-F-8785C[4], closed-loop pole locations are implied. It is also possible to use the technique of a prototype design, such as the ITAE or Bessel responses, for higher order systems. However it is essential to recognise that these techniques deal with pole selection without explicit regard for their effect on control effort.

2.4.2 FLIGHT CONTROL SYSTEM DESIGN

To use the pole-placement technique on problems in which there are reference inputs and/or disturbances, it is frequently desirable to represent these inputs and disturbances by additional state variables. The particular dynamic process to be controlled may be described by the following state equation.

$$\dot{x} = A x + B u + F x_d \qquad (2.25)$$

where x_d is a disturbance vector, which may or may not be subject to direct measurement and u is the control input to the aircraft. In addition it is also desirable that the state x track a reference state x_r . Figure (2.6) is the state-space representation of a system with disturbances and reference input.

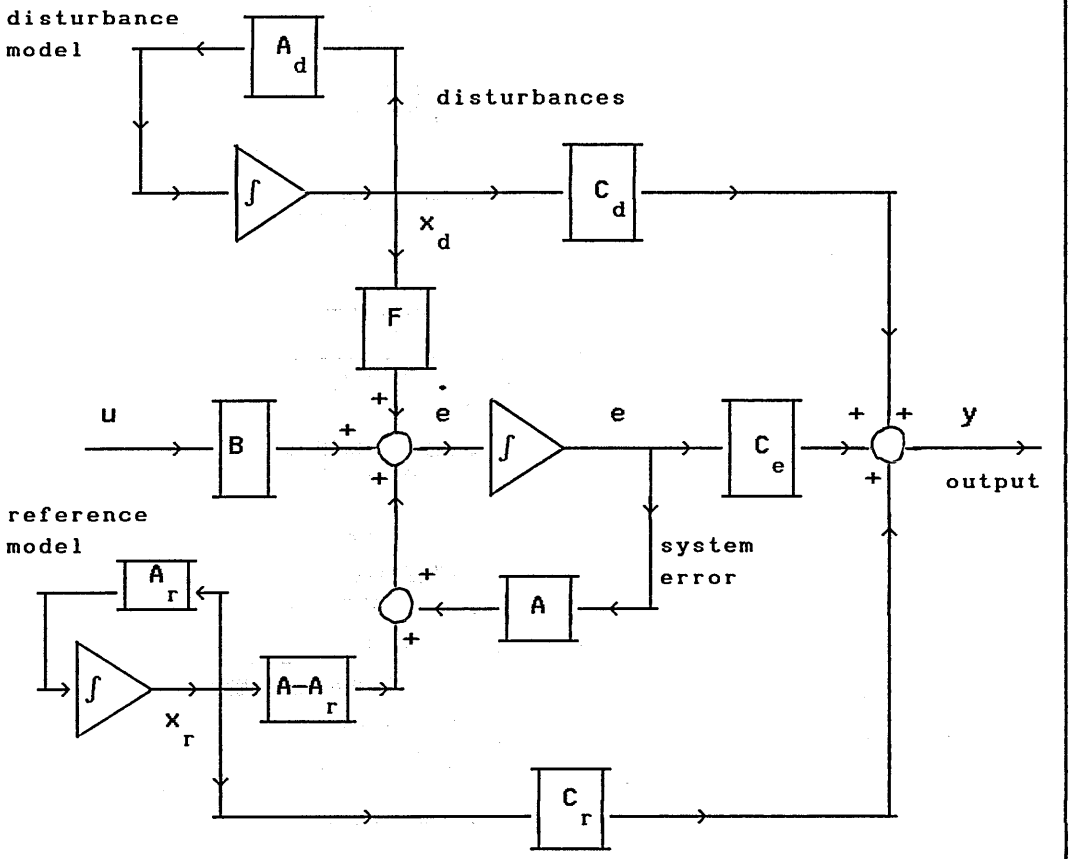

figure 2.6 - State-space representation of a system with disturbance and reference input.

To formulate the problem in terms of state variables, it is often expedient to assume that x_d and x_r satisfy known differential equations :

$$\dot{x}_d = A_d x_d \qquad (2.26)$$

$$\dot{x}_r = A_r x_r \qquad (2.27)$$

These supplementary states are surely not subject to control by the designer, so that these are unforced differential equations. The system comprising x, x_d, and x_r is necessarily uncontrollable. In general the objective is concerned with the error defined by :

$$e = x - x_r \qquad (2.28)$$

So the differential equation for the error using (2.25) and (2.27) will be :

$$\dot{e} = \dot{x} - \dot{x}_r = A(e+x_r) + F\,x_d + B\,u - A_r x_r \qquad (2.29)$$

$$\therefore \quad \dot{e} = A\,e + (A - A_r)x_r + F\,x_d + B\,u \qquad (2.30)$$

$$\text{or,} \quad \dot{e} = A\,e + E\,x_0 + B\,u \qquad (2.31)$$

$$\text{where,} \quad E = \left(A - A_r \,\vdots\, F \right) \qquad (2.32)$$

$$\text{and,} \quad x_0 = \left[\begin{array}{c} x_r \\ \hline x_d \end{array}\right] \qquad (2.33)$$

The vector x_0 represents the exogenous inputs to the system. To the differential equations of the error is adjoined the equations for the reference and disturbance states to produce a system of order 2k+1 having the metastate vector,

$$x = \left[\begin{array}{c} e \\ \hline x_0 \end{array}\right] \qquad (2.34)$$

and satisfying the metastate equation

$$\dot{x} = A\,x + B\,u \qquad (2.35)$$

where, $$A = \left[\begin{array}{c|c} A & E \\ \hline 0 & A_0 \end{array}\right] \qquad (2.36)$$

$$B = \left[\begin{array}{c} B \\ \hline 0 \end{array}\right] \qquad (2.37)$$

and $$A_0 = \left[\begin{array}{c|c} A_r & 0 \\ \hline 0 & A_d \end{array}\right] \qquad (2.38)$$

The design method described here is used in this research program. First it is necessary to refer to figure (2.7) concerning the control system structure.

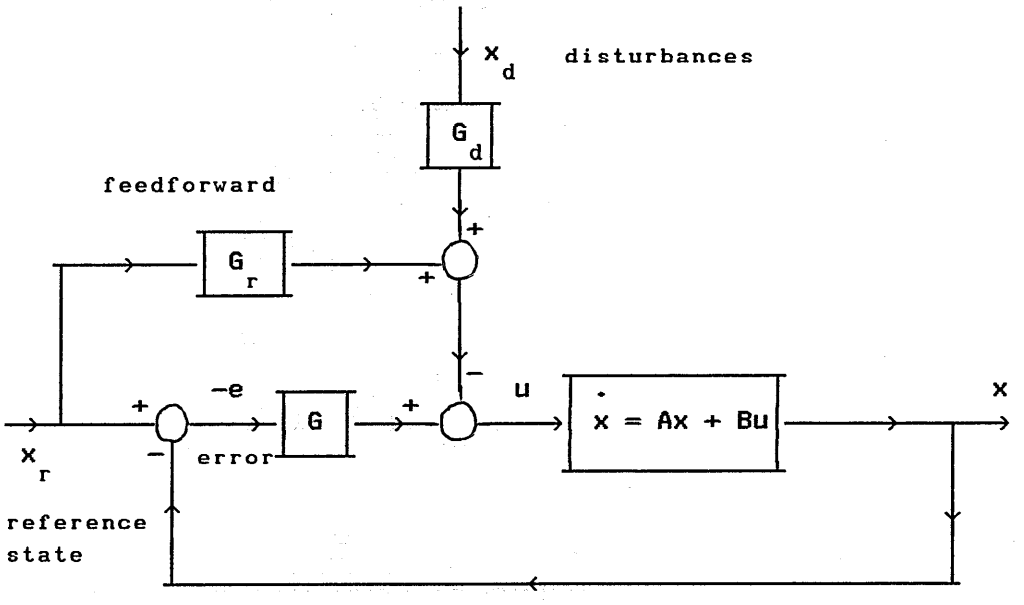

figure 2.7 - Schematic of feedback system for an aircraft with reference state and disturbance input.

This method applies to a more general objective, that is, to control the system error not only for initial disturbances, but also for persistent disturbances, and also to track reference inputs, as required by the Gibson dropback criterion for example.

The error is defined by : $e = x - x_r$ (2.39)

where x is the system state vector

x_r is the reference input vector

and also x_r is assumed to satisfy a differential equation

$$\dot{x}_r = A_r x_r \qquad (2.40)$$

A disturbance x_d is also included and so the error is given by:

$$\dot{e} = A e + (A - A_r)x_r + F x_d + B u \qquad (2.41)$$

$$\dot{e} = A e + B u + E x_0 \qquad (2.42)$$

As in terms of control theory the metasystem is not controllable it is convenient to work directly with the error differential equation (2.42) and so the exogenous vector x_0 is treated as an input just like u. A linear control law is assumed, which takes the general form,

$$u = - G e - G_0 x_0 = - G e - G_r x_r - G_d x_d \qquad (2.43)$$

From figure (2.7) it is possible to see the presence of two signal paths in addition to feedback path. There is a feedforward path with a gain G_r and a path through the gain G_d, and the objective is to minimise the effect of the disturbances x_d. For the present, the objective is limited to the design of the gain matrices G and G_0. The closed loop dynamics are described by,

$$\dot{e} = A e + E x_0 - B(G e + G_0 x_0) \qquad (2.44)$$

which is the differential equation of a linear system excited by x_0. If possible, it is desirable to choose the gains G and G_0 to keep the system error zero, however more reasonable performance objectives are the following:

(a) the closed loop system should be asymptotically stable.

(b) A linear combination of the error state variables is to be zero in the steady state.

In order for the closed loop system to be asymptoticaly stable the closed loop dynamics matrix,

$$A_c = A - B\,G \qquad (2.45)$$

must have its characteristic roots in the left half s-plane. If the system is controllable, this can be accomplished by a suitable choice of the gain matrix. The steady state condition is characterized by a constant error state vector, i.e., in the steady state

$$\dot{e} = 0 \qquad (2.46)$$

and from (2.44), this means that

$$(A - B\,G)e = (B\,G_0 - E)x_0 \qquad (2.47)$$

If the closed loop system is asymptoticaly stable, $A_c = A-BG$ has no characteristic roots at the origin, and so its inverse exists. So the steady state error is given by:

$$e = (A - BG)^{-1}(B\,G_0-E)x_0 \qquad (2.48)$$

It is not reasonable to expect that e be zero, instead it is required that

$$y = C\,e = 0 \qquad (2.49)$$

where C is a singular matrix of suitable dimension.
Then it is possible to write:

$$C\,(A-BG)^{-1}(BG_0-E)x_0 = 0 \qquad (2.50)$$

and it must hold for any x_0 ,that it is possible if and only if the coefficient matrix multiplying x_0 vanishes:

$$C(A-BG)^{-1}(BG_0-E) = 0 \qquad (2.51)$$

or

$$C(A-BG)^{-1}BG_0 = C(A-BG)^{-1}E \qquad (2.52)$$

Now the dimension of C becomes significant.
If the dimension of y is j, then C is a (j x k) matrix, $(A-BG)^{-1}$ is a (k x k) matrix, and B is a (k x m) matrix, where m is the number of control variables. The product of the three matrices multiplying G_0 is thus a (j x k) matrix. If j > k, then (2.52) is overdetermined, there are too many conditions to be satisfied by G_0 and, except for special values of E, no solution to (2.52) for G_0 exists. On the other hand if j < k, then (2.52) is underdetermined, G_0 is not uniquely specified by (2.52). This poses no problem; it only means that G_0 can be choosen to satisfy not only (2.49), but also to satisfy other conditions. Analytically the simplest case is when the number of inputs m is equal to the dimension of y. In this case, when the matrix multiplying G_0 is not singular, the desired gain matrix is given by

$$G_0 = \left[C(A-BG)^{-1}B \right]^{-1} C(A-BG)^{-1} E \qquad (2.53)$$

The big matrix

$$B^{\#} = \left[C(A-BG)^{-1}B \right]^{-1} C (A-BG)^{-1} \qquad (2.54)$$

that multiplies E has the property that

$$B^{\#} B = I \qquad (2.55)$$

and so it is possible to write:

$$G_0 = B^{\#} E \qquad (2.56)$$

It can be shown that $C(A-BG)^{-1}B$ possesses an inverse, see Friedland[13].

2.5 THE LINEAR QUADRATIC OPTIMAL CONTROL TECHNIQUE

2.5.1 INTRODUCTION

There are several good reasons to use optimal control for the design of flight control systems. The first is that in a MIMO system, the pole placement technique does not completely specify the controller or compensator parameters, that is the gains. Another good reason is that the designer may not really know the most satisfactory closed loop pole locations. In fact, the designer who has acquired extensive experience with a particular type of problem generally has an intuitive "feel" about the proper closed loop pole locations. However when faced with a new problem or a lack of time to acquire the necessary insight, the designer will benefit from a design method that can provide an initial design and at the same time acquire "feel" about the problem. Another good reason is that the optimal control theory can be applied to processes which are not controllable in terms of control theory. Optimal control theory was developed to specifically address the issue of achieving a balance between good system response and control effort. It is important to note that Optimal control theory does not provide direct specification of the transient response in the way that other methods do. In fact Optimal control theory selects poles that result in some defined balance between system errors and control effort. The designer can easily examine the relationship between shifts in that balance (by changing the weighting matrices in the performance index) and system root locations, time response, and feedback gains.

2.5.2 THE DESIGN PROCESS

Again, the model considered initially is the same as in the pole placement technique, that is,

$$\dot{e} = A\,e + B\,u + E\,x_0 \qquad (2.57)$$

where x_0 is the exogenous vector, and u the input to the aircraft. As in the pole placement technique x_0 satisfies a known differential equation,

$$\dot{x}_0 = A_0 x_0 \qquad (2.58)$$

and so the entire metastate satisfies the differential equation,

$$\dot{x} = A x + B u \qquad (2.59)$$

where

$$x = \begin{bmatrix} e \\ \hline x_0 \end{bmatrix} \qquad (2.60)$$

$$A = \left[\begin{array}{c:c} A & E \\ \hline 0 & A_0 \end{array}\right] \qquad (2.61)$$

$$B = \begin{bmatrix} B \\ \hdashline 0 \end{bmatrix} \qquad (2.62)$$

An appropriate performance integral is :

$$V = \int_t^\infty (x^T Q\, x + u^T R\, u)\, d\tau \qquad (2.63)$$

thus, the weighting matrix for the metastate is of the form,

$$Q = \left[\begin{array}{c:c} Q & 0 \\ \hline 0 & 0 \end{array}\right] \qquad (2.64)$$

This is the clasical problem of optimal control (LQR), with the matrix M as the solution of the matrix Riccati equation, the theory

and solution of this problem is well described in many books, for example Anderson-Moore[17], and in particular as applied in this work in Friedland[13]. The problem can be solved without theoretical difficulty, and with the partition of the performance matrix M for the metasystem will give:

$$M = \left[\begin{array}{c|c} M_1 & M_2 \\ \hline M_2^T & M_3 \end{array}\right] \qquad (2.65)$$

It is well known that the performance matrix M satisifes the algebraic quadratic equation (algebraic Riccati equation).

$$0 = \bar{M} A + A^T \bar{M} - \bar{M} B R^{-1} B^T \bar{M} + Q \qquad (2.66)$$

and that the optimum gain is given by

$$\bar{G} = R^{-1} B^T \bar{M} \qquad (2.67)$$

The gain matrix $\bar{G}$ for the metasystem is given by,

$$\bar{G} = R^{-1} \left[B^T \,\vdots\, 0 \right] \left[\begin{array}{c|c} M_1 & M_2 \\ \hline M_2^T & M_3 \end{array}\right] \qquad (2.68)$$

$$\bar{G} = \left[R^{-1} B^T M_1 \,\vdots\, R^{-1} B^T M_2 \right] \qquad (2.69)$$

and it is possible to notice that the submatrix M_3 is not needed to solve the problem. Performing the matrix multiplications required by the Riccati equation it is possible to obtain the differential equations for the submatrices in (2.65).

$$-\dot{M}_1 = M_1 A + A^T M_1 - M_1 B R^{-1} B^T M_1 + Q \qquad (2.70)$$

$$-\dot{M}_2 = M_1 E + M_2 A_0 + (A^T - M_1 B R^{-1} B^T) M_2 \qquad (2.71)$$

$$-\dot{M}_3 = M_3 A_0 + A_0^T M_3 + M_2^T E + E^T M_2 - M_2^T B R^{-1} B^T M_2 \qquad (2.72)$$

Due to the special structure of A, B, and Q, the following facts about the submatrices of M emerge:

(a) The solution of M_1 ,and hence the corresponding gain $R^{-1} B^T M_1$, is the same as it would have been with x_0 absent from the problem,i.e., if the design were for the simple regulator problem (clasical optimal control problem), so a steady state solution for M_1 can be obtained if the pair (A,B) is controllable.

(b) The differential equation for M_2, from which the gain $R^{-1} B^T M_2$ is determined, does not depend on M_3, and in fact is a linear equation, which can be written as,

$$-\dot{M}_2 = M_1 E + M_2 A_0 + A_c^T M_2 \qquad (2.73)$$

where $A_c = A - B R^{-1} B^T M_1$ (2.74)

is the closed loop dynamic matrix of the regulator subsystem.

A steady state solution also can be found, and it must satisfy,

$$0 = \bar{M}_1 E + \bar{M}_2 A_0 + A_c^T \bar{M}_2 \qquad (2.75)$$

and so the necessary gains to realize the control law are obtained as:

$$u = - R^{-1}B^T \bar{M}_1 x - R^{-1} B^T \bar{M}_2 x_0 \qquad (2.76)$$

(c) The differential equation for M_3 is also linear. However M_3 is not used in the determination of the gain matrix.

2.5.3 CASE WITH CONSTANT REFERENCE INPUT

The most frequently tracked signal corresponds with the condition, $A_0 = 0$, so for this case the equations for M_2 and M_3 become simply,

$$- \dot{M}_2 = M_1 E + A_c^T M_2 \qquad (2.77)$$

and

$$- \dot{M}_3 = M_2^T E + E^T M_2 - M_2^T B R^{-1} B^T M_2 \qquad (2.78)$$

The correct relationship for M_2 is given by the solution of (2.77) with $M_2 = 0$.

$$\bar{M}_2 = - \left[A_c^T \right]^{-1} \bar{M}_1 E \qquad (2.79)$$

where $\bar{M}_1$ is the steady state solution of (2.70), i.e., the control matrix for the regulator design. Thus the gain for the exogenous variables is,

$$G_0 = -R^{-1}B^T \left[A_c^T \right]^{-1} \bar{M}_1 E = B^* E = G_0^* \qquad (2.80)$$

where

$$B^* = - R^{-1}B^T \left[A_c^T \right]^{-1} \bar{M}_1 \qquad (2.81)$$

2.5.4 COMMENTS ABOUT THE SELECTION OF Q AND R

The question of concern to the control system designer is the selection of the weighting matrices Q and R. To quote, Friedland[13]

" In candor one must admit that minimization of a quadratic integral is rarely the true design objective. The problem, however, is that the true design objective often cannot be expressed in mathematical terms. "

In the performance index two terms contribute to the integrated cost of control: the quadratic form $x^T Q\ x$ which represents a penalty on the deviation of the state x from the origin and the term $u^T R\ u$ which represents the cost of control. It should be obvious that the choice of the state weighting matrix Q depends on what the system designer is trying to achieve. Again Friedland's words are appropriate to be written :

" The relationship between the weighting matrices Q and R and the dynamic behavior of the closed-loop system depend of course on the matrices A and B and are quite complex. "
" It is impratical to predict the effect on closed loop behavior of a given pair of weighting matrices. "

And finally, it is useful to again quote Friedland's words with respect to the design process when working with optimal control. It must also be pointed out that the same advice is given by Brogan[60], and by many other references related to optimal control. So Friedland says :

" A suitable approach for the designer would be to solve for the gain matrices G that result from a range of weighting matrices Q and R, and calculate (or simulate) the corresponding closed-loop response. The gain matrix G that produces the response closest to meeting the design objectives is the ultimate selection. In a few hours time, dozen or more combinations of Q and R can be determined, and a suitable selection of G can be made. "

It is also useful at this time to repeat the guidance given by Brogan[60] about the problem of selection of the weighting matrices Q and R, that is very appropriate to this work :

" For small problems with only a few parameters it may be feasible to parametrically examine the range of possibilities. For most problems a more focussed approach is desirable. The expanded quadratic will contain terms of the form $x_i^2 Q_{ii} + u_i^2 R_{ii}$. If x_i is a position variable with magnitude of thousands of feet, and if u_i is an angle of say 0.01 radian, it is clear that u_i will have no effect on V unless $R_{ii} \gg Q_{ii}$. The point is that scaling units and variable magnitudes are important, as well as the subjective choice of the importance of keeping u_i small compared to keeping x_i small. "

Finally Brogan[60] says about Q and R :

" The relative magnitudes are all that matter "

2.6 OBSERVER DESIGN TECHNIQUE

2.6.1 INTRODUCTION

In order to design the observer two methods have been used, here the design methods are summarised and explained. Both methods are suitable for full order observers or for reduced order observers, however here the discussion relates to the reduced order observer only, which is the one used in this research. The reason for using a reduced order observer is because it requires fewer parameters to be implemented in the flight control system, and so it is more suitable. The reduced order observer has a much higher bandwidth from sensor to control when compared with the full order observer. Therefore, if sensor noise is a significant factor, the reduced order observer is less attractive, since the potential savings in complexity may be more

than offset by the increased sensitivity to noise. In this research, as in the work of Rynaski[5] the sensors are assumed to be essentially noise-free in themselves.

2.6.2 FIRST METHOD

The method here developed can be found in Friedland[13], and Chen[14]. It is assumed that the dynamic system is described by the following state equation,

$$\dot{x} = A\,x + B\,u \qquad (2.82)$$

It is also assumed that it is possible to group the state variables into two sets: those that can be directly measured x_1, and those that depend indirectly on the former x_2. The state vector is partitioned accordingly :

$$x = \left[\begin{array}{c} x_1 \\ \hline x_2 \end{array}\right] \qquad (2.83)$$

with :

$$\dot{x}_1 = A_{11}x_1 + A_{12}x_2 + B_1u \qquad (2.84)$$

$$\dot{x}_2 = A_{21}x_1 + A_{22}x_2 + B_2u \qquad (2.85)$$

The output equation is given by : $y = C_1x_1$ (2.86)

The standard observer for (2.84) and (2.85) is given by :

$$\dot{\hat{x}}_1 = A_{11}\hat{x}_1 + A_{12}\hat{x}_2 + B_1u + K_1(y-C_1\hat{x}_1) \qquad (2.87)$$

$$\dot{\hat{x}}_2 = A_{21}\hat{x}_1 + A_{22}\hat{x}_2 + B_2u + K_2(y-C_1\hat{x}_1) \qquad (2.88)$$

But it is not necessary to implement the observer for x_1 because x_1 is

already available as,

$$x_1 = \hat{x}_1 = C_1^{-1}\, y \qquad (2.89)$$

So the observer for x_2 will be:

$$\dot{\hat{x}}_2 = A_{21}C_1^{-1}y + A_{22}\hat{x}_2 + B_2u \qquad (2.90)$$

which is a dynamic system of the same order as the number of state variables x_2 that cannot be measured directly. The dynamic behaviour of the reduced order observer is governed by the eigenvalues of A_{22} which is a submatrix of the open-loop dynamic matrix A, a matrix over which the engineer has no control. If the eigenvalues of A_{22} are suitable, then (2.90) could be a satisfactory observer. Since there is no assurance that the eigenvalues of A_{22} are suitable it is necessary to devise a more general system to estimate x_2. A suitable general structure for the estimation of x_2 is given by,

$$\hat{x}_2 = L\, y + z \qquad (2.91)$$

with z the state of a (k-1)th order system, and L is the gain matrix of the observer.

$$\dot{z} = F\, z + \bar{G}\, y + H\, u \qquad (2.92)$$

The estimation error is defined by,

$$e = x - \hat{x} = \begin{bmatrix} x_1 - \hat{x}_1 \\ \hline x_2 - \hat{x}_2 \end{bmatrix} = \begin{bmatrix} e_1 \\ \hline e_2 \end{bmatrix} \qquad (2.93)$$

but, $$e_1 = x_1 - \hat{x}_1 = 0 \qquad (2.94)$$

So it is necessary only to consider e_2, described by the differential equation,

$$\dot{e}_2 = \dot{x}_2 - \dot{\hat{x}}_2 = A_{21}x_1 + A_{22}x_2 + B_2u - L\dot{y} - \dot{z} \qquad (2.95)$$

$$\therefore \quad \dot{e}_2 = A_{21}x_1 + A_{22}x_2 + B_2u - L\left[C_1(A_{11}x_1+A_{12}x_2+B_1u)\right] +$$

$$- F\,z - \bar{G}\,y - H\,u \qquad (2.96)$$

but it is known that $\hat{x}_2 = L\,y + z$, equation (2.91), and then

$$z = \hat{x}_2 - L\,y = x_2 - e_2 - L\,y = x_2 - e_2 - LC_1x_1 \qquad (2.97)$$

and

$$\dot{e}_2 = F\,e_2 + (A_{21} - LC_1A_{11} - \bar{G}C_1 + FLC_1)\,x_1 +$$

$$(A_{22} - LC_1A_{12} - F)x_2 + (B_2 - LC_1B_1 - H)u \qquad (2.98)$$

In order for the error to be independent of x_1, x_2 and u, the matrices multiplying x_1, x_2, and u must vanish, that is, the following equations must apply,

$$F = A_{22} - LC_1A_{12} \qquad (2.99)$$

$$H = B_2 - LC_1B_1 \qquad (2.100)$$

$$\bar{G}C_1 = A_{21} - LC_1A_{11} + FLC_1 \qquad (2.101)$$

Then (2.98) becomes $\dot{e}_2 = F\,e_2$ (2.98.a)

and hence, for asymptotic stability, the eigenvalues of F must lie in the left half s-plane.

Having selected the matrix L to place the reduced order observer poles, the matrix H is determined from (2.100) and the matrix $\bar{G}$ is determined from (2.101), that is,

$$\bar{G} = (A_{21} - LC_1A_{11})C_1^{-1} + FL \qquad (2.102)$$

and so:

$$\dot{z} = F\hat{x}_2 + (A_{21} - LC_1A_{11})y + Hu \qquad (2.103)$$

Figure (2.8) represents a block diagram of these equations.

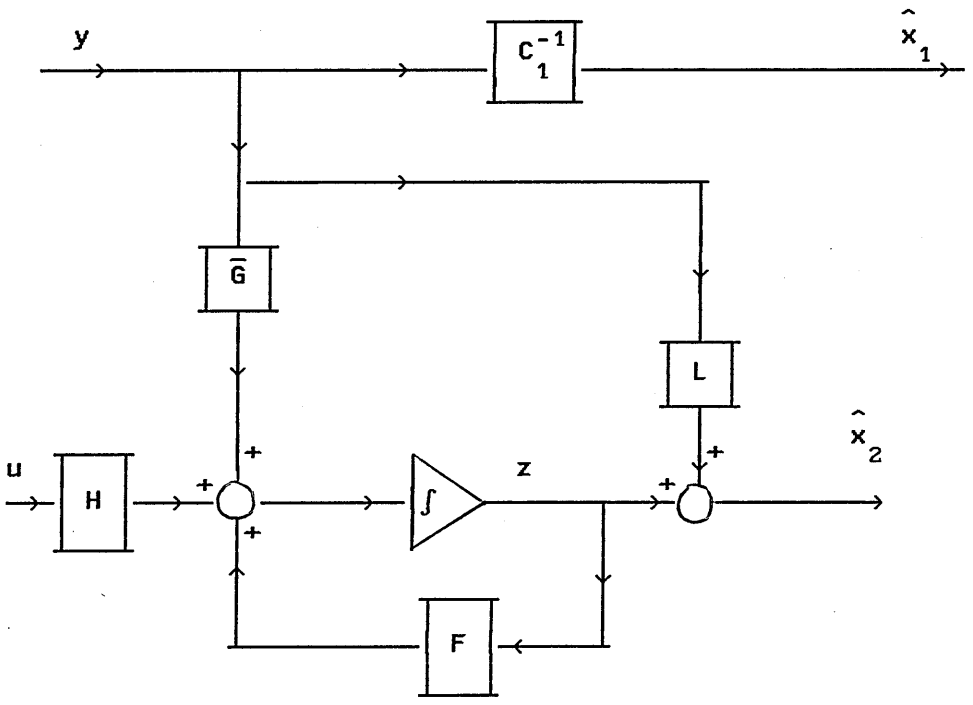

figure 2.8 - Reduced order observer for observation $y = C_1x_1$ with C_1 nonsingular.

The observer is defined by :

$$\dot{z} = F\hat{x}_2 + (A_{21} - LC_1A_{11})y + Hu \qquad (2.104)$$

$$\hat{x}_2 = L\,y + z \qquad (2.105)$$

$$\hat{x}_1 = C_1^{-1}y = x_1 \qquad (2.106)$$

2.6.3 SECOND METHOD

The method here described can be found in Chen[14] as an alternative method when the previous one described is not applicable.
Now consider again the dynamic system given by,

$$\dot{x} = A\,x + B\,u \qquad (2.107)$$

$$y = C\,x \qquad (2.108)$$

where A is a matrix (nxn), B (nxp) and C (qxn)
Suppose again that the observer is given by

$$\dot{z} = F\,z + \bar{G}\,y + H\,u \qquad (2.109)$$

a (n-q) dimensional dynamic equation, with F, $\bar{G}$ and H constant matrices to be designed and with dimensions:
F (n-q)x(n-q), $\bar{G}$ (n-q)xq and H (n-q)xp
In this method the following algorithm is given by Chen[14], and it will be applied in this research,

(1) Choose a real constant matrix F so that all of its eigenvalues have negative real parts and are distinct from those of A.
(2) Choose a matrix $\bar{G}$ so that {F,G} is controllable.
(3) Solve the unique T in : $TA - FT = \bar{G}C$, a Lyapunov equation with T a (n-q) x n matrix.
(4) If the square matrix of order n

$$P = \begin{bmatrix} C \\ T \end{bmatrix} \qquad (2.111)$$

is singular, go back to step (1) and/or step (2) and repeat the process. If P is non nonsingular, compute H = TB. Then the equation (2.109) is an estimate of Tx and so the original state can be estimated by,

$$\hat{x} = \begin{bmatrix} C \\ T \end{bmatrix}^{-1} \begin{bmatrix} y \\ z \end{bmatrix} \qquad (2.113)$$

2.7 THE DOYLE-STEIN OBSERVER

One of the main questions that must be considered when designing an observer is the robustness of the closed loop dynamic process. The observer described in this section was developed by Doyle-Stein[6] and is also discussed by Friedland[13]. Considering first figure (2.9),

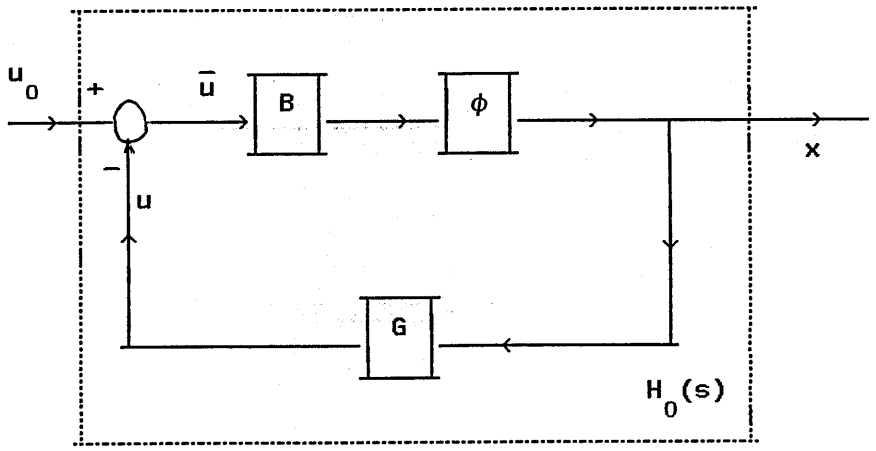

figure 2.9 - schematic of a general feedback control system

Where : $\dot{x} = A\,x + B\,u$ (2.114)

$\bar{u} = u_0 - G\,x = u_0 - u$ (2.115)

and $\phi(s) = (sI-A)^{-1}$ (2.116)

The transfer function from the input u_0 to the state x is ,

$$x(s) = \phi\, B\, \bar{u}(s) \qquad (2.117)$$

Using (2.115) and (2.117),

$$x(s) = (I+\phi BG)^{-1}\phi\ B\ u_0 \qquad (2.118)$$

So the transfer function from u_0 to the state x, using full state feedback, is

$$H_0(s) = (I + \phi\ B\ G)^{-1}\phi\ B \qquad (2.119)$$

$$H_0(s) = [I+(sI-A)^{-1}B\ G]\ (sI-A)^{-1}\ B \qquad (2.120)$$

Now suppose that an observer will be used with the control law as in figure (2.10)

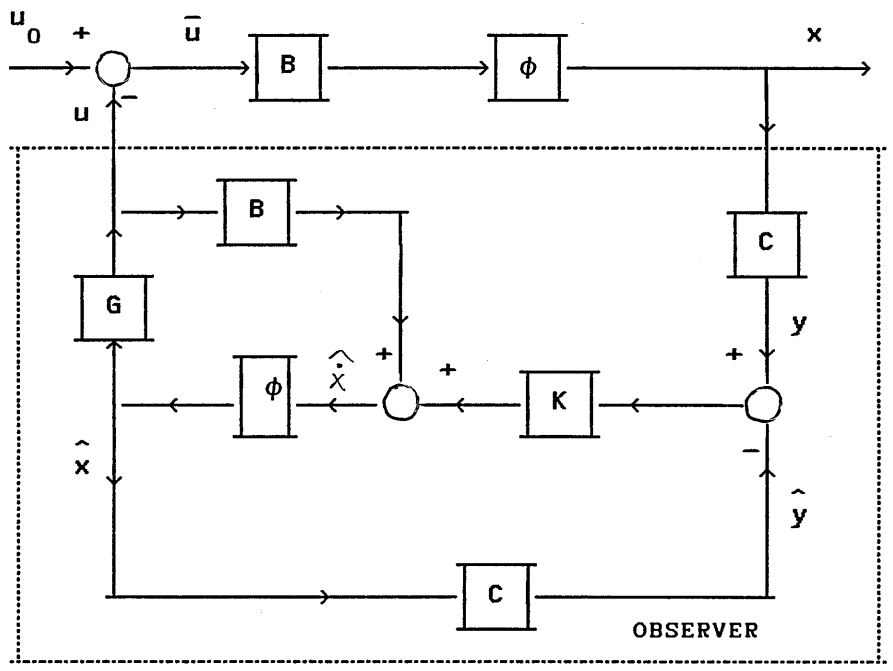

figure 2.10 - schematic of a general control system with control law and observer.

The observer is simply given by,

$$\dot{\hat{x}} = A\ \hat{x} + B\ u + K\ y - KC\ \hat{x} \qquad (2.121)$$

which can be found in Chen[14], described as an asymptotic state estimator, the output of the system is $y = C\ x$ (2.122) and K is the observer gain matrix.

Again, the transfer function from u_0 to x is required, but now the input will be :

$$\bar{u}(s) = u_0 - G\ \hat{x}(s) \qquad (2.123)$$

For an arbitrary gain matrix G, the transfer function from u_0 to x in figure (2.10) will not be the same as that of figure (2.9) unless the transfer function from $\bar{u}$ to $\hat{x}$ in figure (2.10) is the same as that from $\bar{u}$ to x in figure (2.9). The transfer function from $\bar{u}$ to x in figure (2.9) is given by (2.117). From figure (2.10) it is possible to obtain,

$$\hat{x}(s) = (\phi^{-1}+KC)^{-1}[\ B\ u(s) + K\ C\ \phi\ B\ \bar{u}(s)\ ] \qquad (\ 2.124\ )$$

The transfer function from $\bar{u}(s)$ to $\hat{x}(s)$ given by (2.122) is not generally the same as that given by (2.117) as shown by Doyle-Stein[6]. However, they are equal when the Doyle-Stein condition is satisfied

$$K\ (I + C\ \phi\ K)^{-1} = B\ (C\ \phi\ B)^{-1} \qquad (\ 2.125\ )$$

and with the help of the Schur matrix inequality

$$(\phi^{-1}+ KC)^{-1} = \phi - \phi\ K(I+C\ \phi\ K)^{-1}C\ \phi \qquad (\ 2.126\ )$$

it can be shown that (2.124) becomes,

$$\begin{aligned}\hat{x}(s) &= [\phi - \phi\ K(I+C\ \phi\ K)^{-1}C\ \phi]Bu(s) + \\ &\quad [\phi - \phi\ K(I+C\ \phi\ K)^{-1}C\ \phi]K\ C\ \phi\ B\bar{u}(s)\end{aligned} \qquad (\ 2.127\ )$$

Using the Doyle-Stein condition (2.125), the matrix multiplying u(s) becomes zero and the matrix multiplying $\bar{u}(s)$ becomes B.
Then

$$\hat{x}(s) = \phi\ B\ \bar{u}(s)$$

which is the same as (2.117).

What is noted is that the Doyle-Stein condition depends only on the open-loop characteristics of the observer; it is independent of the control gain G. When the Doyle-Stein condition holds, the transfer function from the reference input u_0 to the state x is given by

(2.118), independent of the observer. Therefore the dynamics of the observer do not influence this transfer function.

Another property of a Doyle-Stein observer, i.e. , an observer satisfying the Doyle-Stein condition, is obtained by computing the transfer function from the observable output y to the state estimate $\hat{x}$. Referring to figure (2.10) it is possible to see that:

$$\hat{x} = (\phi^{-1}+KC)^{-1}Ky - (\phi^{-1}+KC)^{-1}BG\,\hat{x} \qquad (2.128)$$

but, by the Doyle-Stein condition,

$$(\phi^{-1}+ KC)^{-1}B = 0 \qquad (2.129)$$

This means that the transfer function from y to the estimated state $\hat{x}$ does not entail feedback of the control signal u. The path from u to z may be omitted. So if K (the observer gain) can be selected to satisfy the Doyle-Stein condition (2.125), the closed-loop system of figure (2.10) can be replaced by that shown in figure (2.11).

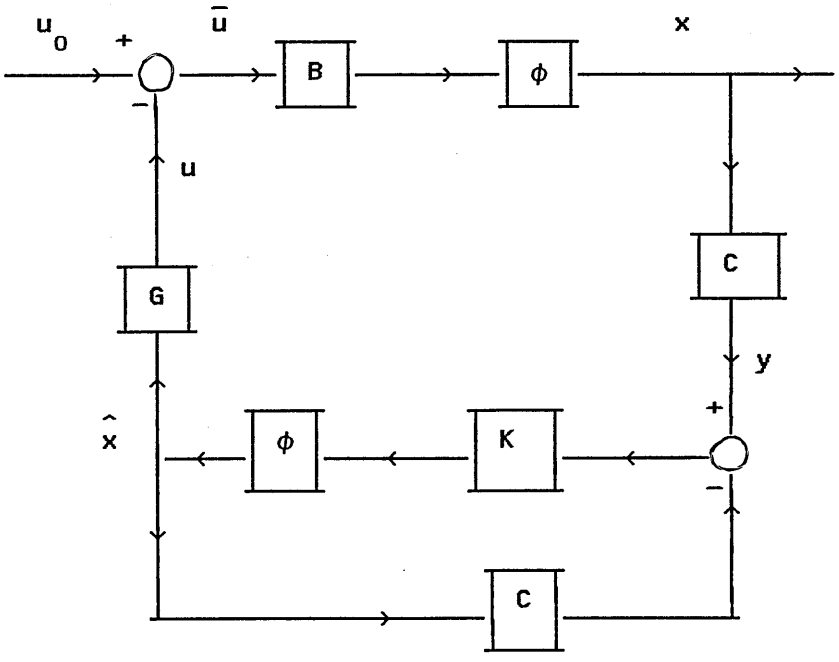

figure 2.11 - schematic of control system with Doyle-Stein observer.

Since there is no feedback from the control u to the observer through the control distribution matrix B, the observer transfer function,

$$H_0(s) = (\phi^{-1} + K C)^{-1} K = (sI - A + KC)^{-1} K \qquad (2.130)$$

is the same as it would be for the unforced system $\dot{x} = A x$, with output equation $y = C x$.

The Doyle-Stein condition has another interesting interpretation, that is, the left hand side of (2.125) can be written as ,

$$K(I+C \phi K)^{1} = K[I+C(sI-A)^{-1}K]^{-1} = (sI-a)(sI-A+KC)^{-1}K \qquad (2.131)$$

and the Doyle-Stein condition can be written as,

$$(sI-A)H_0(s) = B[C(sI-A)^{-1}B]^{-1} \qquad (2.132)$$

thus the transfer function of a Doyle-Stein observer is,

$$H_0(s) = (sI-A)^{-1}B[C(sI-A)B]^{-1} \qquad (2.133)$$

And the closed-loop system of figure (2.11) can be depicted as shown in figure (2.12).

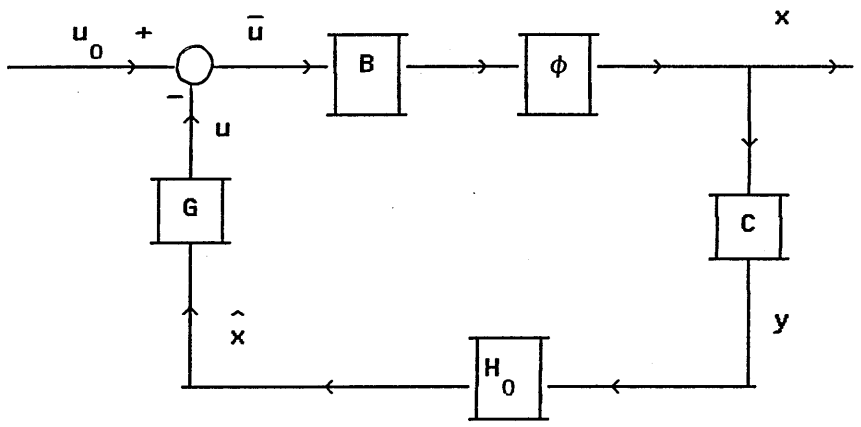

figure 2.12 - Alternate representation of closed-loop system with Doyle-Stein observer.

Referring to figure (2.12) it may be seen that the transfer function from u_0 to x is simply,

$$H_c(s) = \phi\ B\ (I+G\ \phi\ B)^{-1} \qquad (\ 2.134\ )$$

which is the same as the transfer function of the closed loop system when full state feedback is used. From figure (2.9) the following may be obtained,

$$x = \phi\ B\ \bar{u} \qquad (\ 2.135\ )$$

$$\bar{u} = u_0 - G\ \phi\ B\ u \qquad (\ 2.136\ )$$

$$\bar{u} = (I+G\ \phi\ B)^{-1} u_0 \qquad (\ 2.137\ )$$

$$x = \phi\ B(I+G\ \phi\ B)^{-1} u_0 \qquad (\ 2.138\ )$$

The transfer function in the presence of the closed loop process, with a Doyle-Stein observer in place, is the same as it would be for full-state feedback.

In order for a Doyle-Stein observer to exist it is necessary that the open-loop system be square, i.e., that there are exactly as many outputs as inputs. Otherwise the open loop matrix

$$C\ \phi\ B = C(sI-A)^{-1}B$$

would not be a square matrix and its inverse, needed in the calculation of $H_0(s)$ in (2.133) would not be defined. However, the Doyle-Stein condition has been generalized to nonsquare systems by Madiwale and Williams[61].

Note that the transfer function of the Doyle-Stein observer $H_0(s)$ is :

$$H_0(s) = \text{adj}(sI-A)\ B\ \frac{\text{adj}[C\ \text{adj}(sI-A)\ B\ ]}{|\ C\ \text{adj}(sI-A)\ B\ |} \qquad (\ 2.139\ )$$

The denominator of $H_0(s)$ is thus the determinant of the numerator of the transfer matrix of the open loop aircraft, that is, the transmission zeros of the aircraft. Consequently, if the open-loop aircraft has one or more transmission zeros in the right half of the s-plane (that is, nonminimum phase zeros) then a stable Doyle-Stein observer does not exist.
If it is not possible to realize an observer having all the properties of a Doyle-Stein observer, it may be possible to design an observer that has some of its properties. For example,

- Makes the closed-loop transfer function from u_0 to x the same as it is for full state feedback.

- Has its poles at the transmission zeros of the open loop aircraft.

- Does not require feedback of the control signal and thus has a constant transfer function independent of the control gain.

An observer having some, if not all, of these properties might be called a robust observer.

3. CONTROL LAW DESIGN TO SATISFY THE GIBSON DROPBACK CRITERION AND THE MIL-F-8785C FLYING QUALITIES REQUIREMENTS

3.1 INTRODUCTION

In order to design a control law, such that with this control law the aircraft satisfies both MIL-F-8785C[4] (CAP) and the Gibson dropback criterion[1], two methods have been used, pole-placement and an optimal design method. The guidelines to the pole-placement method used are those described above in chapter 2, section 2.4.2, also as described in the notes of Cook[62] and in particular the method developed in Friedland[13].

The method used for the Optimal control law design was also described in chapter 2, sections 2.5.2 and 2.5.3, and also in references such as Friedland[13],Anderson-Moore[17], Lewis[19] and others. The approach developed by Friedland has been followed in this work since his approach is an engineering approach. The subject aircraft used in the design studies was a small perturbation model of the Boeing B-747 since some aerodynamic data was available. The aircraft mathematical model used in the design studies is completely described in Oliva-Cook[12], and data for five flight conditions is given in appendix A. The design was carried out for all 18 flight conditions but only five are presented in this work, that is, one case for each altitude, 1000 ft, 10000 ft, 20000 ft, 30000 ft and 40000 ft, in order to be representative of the flight envelope of the aircraft. The flight conditions analyzed cover the aircraft envelope from sea level to 40000 ft altitude and from Mach 0.30 to Mach 0.90. The aircraft was assumed to be in a cruise configuration at all flight conditions and obviously the control law designs are not valid for other configurations. The data contained in Heffley[11] for the Boeing B-747 is almost all relative to the cruise configuration with few aerodynamic data for landing or take off configurations. The B-747 is considered a class III aircraft according to MIL-F-8785C classification, and for the cruise configuration the flight phase is considered cat.B. So the requirements of MIL-F-8785C for the longitudinal short period mode characteristics are the following :

for level 1 $0.085 \leq CAP \leq 3.6$

for level 2 $0.038 \leq CAP \leq 10.0$

for level 1 $0.30 \leq \zeta_{sp} \leq 2.0$

for level 2 $0.20 \leq \zeta_{sp} \leq 2.0$

for level 3 $\zeta_{sp} \geq 0.15$

For the phugoid mode the requirements are as follows:

for level 1 $\zeta_{ph} \geq 0.040$

for level 2 $\zeta_{ph} \geq 0.0$

for level 3 $T_2 \geq 55$ seconds

where T_2 is the time to double amplitude if the mode is unstable.

Table (3.1) lists the basic aircraft longitudinal characteristics and table (3.2) lists the longitudinal open loop poles of the basic aircraft.

TABLE 3.1 - DYNAMIC CHARACTERISTICS OF THE BASIC AIRCRAFT

FC#	ω_{sp} rad/s	ζ_{sp}	ω_{ph} rad/s	ζ_{ph}	$T_{\theta 2}$ s	CAP s^{-2}	h ft	mach
3	1.619	0.63	0.058	0.083	1.00	0.13	1000	0.60
6	1.338	0.51	0.070	0.040	1.58	0.13	20000	0.70
9	0.992	0.41	0.052	0.062	2.85	0.12	40000	0.80
13	1.070	0.53	0.115	0.050	1.79	0.15	10000	0.40
17	1.100	0.44	0.071	0.051	2.33	0.13	30000	0.70

Obviously the B-747 already satisfies MIL-F-8785C without the addition of a control law, however it does not satisfy the Gibson dropback criterion.

TABLE 3.2 – OPEN LOOP POLES OF THE BASIC AIRCRAFT

FCS	short-period	phugoid	h (ft)	Mach
3	-1.02 ± i 1.25	-0.0049 ± i 0.0580	1000	0.60
6	-0.68 ± i 1.15	-0.0028 ± i 0.0700	20000	0.70
9	-0.40 ± i 0.90	-0.0032 ± i 0.0516	40000	0.80
13	-0.56 ± i 0.91	-0.0061 ± i 0.1158	10000	0.40
17	-0.49 ± i 0.98	-0.0036 ± i 0.0709	30000	0.70

3.2 CONTROL LAW STRUCTURE

The design is carried out for a rate command-attitude hold control law including a proportional plus integral controller acting on pitch rate and angle of attack, both fed back to elevator. Modern aircraft with this structure of controller have shown good handling qualities. The proportional feedback enables the rate command characteristics to be designed as required and the integral feedback drives the error signal to zero, and so good longer term "holding" characteristics are obtained. As the integral of pitch-rate is pitch-attitude the attitude hold characteristic is implicit in this kind of controller.

The design begins with the short period reduced order model of the aircraft,

$$\dot{x}_{RO} = A_{RO}\, x_{RO} + B_{RO}\, \eta \qquad (3.1)$$

where $x_{RO}^T = [\, w \;\; q \,]$ and η is the elevator displacement.

A_{RO} is the state matrix of the short period reduced order model.
B_{RO} is the control matrix of the short period reduced order model.
A_{RO} and B_{RO} are also given in appendix A.

It is necessary to include an extra state in order to allow for the pitch rate error defined by:

$$\dot{\varepsilon}_q = q - q_{dp} \tag{3.2}$$

and

$$\varepsilon_q = \int (q - q_{dp})dt \tag{3.3}$$

where ε_q is the integral of the error.
So, with the addition of this extra state the state equation (3.1) is now given by:

$$\begin{bmatrix} \dot{x}_{RO} \\ \dot{\varepsilon}_q \end{bmatrix} = \left[\begin{array}{cc:c} & & 0 \\ & A_{RO} & 0 \\ \hdashline 0 & 1 & 0 \end{array}\right] \begin{bmatrix} x_{RO} \\ \varepsilon_q \end{bmatrix} + \begin{bmatrix} B_{RO} \\ \hdashline 0 \end{bmatrix} \eta + \begin{bmatrix} 0 \\ 0 \\ \hdashline -1 \end{bmatrix} q_{dp} \tag{3.4}$$

Or, (3.4) can be written as :

$$\dot{x} = A\,x + B\,\eta + E\,q_{dp} \tag{3.5}$$

where now : $x^T = [\, w \quad q \quad \varepsilon_q \,]$ (3.6)

$$A = \left[\begin{array}{cc:c} & & 0 \\ & A_{RO} & 0 \\ \hdashline 0 & 1 & 0 \end{array}\right] \tag{3.7}$$

$$B = \begin{bmatrix} B_{RO} \\ \hdashline 0 \end{bmatrix} \tag{3.8}$$

$$E = \begin{bmatrix} 0 \\ 0 \\ \hdashline -1 \end{bmatrix} \tag{3.9}$$

Now the control law will be of the form:

$$\eta = -G\,x + G_0\,q_{dp} \tag{3.10}$$

which is exactly the form developed in chapter 2, for both design methods, pole-placement and optimal control. Obviously G is the feedback gain vector and G_0 is the feedforward gain. The aircraft with this control law is shown on figure (3.1), and the feedback gain vector will be of the form:

$$G = [\, K_w \quad K_q \quad K_{\varepsilon_q} \,] \tag{3.11}$$

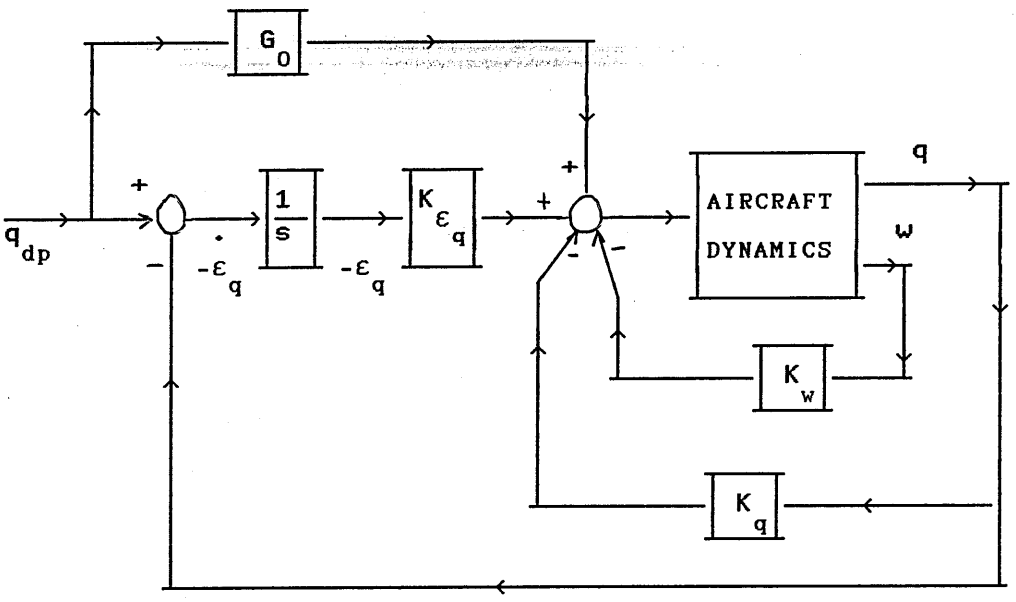

figure 3.1 - control law structure adopted in the design.

Substituting (3.10) into (3.5) the closed loop equation of the system is obtained as :

$$\dot{x} = (A - BG)\,x + (BG_0 + E)\,q_{dp} \qquad (3.12)$$

where q_{dp} is the pilot input to be tracked, or in other words, as in chapter 2, it is the exogenous variable.

3.3 THE POLE-PLACEMENT METHOD

The first design is carried out by pole-placement as described in chapter 2. The problem is to find the feedback gains and the feedforward gain such that the augmented aircraft satisfies:

- MIL-F-8785C, or more specifically CAP requirements.
  (It is known that the aircraft already satisfies the CAP)
- Gibson dropback criterion.

- The augmented aircraft should behave in a second order like way, that is, the additional dynamics introduced by the controller should not be visible to the pilot in the aircraft response to controls.
- The integral term in the control law should have a time constant comparable with the short period natural frequency.

As already known from equation (3.10), G will completely specify the closed loop poles and hence the stability of the closed loop system. It is necessary to choose three poles, as the characteristic equation of the closed loop system is of third order. So with equation (2.9) for CAP and equation (3.14) for dropback, which is derived in appendix B, it is possible to build a system with two equations for two unknowns, that is ω_{sp} and ζ_{sp}.
So the equations:

$$CAP = \frac{g\, T_{\theta 2}\, \omega_{sp}^2}{V_e} \qquad (3.13)$$

and

$$DB = \frac{T_{\theta 2}\omega_{sp} - 2\,\zeta_{sp}}{\omega_{sp}} \qquad (3.14)$$

are the basis for the short period mode pole allocation.
In equation (3.14) by choosing DB = 0 an equation relating ω_{sp} and ζ_{sp} is obtained. Now with equation (3.13) it is possible to assess if the choice of ω_{sp} satisfies the CAP requirement. If so, with the choosen value of ω_{sp} it is possible to obtain ζ_{sp} from equation (3.14). In this way two closed loop poles are specified which satisfy the CAP requirement and the dropback criterion. This procedure to find ω_{sp} and ζ_{sp} is, in fact, a simple iterative procedure. Now, it is necessary to choose the third pole of the characteristic equation of the closed loop system. To choose this third pole it is necessary to take into account that in order to maintain second order like dynamics of the augmented aircraft it is important not to introduce significant changes to the overall gain and phase at frequencies close to the short period natural frequency. As seen from table (3.1) the short period natural frequency is around 1 rad/sec (except for flight conditions 3 and 6), and so this third pole is chosen as s = −1. A better design can be achieved if the pole is chosen based on the short

period natural frequency at each flight condition. However, for simplicity, it is reasonable to consider this third pole constant over the flight envelope. So, in this way, the three closed loop poles have been selected and the closed loop equation to be satisfied is simply:

$$(s^2 + 2\zeta_{sp}\omega_{sp} s + \omega_{sp}^2) (s + 1) = 0 \qquad (3.15)$$

and with the aid of MATLAB the feedback gain vector can easily be obtained.

The feedforward gain G_0 is simply obtained from (2.53), or :

$$G_0 = [C(A-BG)^{-1}B]^{-1}C\ (A-BG)^{-1}E \qquad (3.16)$$

where C is given by : $C = [\ 0\ 1\ 0\ ]$

since $y = C\ x$ and so $y = q$.

A, B, E and G are already defined in (3.7), (3.8), (3.9) and (3.11) respectively.

In table (3.2-A) the control law gains obtained with this design are sumarized and in table (3.3) the corresponding short period characteristics are listed.

TABLE 3.2-A - CONTROL LAW GAINS

FC#	K_w $ft^{-1}sec$	K_q sec	K_{ε_q} rad	G_0 sec	h ft	Mach
3	0.0012	-0.588	-1.219	-1.219	1000	0.60
6	0.0012	-0.889	-1.183	-1.183	20000	0.70
9	0.0011	-1.875	-1.697	-1.697	40000	0.80
13	0.0026	-1.094	-1.270	-1.270	10000	0.40
17	0.0013	-1.249	-1.252	-1.252	30000	0.70

TABLE 3.3 – SHORT PERIOD CHARACTERISTICS OF THE CLOSED LOOP SYSTEM

FC#	POLES		ω_{sp} rad/s	ζ_{sp}	CAP s^{-2}	h ft	Mach
3	−1.08 ± i 1.11	−1	1.55	0.70	0.117	1000	0.60
6	−1.02 ± i 0.63	−1	1.20	0.85	0.101	20000	0.70
9	−1.61 ± i 0.45	−1	0.85	1.21	0.086	40000	0.80
13	−0.58 ± i 0.59	−1	0.83	0.70	0.092	10000	0.40
17	−0.86 ± i 0.25	−1	0.90	0.96	0.087	30000	0.70

From the results it was noticed that in order to satisfy the dropback criterion the CAP at high altitudes (30000 ft and 40000 ft) becomes marginal. This can be explained since in order to satisfy the dropback criterion (3.14) it is necessary to decrease the short period natural frequency. In fact this is not a good design philosopy, since reducing the short period natural frequency also reduces the aircraft bandwidth.

In figure (3.2) plots of the augmented aircraft are shown with respect to the dropback criterion boundaries.

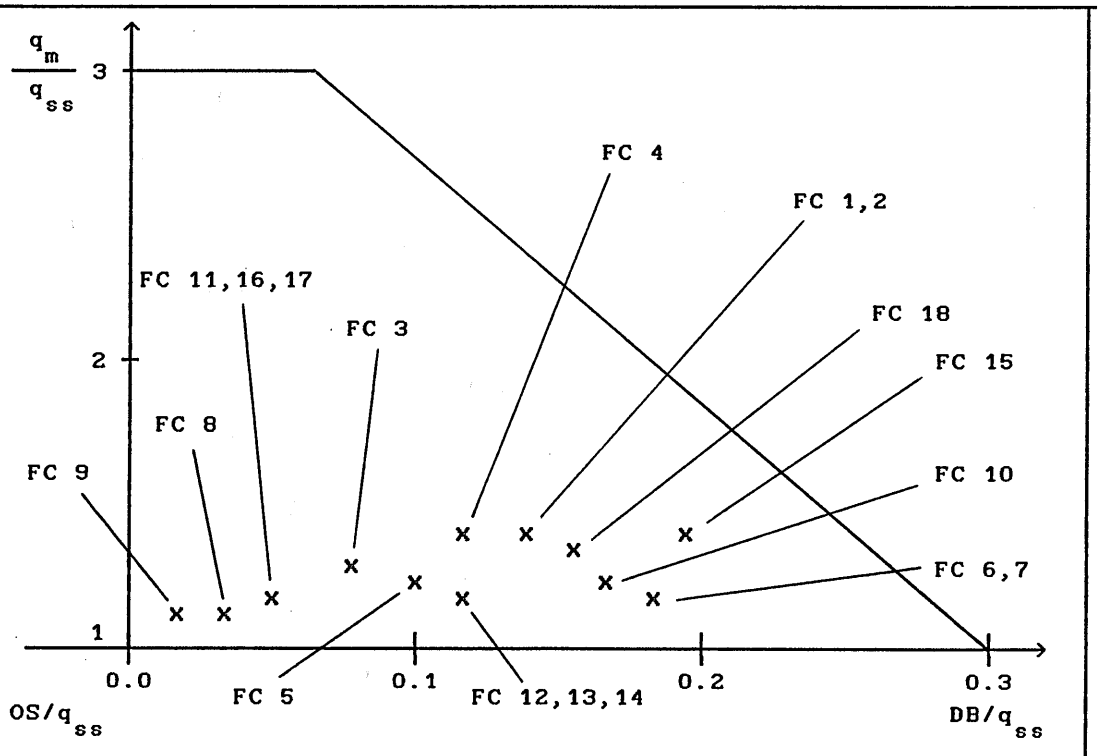

figure 3.2 - Dropback criterion plot of the pole-placement design.

3.4 THE OPTIMAL CONTROL LAW METHOD

An alternative design is now performed using optimal control methods as described in chapter 2. The control law structure is the same as before, but the approach is now completely different. It must be mentioned that a first approach following Athans[63],and then Parker[64] failed to give designs that satisfied the Gibson dropback criterion since both approaches only gave the feedback gains. Obviously, both designs gave zero steady state error at all flight conditions. A better design approach subsequently adopted for this work, is the approach sugested by Friedland[13] which is also described in chapter 2. It is necessary to emphasize again here, that it is not a necessary prerequisite to choose the closed loop poles. The approach now is to work with the performance index:

$$V = \int_{t}^{\infty} (x^{T}Q\, x + \eta^{T} R\, \eta)\, d\tau \qquad (3.17)$$

as described in chapter 2 (alternative performance indices can be found in Lewis-Stevens[18]). The state vector is given by (3.6) and η is the elevator displacement. The matrix Q is the state weighting matrix and the matrix R is the control weighting matrix. In the choice of these two matrices, note that in this case R is a scalar, the guidelines given by Friedland[13] and Brogan[60] are followed; also already described in chapter two. In this problem it is possible to achieve good values for Q and R by means of a parametric study as sugested by Friedland[13]. Obviously Q is a (3x3) matrix and since the design is mainly concerned with the maintenance of zero steady state error only the state " ε_q " will be weighted in the performance index.

In view of this a suitable choice for the state weighting matrix is,

$$Q = \begin{bmatrix} 0 & 0 & 0 \\ 0 & 0 & 0 \\ 0 & 0 & 1 \end{bmatrix} \qquad (3.18)$$

The states w and q are not weighted because it is not as important that they go to zero as it is for ε_q . So with this choice of Q a

parametric study can be performed varying the parameter R, as also advised by Powell-Franklin-Naeimi[7] . For each pair (Q,R) the closed loop poles, feedback gains, CAP, ω_{sp} and ζ_{sp} can be obtained and evaluated against the specification requirements. This is the first step of the design method, and is easily performed with MATLAB Having defined A, B, Q, and R MATLAB gives G and the algebraic Riccati matrix $\bar{M}_1$ (as mentioned in chapter 2) that is required in the calculation of G_0.

It is obvious that G_0 is obtained from equation (2.80) where $\bar{M}_1$ is the algebraic Riccati matrix obtained when the above regulator problem is solved. It is clear that this is an iterative procedure that can be sumarized as follows;

(i) Solve the regulator problem with A, B, Q and R, this will give the feedback gain vector G, and the algebraic Riccati matrix $\bar{M}_1$.

(ii) Look at the closed loop poles obtained. It is not desirable that the closed loop poles be located too far from the open loop poles. Look also at the feedback gain obtained, it is not desirable to obtain high gains say, for example maximum magnitudes of 4. Finally check that CAP is satisfied using equation (3.13).

(iii) Obtain G_0, with the help of equation (2.80)

(iv) With G and G_0 obtained verify that the augmented aircraft satisfies the dropback criterion. Check that the gains are not too high and that CAP is satisfied, if not go back to step (i) and change the parameter R.

This is basically the approach given by Friedland[13], which is an engineering approach. It is also given by Brogan[60] and Powell-Franklin-Naeimi[7] . Experience has shown that this design procedure is very easily performed and compares favourably with the pole placement design procedure. In fact one can obtain the control law gains very quickly with the optimal control method compared with pole-placement design method. In addition, it is clear that no attempt is made to choose the poles of the closed loop equation since, first, it is not necessary in the design procedure, and second, the choice of

one parameter (R) is more easily made than the choice of three poles in the s-plane. It must also be mentioned here that the pole placement method obtains the feedforward gain for perfect zero steady state error, since its calculation is based on pole-zero cancellation. The optimal control method obtains a feedforward gain that does not give a perfect steady state zero error, but for engineering considerations close enough. In fact as the control weight R goes to zero the steady state error also goes to zero.

In table (3.4) the control law gains obtained by optimal control are listed together with the selected control weight R, and this table can be compared with table (3.2) which refers to the pole-placement method. In table (3.5) the short period characteristics obtained with the optimal method are summarized, and can be compared with those of table (3.3) obtained by pole placement.

TABLE 3.4 - CONTROL LAW GAINS

FC#	K_w $ft^{-1}sec$	K_q sec	K_{ε_q} rad	G_0 sec	R	h ft	Mach
3	0.0002	-0.1348	-0.3162	-1.290	10	1000	0.60
6	0.0003	-0.2157	-0.4470	-1.280	5	20000	0.70
9	0.0005	-0.5433	-0.8160	-1.720	1.5	40000	0.80
13	0.0006	-0.2800	-0.4470	-1.910	5	10000	0.40
17	0.0004	-0.2570	-0.4470	-1.540	5	30000	0.70

TABLE 3.5 - SHORT PERIOD CHARACTERISTICS OF THE CLOSED LOOP SYSTEM

FC#	POLES		ω_{sp} rad/s	ζ_{sp}	CAP s^{-2}	h ft	Mach
3	-1.03 ± i 1.27	-0.23	1.64	0.63	0.130	1000	0.60
6	-0.75 ± i 1.20	-0.27	1.42	0.53	0.140	20000	0.70
9	-0.61 ± i 1.03	-0.24	1.19	0.51	0.170	40000	0.80
13	-0.60 ± i 0.93	-0.19	1.11	0.54	0.170	10000	0.40
17	-0.56 ± i 1.03	-0.21	1.18	0.48	0.150	30000	0.70

In figure (3.3) a plot of the augmented aircraft with the optimal control law design with respect to the dropback criterion is shown.

A preliminary comparison of both designs shows that:

- The optimal control law design satisfies the CAP requirement better than the pole-placement design. This can be seen since the poles have moved less with respect to the open loop aircraft in the optimal design than in the pole-placement design.
- In both designs the most difficult flight condition corresponds with 40000 ft, a fact indicating that the design must be carried out for several flight conditions in order to obtain an idea of how it works Thus the analysis of a few flight cases only can sometimes leads to wrong conclusions.
- The optimal design always gives an augmented aircraft with an oscillatory short period mode. This is good since the second order like characteristics are maintained.
- The feedforward gain of the optimal design is always greater than that of the pole-placement design, a fact that leads to a lower frequency integrator pole, but also to a higher control effort with respect to the reference input.
- This preliminary design results in lower feedback gains in the optimal control law design, a fact that gives lower control effort with respect to the regulator characteristics.

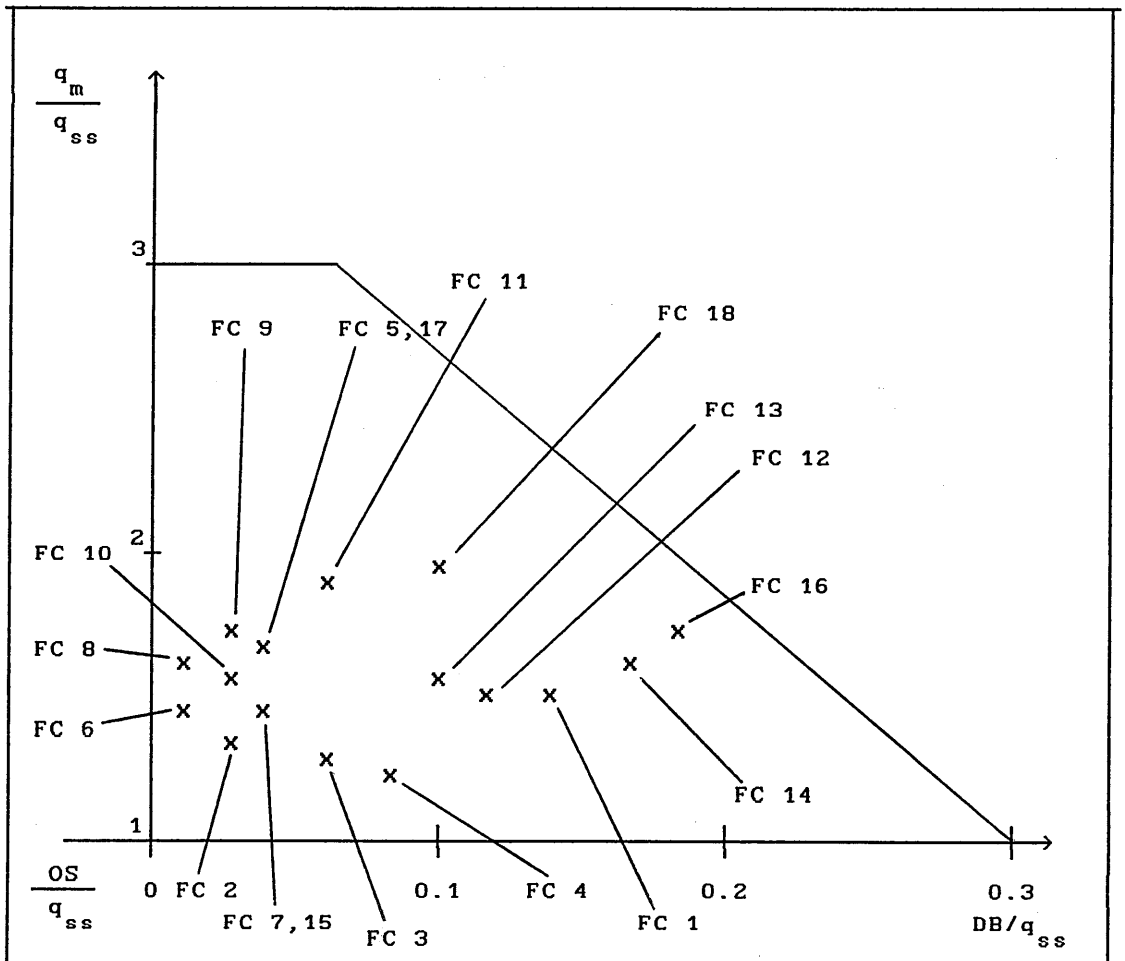

figure 3.3 - Dropback criterion plot of the optimal control design

The results of both design exercises show that the optimal control law design obtains an augmented aircraft that better satisfies not only the dropback criterion but also the CAP (MIL-F-8785C) requirement. To attempt to choose the closed loop pole locations was not as successful as the attempt to choose the control weight R. In the pole placement method the procedure for allocating the short period closed loop poles has lead to the reduction of ω_{sp} in order to satisfy the dropback criterion, which is not good practice, as mentioned. To summarize, it is possible to conclude that the optimal control method offers a better design procedure for meeting both the closed loop pole location requirements as well as handling qualities criteria requirements.

3.5 THE INFLUENCE OF AN ACTUATOR ON CONTROL LAW PERFORMANCE

3.5.1 INTRODUCTION

It is instructive to assess the performance of both control law designs when an actuator is included in the system. First, the study was performed with the reduced short period model of the aircraft. Two actuator models have been used, both described by a second order mathematical model. Obviously, a more searching study could assess actuators with alternative characteristics such as a third order model or a non-linear model. The mathematical models of the actuators are described by the following state equations.

Actuator no.1 is given by :

$$\begin{bmatrix} \dot{\eta} \\ \dot{v}_\eta \end{bmatrix} = \begin{bmatrix} 0 & 0 \\ -450 & -30 \end{bmatrix} \begin{bmatrix} \eta \\ v_\eta \end{bmatrix} + \begin{bmatrix} 0 \\ 450 \end{bmatrix} \eta_c \qquad (3.19)$$

Actuator no.2 is given by :

$$\begin{bmatrix} \dot{\eta} \\ \dot{v}_\eta \end{bmatrix} = \begin{bmatrix} 0 & 0 \\ -100 & -14 \end{bmatrix} \begin{bmatrix} \eta \\ v_\eta \end{bmatrix} + \begin{bmatrix} 0 \\ 100 \end{bmatrix} \eta_c \qquad (3.20)$$

The model is simply: $\dot{x}_A = A_A x_A + B_A \eta_c$ (3.21)

with : $x_A^T = [\ \eta\ v_\eta\ ]$ (3.22)

where η_c is the input to the actuator and v_η is the control rate effort.

Actuator no.1 has a natural frequency of 21.2 rad/sec and a damping ratio of 0.70. Actuator no.2 has a natural frequency of 10 rad/sec and a damping ratio of 0.70. Figure (3.4) shows the aircraft with control law and actuator. The reason for the choice of actuators with these characteristics was due to the fact that the short period

natural frequency is around 1 rad/sec and so it allows to explore their influence on the system performance with respect to stability and flying qualities.

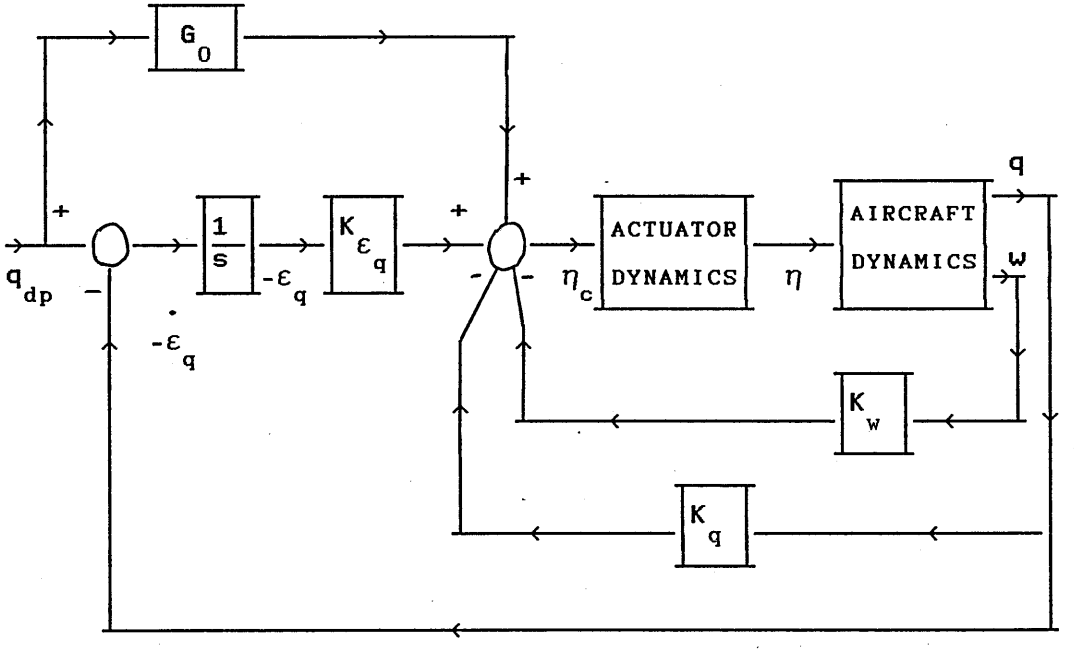

figure 3.4 - control law structure with actuator in the loop.

As before the control law is given by:

$$\eta_c = -G\,x + G_0 q_{dp} \qquad (3.23)$$

where $G = [\,K_w \quad K_q \quad K_{\varepsilon_q}\,]$ and G_0 is simply a single gain.

The aircraft may be described by the state equation,

$$\dot{x} = A\,x + [\,B \;\; Z31\,]\,x_A + E\,q_{dp} \qquad (3.24)$$

where A is given by (3.7) and is a (3x3) matrix, B is given by (3.8) and is a (3x1) vector and E is given by (3.9) and is also a (3x1) vector.

$$Z31^T = [\,0\;0\;0\,] \qquad (3.25)$$

and x is given by (3.6), or $x^T = [\, w \; q \; \varepsilon_q \,]$.

Substituting (3.23) into (3.21) and considering equation (3.24) the closed loop model is given by :

$$\begin{bmatrix} \dot{x} \\ \dot{x}_A \end{bmatrix} = \begin{bmatrix} A & [B \; Z31] \\ -B_A G & A_A \end{bmatrix} \begin{bmatrix} x \\ x_A \end{bmatrix} + \begin{bmatrix} E \\ B_A G_0 \end{bmatrix} q_{dp} \qquad (3.26)$$

With this model it is possible to obtain the trasnfer function of q in response to q_{dp} . The effect of the actuator on the closed loop performance of the aircraft with both control law designs is assessed with particular reference to pitch rate response.

3.5.2 THE RESULTS OF ASSESSMENT

An evaluation was performed with both control laws and both actuators and a summary of the results is listed in tables (3.6), (3.7), (3.8) and (3.9). A review of the assessment leads to the following conclusions.

(i) The inclusion of an actuator in the loop, in general gives an increase in the pitch-rate overshoot of the response in both designs. However, this effect with the pole placement control law design is less than with the optimal design. (tables (3.6) and (3.7)).

(ii) With both actuators the same value for the dropback parameter is obtained.

(iii) The pole-placement control law design has little advantage over the optimal control law design with respect to actuator effects when measured in terms of the dropback criterion. The reasons are clearly seen on tables (3.6) and (3.7).

(iv) The inclusion of the actuator in the loop with the pole placement control law design prevented the aircraft meeting the CAP requirement at pratically all flight conditions. On the other hand, the aircraft with optimal control law design and actuator satisfies CAP level 1 for all flight conditions. This

can be seen in tables (3.8) and (3.9). The short period natural frequency with the pole placement control law design is decreased with respect to the basic aircraft without actuator, the dropback performance is improved but CAP deteriorates.

(v) The speed of aircraft response (t_m) is about the same as seen from tables (3.6) and (3.7).

TABLE 3.6 – INFLUENCE OF THE ACTUATOR WITH RESPECT TO DROPBACK CRITERION IN THE POLE-PLACEMENT DESIGN

FC #	$\frac{q_m}{q_{ss}}$			$\frac{DB}{q_{ss}}$ (sec)			t_m (sec)		
	no act	act 1	act 2	no act	act 1	act 2	no act	act 1	act 2
3	1.251	1.302	1.344	0.09	0.13	0.13	1.4	1.4	1.4
6	1.220	1.250	1.268	0.15	0.20	0.20	1.6	1.6	1.6
9	1.110	1.090	1.090	0.02	-0.05	-0.06	2.1	2.1	2.1
13	1.238	1.250	1.270	0.11	0.12	0.12	2.6	2.6	2.6
17	1.162	1.170	1.180	0.07	0.10	0.11	2.1	2.2	2.1

TABLE 3.7 – INFLUENCE OF THE ACTUATOR WITH RESPECT TO DROPBACK CRITERION IN THE OPTIMAL CONTROL DESIGN

FC #	$\frac{q_m}{q_{ss}}$			$\frac{DB}{q_{ss}}$ (sec)			t_m (sec)		
	no act	act 1	act 2	no act	act 1	act 2	no act	act 1	act 2
3	1.320	1.320	1.340	0.05	-0.06	-0.06	1.2	1.3	1.3
6	1.470	1.470	1.510	0.01	-0.06	-0.07	1.3	1.3	1.4
9	1.490	1.520	1.560	0.02	0.03	0.02	1.5	1.5	1.6
13	1.440	1.450	1.470	0.09	0.10	0.09	1.7	1.8	1.8
17	1.590	1.620	1.650	0.03	0.15	0.14	1.5	1.6	1.6

TABLE 3.8 - INFLUENCE OF THE ACTUATOR WITH RESPECT TO SHORT PERIOD CHARACTERISTICS ON POLE PLACEMENT CONTROL LAW DESIGN

FC #	ω_{sp} (rad/sec)		ζ_{sp}		CAP s^{-2}		h ft	Mach
	no act	act 2	no act	act 2	no act	act 2		
3	1.55	1.46	0.70	0.72	0.117	0.103	1000	0.60
6	1.20	0.94	0.85	0.83	0.101	0.062	20000	0.70
9	0.85	0.60	1.21	1.03	0.086	0.043	40000	0.80
13	0.838	0.78	0.70	0.70	0.092	0.082	10000	0.40
17	0.90	0.71	0.96	0.88	0.087	0.054	30000	0.70

TABLE 3.9 - INFLUENCE OF THE ACTUATOR WITH RESPECT TO SHORT PERIOD CHARACTERISTICS ON OPTIMAL CONTROL LAW DESIGN

FC #	ω_{sp} rad/sec		ζ_{sp}		CAP s^{-2}		h ft	Mach
	no act	act 2	no act	act 2	no act	act 2		
3	1.64	1.67	0.63	0.62	0.13	0.134	1000	0.60
6	1.42	1.46	0.53	0.51	0.14	0.149	20000	0.70
9	1.19	1.25	0.51	0.50	0.17	0.185	40000	0.80
13	1.11	1.11	0.54	0.54	0.17	0.165	10000	0.40
17	1.18	1.19	0.48	0.48	0.15	0.153	30000	0.70

In summary it is possible to conclude that the optimal control law design is more robust with respect to stability requirements (CAP) when an actuator is included in the loop. As can be seen from table (3.9) CAP is maintained for all flight conditions whereas, whith the pole placement design CAP is not maintained as seen in table (3.8). With respect to the dropback criterion both designs have about the

same behaviour as seen in tables (3.6) and (3.7). Therefore, in order that an actuator may be included in the model it is necessary to redesign the optimal control law for flight conditions 3 and 6 in order to meet the dropback criterion and to redesign the pole placement control law for all flight conditions in order to meet CAP.

3.6 ASSESSMENT OF THE CONTROL LAWS WITH THE FULL AIRCRAFT MODEL

3.6.1 INTRODUCTION

Now, it is also necessary to investigate the performance of both control law designs when the phugoid is introduced into the model. The state vector is now given by :

$$x^T = [\, u \; w \; q \; \theta \; \varepsilon_q \,] \tag{3.27}$$

The control law structure is given by figure (3.5).

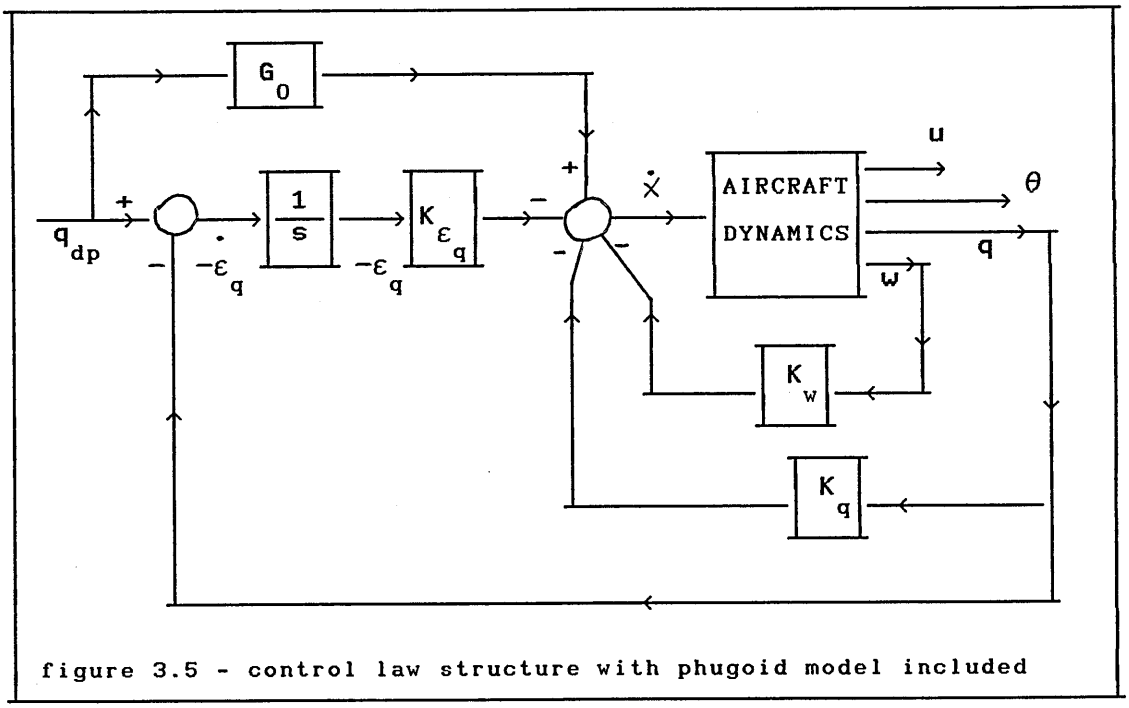

figure 3.5 - control law structure with phugoid model included

The mathematical model is simply:

$$\dot{x} = A\,x + B\,\eta + E\,q_{dp} \tag{3.28}$$

and the aircraft longitudinal model is given in appendix A as :

$$\dot{x}_{LM} = A_{LM}\,x_{LM} + B_{LM}\eta \tag{3.29}$$

$$\text{with ;} \qquad x_{LM}^{T} = [\,u\ w\ q\ \theta\,] \tag{3.30}$$

A_{LM} is the full longitudinal state matrix given in appendix A, and
B_{LM} is the longitudinal control matrix given in appendix A.
Thus,

$$A = \left[\begin{array}{c:c} A_{LM} & \begin{matrix}0\\0\\0\\0\end{matrix} \\ \hdashline [0\ 0\ 1\ 0] & [0] \end{array}\right] \tag{3.31}$$

and

$$B = \left[\begin{array}{c} B_{LM} \\ \hdashline 0 \end{array}\right] \tag{3.32}$$

$$E^{T} = [\,0\ 0\ 0\ 0\ -1\,] \tag{3.33}$$

$$x^{T} = [\,u\ w\ q\ \theta\ \varepsilon_{q}\,] = [\,x_{LM} \,\vdots\, \varepsilon_{q}\,] \tag{3.33.a}$$

again the control law is, $\eta = -\,G\,x + G_{0}\,q_{dp}$ (3.34)

but now the gain vector is given by ;

$$G = [\,0\ K_{w}\ K_{q}\ 0\ K_{\varepsilon_{q}}\,] \tag{3.35}$$

and G_{0} is the same as before.
The closed loop equation is of the same form as equation (3.12), that is ,

$$\dot{x} = (A-BG)x + (BG_{0} + E)q_{dp} \tag{3.36}$$

Based on the solution of equation (3.36) an analysis was performed as for the introduction of the actuator and the findings are as follows :

(i) The inclusion of the phugoid model caused the aircraft with optimal control law design to fail to meet the dropback criterion at any flight condition. The aircraft with pole

placement control law design still satisfies the dropback criterion for some flight conditions.

(ii) Again the aircraft with optimal control law design still satisfies CAP level 1 at all flight conditions but the aircraft with pole placement control law design does not satisfy CAP level 1 at 30000 ft and 40000 ft.

(iii) At 30000 ft , mach 0.50, the aircraft with pole placement control law design has a phugoid that even fails to meet level 3 of MIL-F-8785C requirements.

(iv) The aircraft with optimal control law design has a stable phugoid satisfying level 1 of MIL-F-8785C at all flight conditions.

(v) The optimal control law design fails completely to maintain the relation $(q/q_{dp}) \simeq 1$, at almost all flight conditions. In contrast, the aircraft with pole placement control law design maintains the relation in the range $(0.90 \leq q/q_{dp} \leq 1.10)$ at all flight conditions.

3.6.2 SUMMARY OF AIRCRAFT CHARACTERISTICS WITH BOTH CONTROL LAW DESIGNS

In tables (3.12) and (3.13) the short period characteristics obtained with both control law designs are summarized for comparison. In table (3.14) the steady state pitch rate gain is listed for both control law designs.

In figures (3.6), (3.7) and (3.8) step response time histories for both designs with the full aircraft model are given for comparison. In figures (3.9) and (3.10) a comparative short term step response time histories for both control law designs are shown with the reduced order aircraft model and with the full order aircraft model.

TABLE 3.12 – SHORT PERIOD CHARACTERISTICS OBTAINED WITH THE POLE PLACEMENT CONTROL LAW DESIGN

FC #	REDUCED ORDER MODEL			FULL ORDER MODEL			h	Mach
	ω_{sp} rad/s	ζ_{sp}	CAP s^{-2}	ω_{sp} rad/s	ζ_{sp}	CAP s^{-2}	ft	
3	1.55	0.70	0.117	1.52	0.69	0.113	1000	0.60
6	1.20	0.85	0.101	1.12	0.85	0.089	20000	0.70
9	0.85	1.21	0.086	1.29	1.02	0.205	40000	0.80
13	0.83	0.70	0.092	0.83	0.71	0.097	10000	0.40
17	0.90	0.96	0.087	0.81	0.93	0.068	30000	0.70

TABLE 3.13 – SHORT PERIOD CHARACTERISTICS OBTAINED WITH THE OPTIMAL CONTROL LAW DESIGN

FC #	REDUCED ORDER MODEL			FULL ORDER MODEL			h	Mach
	ω_{sp} rad/s	ζ_{sp}	CAP s^{-2}	ω_{sp} rad/s	ζ_{sp}	CAP s^{-2}	ft	
3	1.64	0.63	0.130	1.664	0.62	0.135	1000	0.60
6	1.42	0.53	0.140	1.445	0.52	0.149	20000	0.70
9	1.19	0.51	0.170	1.199	0.51	0.177	40000	0.80
13	1.11	0.54	0.170	1.116	0.54	0.175	10000	0.40
17	1.18	0.48	0.150	1.176	0.48	0.144	30000	0.70

TABLE 3.14 – STEADY STATE RESPONSE OBTAINED WITH BOTH CONTROL LAW DESIGNS AND THE COMPLETE MODEL

$$\left[q / q_{dp} \right]_{ss}$$

FC #	POLE PLACEMENT DESIGN	OPTIMAL CONTROL DESIGN	h ft	Mach
3	1.06	0.61	1000	0.60
6	1.02	0.58	20000	0.70
9	1.10	0.87	40000	0.80
13	0.81	0.35	10000	0.40
17	1.05	0.52	30000	0.70

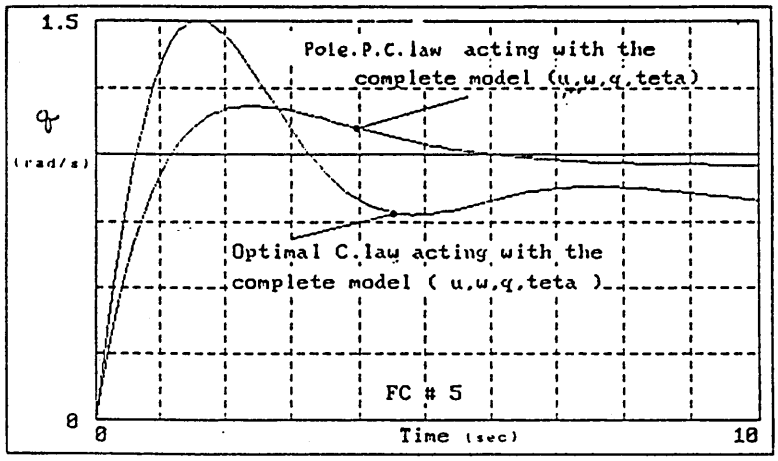

figure 3.6 - pitch-rate time response of both designs with the complete model of the aircraft at 20000 ft, mach 0.50

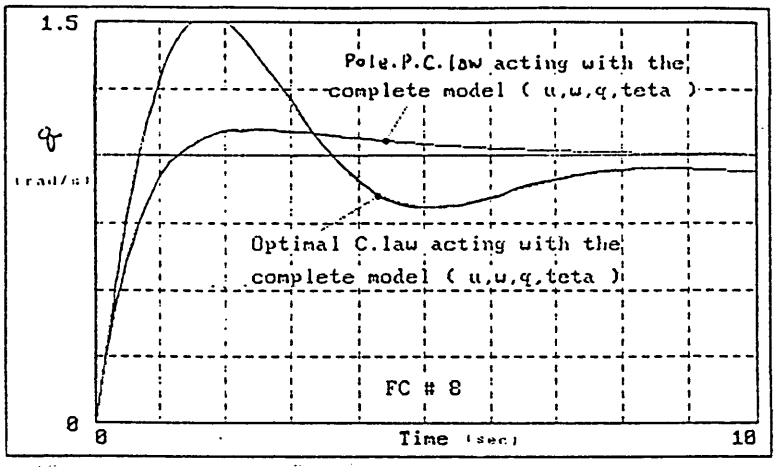

figure 3.7 - pitch-rate time response of both designs with the complete model of the aircraft at 40000 ft, mach 0.70

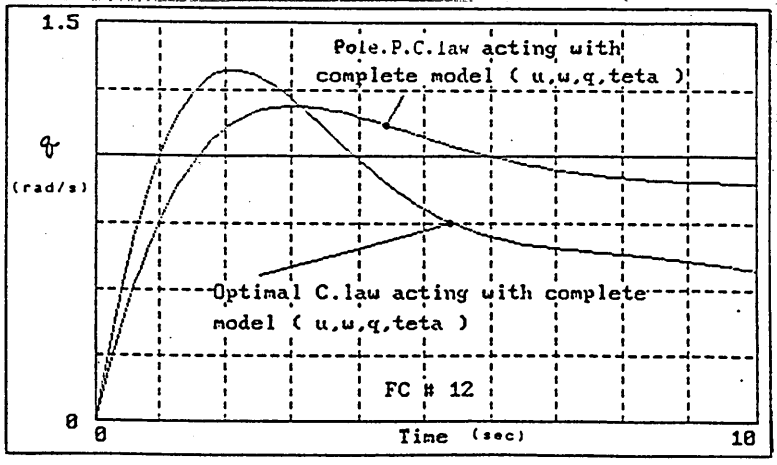

figure 3.8 - pitch-rate time response of both designs with the complete model of the aircraft at 10000 ft, mach 0.30

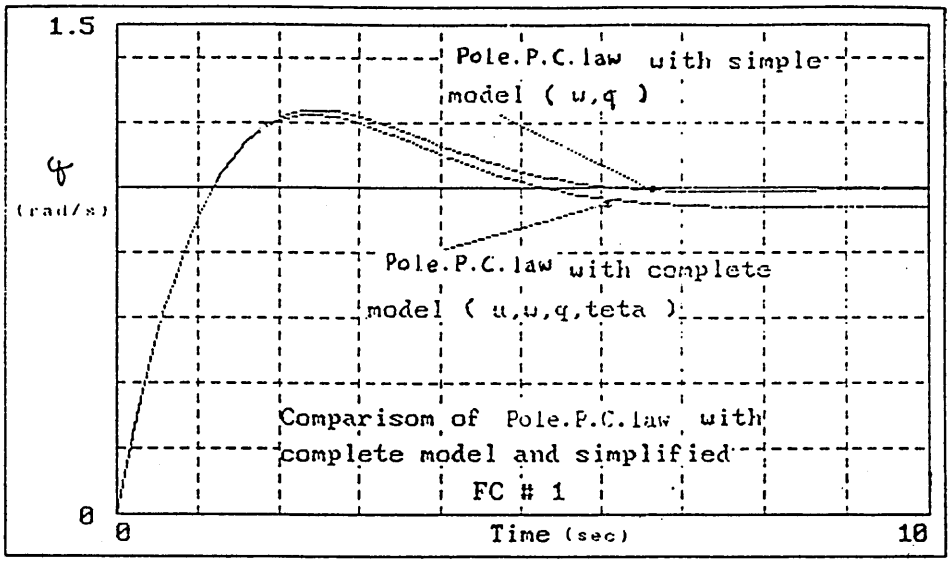

figure 3.9 - effect of the phugoid mode on the aircraft response with pole-placement control law design at 1000 ft mach 0.30

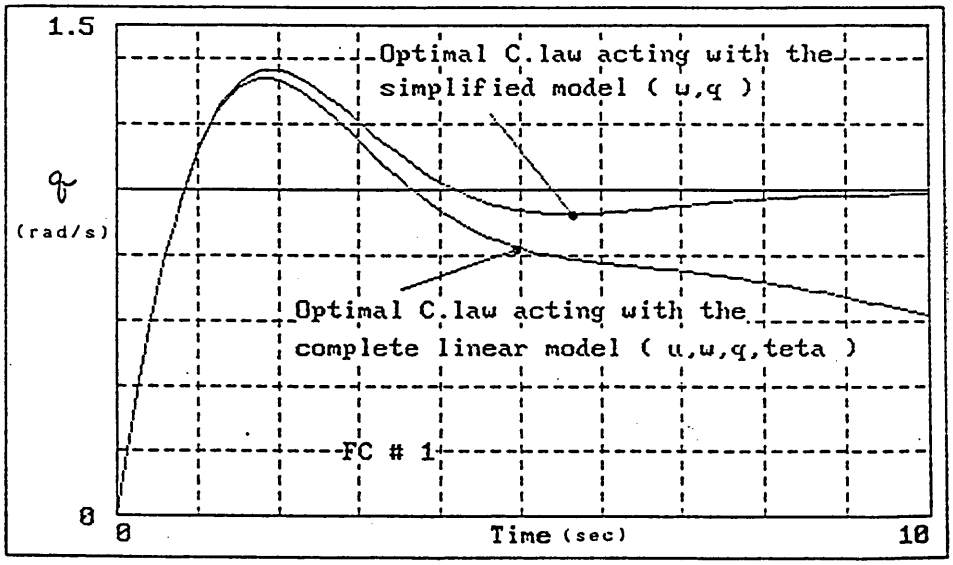

figure 3.10 - effect of the phugoid mode on the aircraft response with optimal control law design at 1000 ft mach 0.30

3.7 THE PERFORMANCE OF BOTH CONTROL LAW DESIGNS WITH THE COMPLETE MODEL OF THE AIRCRAFT AND THE ACTUATOR

Now an evaluation of both control law designs whith the full aircraft model including the actuator is performed. The actuator to be considered is actuator N° 2 from section 3.5, since its natural frequency is closer to the short period natural frequency than the natural frequency of actuator N° 1, and also for simplicity. The control law structure is shown in figure 3.11.

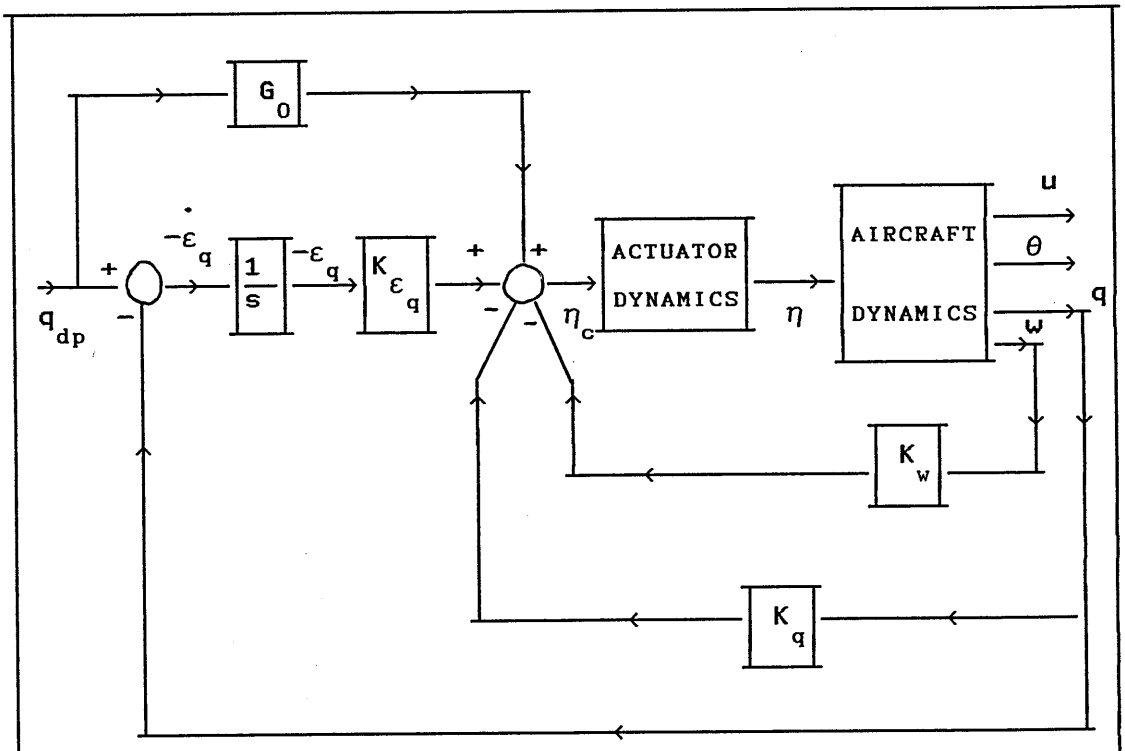

figure 3.11 - control law structure with phugoid model and actuator model included.

Obviously the state vector is now :

$$x^T = [\, u\ w\ q\ \theta\ \varepsilon_q\ \eta\ v_\eta \,] \tag{3.37}$$

The state equation describing the mathematical model is given by:

$$\dot{x} = A\,x + B\,\eta_c + E\,q_{dp} \tag{3.38}$$

Considering

A_{LM} as the state matrix of the aircraft longitudinal model given in appendix A, B_{LM} as the control matrix of the aircraft longitudinal

model as given in appendix A. Then the matrix A in (3.38) can be written

$$A = \left[\begin{array}{cccc:c:cc} & & & & 0 & & 0 \\ & & & & 0 & & 0 \\ & A_{LM} & & & 0 & B_{LM} & 0 \\ & & & & 0 & & 0 \\ \hdashline 0 & 0 & 1 & 0 & 0 & 0 & 0 \\ \hdashline 0 & 0 & 0 & 0 & 0 & & \\ 0 & 0 & 0 & 0 & 0 & A_A & \end{array}\right] \qquad (3.39)$$

A_A is the actuator state matrix defined in section 3.5, equation (3.20). The matrix B is given by,

$$B^T = [\, 0\ 0\ 0\ 0\ 0\ B_A \,] \qquad (3.40)$$

where B_A is the actuator control matrix defined in section 3.5, equation (3.20), and

$$E^T = [\, 0\ 0\ 0\ 0\ -1\ 0\ 0 \,] \qquad (3.41)$$

Again the control law is,

$$\eta_c = -G\,x + G_0 q_{dp} \qquad (3.42)$$

$$\text{but now,}\quad G = [\, 0\ K_w\ K_q\ 0\ K_{\varepsilon_q}\ 0\ 0 \,] \qquad (3.43)$$

and G_0 is the same as before. The closed loop model is given by the state equation,

$$\dot{x} = (A-BG)x + (BG_0 + E)q_{dp} \qquad (3.44)$$

As already mentioned the evaluation was performed only with actuator no.2. Table (3.15) shows a comparison of the dynamic characteristics of the aircraft when it is considered only with the reduced order aircraft model without actuator, as in section (3.3), and with full order aircraft model including actuator, all for the pole-placement control law design. In table (3.16) the same results are listed for the optimal control law design.

TABLE 3.15 – SHORT PERIOD CHARACTERISTICS OBTAINED WITH THE POLE PLACEMENT CONTROL LAW DESIGN

FC #	REDUCED ORDER MODEL NO ACTUATOR			FULL ORDER MODEL WITH ACTUATOR N° 2			h	Mach
	ω_{sp} rad/s	ζ_{sp}	CAP s^{-2}	ω_{sp} rad/s	ζ_{sp}	CAP s^{-2}	ft	
1	0.87	0.70	0.125	0.82	0.72	0.120	1000	0.30
5	0.84	0.85	0.092	0.72	0.85	0.071	20000	0.50
8	0.76	1.17	0.085	1.42	1.19	0.297	40000	0.70
12	0.68	0.70	0.099	0.66	0.72	0.103	10000	0.30
16	0.70	0.90	0.084	0.63	0.86	0.067	30000	0.50

TABLE 3.16 – SHORT PERIOD CHARACTERISTICS OBTAINED WITH THE OPTIMAL CONTROL LAW DESIGN

FC #	REDUCED ORDER MODEL NO ACTUATOR			FULL ORDER MODEL WITH ACTUATOR N° 2			h	Mach
	ω_{sp} rad/s	ζ_{sp}	CAP s^{-2}	ω_{sp} rad/s	ζ_{sp}	CAP s^{-2}	ft	
1	1.02	0.59	0.172	1.04	0.57	0.193	1000	0.30
5	1.11	0.49	0.162	1.13	0.48	0.175	20000	0.50
8	1.05	0.48	0.164	1.07	0.48	0.175	40000	0.70
12	0.86	0.56	0.158	0.88	0.54	0.184	10000	0.30
16	0.91	0.47	0.142	0.91	0.46	0.141	30000	0.50

From these tables it is clear that there is a degradation in CAP with the pole-placement control law design, and again the optimal control law design is more robust with respect to maintenance of CAP. As stated in section 3.1 CAP requirement for level 1 is,

$$0.085 \leq \text{CAP} \leq 3.60$$

The results obtained with both designs with respect to the dropback criterion shows that the optimal design has lost the zero steady state error characteristic $(\varepsilon_q)_{ss} = 0$ for almost all flight conditions, figures (3.12), (3.13) and (3.14) illustrate very well this aspect. In contrast, the pole-placement design has maintained this relation, that

is, $0.80 \leq (q/q_{dp})_{ss} \leq 1.27$ for all flight conditions. In view of this it is clear that, with respect to steady state characteristics, the pole placement design is much more robust than the optimal design. With respect to dropback characteristics both designs no longer meet the criterion. Table (3.17) shows the performance of the pole-placement design with respect to the dropback criterion.

TABLE 3.17 - PERFORMANCE OF THE POLE PLACEMENT DESIGN WITH RESPECT TO DROPBACK CRITERION

FC #	REDUCED ORDER MODEL			FULL ORDER MODEL			h	Mach
	t_m sec	q_m/q_{ss}	DB/q_{ss} sec	t_m sec	q_m/q_{ss}	DB/q_{ss} sec	ft	
1	2.5	1.24	0.12	2.3	1.34	-0.27	1000	0.30
5	2.4	1.19	0.10	2.4	1.25	-0.07	20000	0.50
8	2.5	1.12	0.05	2.2	1.09	-0.22	40000	0.70
12	3.1	1.23	0.11	2.9	1.35	-0.52	10000	0.30
16	2.9	1.17	0.07	2.6	1.22	-0.17	30000	0.50

Table (3.18) shows the steady state pitch rate response obtained with both control law designs applied to the complete model and actuator, and it is clear how the optimal control law design has deteriorated in this respect.

TABLE 3.18 - STEADY STATE RESPONSE OBTAINED WITH BOTH CONTROL LAW DESIGNS AND THE COMPLETE MODEL PLUS ACTUATOR $\left[q / q_{dp} \right]_{ss}$

FC #	POLE PLACEMENT DESIGN	OPTIMAL CONTROL DESIGN	h ft	Mach
1	0.87	0.27	1000	0.30
5	0.80	0.34	20000	0.50
8	1.04	0.55	40000	0.70
12	0.81	0.25	10000	0.30
16	1.09	-0.78	30000	0.50

As a general conclusion, both control law designs require adjustments to satisfy the dropback criterion, however, the pole placement design also requires adjustments to meet CAP level 1. The reasons for the findings can be attributed to the fact that in this preliminary design the pole placement control law has moved the poles from the original open loop position much more than the optimal control law design, which is obvious from the relative feedback gain magnitudes of both designs. The method for obtaining the feedforward gain in each control law design is different. The pole-placement design is more robust with respect to zero steady state error characteristic so, as already shown the feedforward gain of the pole-placement design is based on exact pole-zero cancellation whereas, the feedforward gain in the optimal design is based on the performance index, as explained in chapter 2.

The gains used in flight conditions 1, 5, 8, 12 and 16 are listed in table 3.18-A for the pole placement control law design and also for the optimal control law design. The aircraft data for the same flight conditions are contained in appendix A.

TABLE 3.18-A - CONTROL LAW GAINS

	FC#	K_w $ft^{-1}sec$	K_q sec	K_{ε_q} rad	G_0 sec	R
POLE PLACEMENT CONTROL LAW	1	0.0037	-1.4267	-1.711	-1.711	-
	5	0.0020	-1.3270	-1.346	-1.346	-
	8	0.0013	-2.065	-1.743	-1.743	-
	12	0.0040	-1.828	-1.684	-1.684	-
	16	0.0021	-1.832	-1.544	-1.544	-
OPTIMAL CONTROL LAW	1	0.0005	-0.2131	-0.3162	-2.183	10
	5	0.0005	-0.2723	-0.4472	-1.813	5
	8	0.0006	-0.5297	-0.7071	-1.828	2
	12	0.0008	-0.3782	-0.4472	-2.309	5
	16	0.0006	-0.3492	-0.4472	-1.906	5

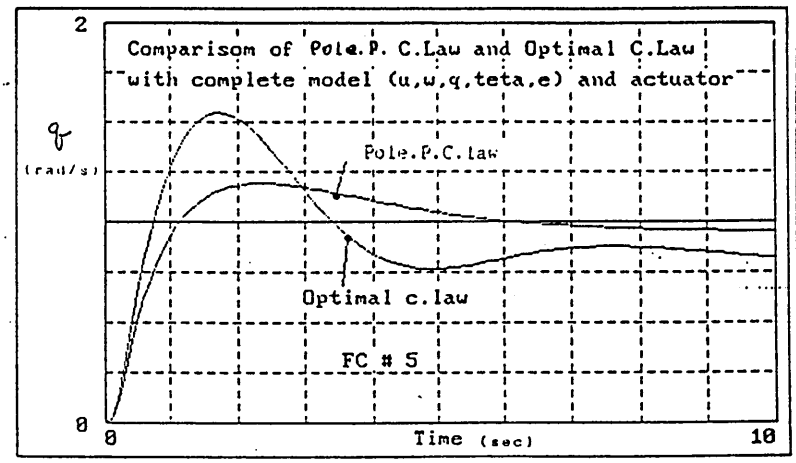

figure 3.12 - pitch-rate time response of both designs with the complete model of the aircraft and actuator at 20000 ft, mach 0.50

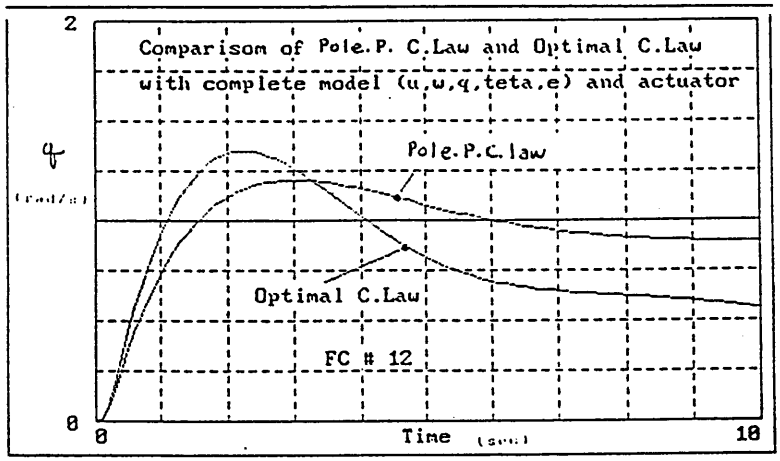

figure 3.13 - pitch-rate time response of both designs with the complete model of the aircraft and actuator at 10000 ft, mach 0.30

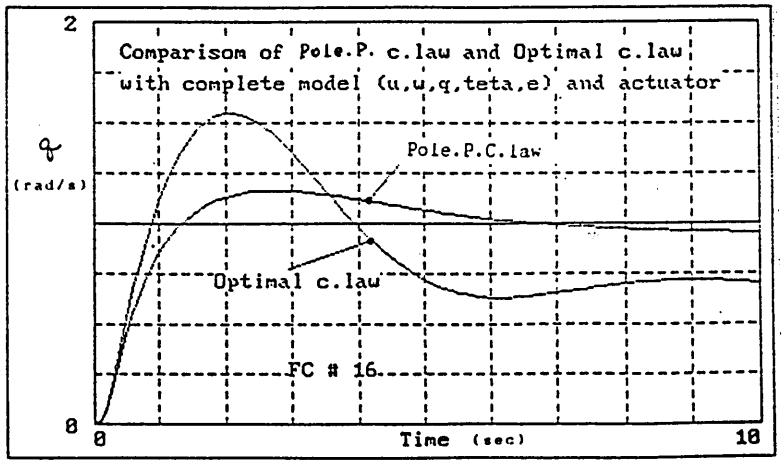

figure 3.14 - pitch-rate time response of both designs with the complete model of the aircraft and actuator at 30000 ft, mach 0.50

3.8 CLOSED LOOP POLE LOCATIONS COMPARISON FOR EACH FLIGHT CONDITION

3.8.1 INTRODUCTION

It is interesting to compare the pole locations for each of the flight conditions studied in order to evaluate the variations.

3.8.2 POLE PLACEMENT CONTROL LAW DESIGN

In table (3.19) the closed loop pole locations for the reduced order short period model are listed, that is, the aircraft obtained in section (3.3), as showed in table (3.3). In table (3.20) the closed loop poles are shown for the case of the reduced order short period model with actuator, that is, the aircraft obtained in section (3.5), as showed in table (3.8). In table (3.21) the closed loop poles of full order aircraft model are listed, that is, the aircraft obtained in section (3.6), as showed in table (3.12). Finally, in table (3.22) the closed loop poles of the full order aircraft model plus actuator are listed, that is, the aircraft obtained in section (3.7), as showed in table (3.15). The actuator referred to is actuator number 2, as above.

TABLE 3.19 - SHORT PERIOD CHARACTERISTICS
REDUCED ORDER MODEL AND CONTROL LAW

FC#	POLES		ω_{sp} rad/s	ζ_{sp}	h ft	Mach
3	-1.08 ± i 1.11	-1	1.55	0.70	1000	0.60
6	-1.02 ± i 0.63	-1	1.20	0.85	20000	0.70
9	-1.61 ± i 0.45	-1	0.85	1.21	40000	0.80
13	-0.58 ± i 0.59	-1	0.83	0.70	10000	0.40
17	-0.86 ± i 0.25	-1	0.90	0.96	30000	0.70

TABLE 3.20 – SHORT PERIOD CHARACTERISTICS

REDUCED ORDER MODEL – C.LAW and ACTUATOR N°2

FC#	POLES		ω_{sp} rad/s	ζ_{sp}	h ft	Mach
3	−1.06 ± i 1.01	−1.36	1.46	0.72	1000	0.60
6	−0.79 ± i 0.52	−2.20	0.94	0.83	20000	0.70
9	−0.78 , −0.47	−3.10	0.60	1.03	40000	0.80
13	−0.54 ± i 0.56	−1.35	0.78	0.70	10000	0.40
17	−0.62 ± i 0.33	−2.26	0.71	0.88	30000	0.70

TABLE 3.21 – SHORT PERIOD CHARACTERISTICS

FULL AIRCRAFT MODEL – CONTROL LAW and NO ACTUATOR

FC#	POLES				ω_{sp} rad/s	ζ_{sp}	h ft	Mach
3	−1.06 ± i 1.08	−1.04	−0.016	0	1.52	0.69	1000	0.60
6	−0.95 ± i 0.59	−1.12	−0.016	0	1.12	0.85	20000	0.70
9	−1.55 , − 1.07	−0.42	−0.015	0	1.29	1.02	40000	0.80
13	−0.59 ± i 0.58	−0.94	−0.038	0	0.83	0.71	10000	0.40
17	−0.75 ± i 0.29	−1.20	−0.014	0	0.81	0.93	30000	0.70

TABLE 3.22 – SHORT PERIOD CHARACTERISTICS

FULL AIRCRAFT MODEL – C.LAW and ACTUATOR N° 2

FC#	POLES				ω_{sp} rad/s	ζ_{sp}	h ft	Mach
3	−1.06 ± i 1.00	−1.35	−0.016	0	1.46	0.72	1000	0.60
6	−0.78 ± i 0.51	−2.21	−0.016	0	0.94	0.84	20000	0.70
9	−0.78 , − 0.45	−3.14	−0.015	0	1.57	1.25	40000	0.80
13	−0.55 ± i 0.55	−1.30	−0.038	0	0.77	0.71	10000	0.40
17	−0.62 ± i 0.33	−2.25	−0.014	0	0.70	0.88	30000	0.70

The following observations resulting from the comparisons may be noted.

(i) table (3.19) with table (3.20)
The influence of the actuator is significant, the closed loop poles have moved considerably with respect to the closed loop poles obtained in table (3.19).

(ii) table (3.19) with table (3.21)
The influence of the phugoid is minimal, the closed loop poles have moved little with respect to the closed loop poles obtained in table (3.19)

(iii) table (3.19) with table (3.22)
Table (3.22) is basically the same as table (3.20), and so the phugoid dynamics do not influence the short period dynamics as much as the actuator does.

3.8.3 OPTIMAL CONTROL CONTROL LAW DESIGN

In table (3.23) the closed loop pole locations for the reduced order short period model are listed, that is, the aircraft obtained in section (3.4), as showed in table (3.5). In table (3.24) the closed loop poles are shown for the case of the reduced order short period model with actuator, that is, the aircraft obtained in section (3.5), as showed in table (3.9). In table (3.25) the closed loop poles of full order aircraft model are listed, that is, the aircraft obtained in section (3.6), as showed in table (3.13). Finally, in table (3.26) the closed loop poles of the full order aircraft model plus actuator are listed, that is, the aircraft obtained in section (3.7), as showed in table (3.16). The actuator referred to is actuator number 2, as above.

TABLE 3.23 – SHORT PERIOD CHARACTERISTICS
REDUCED ORDER MODEL and CONTROL LAW

FC#	POLES		ω_{sp} rad/s	ζ_{sp}	h ft	Mach
3	−1.03 ± i 1.27	−0.23	1.64	0.63	1000	0.60
6	−0.75 ± i 1.20	−0.27	1.42	0.53	20000	0.70
9	−0.61 ± i 1.03	−0.24	1.19	0.51	40000	0.80
13	−0.60 ± i 0.93	−0.19	1.11	0.54	10000	0.40
17	−0.56 ± i 1.03	−0.21	1.18	0.48	30000	0.70

TABLE 3.24 – SHORT PERIOD CHARACTERISTICS
REDUCED ORDER MODEL – C.LAW – ACTUATOR N° 2

FC#	POLES		ω_{sp} rad/s	ζ_{sp}	h ft	Mach
3	−1.03 ± i 1.31	−0.23	1.67	0.62	1000	0.60
6	−0.75 ± i 1.25	−0.27	1.46	0.51	20000	0.70
9	−0.62 ± i 1.08	−0.25	1.25	0.50	40000	0.80
13	−0.60 ± i 0.93	−0.20	1.11	0.54	10000	0.40
17	−0.56 ± i 1.04	−0.21	1.19	0.48	30000	0.70

TABLE 3.25 – SHORT PERIOD CHARACTERISTICS
FULL ORDER AIRCRAFT MODEL – C. LAW and NO ACTUATOR

FC#	POLES			ω_{sp} rad/s	ζ_{sp}
3	−1.04 ± i 1.29	−0.20 ,−0.032	0	1.66	0.62
6	−0.75 ± i 1.23	−0.23 ,−0.032	0	1.45	0.52
9	−0.60 ± i 1.03	−0.23 ,−0.021	0	1.20	0.51
13	−0.60 ± i 0.94	−0.10 ± i0.075	0	1.12	0.54
17	−0.56 ± i 1.03	−0.18 ,−0.033	0	1.17	0.48

TABLE 3.26 – SHORT PERIOD CHARACTERISTICS
FULL ORDER AIRCRAFT MODEL – C.LAW and ACTUATOR N° 2

FC#	POLES			ω_{sp} rad/s	ζ_{sp}
3	−1.03 ± i 1.31	−0.21 ,−0.032	0	1.67	0.62
6	−0.75 ± i 1.25	−0.25 ,−0.032	0	1.46	0.51
9	−0.62 ± i 1.08	−0.24 ,−0.020	0	1.24	0.49
13	−0.60 ± i 0.95	−0.105 ±i0.075	0	1.12	0.81
17	−0.56 ± i 1.05	−0.18 ,−0.033	0	1.19	0.47

The following observations resulting from the comparisons may be noted;

(i) table (3.23) with table (3.24)
The actuator here practically does not affect the pole locations as it does in the case of pole placement control law design. This is probably due to the fact that the integrator pole in the pole placement design is much closer to the actuator dynamics than it is in the optimal control law design.

(ii) table (3.23) with table (3.25)
Again the phugoid dynamics have practically no effect on the pole locations.

(iii) table (3.23) with table (3.26)
Here again table (3.26) is basically the same as table (3.24).

It is noticed that the choice of s = −1 in the pole placement control law design, giving the integrator a time constant close to the short period natural frequency, is not a very good choice or perhaps the choice of ω_{sp} and ζ_{sp} based on equations (3.13) and (3.14) is not so good as the choice of the weighting parameter in the performance index in the optimal control law design. Table (3.20) clearly shows that the inclusion of the actuator influences the pole placement design

much more than it influences the optimal control law design, shown in table (3.24). It appears that optimal design methods can offer a better control law design than methods that directly place closed loop poles on the s-plane. Again, looking at table (3.19) compared to table (3.20) it is evident that flight conditions 3 and 13 are influenced as much as flight conditions 6, 9 and 17, once again this emphasizes that the analysis of just one, or a small number of, flight cases can sometimes lead to wrong conclusions. It must be mentioned that the actuator poles have not been listed in these tables for reasons of simplicity.

4 CONTROL LAW DEVELOPMENT TO SATISFY GIBSON DROPBACK AND PHASE-RATE CRITERIA

4.1 INTRODUCTION

As shown in chapter 3, both control law designs fail to meet the dropback criterion when the phugoid dynamics and actuator are included in the model. So it is necessary to carry out some adjustments to the optimal control law design in order to meet the dropback criterion and to the pole-placement control law design to meet not only the dropback criterion but also CAP. The process adopted in the redesign is described in this chapter.

4.2 THE ADJUSTMENT OF BOTH DESIGNS IN ORDER TO SATISFY THE DROPBACK CRITERION AND CAP REQUIREMENT

4.2.1 THE POLE-PLACEMENT CONTROL LAW DESIGN

As seen in chapter 3, to redesign the pole-placement control law it is necessary to recover the steady state characteristic $(q/q_{dp})_{ss} \simeq 1$, and an acceptable dropback. In order to recover good steady state characteristics it is necessary to adjust the gains K_w and K_{ε_q}, while looking simultaneously at the CAP requirement. To perform this adjustment an analytical approach was followed, and for this approach the actuator dynamics were not included, just the short period mode and phugoid mode together.

The control law is:

$$\eta = -Gx + G_0 q_{dp} \tag{4.1}$$

and for the reduced order model without actuator,

$$x^T = [\, w \; q \; \varepsilon_q \,] \tag{4.2}$$

and

$$G = [\, K_w \; K_q \; K_{\varepsilon_q} \,] \tag{4.3}$$

Now if the phugoid model is included in the dynamics, the state vector becomes,

$$x^T = [\, u \; w \; q \; \theta \,] \tag{4.4}$$

and the basic control law is,

$$\eta = -K_w w - K_q q - K_{\varepsilon_q} \varepsilon_q + G_0 q_{dp} \tag{4.5}$$

however $\dot{\varepsilon}_q = q - q_{dp}$ (4.6)

so, $\varepsilon_q = q/s - q_{dp}/s$ (4.7)

but $\theta = q / s$ (4.8)

and then, $\varepsilon_q = \theta - q_{dp}/s$ (4.9)

substituting (4.9) into (4.5) it is possible to write the control law in the form:

$$\eta = -K_w w - K_q q - K_{\varepsilon_q} \theta + K_{\varepsilon_q} \frac{q_{dp}}{s} + G_0 q_{dp} \tag{4.10}$$

and so, $$\eta = -Gx + \left[\frac{K_{\varepsilon_q}}{s} + G_0 \right] q_{dp} \tag{4.11}$$

now with $x^T = [\, u \; w \; q \; \theta \,]$ (4.12)

and $G = [\, 0 \; K_w \; k_q \; K_{\varepsilon_q} \,]$ (4.13)

So the analytical approach to adjust K_w and K_{ε_q} was obtained with the state vector (4.12) and the control law (4.11). From the mathematical model for the closed loop system it is possible to obtain the transfer function of q to q_{dp}, which is of the form:

$$\frac{q}{q_{dp}} = \frac{N_3 s^3 + N_2 s^2 + N_1 s + N_0}{\Delta_4 s^4 + \Delta_3 s^3 + \Delta_2 s^2 + \Delta_1 s + \Delta_0} \tag{4.14}$$

Applying the final value theorem to (4.14), it is possible to obtain a relationship :

$$\left[\frac{q}{q_{dp}} \right]_{ss} = \frac{N_0}{\Delta_0} = K_{ss} \tag{4.15}$$

as N_0 and Δ_0 are functions of the aircraft aerodynamics, K_w and K_{ε_q}, (4.15) can be written as: K_{ss} = function (K_w, K_{ε_q}), and so it is possible to obtain an approximation for K_{ε_q} as a function of K_w and K_{ss} where K_{ss} is simply the desired steady state constant to be achieved.

If K_{ss} is choosen around 1, lets say in the range 0.98 to 1.02, then it is possible to adjust K_w and K_{ε_q} whilst monitoring the value of CAP. It must be mentioned that it is not possible to choose K_{ss} exactly 1 due to numerical problem in the calculation of K_{ε_q}. In this way new gains K_w and K_{ε_q} were obtained for all flight conditions. It is useful now to remember from chapter 3 that the zero steady state characteristic of the pole placement control law design was well behaved even when the actuator was included, and so the method is a good approximation for finding new feedback gains K_w and K_{ε_q}.

The method can be summarized as:

(i) choose a constant K_{ss} (0.98 to 1.02)

(ii) with the old K_w (from the reduced order model) obtain a new K_{ε_q}

(iii) with the new gains K_w ,K_{ε_q} and old K_q find the CAP with the complete model and actuator. If CAP is satisfyied, then it is all right (as is the case of flight conditions 9 and 17). If not go back to (ii) with a small change in K_w.

This procedure will recover good CAP and good steady state characteristics, it remains now to recover good dropback. The dropback characteristics will be recovered by the feedforward gain G_0. The technique for obtaining a new G_0 is simple and widely used in the aeronautical industry, by simulating the aircraft response and adjusting the gain G_0 based on the original value obtained with the reduced order model.

With the new feedback gains and the original feedforward gain obtain the dropback parameter, if it satisfies the criterion then no adjustment is necessary, if the criterion is not satisfied then change the G_0 just a little, beginning with 5% change. Obtain the aircraft response, and so on until the criterion is satisfied. The convergence is fast, with few iterations. Around five iterations are required to obtain a new value of the feedforward gain.

With this procedure the new gains obtained are listed in table (4.1). and in table (4.2) the new short period characteristics are compared to the original short period characteristics.

TABLE 4.1 – NEW GAINS COMPARED WITH THE OLD GAINS FOR THE POLE-PLACEMENT CONTROL LAW

	FC #	3	6	9	13	17
K_w	old	0.0012	0.0012	0.0011	0.0026	0.0013
$ft^{-1}s$	new	0.0009	0.0018	0.0011	0.0030	0.0013
K_q	old	-0.588	-0.889	-1.875	-1.094	-1.249
s	new	-0.588	-0.889	-1.875	-1.094	-1.249
K_{ε_q}	old	-1.219	-1.183	-1.697	-1.270	-1.252
rad	new	-1.600	-2.857	-2.200	-3.755	-3.429
G_0	old	-1.219	-1.183	-1.697	-1.270	-1.252
s	new	-1.389	-0.592	-2.036	-1.600	-1.410

TABLE 4.2 – NEW SHORT PERIOD CHARACTERISITCS COMPARED WITH THE OLD SHORT PERIOD CHARACTERISTICS

	FC #	3	6	9	13	17
ω_{sp}	old	1.55	1.20	0.85	0.83	0.90
rad/s	new	2.03	2.19	1.91	1.88	2.42
ζ_{sp}	old	0.70	0.85	1.21	0.70	0.96
	new	0.57	0.50	0.99	0.35	0.45
CAP	old	0.117	0.101	0.086	0.092	0.087
s^{-2}	new	0.099	0.156	0.235	0.264	0.252

In table (4.3) the new and old dropback charactristics are compared, and some comments are in order now:

i It is seen from table 4.1 that K_w has changed very little but K_{ε_q} has changed more, this is due to the fact that K_{ε_q} has the main influence in the steady state error.

ii The feedforward gain has in general increased with respect to the old values, in fact this is not so good, since it represents higher control effort.

iii The damping ratio has decreased in all flight conditions, but still satisfies level 1 of MIL-F-8785C.

iv It is interesting to note that the short period natural frequency has increased in all flight conditions, a fact that contradicts the approach followed in the pole placement control law design followed in chapter 3.

v The aircraft response is now faster than it was before, that is, t_m is now lower.

TABLE 4.3 - NEW DROPBACK CHARACTERISTICS COMPARED WITH THE OLD DROPBACK CHARACTERISTICS

	FC #	3	6	9	13	17
$\frac{q_m}{q_{ss}}$	old	1.25	1.22	1.11	1.24	1.16
	new	1.44	1.48	1.21	1.51	1.46
$\frac{DB}{q_{ss}}$ (sec)	old	0.09	0.15	0.02	0.11	0.07
	new	0.05	0.16	0.24	0.12	0.08
t_m (sec)	old	1.4	1.6	2.1	2.6	2.1
	new	1.1	1.4	1.2	1.4	1.1
q_{ss} (rad/s)	old	1	1	1	1	1
	new	0.99	1	1	0.98	1

4.2.2 THE OPTIMAL CONTROL LAW DESIGN

It was necessary to make changes to the optimal control law design in order to recover good dropback characteristics, the gains were adjusted as follows. In the initial design process a constant state weighting matrix Q was used and the control weighting matrix was varied. Here the procedure is reversed, that is, a constant control weighting matrix R is used, in this case R is taken to be equal to 1, and the state weighting matrix Q is varied. Only the element Q(3,3) is varied as in the preliminary design. The procedure can be summarized as:

i With the reduced order short period model, that is with the same model used in chapter 3 to design the control law, obtain a set of new feedback gains varying only the element Q(3,3). The design attempts to ensure that the closed loop poles don't move too far from the open loop poles and that the gain magnitudes are not too high (say no more than 4). By varying Q(3,3) from 0.01 to 20 a set of feedback gains and feedforward gains were obtained, in the same way as described in chapter 3, for each flight condition.

ii Evaluate the steady state error response of the full aircraft model with actuator and the new gains obtained in (i). Choose the set of gains that offer the best steady sate error response recovery.

iii Obtain the dropback characteristics with the new set of feedback gains and feedforward gain obtained in (ii). If acceptable do not change the feedforward gain. If not acceptable try a new feedforward gain based on the value obtained in (ii) and changing it by 5%, 10% and so on until the dropback criterion is satisfied.

It must be mentioned here that in this case it is possible to obtain analytically full state feedback gains with the full model, that is, with the state vector:

$$x^T = [\ u\ w\ q\ \theta\ \varepsilon_q\ \eta\ v_\eta\ ] \qquad (4.15.a)$$

However, since the design was not intended to have feedbacks of u, η and v_η, this approach was not adopted. In contrast with pole-placement method, it is not possible to obtain analyticaly the gains with the full model since the system is not controllable in terms of control theory. After the redesign the new gains obtained are listed in table (4.4) compared with the old gains. Table (4.5) shows the new and old short period characterisitcs and table (4.6) shows the new and old dropback characterisitcs.

TABLE 4.4 – NEW GAINS COMPARED WITH THE OLD GAINS FOR THE OPTIMAL CONTROL LAW DESIGN

	FC #	3	6	9	13	17
K_w $ft^{-1}s$	old	0.0002	0.0003	0.0005	0.0006	0.0004
	new	0.0008	0.0007	0.0009	0.0014	0.0008
K_q s	old	-0.135	-0.216	-0.543	-0.280	-0.257
	new	-0.898	-1.016	-1.343	-1.356	-1.228
K_{ε_q} rad^q	old	-0.316	-0.447	-0.816	-0.447	-0.447
	new	-2.236	-2.236	-2.236	-2.236	-2.236
G_0 s	old	-1.290	-1.280	-1.720	-1.910	-1.540
	new	-1.927	-1.973	-2.188	-3.230	-2.282

TABLE 4.5 – NEW SHORT PERIOD CHARACTERISITCS COMPARED WITH THE OLD SHORT PERIOD CHARACTERISTICS

	FC #	3	6	9	13	17
ω_{sp} rad/s	old	1.64	1.42	1.19	1.11	1.18
	new	2.59	2.56	1.95	1.74	2.13
ζ_{sp}	old	0.63	0.53	0.51	0.54	0.48
	new	0.61	0.59	0.59	0.60	0.59
CAP s^{-2}	old	0.13	0.14	0.17	0.17	0.15
	new	0.127	0.182	0.240	0.245	0.222

TABLE 4.6 – NEW DROPBACK CHARACTERISTICS COMPARED WITH THE OLD DROPBACK CHARACTERISTICS

	FC #	3	6	9	13	17
$\frac{q_m}{q_{ss}}$	old	1.32	1.47	1.49	1.44	1.59
	new	1.56	1.60	1.47	1.74	1.60
$\frac{DB}{q_{ss}}$ (sec)	old	0.05	0.01	0.02	0.09	0.03
	new	0.07	0.12	0.03	0.01	0.15
t_m (sec)	old	1.20	1.30	1.50	1.70	1.50
	new	0.90	0.90	1.10	1.10	1.00
q_{ss} (rad/s)	old	1	1	1	1	1
	new	0.99	1	0.99	0.94	0.98

4.2.3 CONCLUSIONS AND OBSERVATIONS

The results obtained with the revised pole placement control law design and optimal control law design led to the following observations:

i Again the optimal control law design requires higher feedforward gains than the pole placement control law design. This is not a good feature with respect to control effort.

ii Although the feedback gain K_{ε_q} has increased with respect to the original value in the optimal control law design, it is constant over the flight envelope, which is very good in terms of implementation, since it is not required to be scheduled.

iii Again the optimal control law design satisfyies CAP requirement much better than the pole-placement control law design. In the process of gain adjustment some difficulty was experienced in trying to keep CAP in level 1 with the pole placement control law design for some flight conditions.

iv Again the pole placement control law design gives better steady state characteristics than the optimal control law design. This was already known since the method of calculation of the feedforward gain used in the pole placement method is based on pole-zero cancellation (chapter 2).

v The aircraft with optimal control law design continues to present a greater pitch-rate overshoot compared with the aircraft with pole placement control law design.

vi The short period damping is pratically unchanged in the optimal control law design. Since it was already satisfying the CAP requirement the redesign of the optimal control law was basically concerned with the dropback criterion.

vii The optimal control law design still gives the better phugoid performance with respect to MIL-F-8785C.

viii The pole placement control law design gives a greater phase and gain margin than the optimal control law design. In optimal control design methods one can expect to obtain better phase and gain margin characteristics than with other methods, however, this is true only when full state feedback is used, which is not the case here.

ix The optimal control law design results in higher bandwidth and resonant peak than the pole placement control law design. However, both designs give a performance which falls outside the desired bandwidth range as specified in D'Sousa[65].

x As seen, the feedforward gain G_0 in both designs was finely adjusted by trial and error about the nominal feedforward gain value obtained in the redesign. Adjustment by simulation is very straightforward, in fact no more than four or five iterations were necessary in order to obtain the final G_0.

Table (4.7) shows the gain margin G_M, and phase margin P_M obtained for the augmented aircraft with both designs and also the resonant peak M_P, and bandwidth ω_b.

TABLE 4.7 – DYNAMIC CHARACTERISTICS OF THE AUGMENTED AIRCRAFT WITH BOTH DESIGNS

	FC #	3	6	9	13	17
G_M (dB)	PPCL	12.8	13.6	12.5	15.3	12.4
	OCL	9.4	9.4	12.5	11.6	10.5
P_M (deg)	PPCL	82	62	110	64	70
	OCL	62	60	80	74	70
ω_b (rad/s)	PPCL	4.9	3.7	4.7	3.3	4.6
	OCL	6.7	6.8	4.9	5.3	5.8
M_P (dB)	PPCL	4.4	4.6	1.8	6.8	4.9
	OCL	5.3	5.8	4.8	6.2	5.7

In figure (4.1) the time response of both designs are compared. In figure (4.2) the frequency response of both designs are compared on the Nichols chart and in figure (4.3) the frequency response of both designs are compared on the bode plot. All these figures refer to flight condition 6.

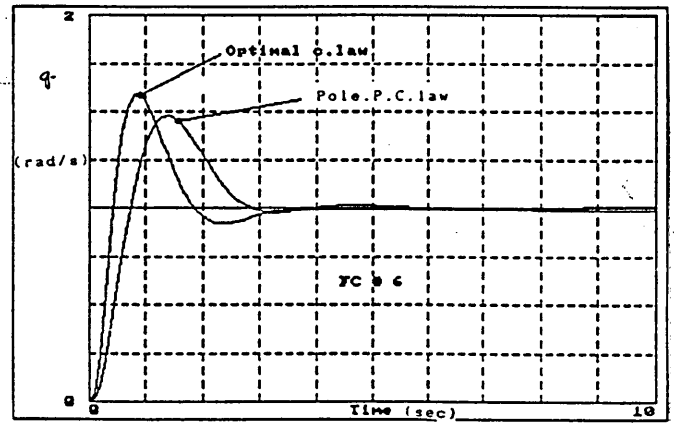

figure 4.1 - pitch-rate time response of both designs at 20000 ft mach 0.70

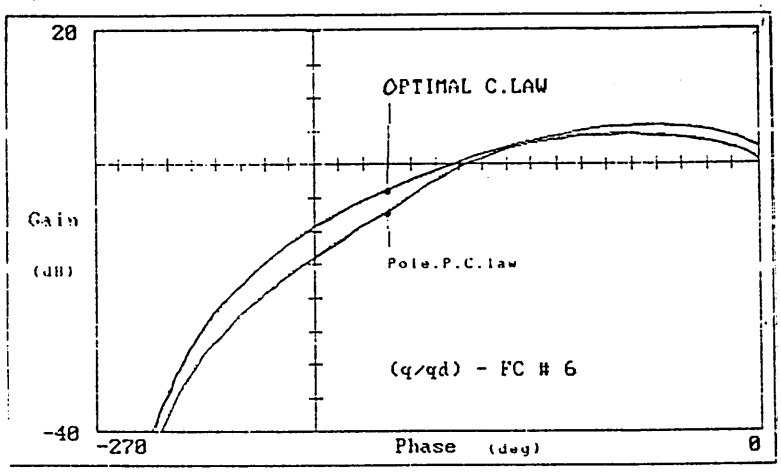

figure 4.2 - Nichols plot of pitch-rate frequency response of both designs at 20000 ft, mach 0.70

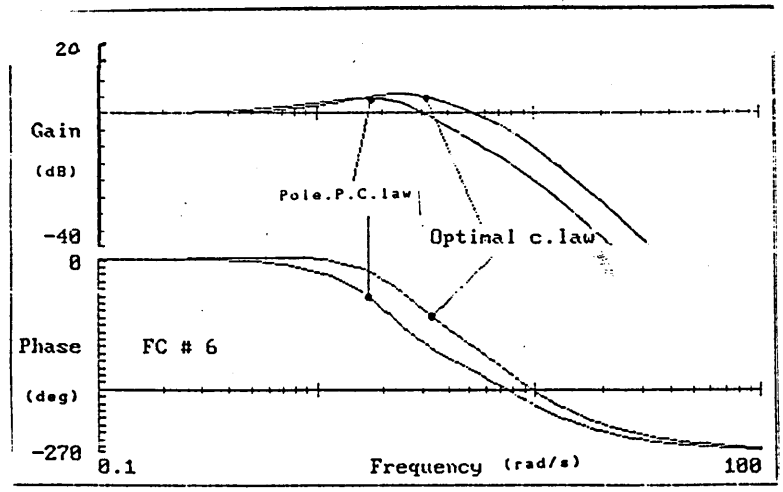

figure 4.3 - Bode plot of pitch-rate frequency response of both designs at 20000 ft, mach 0.70

4.3 FURTHER DEVELOPMENT OF THE CONTROL LAWS TO MEET THE PHASE-RATE CRITERION

4.3.1 INTRODUCTION.

The Gibson phase-rate criterion was developed specially to deal with the problem of pilot induced oscillations (PIO), which occurs mainly in approach and flare. However, here the study is carried out for the cruise configuration only, since the reference used, Heffley[11], does not contains aerodynamic data for the landing configuration. Other useful references concerned with the PIO problem are Hess-Kalteis[66] and Powers[67]. In particular Hess-Kalteis[66] offers an interesting method for dealing with the PIO problem based on the use of optimal control methods.

4.3.2 EVALUATION OF BOTH CONTROL LAWS RELATIVE TO THE PHASE-RATE CRITERION

To evaluate both control law designs with respect to the phase-rate criterion the aircraft model considered is that described in chapter 3, section 3.7, the state vector as given by equation (3.37) is,

$$x^T = [\ u\ w\ q\ \theta\ \varepsilon_q\ \eta\ v_\eta\ ] \tag{4.16}$$

and describes the full aircraft model plus actuator. From this point on actuator no.2 is used in this work. The aircraft model is given by the following state equation (3.38),

$$\dot{x} = A\,x + B\,\eta + E\,q_{dp} \tag{4.17}$$

So the control law structure is that given in Figure (3.11). The closed loop model is,

$$\dot{x} = (A - BG)x + (BG_0 + E)q_{dp} \tag{4.18}$$

with A given by equation (3.39), B given by equation (3.40), E given by equation (3.41) and the gain vector G is given in table(4.1) for

the pole placement control law, and in table (4.4) for the optimal control law. Plotting the closed loop attitude frequency response on Nichols chart it is possible to obtain the necessary data to evaluate the control law designs with respect to the phase-rate criterion. Referring to figure (4.4),

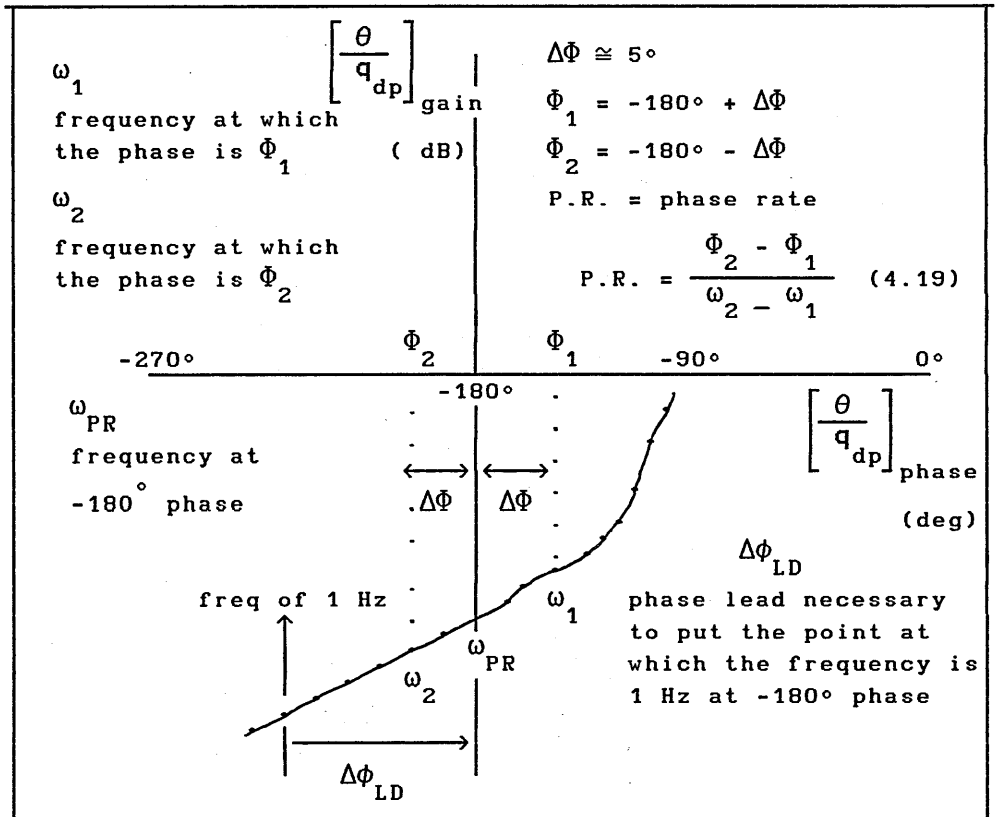

figure 4.4 - Necessary parameters for evaluation of the phase rate criterion obtained from the closed loop attitude frequency response on the Nichols chart.

which describes the parameters needed in order to evaluate the criterion, these parameters were obtained for both control laws and the findings are listed in table (4.8).

Figure (4.5) shows the performance of both control law designs with respect to the phase rate criterion. From this figure it is obvious that the optimal control law is always located in the region of moderate PIO whereas, the pole placement control law design shows greater variations since it is located in this region and also in the region of severe PIO. To bring both designs into the optimum region it is necessary to introduce of a lead filter into the command path of the control laws,as described in chapter 2, section 2.3.4.

TABLE 4.8 – PHASE–RATE PARAMETERS FOR BOTH DESIGNS

FC #	POLE-PLACEMENT DESIGN			OPTIMAL DESIGN		
	P.R. (deg/Hz)	$\Delta\Phi_{LD}$ (deg)	ω_{PR} (Hz)	P.R. (deg/Hz)	$\Delta\Phi_{LD}$ (deg)	ω_{PR} (Hz)
3	–147	49.7	0.52	–160	46	0.60
6	–317	77.8	0.38	–163	48	0.60
9	–129	46.4	0.60	–149	52	0.50
13	–344	66.8	0.36	–136	50	0.50
17	–243	63.8	0.45	–156	50	0.55

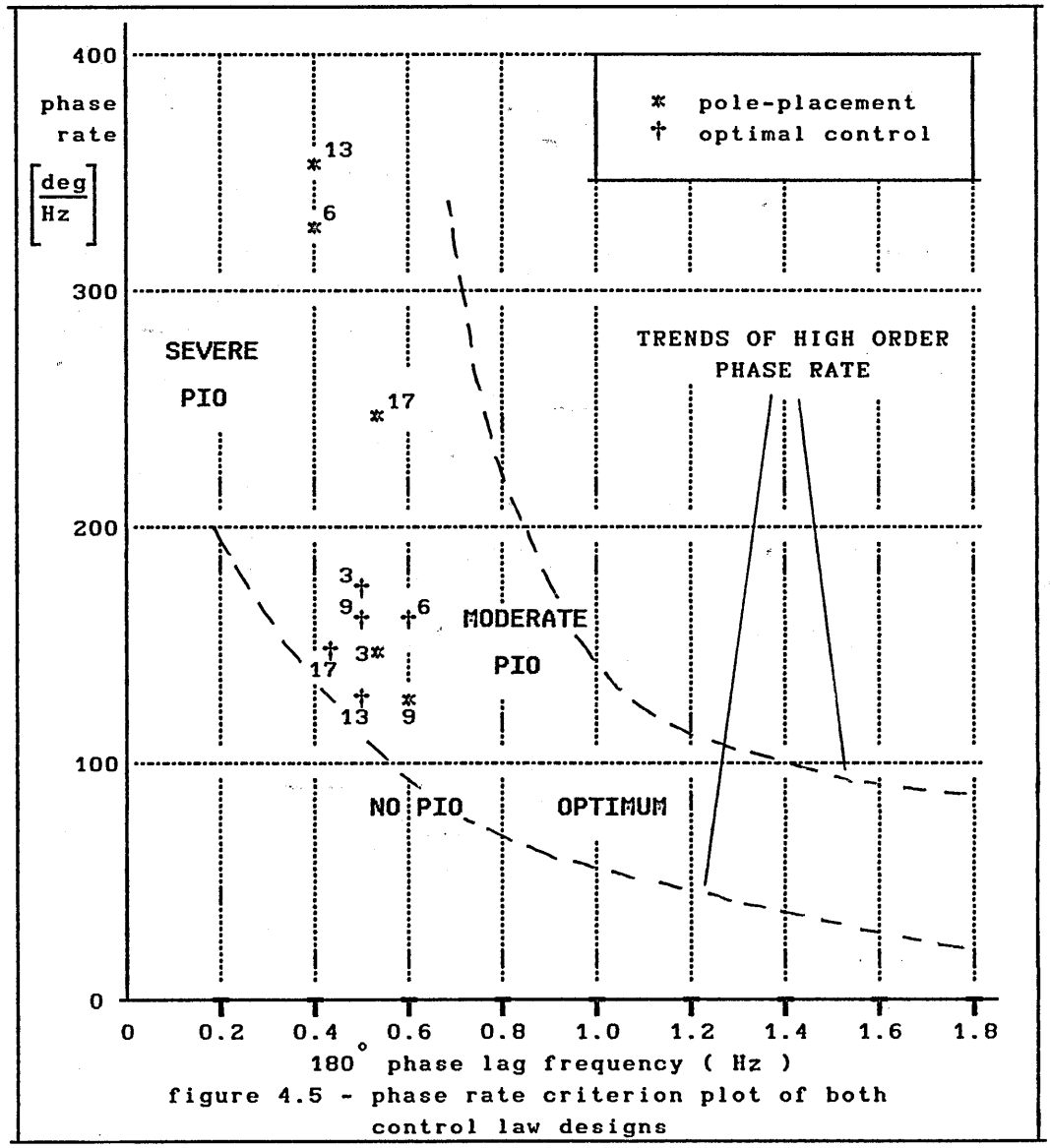

figure 4.5 - phase rate criterion plot of both control law designs

With the extra dynamics of the lead filter in the system it can be represented as in Figure 4.6 below.

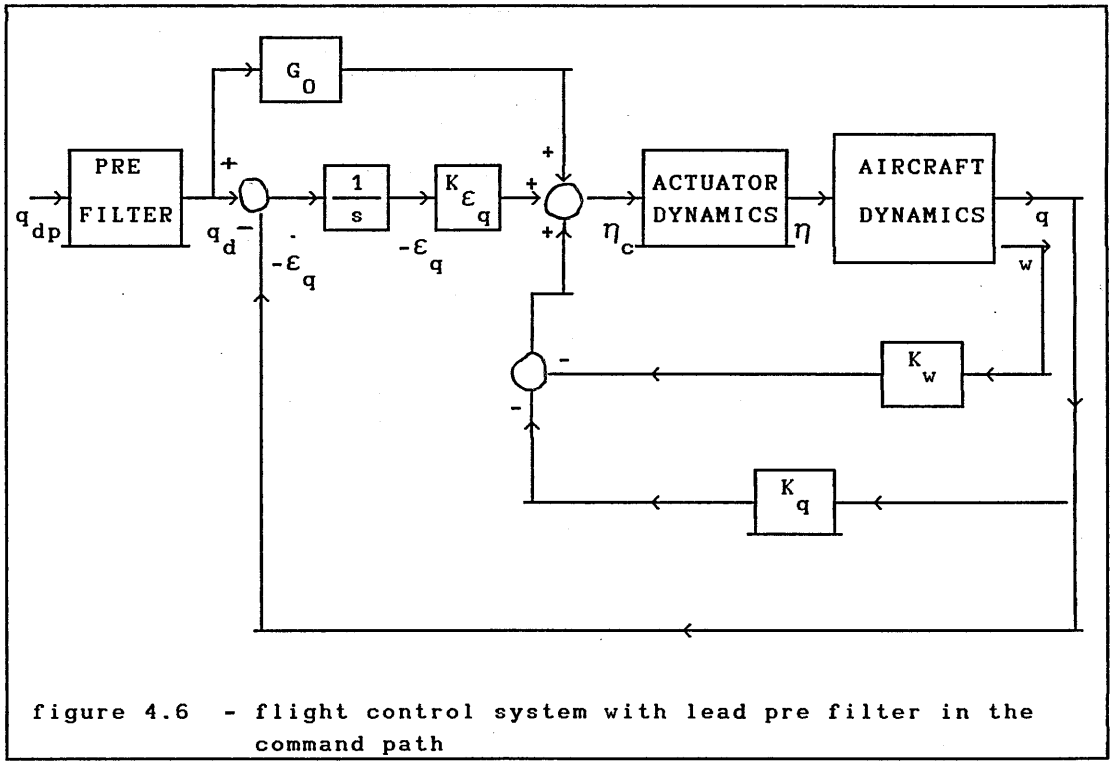

figure 4.6 - flight control system with lead pre filter in the command path

Referring to figure (4.6) the error is now given by,

$$\dot{\varepsilon}_q = q - q_d \qquad (4.20)$$

With the introduction of the lead filter in the command path the good dropback characteristics obtained in chapter 3 are degraded for both control law designs, and so it is necessary to adjust the gains of both control law designs. Certainly it can be predicted that the gain adjustment will be more difficult for the pole placement control law design than for the optimal control law design since the performance of the pole placement control law design falls almost entirely in the region of severe PIO. With reference to table (4.8) it is noticed that the maximum phase rate of the optimal control law is about -136 deg/Hz, and the minimum is about -165 deg/Hz. For the pole placement control law the maximum phase rate is about -124 deg/Hz and the minimun about -317 deg/Hz. Thus it is clear that the optimal control

law design comes closer to meeting the criterion than the pole-placement control law design. As seen in chapter 2, section 2.3.4, a desirable phase rate is less than 100 deg/Hz. Also, a comparison of the phase lead $\Delta\Phi_{LD}$ necessary to bring the design into agreement with the criterion, that is to put the frequency of 1 Hz in the closed loop attitude frequency response on the Nichols chart at -180° phase, for both designs shows that,

(i) For the optimal c.l.design $45.1^{\circ} \leq \Delta\Phi_{LD} \leq 51.7^{\circ}$

(ii) For the pole p.c.l. design $44.9^{\circ} \leq \Delta\Phi_{LD} \leq 77.8^{\circ}$

And it is clear that the values of phase adjustment required by the pole placement control law design for some flight conditions can not be obtained with phase lead only but, require some redesign of the control law gains as well.

4.3.3 THE POLE-PLACEMENT CONTROL LAW DESIGN

To design the lead filter the method of Kuo[68] has been followed. The transfer function of the phase lead filter can be written as;

$$\frac{E_2}{E_1} = \frac{1 + aTs}{1 + Ts} \qquad a > 1 \tag{4.21}$$

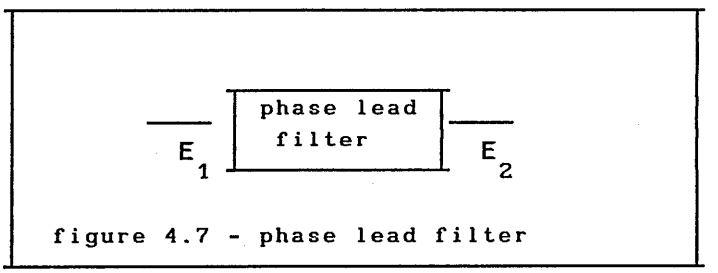

figure 4.7 - phase lead filter

Shown on the bode plot, the phase lead controller has two corner frequencies, one at $\omega = 1/(aT)$ and the other at $\omega = 1/T$. A relation of ω_m and Φ_m with a and T is obtained in Kuo[68] as;

$$\omega_m = \frac{1}{\sqrt{a}\,T} \quad (4.22) \qquad \text{and} \quad \sin \Phi_m = \frac{a-1}{a+1} \quad (4.23)$$

In figure 4.8 the bode plot of the phase lead controller is shown.

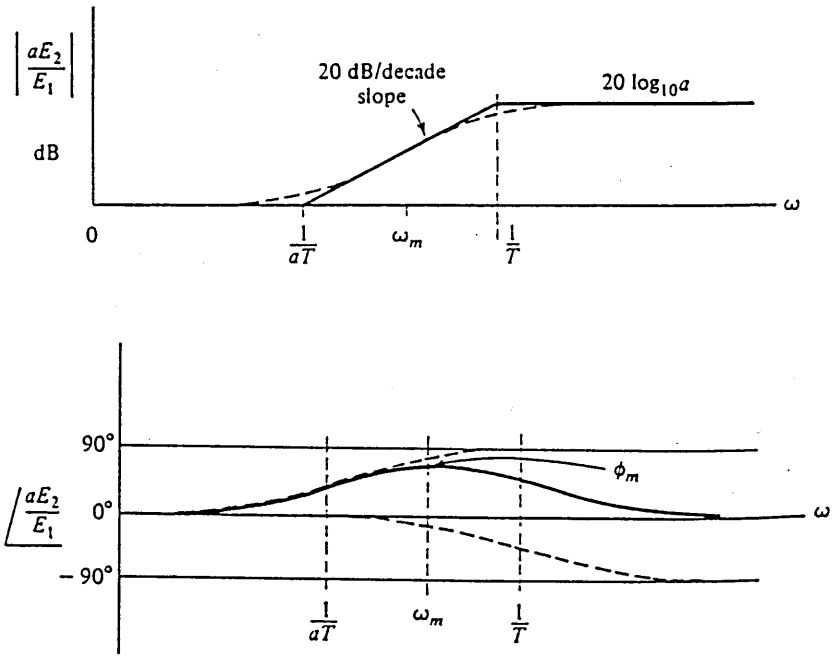

figue 4.8 - bode plot of the phase lead controller

As Φ_m is the maximum phase lead obtained at the frequency ω_m. In this case ω_m is 1 Hz for all flight cases and the required Φ_m varies with flight case. Since the average phase lead required by the pole placement control law design is around 57°, before attempting to design the lead filter it was decided to redesign the control law gains for the flight conditions located in the region of severe PIO. The redesign procedure was carried out for flight conditions at 10000 ft, 20000 ft and 30000 ft only, that is flight conditions 6, 13 and 17. The redesign was performed based on the gains obtained in the preliminary design with the reduced order model, chapter 3, section 3.3, and by choosing to adjust K_w only. So flight condition 3 and 9 have no changes in the feedback gains, they are the same as obtained in section 4.2.1. To obtain the new feedback gain K_w for flight cases 6, 13 and 17 the starting point was the gains obtained in section 3.3 , K_w, K_q and K_{ε_q}.

The redesign was made by adjusting K_w in order to obtain a phase rate lower than 200 deg/Hz, and an acceptable CAP. This choice was based mainly on the option to keep the changes as simple as possible. The new feedback gains obtained by this procedure are listed in table 4.9.

TABLE 4.9 – NEW GAINS COMPARED WITH THE OLD GAINS FOR THE POLE-PLACEMENT CONTROL LAW

	FC #	3	6	9	13	17
K_w	old	0.0009	0.0018	0.0011	0.0030	0.0013
$ft^{-1}s$	new	0.0009	0.0010	0.0011	0.0026	0.0010
K_q	old	-0.588	-0.889	-1.875	-1.094	-1.249
s	new	-0.588	-0.889	-1.875	-1.094	-1.249
K_{ε_q}	old	-1.600	-2.857	-2.200	-3.755	-3.429
rad	new	-1.600	-1.183	-2.200	-1.270	-1.252
G_0	old	-1.389	-0.592	-2.036	-1.600	-1.410
s	new	-0.834	-1.065	-1.629	-1.461	-1.439

The steps in the procedure can be summarized;

(i) for flight cases 6, 13 and 17 go back to the feedback gains obtained in table (3.3). For flight conditions 3 and 9 the feedback gains K_w, K_q and K_{ε_q} are maintained at the same values obtained in table (4.1).

(ii) Maintain K_{ε_q} and K_q at the values of table (3.3), for flight conditions 6, 13 and 17.

(iii) For flight conditions 6, 13 and 17 the following procedure was adopted;

Adjust K_w in order to obtain a CAP that satisfies Level 1, a reasonable phase-rate (less than 200° deg/Hz), a reasonable $\Delta\Phi_{LD}$ and a good $(q/q_{dp})_{ss} \simeq 1$. This adjustment was performed by simulating the system and looking for these parameters iteractively. As convergence is not difficult to obtain.

(iv) The new feedback gains are then determined.

(v) Design the lead filter based on the results obtained in (iii) for

$\Delta\Phi_{LD}$ and P.R.

(vi) With the lead filter, actuator, full aircraft model, feedback gains obtained in (iv), and the feedforward gain obtained in table(4.1), obtain the dropback characteristics. If the dropback criterion is satisfied then it is not necessary to change G_0. If the criterion is not satisfied then adjust G_0 by simulation using the value in table (4.1) as the starting point. After a few iterations the new G_0 is obtained and the redesign is then completed.

It should be noted that in steps (i), (ii), (iii) and (iv) no filter is included in the process, and in the steps (v) and (vi) then the lead filter is considered in the process. With this redesign of feedback gains, the pole placement control law is now located entirely in the region of moderate PIO. Table (4.10) shows the aircraft characteristics for the control law with redesigned gains but excluding the effects of the lead filter.

TABLE 4.10 - NEW AIRCRAFT CHARACTERISTICS WITH THE NEW FEEDBACK GAINS

FC #	CAP s^{-2}	$\left[\frac{q}{q_{dp}}\right]_{ss}$	P.R. deg/Hz	$\Delta\Phi_{LD}$ deg
3	0.099	0.99	-147	49.7
6	0.109	0.95	-122	46.6
9	0.235	1.07	-129	46.4
13	0.109	0.80	-120	53.0
17	0.157	0.93	-122	48.3

A comparison with table (4.8) shows the improvements obtained.

Now that the performance at all flight conditions is improved with respect to the requirements of the phase rate criterion, that is, they now require less than 50° of phase lead and they have less than

150°/Hz of phase rate, it is possible to design the phase lead filter. The filter was designed choosing the phase lead as 49.5° at 1 Hz, for all flight conditions. The resulting lead filter is:

$$PLF = \frac{(1 + 0.431\ s)}{(1 + 0.059\ s)} \tag{4.24}$$

or,

$$PLF = 7.3\ \frac{(s + 2.32)}{(s + 17)} \tag{4.25}$$

The 7.3 represents the necessary gain compensation in order to keep the slope of the closed loop attitude frequency response plot at a reasonable value at cross over, that is, lower than 100°/Hz . With this lead filter and the redesigned feedback gains, the control law satisfies CAP and the phase rate criterion. However, it must also satisfy the dropback criterion obtained with the redesign of the feedforward gain G_0 as already described before. Table (4.11) shows the phase rate criterion and dropback criterion parameters for the aircraft with the redesigned control law.

TABLE 4.11 – FINAL DROPBACK AND PHASE RATE OBTAINED

FC #	3	6	9	13	17
DB (rad)	0.05	0.06	0.18	0.09	0.01
P.R. (deg/Hz)	-76.5	-90.4	-100	-76.1	-91.2

It was noticed that, for some flight conditions the dropback is very sensitive to changes in the feedforward gain, as can be seen from the example of table (4.12). Thus the robustness of this design is poor with respect to dropback criterion when the feedforward gain is varied. If the design were performed for just one flight condition this problem would not be visible, which also shows that in order to get some "feel" for the design several flight cases must be analyzed.

TABLE 4.12 – VARIATIONS IN DB WITH CHANGES IN THE FEEDFORWARD GAIN AT 20000 FT MACH 0.80

G_0 (s)	DB (rad)
-1.135	-0.008
-1.156	-0.041
-1.245	0.170

4.3.4 THE OPTIMAL CONTROL LAW DESIGN

To adjust the optimal control law to satisfy the phase rate criterion it was not necessary to redesign the feedback gains as in the case of the pole placement control law. Since all the flight cases are located in the region of moderate PIO, and the phase rate obtained is less than 200°/Hz a phase lead filter can be designed directly. Considering the average phase lead required for all flight cases as 48.5° the resulting filter is:

$$PLF = 6.96 \frac{(s + 2.38)}{(s + 16.58)} \qquad (4.26)$$

With the introduction of this filter in the command path the phase rate criterion and CAP are satisfied, but, the dropback criterion is not satisfied. So it is necessary to redesign the feedforward gain only in order to restore good dropback characteristics. The redesign is based on the feedforward gain obtained in chapter 3, section 3.4, as the starting point for iterative adjustment. A new feedforward gain was obtained by simulating the aircraft response with full model, actuator, lead filter and control law with original feedback gains. Then with small changes to the initial value of G_0 it is easy to find a new value that satisfies the dropback criterion. Here the convergence is very fast, and the sensitivity of dropback to variations in G_0 is not a problem as with the pole placement control law design. So with this procedure the redesign is completed and the resulting feedforward gain, dropback and phase rate are listed in table (4.13)

TABLE 4.13 – FINAL FEEDFORWARD GAINS, DROPBACK AND PHASE–RATE OBTAINED

FC #	G_0 (s)		DB (rad)		P.R. (deg/Hz)
	old	new	old	new	
3	-1.927	-1.156	0.07	0.08	-91
6	-1.973	-1.184	0.12	0.09	-92
9	-2.188	-1.641	0.03	0.06	-83
13	-3.230	-2.584	0.01	0.12	-81
17	-2.282	-1.255	0.15	0.02	-84

4.3.5 CONCLUSIONS AND OBSERVATIONS

The final design characteristics of the aircraft with pole placement control law design are summarized in table (4.14) and the corresponding results for the aircraft with the optimal control law design are included in table (4.15). Now the following observations may be made,

(i) The optimal control law design has a greater pitch rate overshoot than the pole placement control law design as well as giving a faster response.

(ii) The optimal control law design results in a greater bandwidth than the pole placement control law design.

(iii) The pole placement control law design always has a greater phase and gain margin.

(iv) The inclusion of the phase lead filter has increased the bandwidth, phase margin and gain margin in both control law designs compared with the aircraft without lead filter.

(v) The magnitude of the feedforward gains has decreased in both designs, which is a good feature, since it represents lower control effort.

(vi) In the pole placement design the feedback gain K_{ε_q} has also decreased, which also represents lower control effort.

(vii) The dropback characteristic has been improved in both designs.

(viii) The pole placement design is not so robust as the optimal design with respect to the dropback characteristic when the feedforward gain is changed.

TABLE 4.14 – FINAL RESULTS WITH THE POLE-PLACEMENT DESIGN

FC #	q_m rad/sec	t_m sec	q_{ss} rad/sec	DB rad	ω_b rad/sec	M_p dB	G_M dB	P_M deg	P.R. deg/Hz
3	1.34	0.80	0.99	0.05	7.60	3.92	14.2	103	-76.5
6	1.32	0.60	0.99	0.06	9.30	2.65	12.4	90	-90.4
9	1.34	0.60	1.00	0.18	9.40	2.40	11.9	78	-100
13	1.31	1.70	0.92	0.09	5.50	3.50	15.6	133	-76.1
17	1.30	0.60	0.98	0.01	9.50	2.40	12.3	85	-91.2

TABLE 4.15 – FINAL RESULTS WITH THE OPTIMAL DESIGN

FC #	q_m rad/sec	t_m sec	q_{ss} rad/sec	DB rad	ω_b rad/sec	M_p dB	G_M dB	P_M deg	P.R. deg/Hz
3	1.56	0.60	0.99	0.08	10.0	5.30	10.9	64	-90.9
6	1.61	0.60	0.99	0.09	10.0	5.75	10.3	63	-91.6
9	1.49	0.70	0.99	0.06	9.0	5.00	12.3	82	-82.8
13	1.68	0.60	0.94	0.12	10.3	6.42	10.9	68	-81.3
17	1.41	0.70	0.99	0.02	8.5	4.40	13.0	91	-83.5

In addition the optimal control law design is more tolerant to adjustment than the pole placement control law design. As mentioned in Powell[7], the fact that the optimal design procedure is based on the choice of just one parameter, the weight matrix, simplifies the design very much. Whereas,the pole placement design is based on the direct choice of closed loop poles, i.e.,more than one parameter. In figure (4.9) the time response of both designs are compared, in figure (4.10) the frequency response of both designs are compared on the Nichols chart and in figure (4.11) on the bode plot, all for flight condition 6. Finally figure (4.12) shows the performance of the final pole placement design with respect to the dropback criterion and figure 4.13 shows the performance of the final optimal control law design with respect to the dropback criterion.

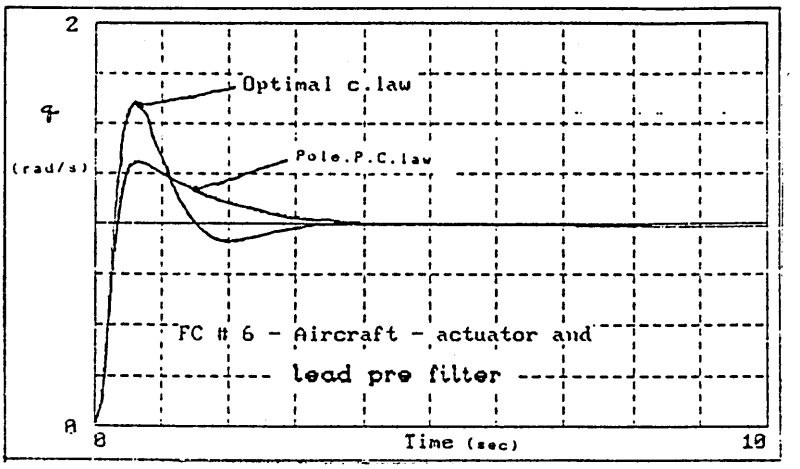

figure 4.9 - pitch-rate time response of both designs with command path filter at 20000 ft, mach 0.70.

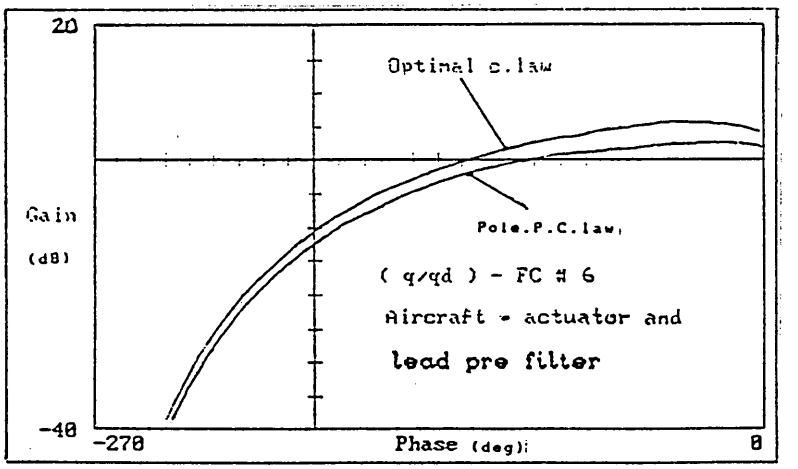

figure 4.10 - Nichols plot of pitch-rate frequency response of both designs with command path filter at 20000 ft, mach 0.70

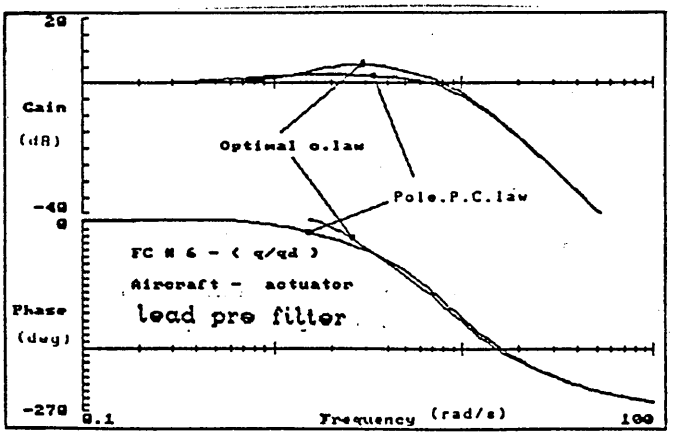

figure 4.11 - Bode plot of pitch-rate frequency response of both designs with command path filter at 20000 ft, mach 0.70

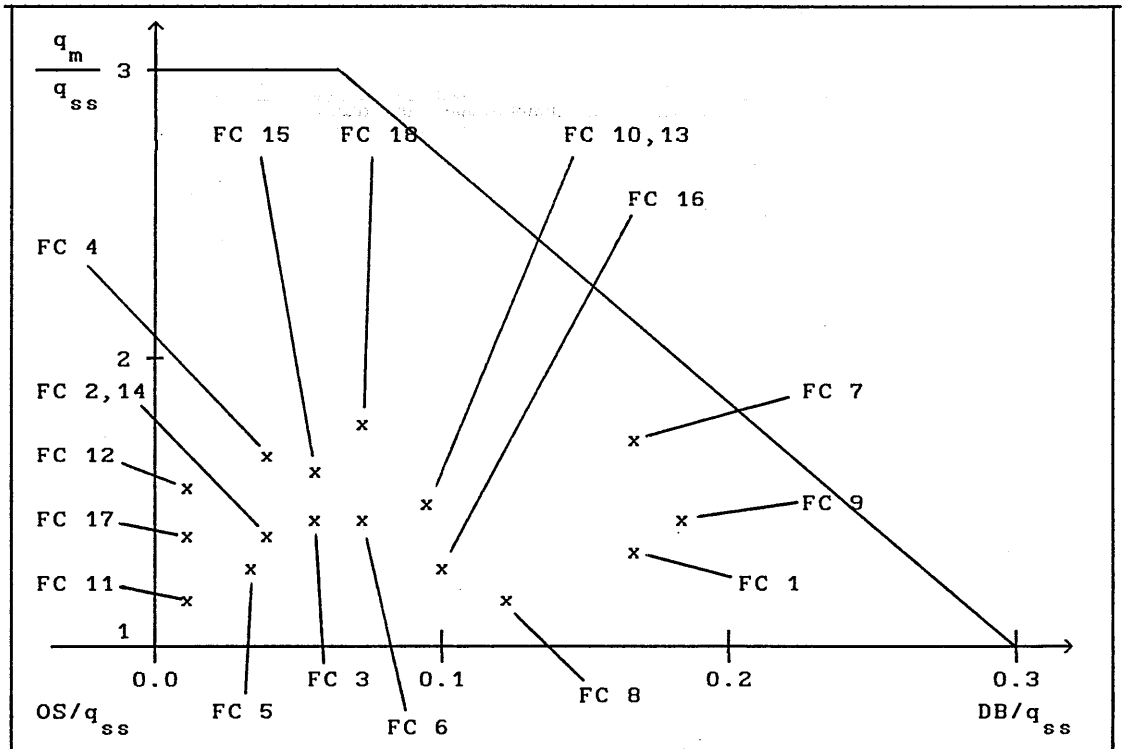

figure 4.12 - Dropback criterion plot of the augmented aircraft with command path lead filter and pole-placement design

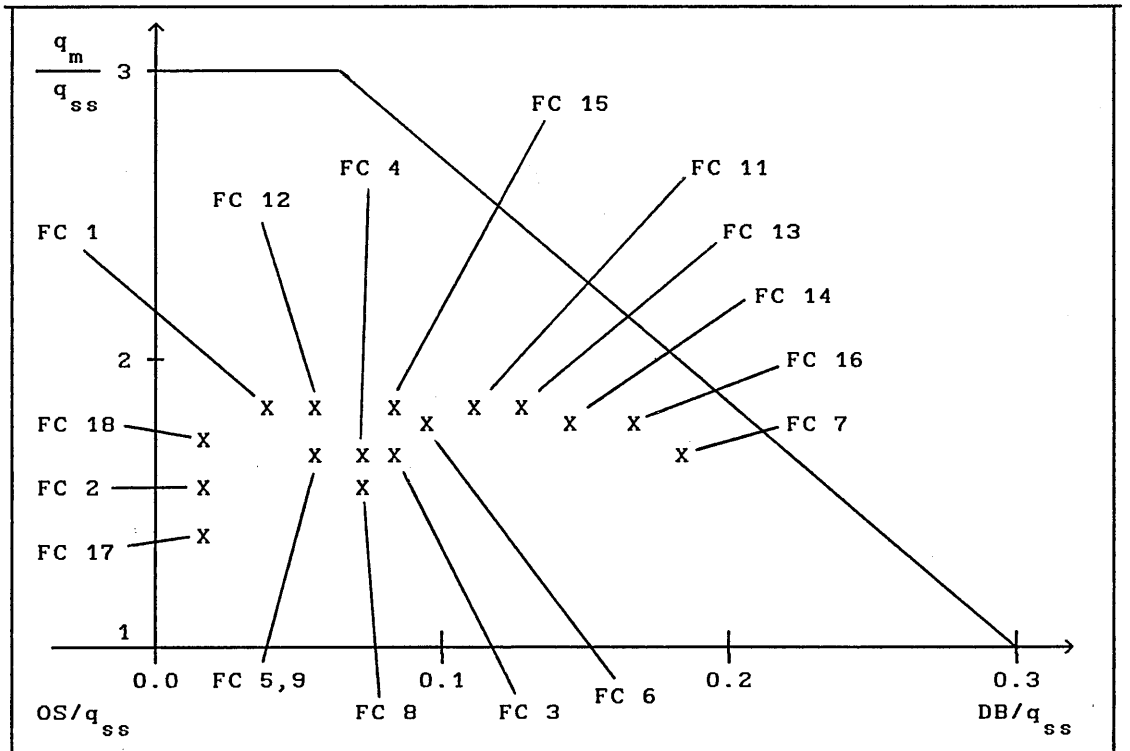

figure 4.13 - Dropback criterion plot of the augmented aircraft with command path lead filter and optimal control law design

5. FLIGHT CONTROL SYSTEM DESIGN USING THE DOYLE STEIN OBSERVER

5.1 INTRODUCTION

Having designed a satisfactory control law the design will now be extended to incorporate a Doyle-Stein observer. The inclusion of an observer is useful because it will allow the introduction of redundancy in the designed flight control system with respect to sensor failures. The Doyle-Stein observer is described in chapter 2, section 2.7, and also in the Doyle-Stein[6] classical paper. In the design a reduced order observer is used and the two methods of design described in chapter 2 will be used. Other references that also present comparable methods for observer design are Miron[69],Nelson[70] and D'Azzo[59].It is useful to remember that the Doyle-Stein observer has the following important properties:

(i) It Makes the closed loop transfer function from the reference input to the output the same as it is for full state feedback.
(ii) It has its poles at the transmission zeros of the open-loop system.
(iii) It does not require feedback of the control signal and thus has a constant transfer function, independent of the control gain.

Three observers will be designed, as follows:

(i) Observer when the sensed output of the aircraft is w
(ii) Observer when the sensed output of the aircraft is q
(iii) Observer when the sensed output of the aircraft is θ

The observer (i) is designed by the first method described in chapter 2, section 2.6.2, and the observers (ii) and (iii) are designed by the second method described in chapter 2, section 2.6.3.

5.2 THE DOYLE-STEIN OBSERVER WHEN THE OUTPUT IS w

When the output of the aircraft is w, normal velocity, the first design method is used. The aircraft state equation is given by,

$$\dot{x} = A\,x + B\,\eta \tag{5.1}$$

and it can be partitioned as,

$$\begin{bmatrix} \dot{x}_1 \\ \dot{x}_2 \end{bmatrix} = \begin{bmatrix} A_{11} & A_{12} \\ A_{21} & A_{22} \end{bmatrix} \begin{bmatrix} x_1 \\ x_2 \end{bmatrix} + \begin{bmatrix} B_1 \\ B_2 \end{bmatrix} \eta \tag{5.2}$$

with $x_1 = w$ (5.3)

and $x_2^T = [\, u \;\; q \;\; \theta \,]$ (5.4)

obviously $y = C_1\, x_1 = w$ (5.5)

and $C_1 = 1$, or I the identity matrix (5.5.a)

As described in chapter 2, the observer is of the form,

$$\dot{z} = F\,z + \bar{G}\,y + H\,\eta \tag{5.6}$$

$$\hat{x}_2 = L\,y + z \tag{5.7}$$

and figure 5.1 represents the aircraft plus the observer.

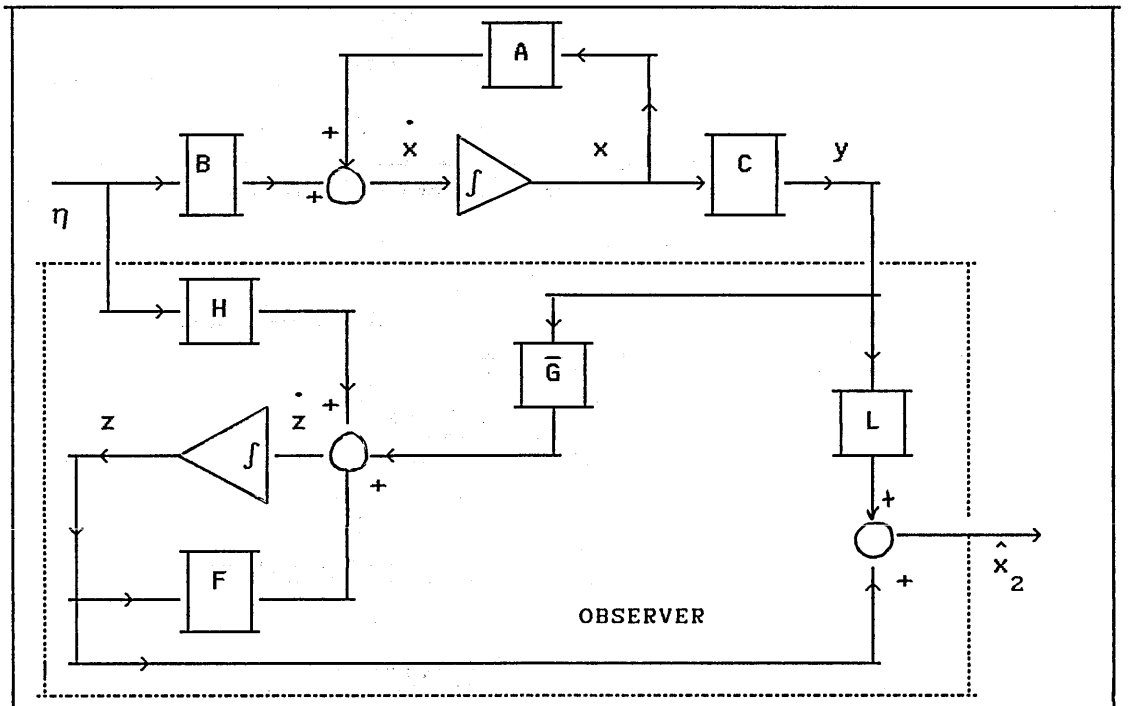

figure 5.1 - aircraft and observer block diagram for the first method of observer design.

the state $\hat{x}_2$ is the estimate of x_2 and the matrices F, $\bar{G}$, and H are obtained as in (2.99), (2.100) and (2.102) respectively and take the form:

$$F = A_{22} - L\,C_1 A_{12} \tag{5.8}$$

$$\bar{G} = (A_{21} - L\,C_1 A_{11})\,C_1^{-1} + F\,L \tag{5.9}$$

$$H = B_2 - L\,C_1 B_1 \tag{5.10}$$

L is called the gain matrix of the observer. It is clear in this method that to obtain the condition of zero feedback from the control input signal to the observer it is necessary that H = 0. It is interesting to note that this is not always possible, and when it is not possible then it is necessary to use the second design method. So for H = 0 it is necesary that;

$$B_2 - L\,C_1 B_1 = 0 \tag{5.11}$$

Solving equation (5.11) the gain matrix L of the observer can be found. With L determined it is possible, in equation (5.8), to obtain F and then in equation (5.9) to obtain $\bar{G}$. With this procedure the poles of the observer are automatically located at the transmission zeros of the open loop system, this is shown in Friedland[13]. In this case the zeros fall exactly on the transmission zeros of the open loop transfer function w/η . In this way the Doyle-Stein observer is designed, and its properties are maintained. In appendix D the matrices L, F and $\bar{G}$ obtained are listed for the flight cases studied, for example these matrices for flight case 3 are,

$$L = \begin{bmatrix} -0.011 \\ 0.056 \\ 0.0 \end{bmatrix} = \begin{bmatrix} l_{11} \\ l_{21} \\ l_{31} \end{bmatrix} \tag{5.12}$$

It is noted that $l_{31} = 0$ for all flight cases and l_{21} is pratically constant with flight case.

$$\bar{G} = \begin{bmatrix} 0.0482 \\ -2.1774 \\ 0.0564 \end{bmatrix} = \begin{bmatrix} \bar{g}_{11} \\ \bar{g}_{21} \\ \bar{g}_{31} \end{bmatrix} \qquad (5.13)$$

It is noted that $\bar{g}_{31} = l_{21}$ for all flight cases.

$$F = \begin{bmatrix} -0.0099 & -0.0550 & -32.2 \\ 0.0082 & -39.62 & 0.0217 \\ 0 & 1 & 0 \end{bmatrix} = \begin{bmatrix} f_{11} & f_{12} & f_{13} \\ f_{21} & f_{22} & f_{23} \\ f_{31} & f_{32} & f_{33} \end{bmatrix} \qquad (5.14)$$

It is noted that for all flight cases $f_{31} = 0$, $f_{32} = 1$, $f_{33} = 0$ and f_{13} is constant. Such features are very good in terms of implementation. So this observer design requires that the following gains are scheduled with flight condition,

$$l_{11}\ ,\ \bar{g}_{21}\ ,\ \bar{g}_{11}\ ,\ f_{11}\ ,\ f_{12}\ ,\ f_{21}\ ,\ f_{22} \text{ and } f_{23}$$

that is 8 parameters.

5.3 THE DOYLE STEIN OBSERVER WHEN THE OUTPUT IS q

5.3.1 INTRODUCTION

When the output is pitch rate q, the same method can be applied to design the observer. However, in this case, the design will have a problem because one of the transmission zeros of the transfer function q/η is zero, and so one of the observer poles will be located at zero. Then the closed loop aircraft will therefore have two poles at zero since the aircraft already has a pole at zero. With two poles at zero the aircraft will not be BIBO stable and so it is impossible to implement this observer design. The solution is to use a second method to design the observer, as described in chapter 2, section 2.6.3.

5.3.2 THE DESIGN

The procedure for design is as follows. The observer dynamics are again given by,

$$\dot{z} = F z + \bar{G} y + H \eta \tag{5.15}$$

the estimated vector is now given by,

$$\hat{x}_2 = M y + N z \tag{5.16}$$

Again the aircraft state equation is,

$$\dot{x} = A x + B \eta \tag{5.17}$$

$$y = C x = q \tag{5.17.a}$$

$$C = [\ 1\ 0\ 0\ 0\ ] \tag{5.17.b}$$

and again it can be partitioned as ;

$$\begin{bmatrix} \dot{x}_1 \\ \dot{x}_2 \end{bmatrix} = \begin{bmatrix} A_{11} & A_{12} \\ A_{21} & A_{22} \end{bmatrix} \begin{bmatrix} x_1 \\ x_2 \end{bmatrix} + \begin{bmatrix} B_1 \\ B_2 \end{bmatrix} \eta \tag{5.18}$$

with, $x_1 = q$ (5.19)

$$x_2^T = [\ u\ w\ \theta\ ] \tag{5.20}$$

and $$\hat{x}_2^T = [\ \hat{u}\ \hat{w}\ \hat{\theta}\ ] \tag{5.20.a}$$

Figure 5.2 shows a block diagram representation of the aircraft plus observer in this case.

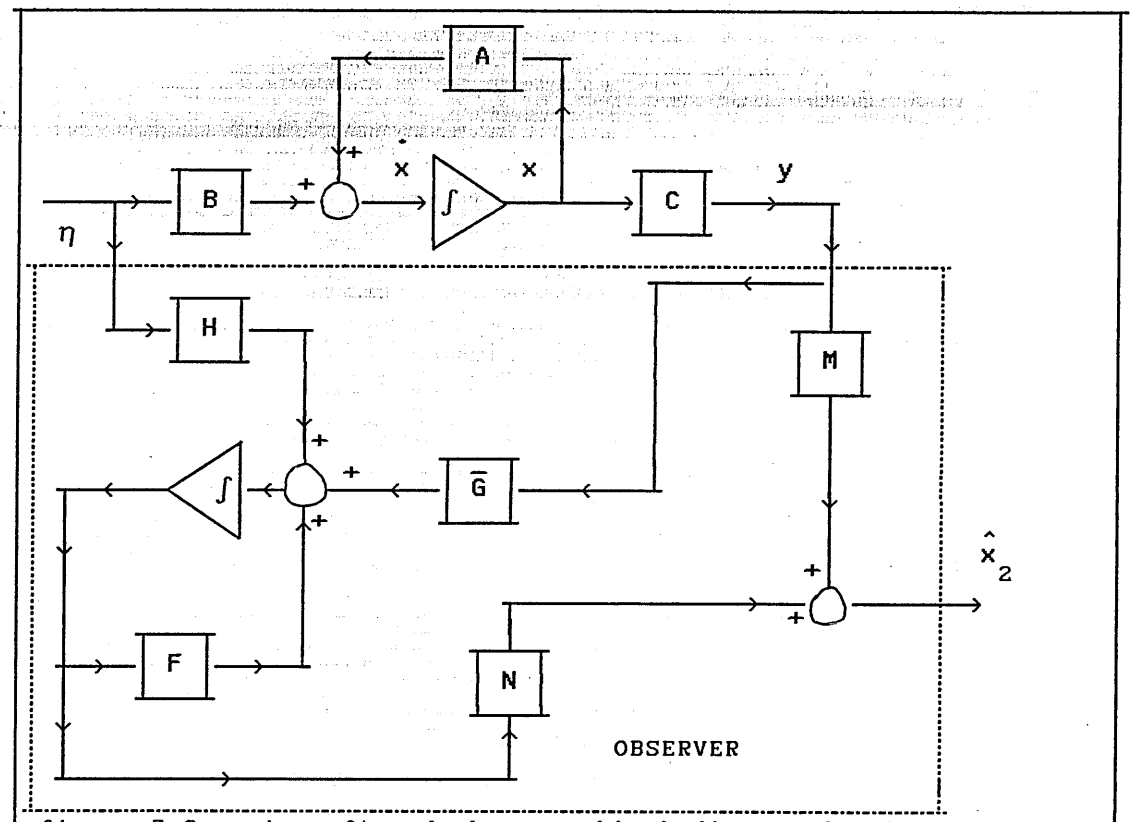

figure 5.2 - aircraft and observer block diagram for the second method of observer design.

As already explained in chapter 2, it is necessary first to choose the observer poles, that is, the eigenvalues of the F matrix. However, since the design is for a Doyle-Stein observer, the observer poles must be located at the transmission zeros of the open loop system. Then F is choosen as a diagonal matrix with the transmission zeros of the open loop tranfer function q/η in the main diagonal. One of the transmission zeros of q/η is zero and, as explained before, it is not possible to use this transmission zero, but it is possible to use a negative number as close as possible to zero to replace this particular transmission zero. The first choice for all flight cases was -0.01, and the results have shown that this value works quite well. This choice can be made based on the performance of the system, so it is iterative. That is , once a value is choosen the performance of the aircraft with observer is assessed, if satisfactory this pole is obviously a good choice if not, then try other pole. The convergence is very fast with the available software in these days.

Now, it is also necessary to choose $\bar{G}$, and the method says to choose $\bar{G}$ with the condition that the pair $(F,\bar{G})$ be controllable. For simplicity $\bar{G}$ was choosen initially as

$$\bar{G}^T = [\ 1\ 1\ 1\ ] \tag{5.21}$$

This choice was maintained for all flight cases, and the controlability of the pair $(F,\bar{G})$ for each flight case was checked in order to proceed with the design.

The next step is to find H, obtained as a solution of,

$$H = T\ B \tag{5.22}$$

where T is given by solving the Lyapunov equation,

$$F\ T + T\ (-A) = -\ \bar{G}\ C \tag{5.23}$$

and the estimated state vector will be:

$$\hat{x} = \begin{bmatrix} C \\ \cdots\cdots \\ T \end{bmatrix}^{-1} \begin{bmatrix} y \\ \cdots\cdots \\ z \end{bmatrix} = P^{-1} \begin{bmatrix} y \\ \cdots\cdots \\ z \end{bmatrix} \tag{5.24}$$

where, $\hat{x}^T = [\ \hat{x}_1 \vdots \hat{x}_2\ ]$ (5.25)

$$P = \begin{bmatrix} C \\ \cdots\cdots \\ T \end{bmatrix} \tag{5.25.a}$$

and, $\hat{x}_2$ can be expressed as equation (5.10)

$$\hat{x}_2 = M\ y + N\ z \tag{5.26}$$

So the matrices M and N are simply submatrices of P^{-1} and the design is completed. By way of eaxmple these matrices are listed here for flight condition 3, the remaining flight conditions are contained in appendix E.

$$H = \begin{bmatrix} 0 \\ 0 \\ -0.016 \end{bmatrix} = \begin{bmatrix} h_{11} \\ h_{21} \\ h_{31} \end{bmatrix} \tag{5.26.a}$$

$$M = \begin{bmatrix} 35.4 \\ 12.6 \\ -0.019 \end{bmatrix} = \begin{bmatrix} m_{11} \\ m_{21} \\ m_{31} \end{bmatrix} \qquad (5.26.b)$$

$$N = \begin{bmatrix} 4482 & -102 & -4349 \\ -658 & 704 & 634 \\ -1.4 & 0.03 & 2.3 \end{bmatrix} = \begin{bmatrix} n_{11} & n_{12} & n_{13} \\ n_{21} & n_{22} & n_{23} \\ n_{31} & n_{32} & n_{33} \end{bmatrix} \qquad (5.26.c)$$

$$F = \begin{bmatrix} -0.0175 & 0 & 0 \\ 0 & -0.9859 & 0 \\ 0 & 0 & -0.01 \end{bmatrix} = \begin{bmatrix} f_{11} & f_{12} & f_{13} \\ f_{21} & f_{22} & f_{23} \\ f_{31} & f_{32} & f_{33} \end{bmatrix} \qquad (5.26.d)$$

In this case it is necessary to schedule the following parameters:

$$f_{11}\ ,\ f_{22}\ ,\ m_{11}\ ,\ m_{21}\ ,\ n_{11}\ ,\ n_{12}$$
$$n_{13}\ ,\ n_{21}\ ,\ n_{22}\ ,\ n_{23}\ ,\ n_{31}\ ,\ h_{31}$$

That is, 12 parameters, this is a disadvantage with respect to the previous design in terms of implementation.

The parameters m_{31}, n_{32} and n_{33} are basically constant for all flight cases. It is also noticed that the element h_{31} in the matrix H is not exactly zero and, as expected, this is due to the fact that an approximation to the exact transmission zero was used in the design. For this flight case, and all other flight cases, this element is very small, and as will be seen later its influence on performance can be regarded as negligible.

5.4 THE DOYLE–STEIN OBSERVER WHEN THE OUTPUT IS θ

Here the design method is the same as in the previous section. So again, the aircraft state equation is;

$$\dot{x} = A\,x + B\,\eta \qquad (5.27)$$

the observer is given by; $\dot{z} = F\,z + \bar{G}\,y + H\,\eta$ (5.28)

the estimated state is ; $\hat{x}_2 = M\,y + N\,z$ (5.29)

The design procedure is the same as in the previous section. However,

here the problem is not that one of the transmission zeros of θ/η is zero but, one of the transmission zeros of θ/η is at infinity, thus the design is based on the choice of an approximate pole as close as possible to infinity. The choice must be made based on the performance obtained, so one must choose a value for this third pole (θ/η has two real transmission zeros). Design the observer, check that all elements of H are close to zero, compare the frequency response of the aircraft with control law and the observer with the frequency response of the aircraft and control law, if so, then the choice is acceptable. If not, then another choice must be made and the problem repeated. This iterative procedure is in fact fast, for this design three choices were evaluated, s = -50 ; s = - 15 , and s = - 4 , and the analysis showed that s = -4 has an acceptable performance. That is, the aircraft with control law and observer including this pole and the other two poles in the real transmission zeros of θ/η, has a performance that matches the aircraft with only the control law and no observer. Also the matrix H has its elements close to zero.

The results obtained for flight condition 3 for example are listed here. Appendix F contains the observer matrices for the other flight cases studied.

$$H = \begin{bmatrix} -0.0001 \\ -0.0008 \\ 0.1433 \end{bmatrix} \qquad (5.29.a)$$

$$N = \begin{bmatrix} 43.6 & -33.2 & 2.6 \\ -677 & 4.9 & 247 \\ 0.52 & -0.002 & -14 \end{bmatrix} \qquad (5.29.b)$$

$$M = \begin{bmatrix} -7.3 \\ 737 \\ 3 \end{bmatrix} \qquad (5.29.c)$$

$$F = \begin{bmatrix} -0.9859 & 0 & 0 \\ 0 & -0.0175 & 0 \\ 0 & 0 & -4 \end{bmatrix} \qquad (5.29.d)$$

For this case the elements; f_{11}, f_{22}, h_{31}, m_{11}, m_{21}

n_{11}, n_{13}, n_{21}, n_{22}, n_{31}

must be scheduled with flight condition. It is noted that in this design the element h_{31} is not so close to zero as in the previous cases. The performance of the design shows that this does not destroy the Doyle-Stein condition. So the Doyle-Stein observer has some degree of robustness with respect to variations in the elements of the matrix H, that is variations in H within reasonable limits do not destroy the match between the frequency response of the sensor based control law and the observer based control law or, as the literature of today says, the loop tranfer recovery (Stevens-Lewis[18]).

5.5 A COMPARISON OF THE PERFORMANCE OF THE OBSERVER BASED CONTROL LAW WITH THE PERFORMANCE OF THE SENSOR BASED CONTROL LAW

5.5.1 INTRODUCTION

Having designed the alternative observers for a range of flight conditions these were evaluated with the previously designed pole-placement or optimal control law designs. Since various combinations were evaluated the following identification is used;

CL_SB sensor based control law, with the pole placement or with the optimal design. The baseline control law for comparative purposes.

CL_OB_w observer based control law, that is the control law with observer when the output of the aircraft is w, again with the optimal design or with the pole-placement design.

CL_OB_q observer based control law, that is the control law with observer when the output of the aircraft is q, again with the optimal design or with the pole-placement design.

CL_OB_θ observer based control law, that is the control law with observer when the output of the aircraft is θ, again with the optimal design or with the pole-placement design.

The study was performed by simulating each complete control law system with an ACSL program, and by comparing the results. An analytical study was also performed in order to compare the frequency response of each system as well as the time response. The same reference input was applied in each case and the results, comprising the time histories appropriate to a height of 20000 ft at mach 0.70 only are shown, also shown is the frequency response comparison.

5.5.2 SENSOR BASED CONTROL LAW

The control law designs considered here are those obtained in chapter 4, that is, a control law that satisfyies CAP, dropback criterion and phase-rate criterion. Considering figure 4.6 which defines the basic control law, that is, the sensor based control law.

$$\dot{\varepsilon}_q = q - q_d \tag{5.30}$$

and $$\eta_c = -K_w w - K_q q - K_{\varepsilon_q} \varepsilon_q + G_0 q_d \tag{5.31}$$

where η_c is the input to the actuator.
now q_d is the output of the lead filter introduced in chapter 4 ,and shown in figure 4.6, and q_{dp} is the reference input, that now is also the input to the lead filter.

It is possible to write ; $\dot{\theta} = q$ (5.32)

and so , $\theta = \frac{q}{s}$ (5.33)

From (5.30) $\varepsilon_q = \frac{q}{s} - \frac{q_d}{s}$ (5.34)

Defining $\theta_d = \frac{q_d}{s}$ (5.35)

than $\varepsilon_q = \theta - \theta_d$ (5.36)

substituting into (5.31)

$$\eta_c = -K_w w - K_q q - K_{\varepsilon_q} \theta + K_{\varepsilon_q} \theta_d + G_0 q_d \tag{5.37}$$

$$\eta_c = -\begin{bmatrix} 0 & K_w & K_q & K_{\varepsilon_q} \end{bmatrix} x + K_{\varepsilon_q} \theta_d + G_0 q_d \tag{5.38}$$

the state vector is $x^T = [\ u\ w\ q\ \theta\ ]$ (5.39)

The system can be represented by figure (5.3).

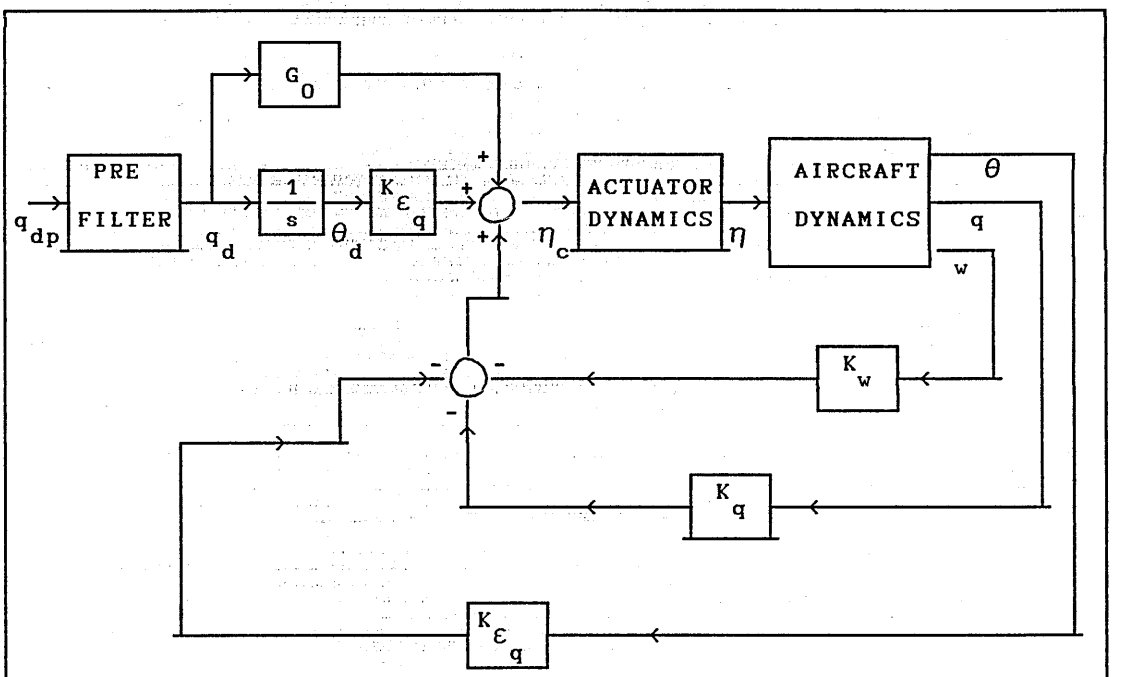

figure 5.3 - alternative representation of control law design obtained from figure 4.6

The lead filter considered was obtained in chapter 4, section 4.3.3 for the pole placement control law design and section 4.3.4 for the optimal control law design. In state space model form the lead filter can be written as:

$$\dot{x}_{LF} = a_{LF}\, x_{LF} + b_{LF}\, q_{dp} \tag{5.40}$$

$$q_d = c_{LF}\, x_{LF} + d_{LF}\, q_{dp} \tag{5.41}$$

For the pole-placement control law design the filter parameters are:

$$a_{LF} = -16.95\ ,\ b_{LF} = 1\ ,\ c_{LF} = -106.8\ ,\ d_{LF} = 7.3$$

and for the optimal control law design,

$$a_{LF} = -16.66\ ,\ b_{LF} = 1\ ,\ c_{LF} = -100.0\ ,\ d_{LF} = 7.0$$

the mathematical model of the actuator can be given as ;

$$\dot{x}_A = A_A x_A + B_A \eta_c \tag{5.42}$$

$$\text{with} \quad x_A^T = [\ \eta \ v\ ] \tag{5.43}$$

and the actuator considered is actuator no.2 used in chapter 3. The aircraft dynamics can be written as ;

$$\dot{x} = A\, x + [\ B\ Z41\ ]\, x_A \tag{5.44}$$

$$\text{with} \quad Z41^T = [\ 0 \quad 0 \quad 0 \quad 0\ ] \tag{5.45}$$

The matrix A, and matrix B are given in appendix A for the flight cases studied , and the state vector of the aircraft is ,

$$x^T = [\ u\ w\ q\ \theta\ ] \tag{5.46}$$

The control law is given by,

$$\eta_c = -G\, x + G_0 q_d + K_{\varepsilon_q} \theta_d \tag{5.47}$$

$$\text{with} \quad G = [\ 0 \quad K_w \quad K_q \quad K_{\varepsilon_q}\ ] \tag{5.48}$$

and θ_d is defined in (5.35). With these equations the closed loop model can be obtained as follows,

$$\begin{bmatrix} \dot{x} \\ \dot{x}_A \\ \dot{x}_{LF} \\ \dot{\theta}_d \end{bmatrix} = \begin{bmatrix} A & [B\ Z41] & Z41 & Z41 \\ -B_A G & A_A & B_A G_0 c_{LF} & B_A K_{\varepsilon_q} \\ Z14 & Z12 & a_{LF} & 0 \\ Z14 & Z12 & c_{LF} & 0 \end{bmatrix} \begin{bmatrix} x \\ x_A \\ x_{LF} \\ \theta_d \end{bmatrix} + \begin{bmatrix} 0 \\ B_A G_0 d_{LF} \\ b_{LF} \\ d_{LF} \end{bmatrix} q_{dp} \tag{5.49}$$

$$\text{with} \quad Z14 = [\ 0\ 0\ 0\ 0\ ]\ , \quad Z12 = [\ 0\ 0\ ]$$

That is, the control law will be considered as if implemented with three sensors, for w, for q and for θ, as in figure 5.3. The reference command input used in the ACSL simulations is shown in figure (5.4). It is commonly used to represent a pilot input to the aircraft since it is more representative of reality than a step.

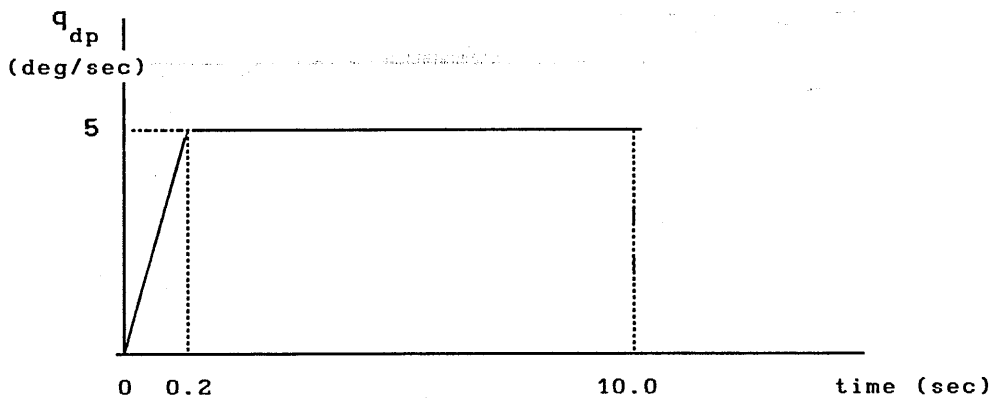

figure 5.4 - pilot input used in the ACSL simulations.

In figure (5.5) the time histories obtained with the optimal control law at 20000 ft, mach 0.70 with CL_SB are shown. The study has shown that the dropback criterion was satisfied as already reported in chapter 4. In figure 5.6 the frequency response of the closed loop system is reported and is used for comparison with the observer based control laws.

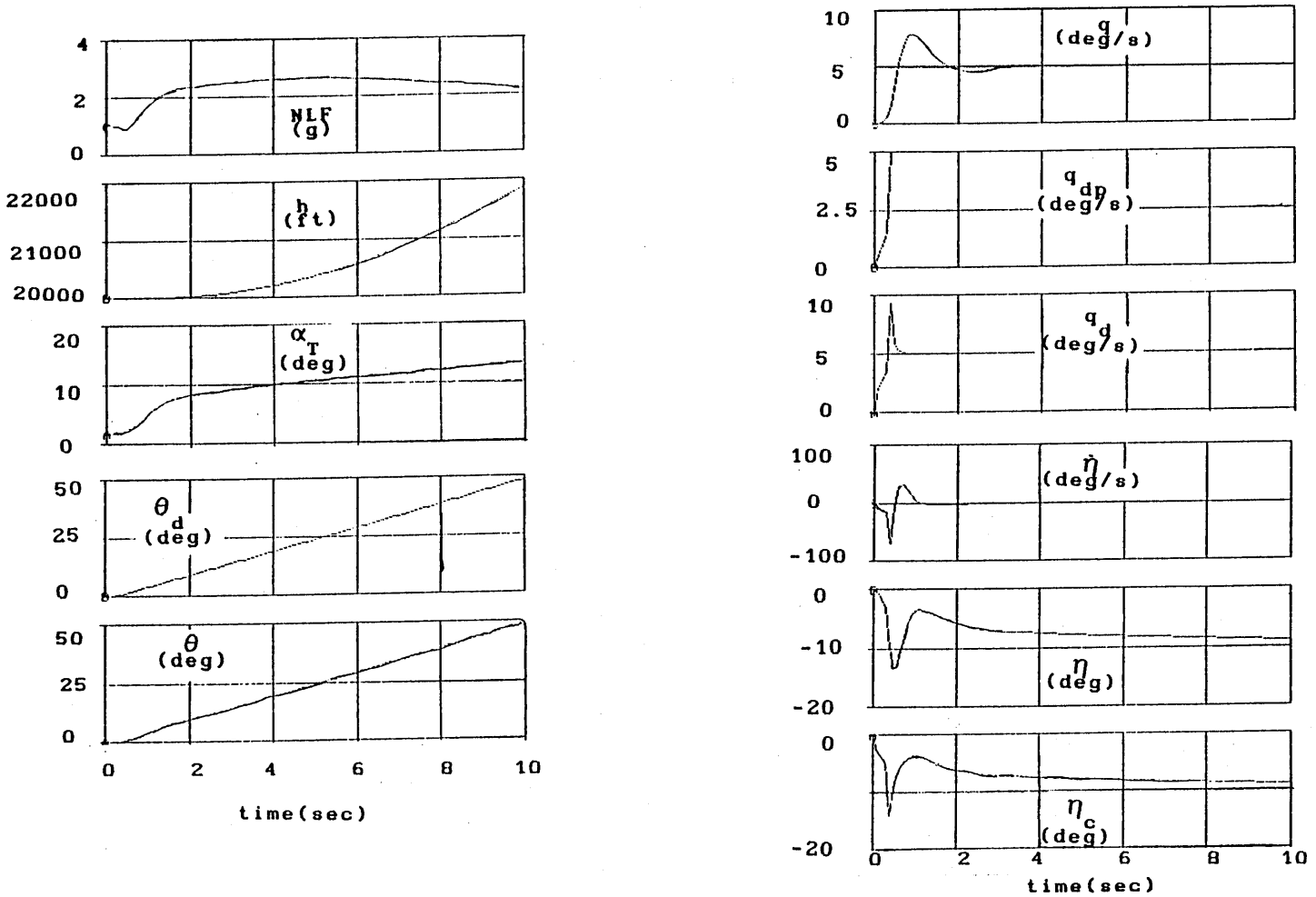

figure 5.5 - time histories of the aircraft with the optimal control law design and control law CL_SB at 20000 ft mach 0.70 .

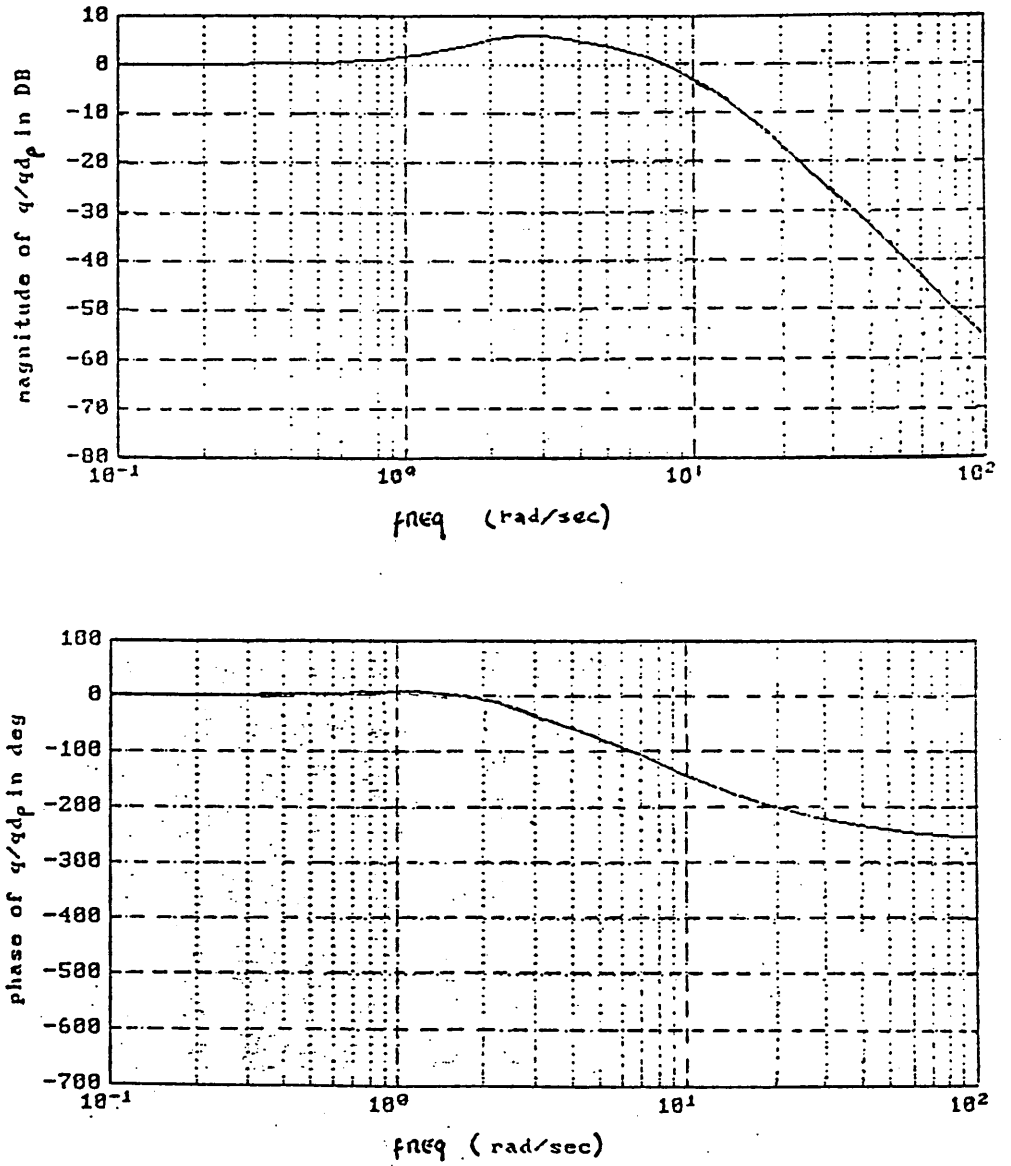

figure 5.6 - pitch-rate frequency response of the aircraft with optimal control law design CL_SB at 20000 ft mach 0.70

5.5.3 OBSERVER BASED CONTROL LAW CL_OB_w

The same simulation exercise was performed with the aircraft and observer based control law CL_OB_w, that is, with an angle of attack sensor only. Figure 5.7 shows the structure considered:

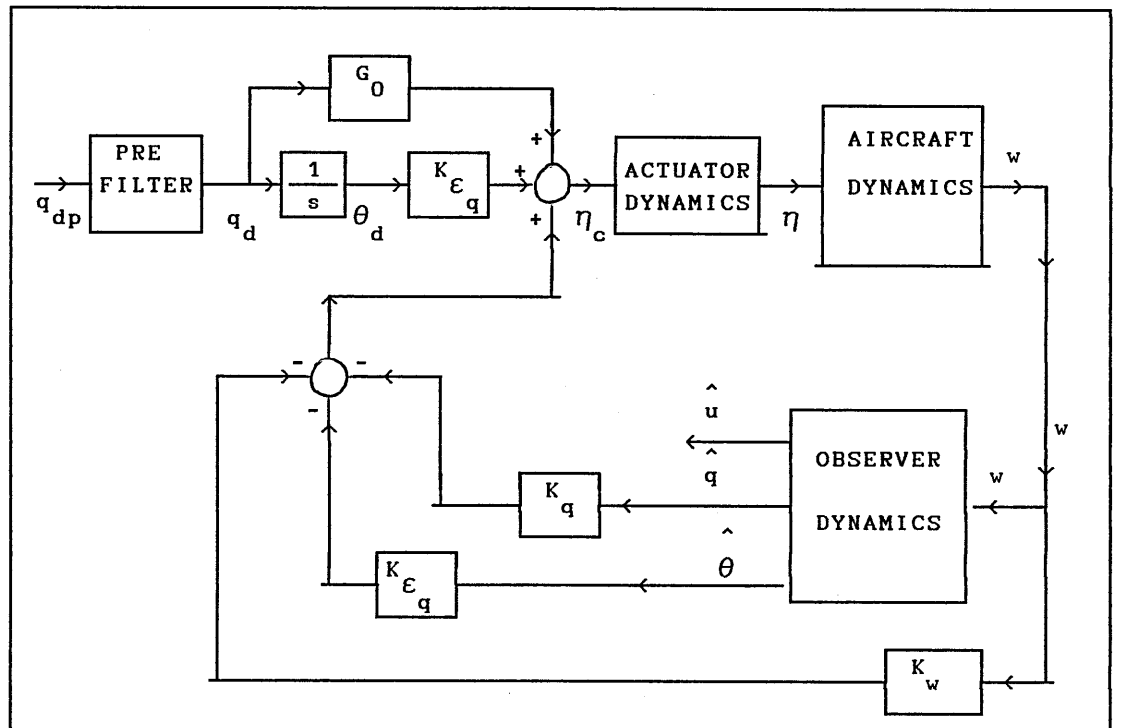

figure 5.7 structure of the observer-based control law CL_OB_w

The lead filter is again given by,

$$\dot{x}_{LF} = a_{LF} x_{LF} + b_{LF} q_{dp} \tag{5.50}$$

$$q_d = c_{LF} x_{LF} + d_{LF} q_{dp} \tag{5.51}$$

Again the actuator is actuator no.2 with the mathematical model,

$$\dot{x}_A = A_A x_A + B_A \eta_c \tag{5.52}$$

with $x_A^T = [\ \eta\ v_\eta\ ]$ (5.53)

Now the aircraft is given by,

$$\dot{x}_1 = A_{11} x_1 + A_{12} x_2 + [B_1 \; 0]\, x_A \tag{5.54}$$

$$\dot{x}_2 = A_{21} x_1 + A_{22} x_2 + [B_2 \; Z31]\, x_A \tag{5.55}$$

$$\text{with } Z31^T = [\,0\;0\;0\,] \tag{5.55.a}$$

$$\text{with } x_1 = w \tag{5.56}$$

$$\text{and } x_2^T = [u\; q\; \theta] \tag{5.56.a}$$

The observer dynamics are described by,

$$\dot{z} = F z + \bar{G} x_1 + H \eta \tag{5.57}$$

$$\hat{x}_2 = L x_1 + z \tag{5.58}$$

$$\text{with} \quad \hat{x}_2^T = [\,\hat{u}\;\hat{q}\;\hat{\theta}\,] \tag{5.59}$$

F, $\bar{G}$, H and L are obtained as explained in section (5.2) and are listed in appendix D for the flight cases analyzed. The control law is given by ;

$$\eta_c = -G_1 x_1 - G_2 \hat{x}_2 + G_0 q_d + K_{\varepsilon_q} \theta_d \tag{5.60}$$

$$\text{with } G_1 = K_w \tag{5.61}$$

$$\text{and } G_2 = [\,0\; K_q\; K_{\varepsilon_q}\,] \tag{5.62}$$

The closed loop model is then,

$$\dot{x} = A x + B u \tag{5.63}$$

$$\text{with } x^T = [\,x_1\; x_2\; x_A\; z\; q_d\; x_{LF}\,] \tag{5.64}$$

$$\text{and } u = q_{dp} \tag{5.65}$$

$$A = \begin{bmatrix} A_{11} & A_{12} & [B_1\ 0] & Z13 & 0 & 0 \\ A_{21} & A_{22} & [B_2\ Z31] & Z33 & Z31 & Z31 \\ -B_A(G_1+G_2L) & Z23 & A_A & -B_A G_2 & B_A K_{\varepsilon_q} & B_A G_{c_{LF}} \\ \bar{G} & Z33 & [H\ Z31] & F & Z31 & Z31 \\ 0 & Z13 & Z12 & Z13 & 0 & c_{LF} \\ 0 & Z13 & 0 & Z13 & 0 & a_{LF} \end{bmatrix} \quad (5.66)$$

$$B^T = [\ 0\ \ Z31\ \ B_A G_{d_{LF}}\ \ Z31\ \ d_{LF}\ \ b_{LF}\ ] \quad (5.67)$$

where ; $Z31^T = [\ 0\ 0\ 0\ ]$ (5.67.a)

$$Z23 = \begin{bmatrix} 0 & 0 & 0 \\ 0 & 0 & 0 \end{bmatrix} \quad (5.67.b)$$

$$Z33 = \begin{bmatrix} 0 & 0 & 0 \\ 0 & 0 & 0 \\ 0 & 0 & 0 \end{bmatrix} \quad (5.67.c)$$

$$Z13 = [\ 0\ \ 0\ \ 0\ ] \quad (5.67.d)$$

In Figure (5.8) the time histories obtained with the optimal control law design are shown and a comparison with the results of figure 5.5 shows a very good agreement between both. The match between CL_SB and CL_OB_w is not exactly perfect because CL_OB_w was designed with a MATLAB model incorporating the matrix A and B of the aircraft but, in the ACSL model the A and B matrix of the aircraft were a little different from those used in the aircraft MATLAB model. The differences in the elements of both matrices are around 12 % and arise due to the fact that the ACSL model takes the values of the elements from an aerodynamic data base and so uses interpolation functions to obtain the values whereas, the values used in the MATLAB model were taken directly from Heffley[11]. This fact has shown that CL_OB_w is not so robust to aircraft parameter variations when compared with CL_SB. This means that if the aircraft parameters vary then the time histories obtained with the aircraft augmented with CL_OB_w will not

be exactly the same as the time histories obtained with the aircraft augmented with CL_SB. Figure 5.9 shows the bode plot frequency response of the pitch rate transfer function of the aircraft with CL_OB_w, and a comparison with figure 5.6 shows a very good agreement, and so it shows that the Doyle-Stein observer works perfectly. This was expected since CL_OB_w was designed with an observer with poles exactly at the transmission zeros of the open loop tranfer function w/η.

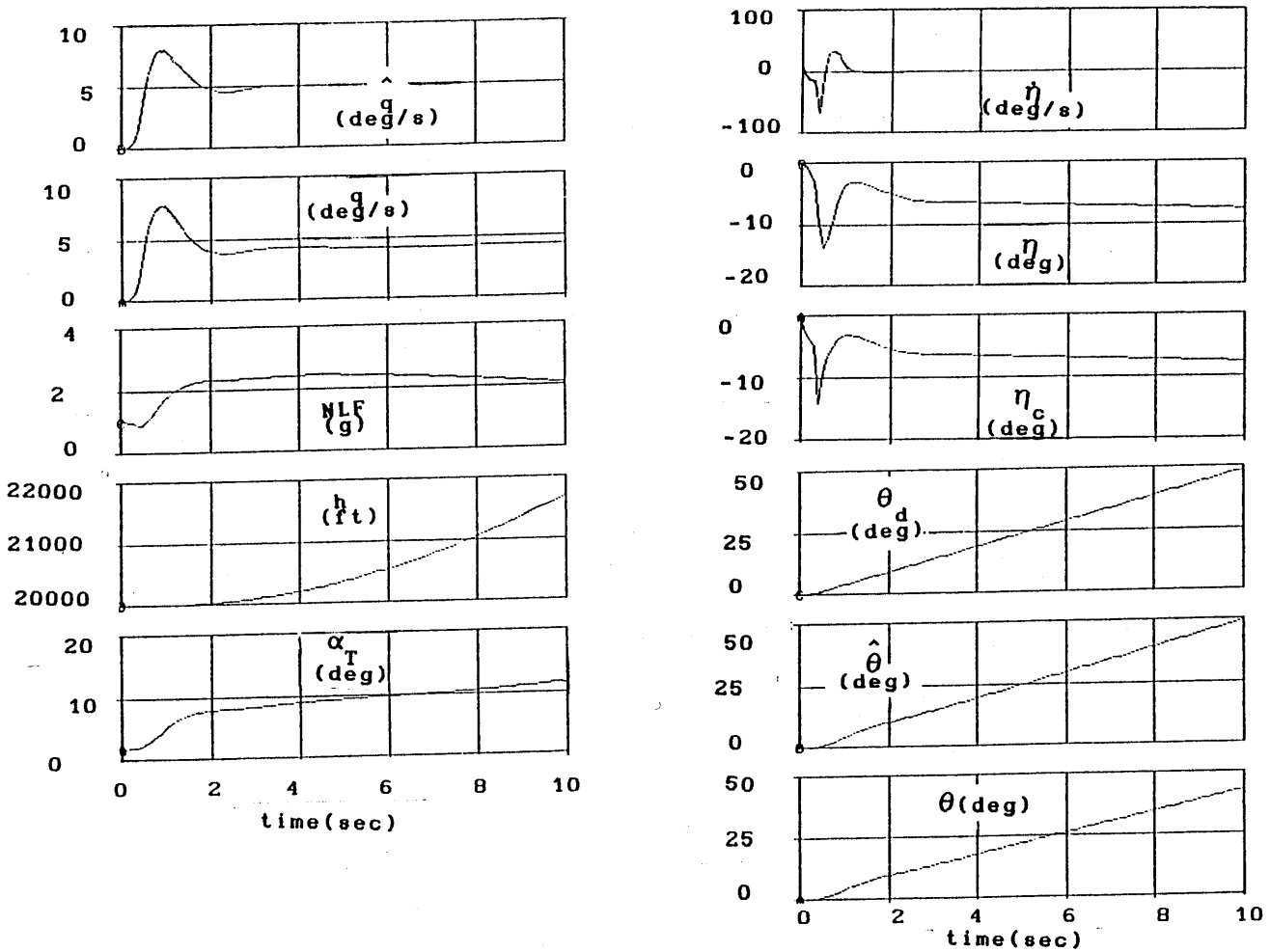

figure 5.8 - time histories of the aircraft with the optimal control law design and control law CL_OB_w at 20000 ft mach 0.70

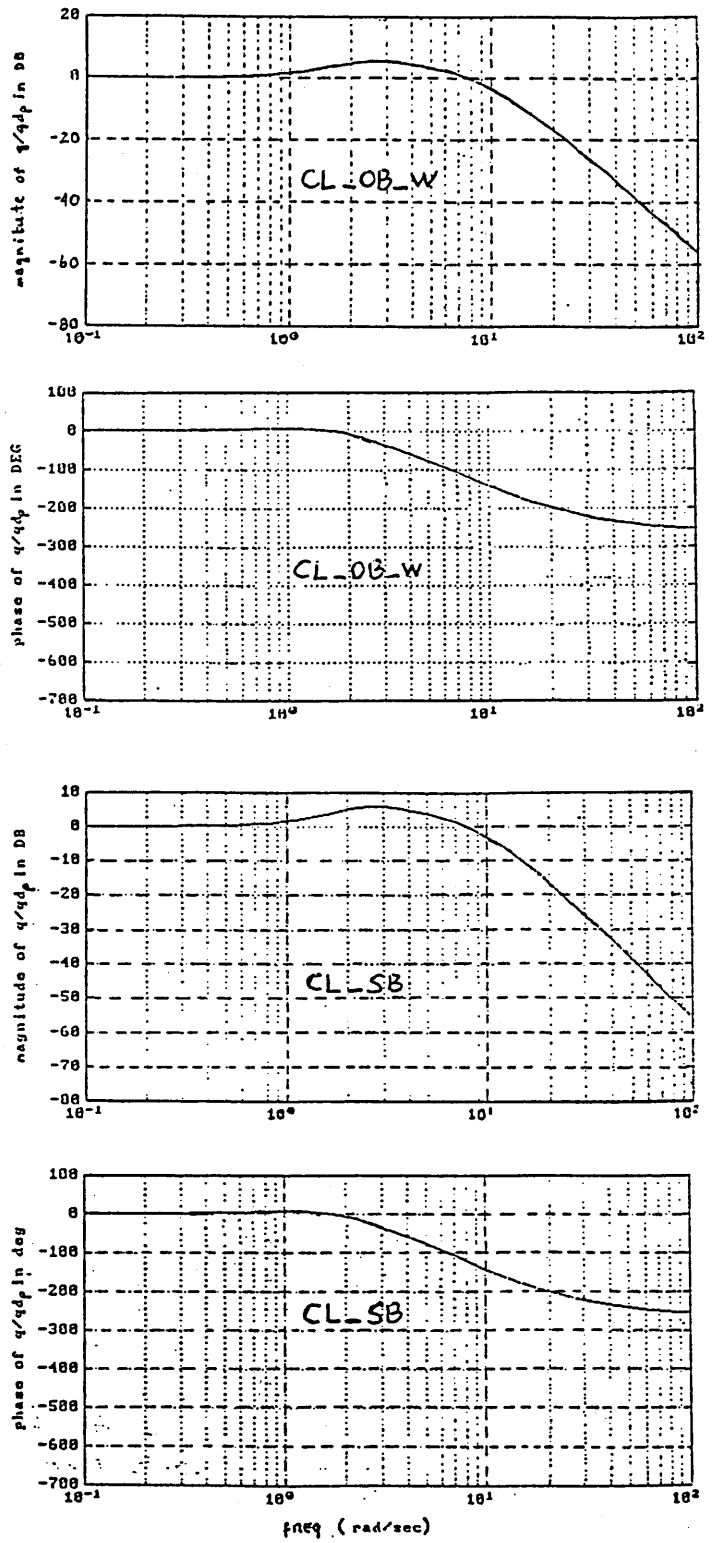

figure 5.9 - pitch-rate frequency response of the aircraft with optimal control law design CL_OB_w at 20000 ft mach 0.70

5.5.4 OBSERVER BASED CONTROL LAW CL_OB_q

Figure 5.10 shows the aircraft augmented with the observer based control law CL_OB_q .

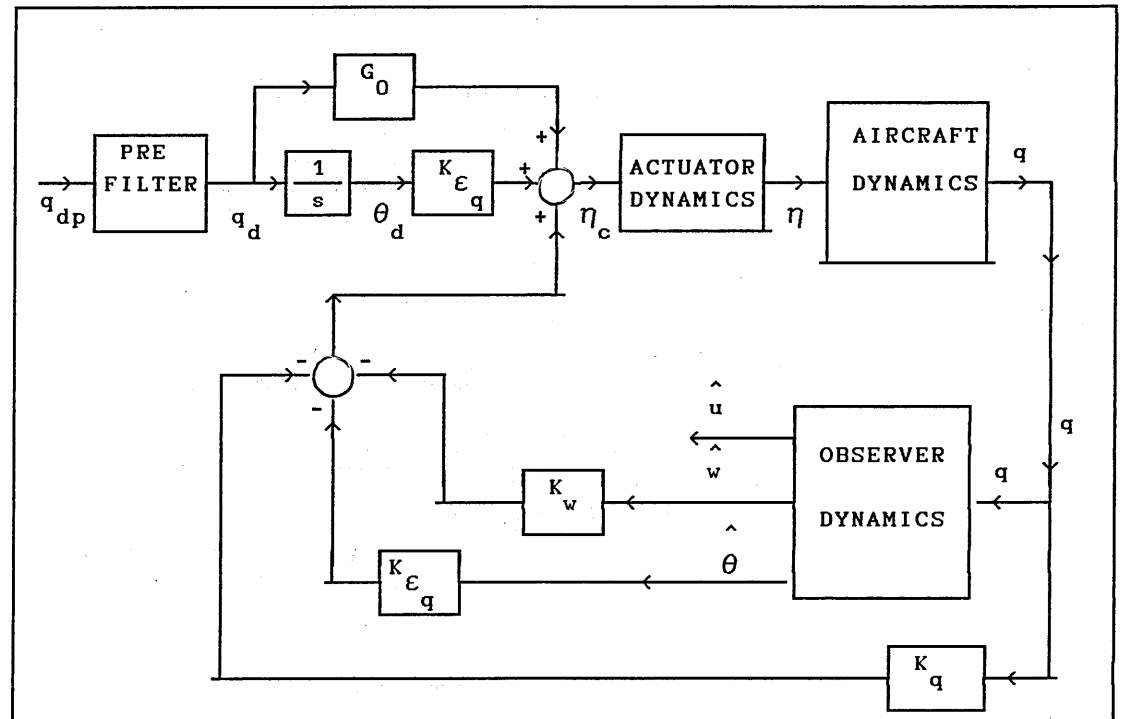

figure 5.10 structure of the observer-based control law CL_OB_q

In this case the observer dynamics are written as ,

$$\dot{z} = F\, z + \bar{G}\, x_1 + H\, \eta \qquad (5.68)$$

$$\hat{x}_2 = M\, x_1 + N\, z \qquad (5.69)$$

F, $\bar{G}$, H , M and N are obtained in section (5.3) and are listed in appendix E for the analyzed flight cases. Here $x_1 = q$ (5.70)

and $x_2^T = [\, u\ w\ \theta\,]$ (5.71)

The control law is ,

$$\eta_c = -G_1 x_1 - G_2 \hat{x}_2 + G_0 q_d + K_{\varepsilon_q} \theta_d \qquad (5.72)$$

with $G_1 = K_q$ (5.73)

and $G_2 = [0\ K_w\ K_{\varepsilon_q}]$ (5.74)

the aircraft model, actuator model and lead filter are the same as described in section 5.5.3. The closed loop model is,

$$\dot{x} = A\,x + B\,u \tag{5.75}$$

with $x^T = [\,x_1\ x_2\ x_A\ z\ \theta_d\ x_{LF}\,]$ (5.76)

$$u = q_{dp} \tag{5.76.a}$$

$$A = \begin{bmatrix} A_{11} & A_{12} & [B_1\ 0] & Z13 & 0 & 0 \\ A_{21} & A_{22} & [B_2\ Z31] & Z33 & Z31 & Z31 \\ -B_A(G_1+G_2M) & Z23 & A_A & -B_A G_2 N & B_A K_{\varepsilon_q} & B_A G_0 c_{LF} \\ \bar{G} & Z33 & [H\ Z31] & F & Z31 & Z31 \\ 0 & Z13 & Z12 & Z13 & 0 & c_{LF} \\ 0 & Z13 & Z12 & Z13 & 0 & a_{LF} \end{bmatrix} \tag{5.77}$$

$$B^T = [\,0\ \ Z31\ \ B_A G_0 d_{LF}\ \ Z31\ \ d_{LF}\ \ b_{LF}\,] \tag{5.78}$$

with $Z12 = [0\ 0]$ (5.78.a)

and Z31, Z13, Z33 , Z23 have been defined previously. Similar simulations were performed with CL_OB_q and the resulting time histories are shown on Figure 5.11, these plots show a very good agreement between CL_SB and CL_OB_q which also shows that CL_OB_q has more robustness with respect to aircraft parameters variations than CL_OB_w when compared with CL_SB in terms of aircraft response. Figure 5.12 shows the pitch rate frequency response bode plot obtained with CL_OB_q, and a comparison with figure 5.6 also shows a very good match between both. In this case the observer was designed with a pole close to zero to approximate the zero transmission zero of q/η and the results show that both frequency responses are very close so maintaining the same frequency response characteristics of the sensor based control law as required.

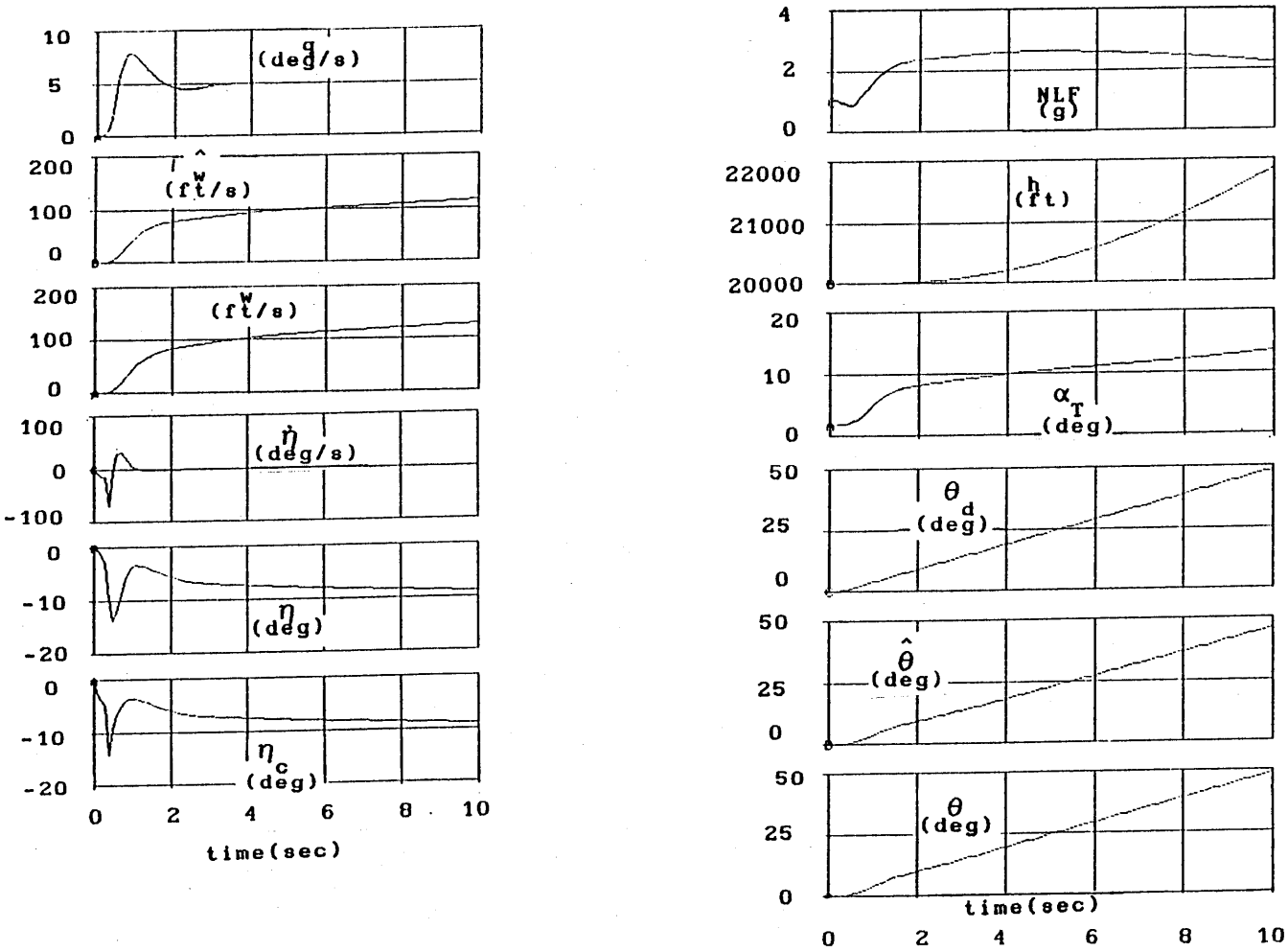

figure 5.11 - time histories of the aircraft with the optimal control law design and control law CL_OB_q at 20000 ft mach 0.70

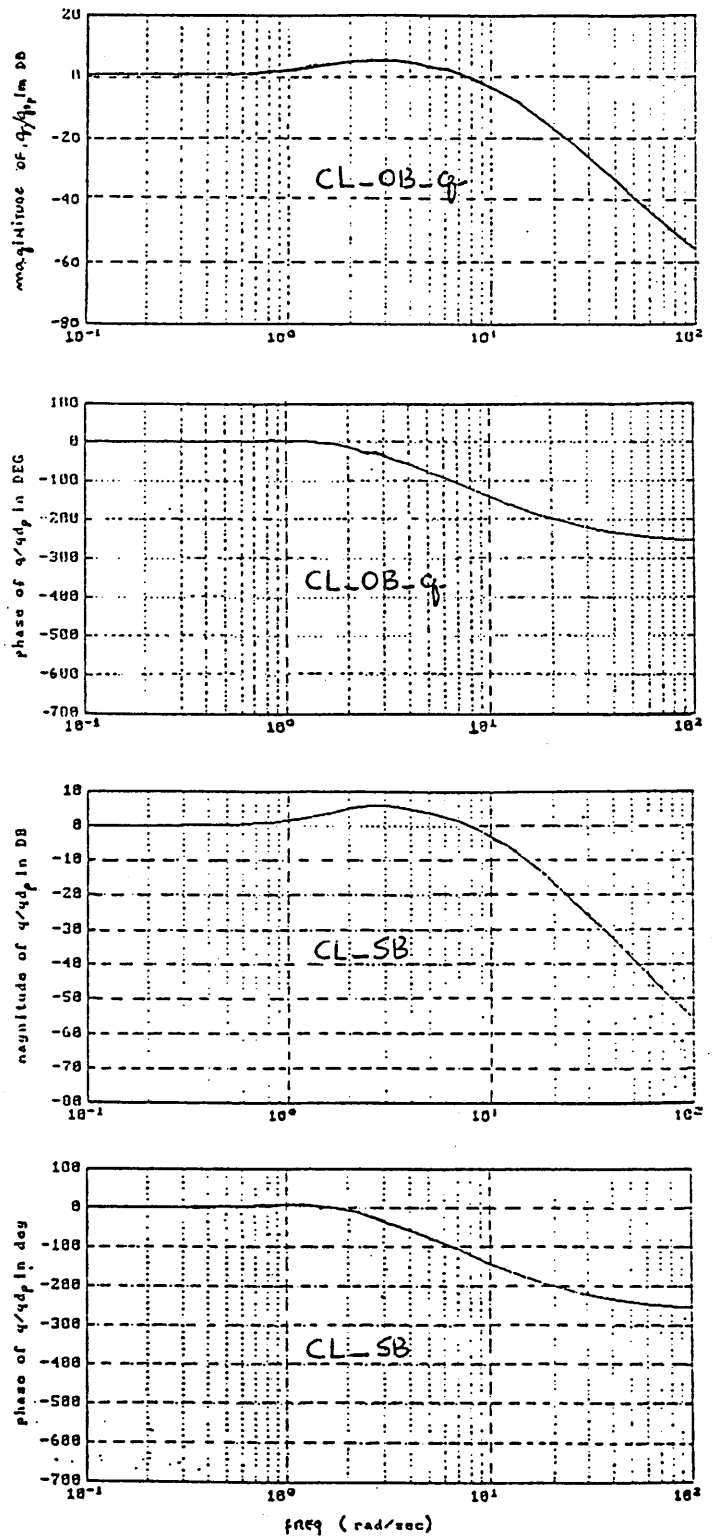

figure 5.12 - pitch-rate frequency response of the aircraft with optimal control law design CL_OB_q at 20000 ft mach 0.70

5.5.5 THE OBSERVER BASED CONTROL LAW CL_OB_θ

In this case figure 5.13 represents the augmented aircraft with observer based control law CL_OB_θ .

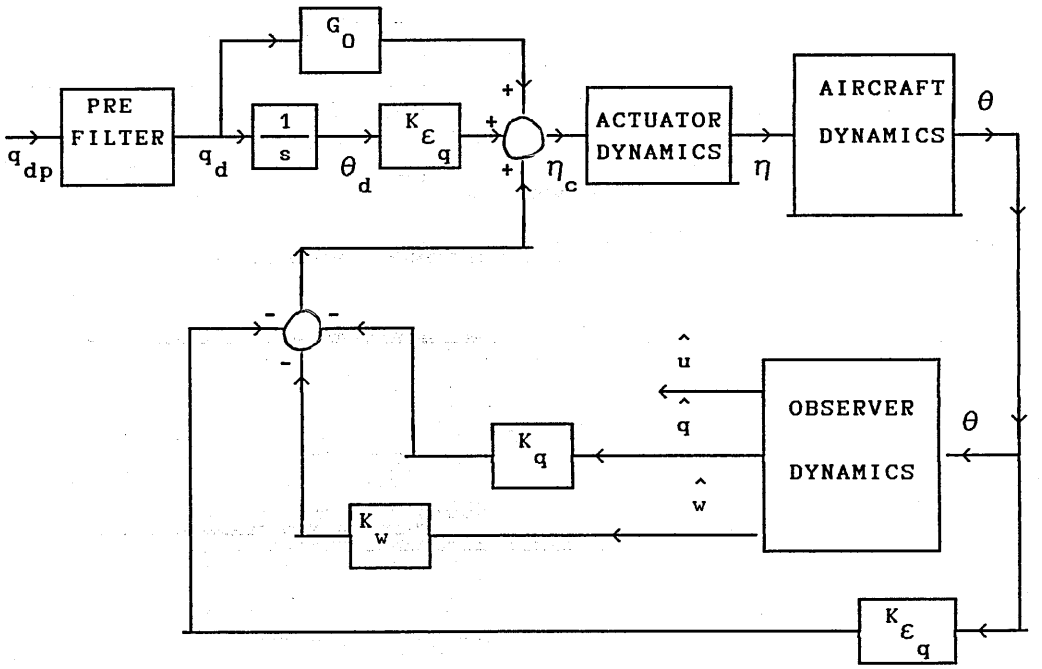

figure 5.13 - structure of the observer-based control law CL_OB_θ

The mathematical model is similar to that described in section 5.5.4 the differences now are,

$$x_1 = \theta \tag{5.79}$$

and $$x_2^T = [\, u \; w \; q \,] \tag{5.80}$$

$$\hat{x}_2^T = [\, \hat{u} \; \hat{w} \; \hat{q} \,] \tag{5.81}$$

and $$G_1 = K_{\varepsilon_q} \tag{5.82}$$

$$G_2 = [\, 0 \; K_w \; K_{\varepsilon_q} \,] \tag{5.83}$$

Performing the simulations as before the results are shown in figure 5.14, and again the agreement with CL_SB is also very good, possible better than CL_OB_q. In figure 5.15 the pitch rate frequency response bode plot of the aircraft augmented with CL_OB_θ is presented, and if compared with those of the CL_SB in figure 5.6 a very good agreement is seen. Again the Doyle-Stein condition is maintained showing good robustness of this design with respect to observer pole selection, that is, when the observer poles are not exactly at the transmission zeros of the open loop transfer function θ/η in this case.

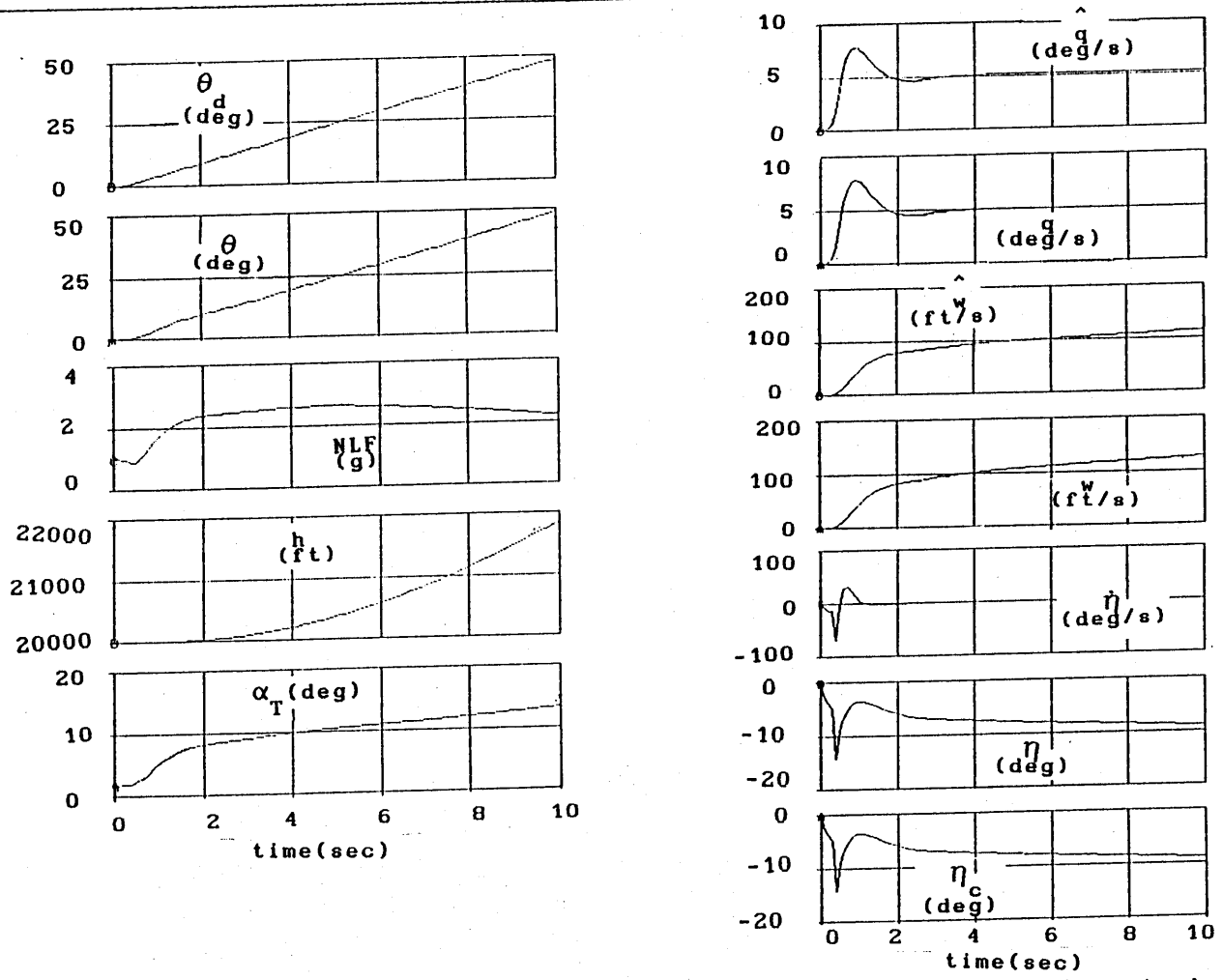

figure 5.14 - time histories of the aircraft with the optimal control law design and control law CL_OB_θ at 20000 ft mach 0.70

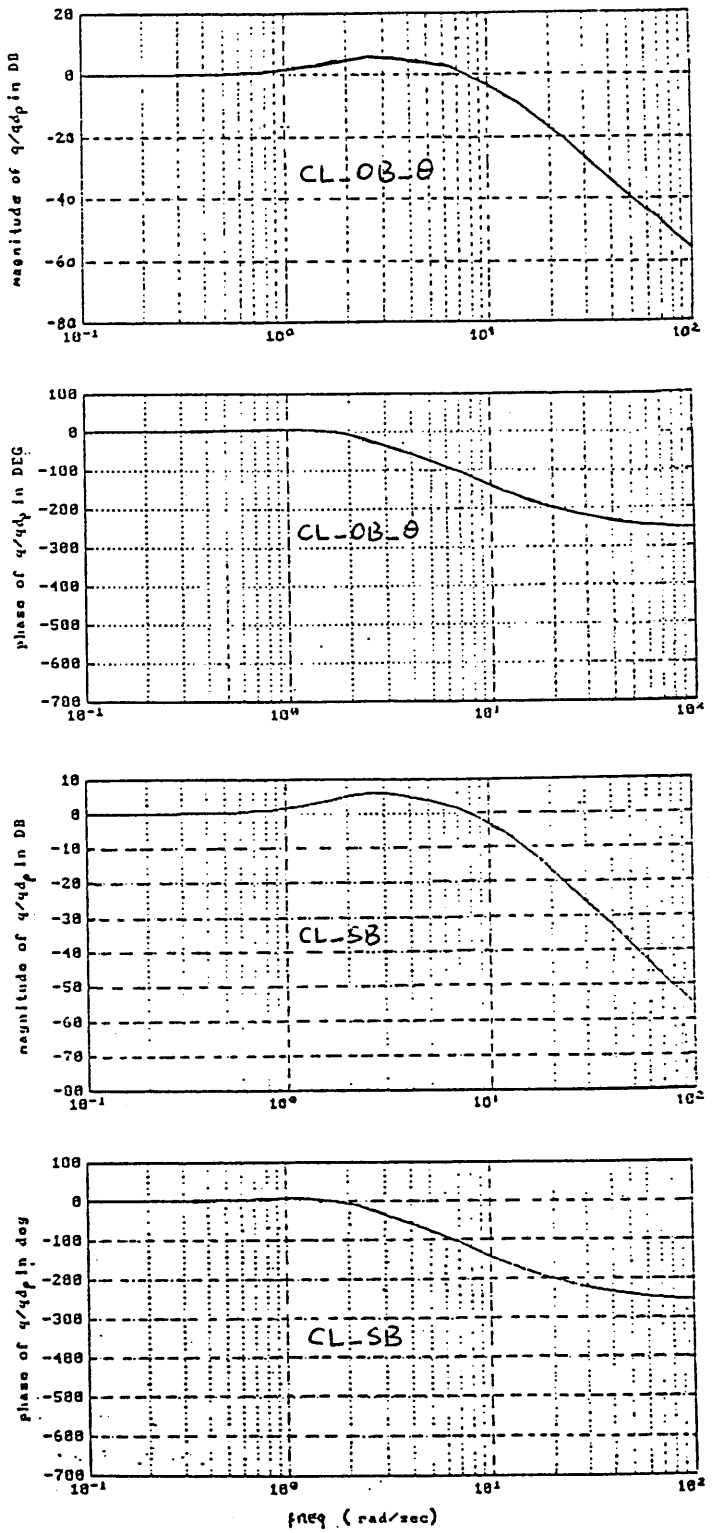

figure 5.15 - pitch-rate frequency response of the aircraft with optimal control law design CL_OB_θ at 20000 ft mach 0.70

5.5.6 COMPARISON OF THE RESULTS

The figures presented above show the results obtained and can be used to form a comparative idea of the performance of each design with respect to the sensor based control law as well as with respect to the Doyle-Stein observer condition. However, to quantify the results the four control law designs are compared in the following tables.

5.5.6.1 THE DROPBACK CHARACTERISTICS

From the simulations performed the attitude dropback parameter was obtained for each control law implementation, and summarized in table (5.1) ,

TABLE 5.1 – DROPBACK CHARACTERISTICS
DROPBACK ATTITUDE (DB) (in deg)

	OPTIMAL C.LAW DESIGN				POLE-PLACEMENT C.LAW DESIGN			
FC	CL_SB	CL_OB_w	CL_OB_q	CL_OB_θ	CL_SB	CL_OB_w	CL_OB_q	CL_OB_θ
3	0.54	-4.0	0.40	0.32	0.37	-4.1	0.13	0.00
6	0.43	-6.1	0.26	0.13	1.18	-5.6	0.59	0.40
9	0.70	-4.3	0.37	0.13	1.65	-3.6	0.59	0.84
13	0.80	1.9	0.52	0.59	1.70	2.6	0.62	0.62
17	0.13	-4.3	-0.13	-0.33	1.00	-3.4	0.37	0.00

It is obvious that CL_OB_w has the worst performance as already noticed from the time histories. It is known that the aircraft parameters used in the ACSL model are little different from those used in the MATLAB model, as mentioned the differences are around 12 % . So, looking at table 5.1 it is seen that the baseline control law with the optimal design offers a better robustness, with respect to aircraft parameter variations, than the baseline control law with the pole-placement design, relative to the attitude dropback paramameter. In both designs (pole-placement and optimal) the CL_OB_w has a poor robustness with respect to aircraft parameter variations considering the dropback attitude parameter. This can be attributed to the fact

that the complex pair of poles of the observer in CL_OB_w are very close to the origin in the s-plane, consequently the poles have some influence on the dynamics of the closed loop system. In the other observers there is no one pole so close to the origin as in this case. Here perhaps the observer design method as used in CL_OB_q and CL_OB_θ would give a better performance by using an approximation for the transmission zeros of w/η very close to the origin. It is also noted that CL_OB_q or CL_OB_θ both have a very good performance and so both are tolerant to variations in the aircraft parameters with respect to the dropback criterion.

5.5.6.2 CONTROL RATE EFFORT $\dot{\eta}$

The control rate effort required by each control law is compared in tables 5.2 and 5.3, below,

TABLE 5.2 - CONTROL RATE EFFORT $\dot{\eta}$
FOR THE OPTIMAL CONTROL LAW DESIGN

FC	CL_SB (deg/sec)		CL_OB_w (deg/sec)		CL_OB_q (deg/sec)		CL_OB_θ (deg/sec)	
	$\dot{\eta}_{min}$	$\dot{\eta}_{max}$	$\dot{\eta}_{min}$	$\dot{\eta}_{max}$	$\dot{\eta}_{min}$	$\dot{\eta}_{max}$	$\dot{\eta}_{min}$	$\dot{\eta}_{max}$
3	-72	28	-72	27	-72	27	-72	28
6	-72	30	-72	32	-72	32	-72	32
9	-96	43	-95	43	-95	42	-95	43
13	-144	65	-145	64	-145	64	-145	65
17	-78	30	-78	29	-78	32	-78	30

From both tables it is clear that the pole placement control law design demands less control rate effort than the optimal control law design, and that was already expected from the analysis of chapter 3 and 4. It is also observed that for either control law, baseline or

observer-based, the control rate effort is much the same irrespective of the choice of CL_SB, CL_OB_w, CL_OB_q or CL_OB_θ control laws.

TABLE 5.3 - CONTROL RATE EFFORT $\dot{\eta}$
FOR THE POLE PLACEMENT C.LAW DESIGN

FC	CL_SB (deg/sec)		CL_OB_w (deg/sec)		CL_OB_q (deg/sec)		CL_OB_θ (deg/sec)	
	$\dot{\eta}_{min}$	$\dot{\eta}_{max}$	$\dot{\eta}_{min}$	$\dot{\eta}_{max}$	$\dot{\eta}_{min}$	$\dot{\eta}_{max}$	$\dot{\eta}_{min}$	$\dot{\eta}_{max}$
3	-56	16	-56	16	-55	16	-56	16
6	-62	27	-61	27	-64	27	-64	27
9	-95	48	-95	48	-95	49	-95	51
13	-84	32	-83	32	-83	32	-83	32
17	-83	40	-80	40	-80	42	-81	41

5.5.6.3 CONTROL EFFORT η

The minimum control effort required for each control law design is summarized in table 5.4 below,

TABLE 5.4 - CONTROL EFFORT in degrees

	FC #	3	6	9	13	17
CL_SB	P.P.C.L.	-10.0	-11.4	-17.8	-16.1	-15.0
	O.C.L.	-13.6	-13.9	-18.0	-27.2	-14.5
CL_OB_w	P.P.C.L.	-10.0	-11.4	-17.8	-16.0	-15.0
	O.C.L.	-13.6	-13.9	-18.0	-27.0	-14.4
CL_OB_q	P.P.C.L.	-10.0	-11.4	-17.8	-15.8	-15.0
	O.C.L.	-13.6	-13.9	-18.0	-27.0	-14.5
CL_OB_θ	P.P.C.L.	-10.0	-11.7	-17.8	-16.1	-15.0
	O.C.L.	-13.6	-14.4	-18.0	-27.2	-14.4

Again, the pole placement control law design requires less control effort than the optimal control law design, and again the control effort is much the same for both control law designs irrespective of the choice of CL_SB, CL_OB_w, CL_OB_q or CL_OB_θ control laws.

5.6 INTERIM CONCLUSIONS AND OBSERVATIONS

From the study performed it was observed that the control laws CL_OB_w, CL_OB_q and CL_OB_θ can offer the same level of flying qualities and stability in the event that a full complement of sensors is not available. That is, they are able to maintain the same CAP as obtained with CL_SB, the same performance with respect to dropback criterion (except CL_OB_w) and the same performance with respect to the phase-rate criterion. It was obvious from the analysis that CL_OB_q and CL_OB_θ give a better performance than CL_OB_w, but only with respect to the dropback criterion. So in the event of a sensor failure it is best to first switch to CL_OB_q or CL_OB_θ, and only in the event of a second failure to switch to CL_OB_w. Although it has not been reported, the maximum pitch rate q_m handling parameter is about the same with each control law as is the steady state pitch-rate q_{ss}. It has also been verified that other response parameters, such as normal load factor, altitude and angle of attack in all the observer-based control laws evaluated maintain a similar response to CL_SB. In conclusion, control law CL_OB_w needs some improvement in order to be able to maintain the same dropback performance as CL_SB. An improvement could be tried by designing the observer by the second method, that is, by using an approximation to the transmission zeros that are very close to the origin in the s-plane.

With respect to the number of parameters to be scheduled, it has been noticed that CL_OB_w requires only 8 parameters, CL_OB_q requires 12 and CL_OB_θ requires 10, so in this respect CL_OB_w has an advantage over CL_OB_q and CL_OB_θ, a fact that suggests that the second method used to design the observer in general requires more parameters to be scheduled with flight condition. Therefore it has been demosntrated

that the incorporation of an observer operating on one output variable only can confer some analytical redundancy to the original control law design, whilst maintaining the same stability level and flying qualities of the baseline control law.

6 THE FAILURE ANALYSIS OF THE CONTROL LAWS AND ROBUSTNESS TO GAIN VARIATIONS

6.1 INTRODUCTION

Having designed the control laws to meet the requirements, a failure analysis was carried out to evaluate the effect of loosing feedback paths. The control laws were also investigated to see how robust they are with respect to gain variation. That is, if the control law gains experience some variation how does this variation affect the aircraft response and the ability of the augmented aircraft to meet the dropback criterion, MIL-F8785C and phase rate criterion. Finally, an investigation was carried out to evaluate the effect of a failure in some of the feedback paths followed by the system switching from one control law to another. In particular, when the aircraft is working with the baseline control law and a sensor failure occurs, then the aircraft switches to an observer-based control law. In this final study the threshold detection time, the time elapsed from the moment that the failure happens until the moment when the aircraft switches to the reversionary control law, was also varied and sensor signals were varied to represent maximum, minimum, zero and passive failures for steady flight, and manoeuvering flight.

6.2 CONDITIONS ANALYZED IN THE STUDY

In the analytical study only the sensor based control laws were considered and the study was split into two cases :

(i) control law implemented with w and q sensors.
(ii) control law implemented with w, q and θ sensors.

In the first case two conditions were studied :

(i.i) complete loss of w feedback

(i.ii) complete loss of q feedback

In the second case the following conditions were studied :

(ii.i) complete loss of q feedback

(ii.ii) complete loss of θ feedback

In this case the condition of complete loss of w feedback was not studied since it is the same as in the first case.

6.2.1 CONTROL LAW IMPLEMENTED WITH w AND q SENSORS COMPLETE LOSS OF w FEEDBACK

In this case figure 6.1 is the baseline control system for the analysis.

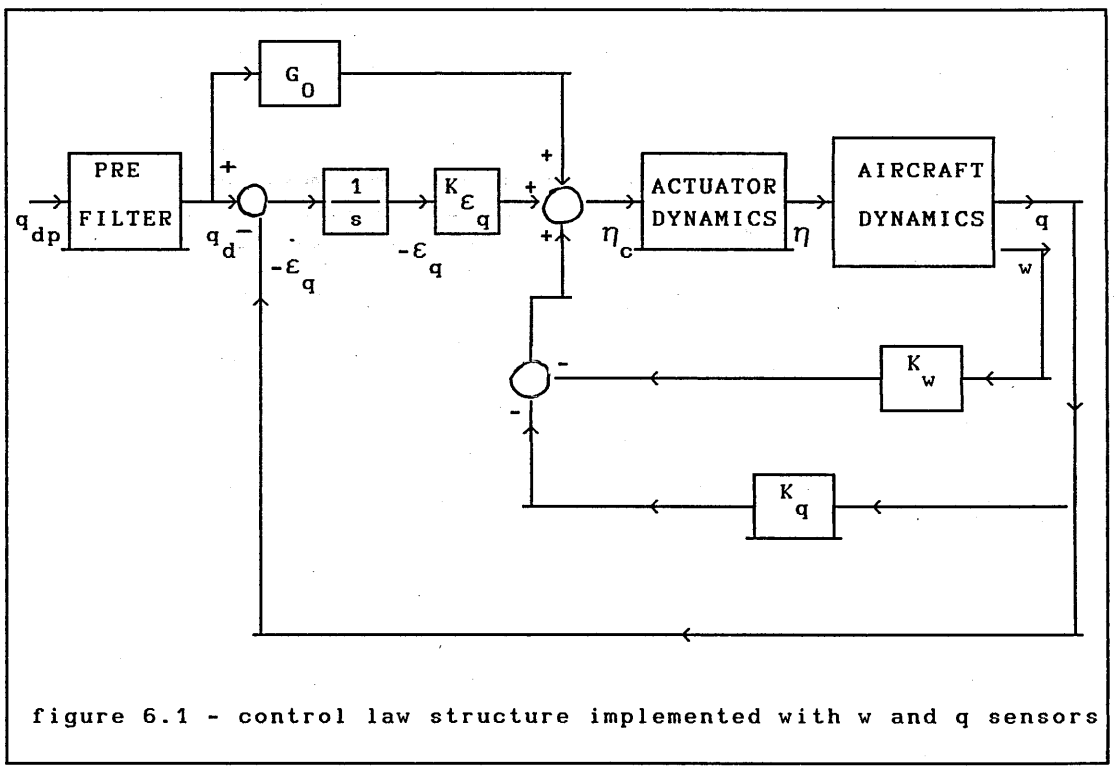

figure 6.1 - control law structure implemented with w and q sensors

The mathematical model of the lead filter can be written as,

$$\dot{x} = a_{LF} x_{LF} + b_{LF} q_{dp} \tag{6.1}$$

$$q_d = c_{LF} x_{LF} + d_{LF} q_{dp} \tag{6.2}$$

and as already known $\dot{\varepsilon}_q = q - q_d$ (6.3)

The control law is,

$$\eta_c = -K_w w - K_q q - K_{\varepsilon_q} \varepsilon_q + G_0 q_d \tag{6.4}$$

With $G = [\ 0\ K_w\ K_q\ 0\ ]$, then (6.4.a)

$$\eta_c = -G x - K_{\varepsilon_q} \varepsilon_q + G_0 q_d \tag{6.4.b}$$

but when w feedback is lost the control law becomes,

$$\eta_c = -K_q q - K_{\varepsilon_q} \varepsilon_q + G_0 q_d \tag{6.5}$$

or,with $G_f = [\ 0\ 0\ K_q\ 0\ ]$ then, (6.5.a)

$$\eta_c = -G_f x - K_{\varepsilon_q} \varepsilon_q + G_0 q_d \tag{6.5.b}$$

The actuator model is represented by the state equation,

$$\dot{x}_A = A_A x_A + B_A \eta_c \tag{6.6}$$

$$x_A^T = [\ \eta\ \ v_\eta\ ] \tag{6.7}$$

The aircraft mathematical model is represented by the state equation,

$$\dot{x} = A x + [B\ Z41] x_A \tag{6.8}$$

where, $Z41^T = [\ 0\ \ 0\ \ 0\ \ 0\ ]$ (6.8.a)

and, with $x^T = [\ u\ w\ q\ \theta\ ]$ (6.9)

The A and B matrices are given in appendix A, the lead filter was developed in chapter four, the actuator is actuator no.2 of chapter 3, and the gains were obtained in chapter 4. With this is mind the closed loop model is simply,

$$\dot{x} = A x + B u \tag{6.10}$$

$$\text{with} \quad x^T = [\, x \;\; x_A \;\; x_{LF} \;\; \varepsilon_q \,] \tag{6.10.a}$$

$$\text{and,} \qquad u = q_{dp} \tag{6.10.b}$$

$$A = \begin{bmatrix} A & [B\ Z41] & Z41 & Z41 \\ -B_A G_f & A_A & B_A G_0 c_{LF} & -B_A K_{\varepsilon_q} \\ [0\ 0\ 0\ 0] & [0\ 0] & a_{LF} & 0 \\ [0\ 0\ 1\ 0] & [0\ 0] & -c_{LF} & 0 \end{bmatrix} \tag{6.10.c}$$

$$B^T = [\, Z41 \;\; B_A G_0 d_{LF} \;\; b_{LF} \;\; -d_{LF} \,] \tag{6.10.d}$$

In figures 6.2 and 6.3 the time history comparison for both control law designs respectively are shown for flight condition 6. The results show that the failed aircraft has an increase in the short period natural frequency compared with the baseline aircraft, and the failed aircraft has a decrease in the short period damping ratio compared with the baseline aircraft. It has also been noted that the failed aircraft no longer satisfies the dropback criterion, however the deterioration is only small. Table 6.1 shows the short period dynamic parameters compared.

TABLE 6.1 – SHORT PERIOD DYNAMIC CHARACTERISTICS OF THE NON FAILED AIRCRAFT AND THE FAILED AIRCRAFT WITH THE OPTIMAL CONTROL LAW DESIGN

FC #		3	6	9	13	17
non failed	ω_{sp} rad/s	2.59	2.56	1.95	1.74	2.13
	ζ_{sp}	0.61	0.59	0.59	0.59	0.59
failed	ω_{sp} rad/s	2.98	2.88	2.19	2.00	2.41
	ζ_{sp}	0.52	0.50	0.51	0.52	0.51

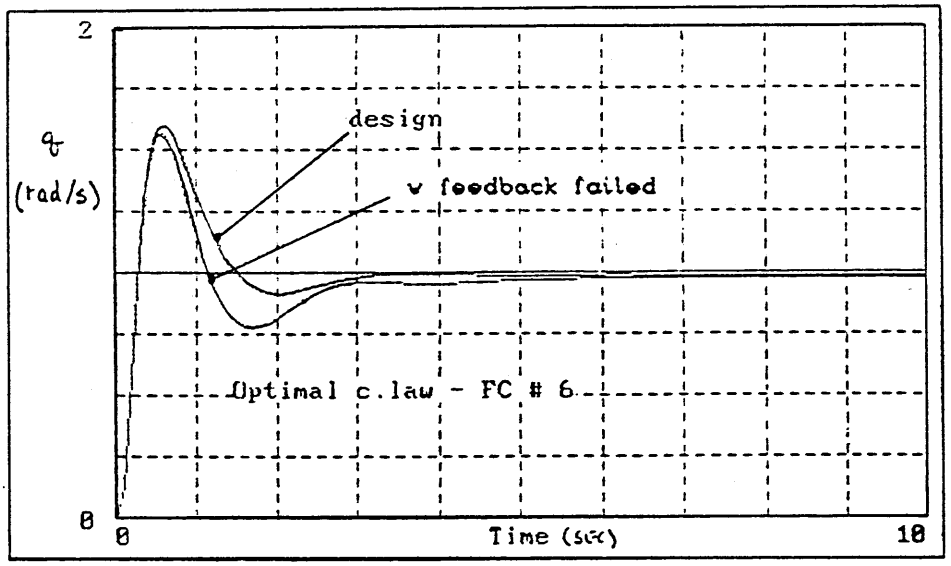

figure 6.2 - pitch-rate time response of the aircraft with optimal design at 20000 ft mach 0.70 with w feedback failed

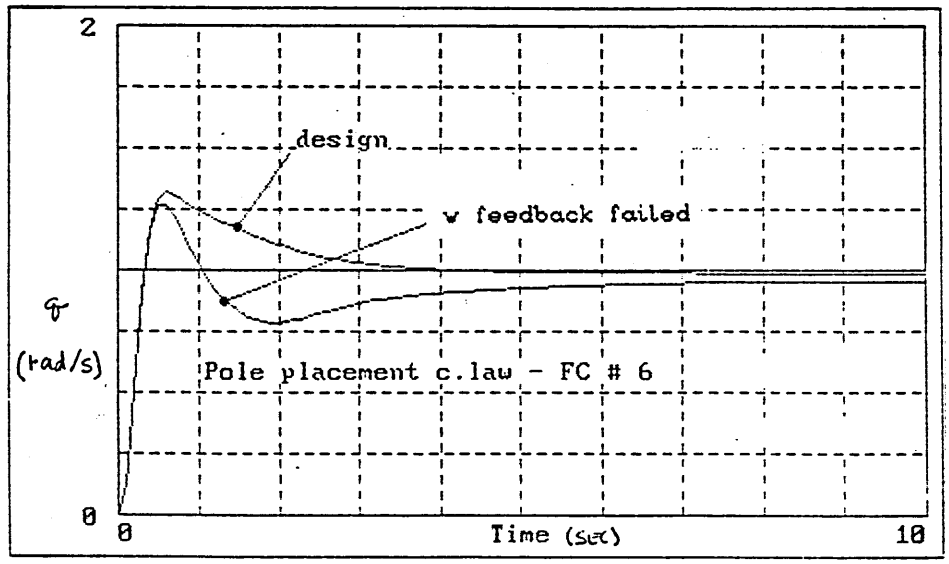

figure 6.3 - pitch-rate time response of the aircraft with pole placement design at 20000 ft mach 0.70 with w feedback failed

The CAP is satisfied with both control law designs in the failed condition, and so the stability level is not changed significantly. The study also showed that q_m, t_m and q_{ss} are very little changed with respect to the non failed condition. As a general conclusion it can be said that both designs demonstrate good tolerance to this kind of failure, in particular the optimal control law design, is better since its K_w gain is lower than the corresponding K_w of the pole placement design and so it is less susceptible to this failure.

6.2.2 CONTROL LAW IMPLEMENTED WITH w AND q SENSORS COMPLETE LOSS OF q FEEDBACK

In this case figure 6.1 is the reference control system again. The lead filter is the same as before, given by (6.1) and (6.2), the control law is :

$$\eta_c = -G \times -K_{\varepsilon_q} \varepsilon_q + G_0 q_d \qquad (6.11)$$

with $x^T = [\ u\ w\ q\ \theta\ ]$ (6.12)

and, $G = [\ 0\ K_w\ K_q\ 0\ ]$ (6.13)

Now the failed control law is given by ;

$$G_f = [\ 0\ K_w\ 0\ 0\ ] \tag{6.14}$$

but, $\dot{\varepsilon}_q = q - q_d$ (6.15)

So when q feedback is lost and then ; $\varepsilon_q = -q_d$ (6.16)

and the control law can be written,

$$\eta_c = -G_f x - K_{\varepsilon_q} \varepsilon_q + G_0 q_d \tag{6.17}$$

The aircraft is again given by,

$$\dot{x} = A\,x + [B\ Z41]x_A \tag{6.18}$$

and the actuator by ,

$$\dot{x}_A = A_A x_A + B_A \eta_c \tag{6.19}$$

with $x_A^T = [\ \eta\ \ v_\eta\ ]$ (6.20)

The closed loop model is given by, $\dot{x} = A\,x + B\,u$ (6.21)

where $x^T = [\ x\ \ x_A\ \varepsilon_q\ \ x_{LF}\ ]$ (6.21.a)

and $u = q_{dp}$ (6.21.b)

Thus,

$$A = \begin{bmatrix} A & [B\ Z41] & Z41 & Z41 \\ -B_A G_f & A_A & -B_A K_{\varepsilon_q} & B_A G_0 c_{LF} \\ Z14 & Z12 & 0 & -c_{LF} \\ Z14 & Z12 & 0 & a_{LF} \end{bmatrix} \tag{6.21.c}$$

and,

$$B^T = [\ Z41\ \ B_A G_0 d_{LF}\ \ -d_{LF}\ \ b_{LF}\ ] \tag{6.21.d}$$

The analysis of the closed loop characteristic equation when the aircraft is subject to this kind of failure shows two poles at zero, that is s = 0. Thus the system is not BIBO stable. Table 6.2 shows a comparison between the closed loop poles location of the non failed aircraft and the failed aircraft.

TABLE 6.2 – CLOSED LOOP POLE LOCATIONS OF THE FAILED AND THE NON FAILED AIRCRAFT

FC #	OPTIMAL CONTROL LAW	
	NON FAILED	FAILED
6	−1.5 ± i 2.07 −0.576 −0.018 0	−0.75 ± i 0.49 −0.0026 ± i 0.066 0.0 0
13	−1.035 ± i 1.39 −0.462 −0.040 0	−0.604 ± i 0.44 −0.0011 ± i 0.1318 0 0
	POLE PLACEMENT CONTROL LAW	
6	−1.45 ± i 0.50 −0.819 −0.0175 0	−1.259 −0.289 −0.0043 ± i 0.055 0 0
13	−0.55 ± i 0.54 −1.30 −0.0378 0	−1.218 −0.1515 0.053 ± i 0.152 0 0

Note that at some flight conditions the pole placement control law design has a pole located on the right half s-plane, and that the short period characteristics are very deteriorated. This was expected since q feedback is a critical feedback. As the system is no longer BIBO stable the aircraft response diverges very quickly. In conclusion, if q feedback is lost the aircraft will demonstrate dangerous characteristics if the control law is implemented as in figure 6.1.

6.2.3 CONTROL LAW IMPLEMENTED WITH w, q AND θ SENSORS FOLLOWED BY COMPLETE LOSS OF q FEEDBACK

Now figure 6.4 must be considered as the implementation of the control law.

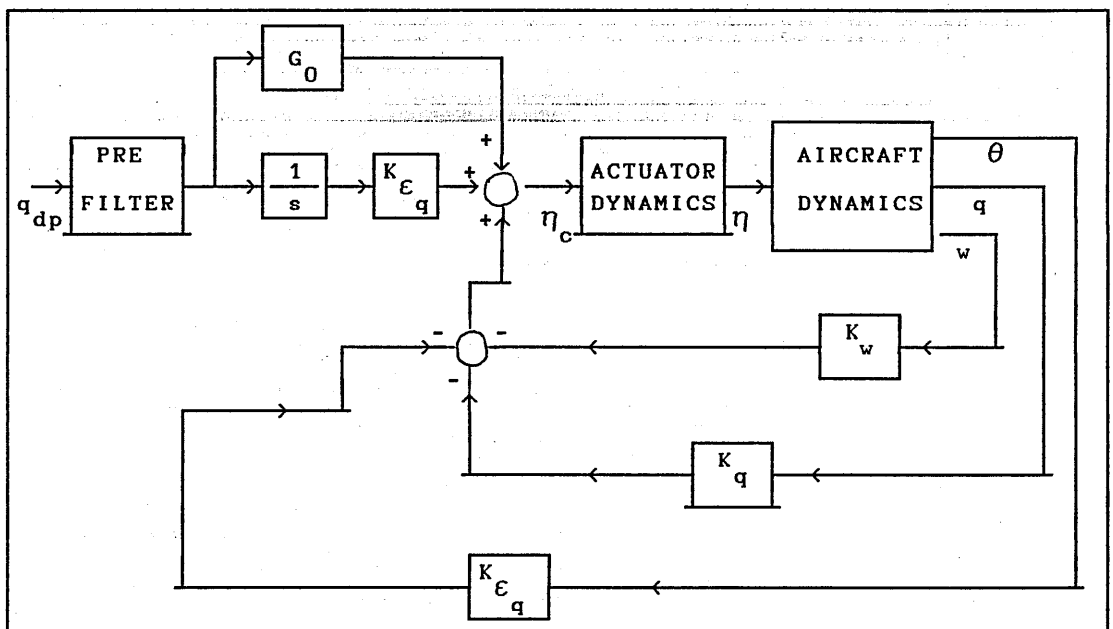

figure 6.4 - control law structure implemented with " w ", " q ", and " θ " sensors

The state vector is again $x^T = [\, u \; w \; q \; \theta \,]$ (6.22)

the control law is now, $\eta_c = -K_w w - K_q q - K_{\varepsilon_q} \varepsilon_q + K_{\varepsilon_q} \theta_d + G_0 q_d$ (6.23)

with, $\dot{\theta}_d = q_d$, where, (6.24)

$$\eta_c = -G\,x + K_{\varepsilon_q}\,\theta_d + G_0\,q_d \tag{6.25}$$

and, In the failed condition $G = [\, 0 \;\; K_w \;\; K_q \;\; K_{\varepsilon_q} \,]$ (6.26)

$$\eta_c = -K_w w - K_{\varepsilon_q} \theta + K_{\varepsilon_q} \theta_d + G_0 q_d \tag{6.27}$$

or, $\eta_c = -G_f x + K_{\varepsilon_q} \theta_d + G_0\, q_d$ (6.28)

where, $G_f = [\, 0 \; K_w \; 0 \; K_{\varepsilon_q} \,]$ (6.29)

The aircraft state equation is, $\dot{x} = A\,x + [B \; Z41]\, x_A$ (6.30)

and the actuator state equation is, $\dot{x}_A = A_A x_A + B_A \eta_c$ (6.31)

with $x_A^T = [\, \eta \;\; v_\eta \,]$ (6.32)

The matrices A and B of the aircraft model are contained in appendix A. Thus, the closed loop model is given by,

$$\dot{x} = A x + B u \tag{6.33}$$

where $x^T = [\, x \;\; x_A \;\; x_{LF} \;\; \theta_d \,]$ (6.33.a)

$$u = q_{dp} \tag{6.33.b}$$

$$A = \begin{bmatrix} A & [B\ Z41] & Z41 & Z41 \\ -B_A G_{Af} & A_A & B_A G_{c_{0LF}} & B_A K_{\varepsilon_q} \\ Z14 & Z12 & a_{LF} & 0 \\ Z14 & Z12 & c_{LF} & 0 \end{bmatrix} \tag{6.33.c}$$

$$B^T = [\; Z41 \;\; B_A G_{d_{0LF}} \;\; b_{LF} \;\; d_{LF} \;] \tag{6.33.d}$$

In figures 6.5 and 6.6 the pitch-rate time response comparison for the optimal control law design is shown, for flight cases 3 and 6 respectively, for the failed and non failed aircraft. The failed control law no longer satisfies the dropback criterion however, the aircraft remains stable at all flight conditions. The results also show that the short period damping is very much reduced whilst the frequency is practically unaffected. The pitch-rate response with the failed control law takes longer to reach the steady state than is the case with the non failed aircraft. In conclusion, a failure of q feedback is not so critical when the control law is implemented as in figure 6.4. However, if the implementation shown in figure 6.1 is used this kind of failure can be very dangerous.

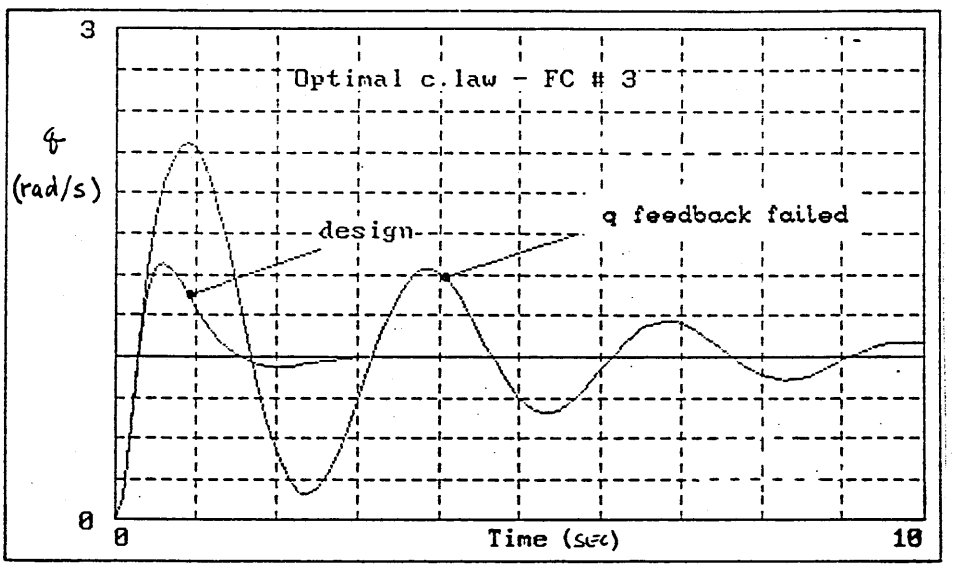

figure 6.5 - pitch-rate time response of the aircraft with optimal design at 1000 ft mach 0.60 with q feedback failed

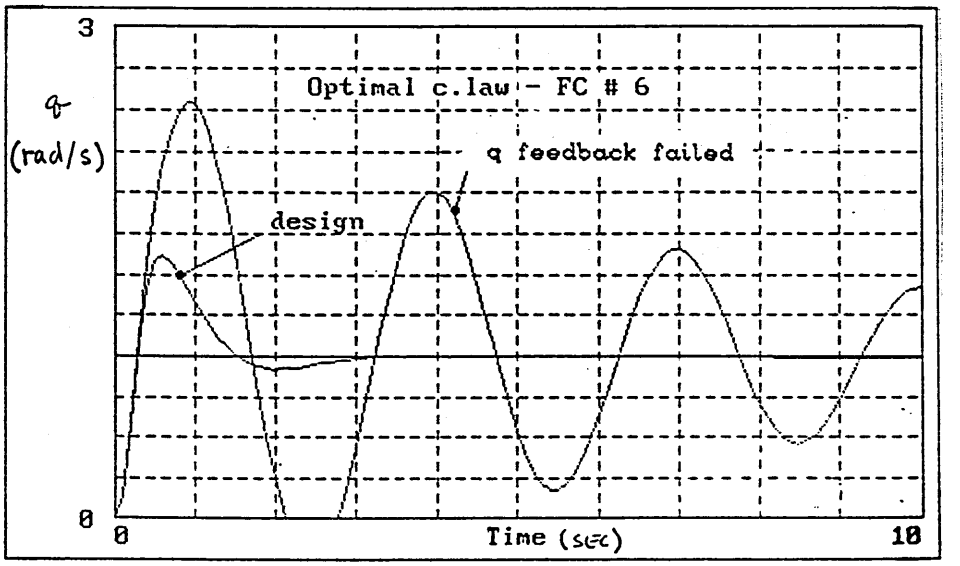

figure 6.6 - pitch-rate time response of the aircraft with pole placement design at 20000 ft mach 0.70 with q feedback failed

6.2.4 CONTROL LAW IMPLEMENTED WITH w, q AND θ SENSORS FOLLOWED BY COMPLETE LOSS OF θ FEEDBACK

The implementation considered here is also that of figure 6.4, but since θ feedback is lost it is necessary to write,

$$G_f = [\ 0\ K_w\ K_q\ 0\ ] \tag{6.34}$$

Otherwise the equations are exactly the same as in section 6.2.3, except that it is necessary to use (6.34) instead of (6.29) in the closed loop model. The analysis shows that in this case the steady state response characteristic of $(q/q_{dp}) \simeq 1$ is no longer maintained. Referring to the characterisitc equation of the closed loop system, it is evident that the stability is maintained in all flight conditions with the optimal control law design, but not with the pole placement control law design. Table 6.3 shows a comparison of the poles for the two control law designs.

TABLE 6.3 - CLOSED LOOP POLES COMPARISON FOR THE FAILED AND NON FAILED C.LAW AT FC # 9

OPTIMAL CONTROL LAW	
NON FAILED	FAILED
-1.15 ± i 1.57	-2.88
-0.317	-0.416
-0.0176	-0.0071 ± i 0.0156
0	0
POLE PLACEMENT CONTROL LAW	
NON FAILED	FAILED
-1.89 ± i 0.21	-4.67
-0.398	-0.23
-0.016	-0.0567
0	0.0285
	0

With respect to stability robustness, the optimal control law is more robust than the pole placement control law with this kind of failure because, in no one flight condition the optimal design gives a positive pole in the s-plane. However this kind of failure is not so important as the others studied, since if θ feedback is lost it is possible to obtain θ by integrating q (pitch-rate), so it is possible to say that in this respect, figure 6.4 is also a redundant implementation of figure 6.1.

6.3 ROBUSTNESS TO GAIN VARIATIONS

Now it is useful obtain some idea of how robust or tolerant the control laws are with respect to variations in the magnitude of the designed gains. To perform this evaluation the control law implementation is that described in figure 6.1. The closed loop model is given by (6.10) except that instead of using G_f (6.5.a), G is used as in (6.4.a). The gains considered in the study are K_w, K_q, K_{ε_q} and G_0. Two conditions have been analyzed, the first is called +10% and is obtained by multiplying the nominal gains by 1.10, the second one is called -10%, and is obtained by multiplying the nominal gains by 0.90. So, as the nominal control law is given by

$$G_{nom} = [\, K_w \quad K_q \quad K_{\varepsilon_q} \,] \tag{6.35}$$

$$G_{0_{nom}} = G_0 \tag{6.35.a}$$

the condition of 10% is obtained by writing,

$$G_{+10\%} = 1.10\, G_{nom} \tag{6.36}$$

$$G_{0_{+10\%}} = 1.10\, G_{0_{nom}} \tag{6.36.a}$$

and the condition of -10% is obtained by writing,

$$G_{-10\%} = 0.90\, G_{nom} \tag{6.37}$$

$$G_{0_{-10\%}} = 0.90\, G_{0_{nom}} \tag{6.37.a}$$

So all gains are varied simultaneously by the same percentage. Obviously a more detailed study could be performed by varying one gain at a time. The results of this study show that the pole placement control law design is more sensitive to this kind of variation in the gains than the optimal control law design when the short period characteristics are considered. In figure 6.7, the pitch-rate frequency response of the optimal control law design is shown with nominal gains and with the variations in the gains. It is clear that an increase in the gains results in a small decrease in gain and phase margin, that is, about 10° in phase margin and 2 dB in gain margin. Figure 6.8 shows the corresponding pitch-rate time response of the optimal control law design and figure 6.9 shows the pitch-rate time response of the pole placement control law design. It is clear that small variations in the gains (± 10%) has little effect on control law performance with either control law design. Table 6.4 gives some indication of the variation in short period characteristics with nominal gains and with the variations.

TABLE 6.4 – SHORT PERIOD CHARACTERISTICS WITH GAIN VARIATIONS TO FLIGHT CONDITION 6

CONTROL LAW	ω_{sp} (rad/sec)			ζ_{sp}		
	-10%	nominal	+10%	-10%	nominal	+10%
O.C.L.	2.42	2.56	2.71	0.56	0.59	0.61
P.P.C.L	1.58	1.54	1.02	0.86	0.94	0.95

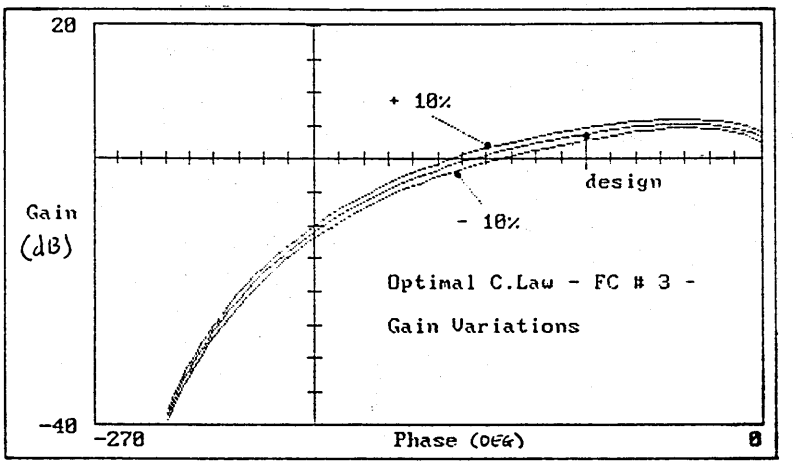

figure 6.7 - pitch-rate frequency response of the aircraft with optimal design at 1000 ft mach 0.60 with gain variations

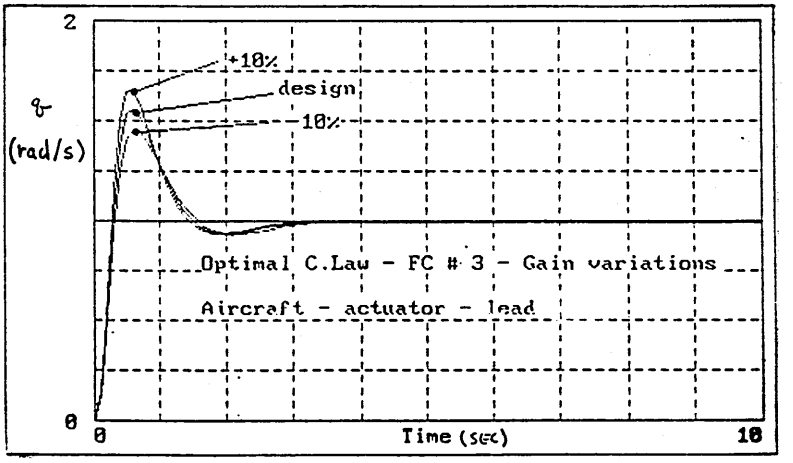

figure 6.8 - pitch-rate time response of the aircraft with optimal design at 1000 ft mach 0.60 with gain variations

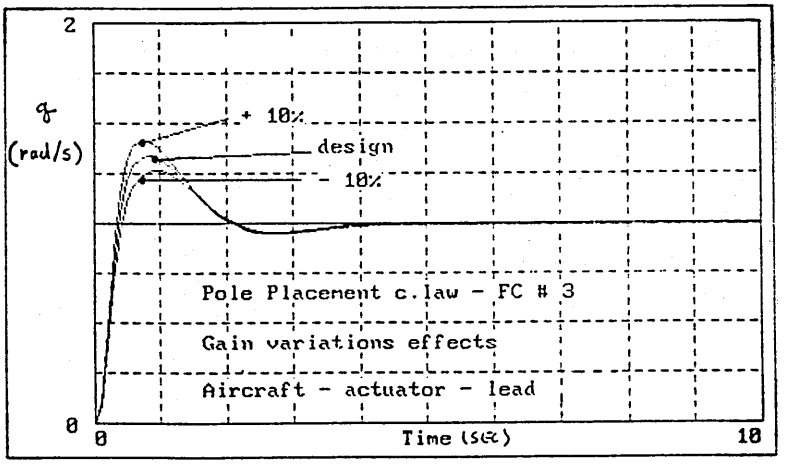

figure 6.9 - pitch-rate time response of the aircraft with pole placement design at 1000 ft mach 0.60 with gain variations.

The dropback criterion, phase rate criterion and CAP continue to be satisfied with this magnitude of gain variation. A more searching study could be performed by increasing the magnitude of the gain variation to find the tolerance limits of the control laws. That could be a useful study to perform since the gains must be scheduled and some errors might occur in the schedules. Thus the study could guide the designer by defining the acceptable tolerance in gain scheduling. The results also show that the closed loop poles with the optimal control law design would seem to be marginally better with respect to changes in the closed loop poles location.

6.4 INTERIM CONCLUSIONS

From the performed study some useful conclusions can be drawn :

i The control law implementation shown in figure 6.4 is safer than the implementation shown in figure 6.1. It is also more robust to the effects of q feedback failure with respect to the maintenance of stability , dropback criterion and phase rate criterion.

ii The control law is much more robust with respect to the effects of failures in w feedback than in either q or θ feedback with respect to stability and flying qualities maintenance. This was expected since the magnitude of K_w is smaller than the magnitude of K_q and $K_{\dot{\varepsilon}_q}$. In particular, the optimal control law is more robust than the pole placement control law.

iii The optimal control law is more robust with respect to feedback gain variations and also to feedback path failures than the pole placement control law.

iv In conclusion the implementation of figure 6.4 is advisable with the optimal design, since it is safer and more robust.

6.5 THE SIMULATION STUDY

6.5.1 INTRODUCTION

The computer simulation was used to study the dynamic failure characteristics of both control laws that is, the sensor based and the observer-based. The study considered the following failure modes;

(i) The signal of a sensor fails to zero, called a zero failure.
(ii) The signal of a sensor fails to its maximum positive or maximum negative value, called a hardover failure.
(iii) The signal of a sensor fails to its present value, called a passive failure.

Also two conditions have been considered as follows,

(a) steady-state-flight
That is, there is no pilot input and the aircraft is considered to be flying in trimmed steady flight. In this condition 10 seconds of flight was simulated and the failure occurs after 0.10 seconds.
(b) pilot manoeuvering
That is, there is a pilot input, again 10 seconds of flight have been simulated, and the failure occurs after 0.30 seconds.

The study was performed for one flight condition only, 20000 ft at mach 0.70. The optimal control law design only was used. The study also considered two values of failure detection threshold time , 0.10 seconds and 0.30 seconds.

6.5.2 THE FAILURE DYNAMICS

The failure dynamics were studied by first assuming the aircraft to be fully controlled by the sensor based control law. After a short predetermined time a fault situation was applied and after the threshold detection delay the control law was reconfigured to an

observer based alternative (reversionary control law). Figure 6.10 shows the sequence of events in the steady-state-flight situation.

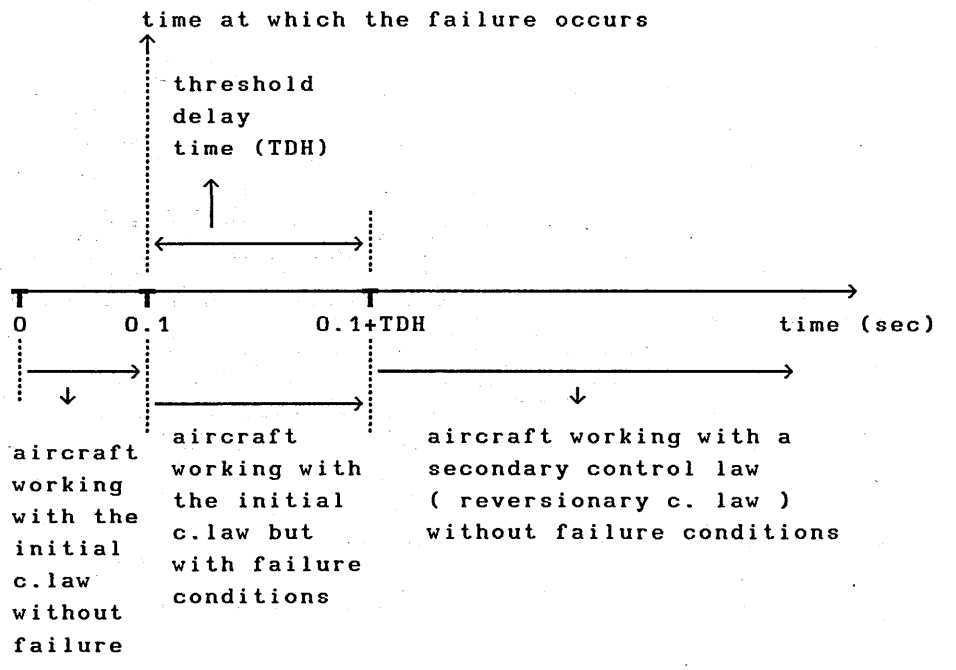

figure 6.10 - sequence of events in the steady-state flight failure conditions

In this study for reasons of simplicity the failure is assumed to be instantaneous, that is, there are no dynamics associated with the signal of the failed sensor as it changes to its failed value.
The study have considered primary failures, which means that the control of the aircraft switches from the sensor based control law to an observer-based control law, and also secondary failures, which means that the control of the aircraft switches from an observer-based control law to an alternative observer-based control law. Figure 6.11 illustrates the situation, for primary failures and figure 6.12 the possible situations for secondary failures.

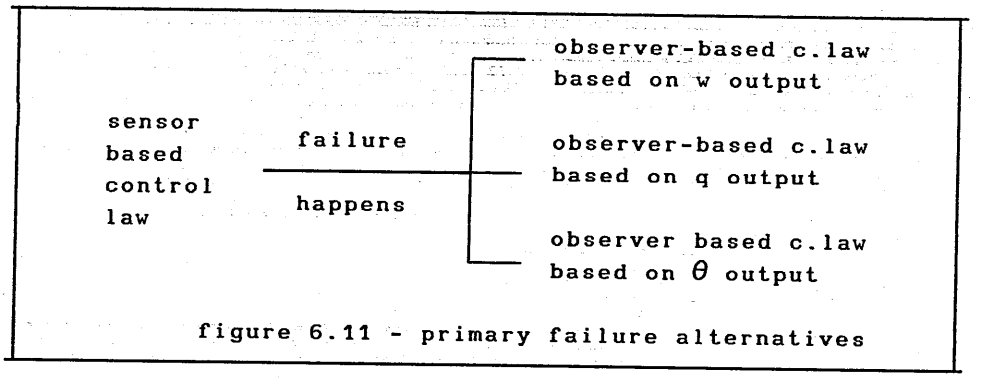

figure 6.11 - primary failure alternatives

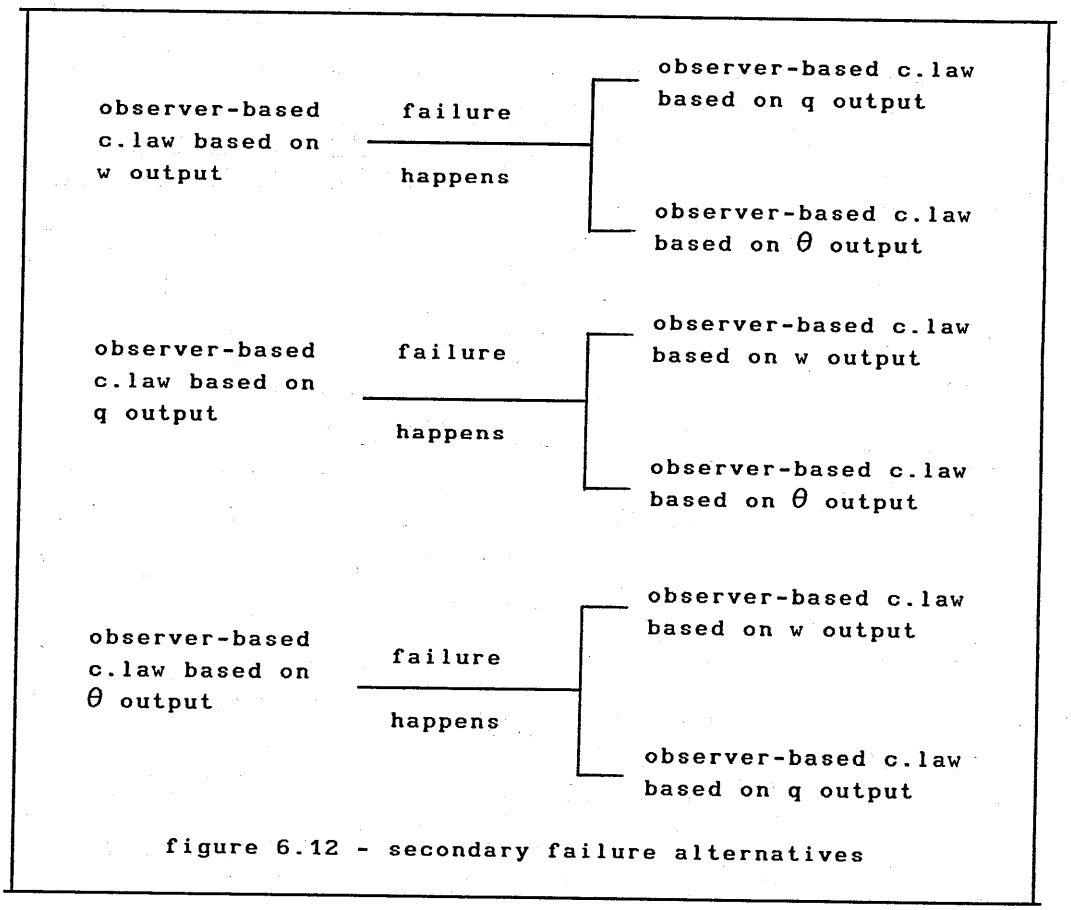

figure 6.12 - secondary failure alternatives

The pilot input used to simulate manoeuvering is shown in figure 6.13 together with the sequence of events representing the failure with pilot input. This input was chosen in order to be more representative of a typical flight situation.

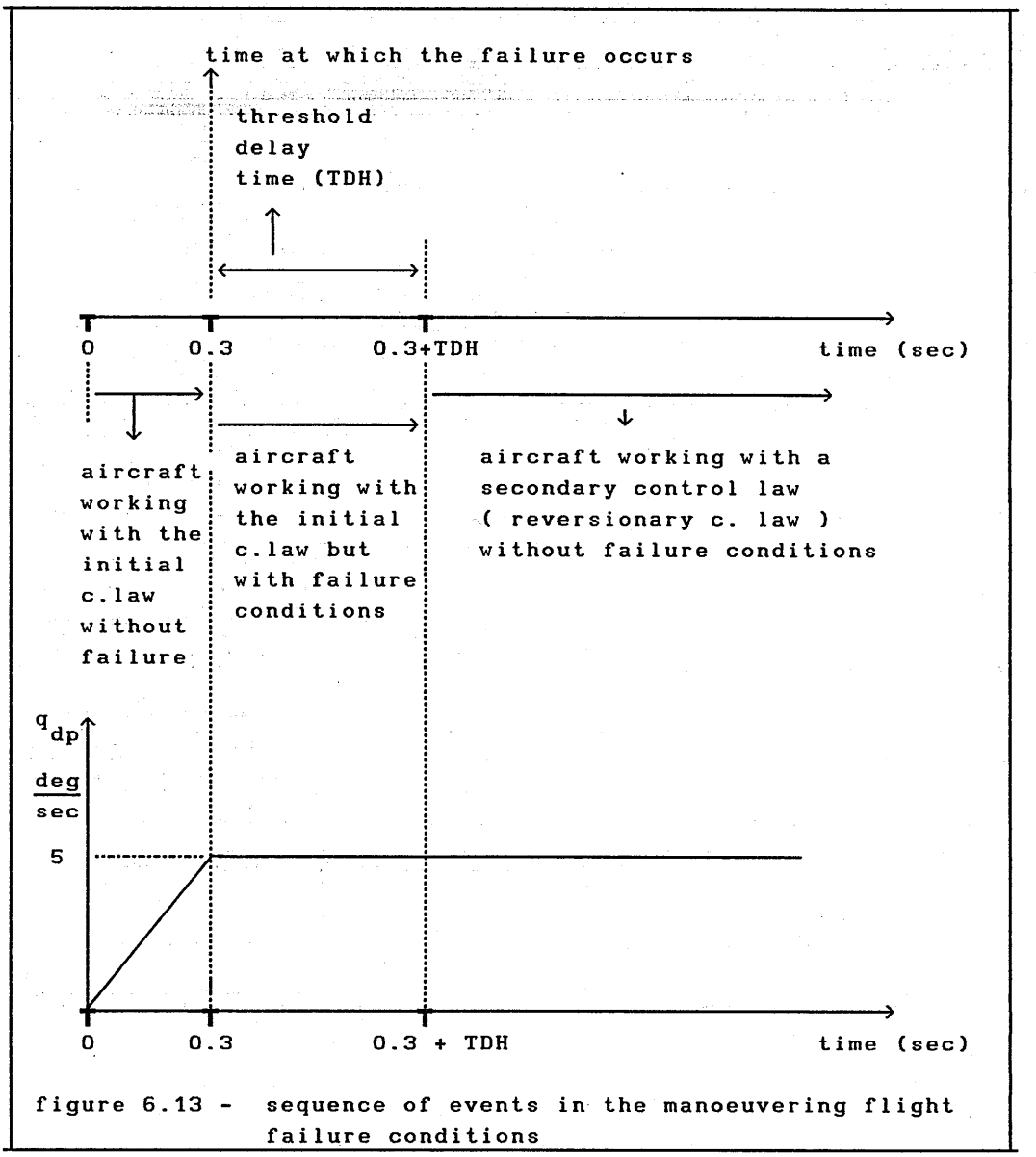

figure 6.13 - sequence of events in the manoeuvering flight failure conditions

6.5.2.1 PRIMARY FAILURES ANALYZED

In order to identify the cases analyzed the following shorthand identification is adopted from here on. There are six possible cases of primary failures,

(i) CL_SB ——————→ CL_OB_w

The aircraft is initially controlled by sensor based control law (CL_SB) and switches to observer-based control law CL_OB_w, following a failure of the q sensor. This failure is identified as SBOw_q, that is, mode failure from CL_SB to CL_OB_w following failure of q sensor.

(ii) CL_SB ——————→ CL_OB_w

The aircraft is initially controlled by sensor based control law (CL_SB) and switches to observer-based control law CL_OB_w, following a failure of the θ sensor. This failure is identified as SBOw_θ, that is, mode failure from CL_SB to CL_OB_w following failure of θ sensor.

(iii)CL_SB ——————→ CL_OB_q

The aircraft is initially controlled by sensor based control law (CL_SB) and switches to observer-based control law CL_OB_q, following a failure of the θ sensor. This failure is identified as SBOq_θ, that is, mode failure from CL_SB to CL_OB_q following failure of θ sensor.

(iv) CL_SB ——————→ CL_OB_q

The aircraft is initially controlled by sensor based control law (CL_SB) and switches to observer-based control law CL_OB_q, following a failure of the w sensor. This failure is identified as SBOq_w, that is, mode failure from CL_SB to CL_OB_q following failure of w sensor.

(v) CL_SB ——————→ CL_OB_θ

The aircraft is initially controlled by sensor based control law (CL_SB) and switches to observer-based control law CL_OB_θ, following a failure of the q sensor. This failure is identified as SBOθ_q, that is, mode failure from CL_SB to CL_OB_θ following failure of q sensor.

(vi) CL_SB ——————→ CL_OB_θ

The aircraft is initially controlled by sensor based control law

(CL_SB) and switches to observer-based control law CL_OB_θ, following a failure of the w sensor. This failure is identified as SBOθ_w, that is, mode failure from CL_SB to CL_OB_θ following failure of w sensor.

For the hardover failures the following limiting values are assumed,

$$\theta_{max} = 50^{\circ} \qquad \theta_{min} = -50^{\circ}$$

$$q_{max} = 50^{\circ}/s \qquad q_{min} = -50^{\circ}/s$$

$$\alpha_{max} = 30^{\circ} \qquad \alpha_{min} = -30^{\circ}$$

These values are assumed for the purposes of this exercise, and are representative of a typical failure. In a real design situation the engineer will have access to sensor data enabling him to perform a more realistic analysis.

6.5.2.2 SECONDARY FAILURES ANALYZED

Six secondary failure cases are also analyzed and these cases are identified by the following shorthand identification,

(i) CL_OB_w ——→ CL_OB_q

The aircraft is initially controlled by the observer-based control law (CL_OB_w) and switches to the observer-based control law CL_OB_q, obviously following an α sensor failure identified simply by, OwOq_w

(ii) CL_OB_w ——→ CL_OB_θ

The aircraft is initially controlled by the observer-based control law (CL_OB_w) and switches to the observer-based control law CL_OB_θ, obviously following an α sensor failure identified simply by, OwOθ_w

(iii)CL_OB_q ——→ CL_OB_w

The aircraft is initially controlled by the observer-based

control law (CL_OB_q) and switches to the observer-based control law CL_OB_w, obviously following a q sensor failure identified simply by, 0q0w_q.

(iv) CL_OB_q ——————→ CL_OB_θ

The aircraft is initially controlled by the observer-based control law (CL_OB_q) and switches to the observer-based control law CL_OB_θ, obviously following a q sensor failure identified simply by, 0q0θ_q.

(v) CL_OB_θ ——————→ CL_OB_w

The aircraft is initially controlled by the observer-based control law (CL_OB_θ) and switches to the observer-based control law CL_OB_w, obviously following a θ sensor failure identified simply by, 0θ0w_θ.

(vi) CL_OB_θ ——————→ CL_OB_q

The aircraft is initially controlled by the observer-based control law (CL_OB_θ) and switches to the observer-based control law CL_OB_q, obviously following a θ sensor failure identified simply by, 0θ0q_θ.

6.5.3 THE RESULTS AND CONCLUSIONS

For each failure mode 12 cases were simulated and the total number of simulations performed was 144. So it is impratical to show time histories representative of all cases. Thus a summary of the findings only is reported. The analysis of the results has shown that the most hazardous case is the θ sensor failure mode, the q sensor failure is less hazardous and the least hazardous is the w sensor failure. This is due to the fact that the gain K_{ε_q} has a greater magnitude than the gains K_w or K_q. The simulations were performed without limits on η or $\dot{\eta}$. The actual aircraft has the following hard elevator control limits,

$$\delta_{e_{min}} = -23^{\circ} \qquad \delta_{e_{max}} = 17^{\circ}$$

$$\dot{\delta}_{e_{min}} = -37^{\circ}/s \qquad \dot{\delta}_{e_{max}} = 37^{\circ}/s$$

However, in the context of the present day technology it is considered reasonable to have a control rate limit greater than $37^{\circ}/s$, and a reasonable value is assumed to be $100^{\circ}/s$. In order to avoid dangerous failure transients it is advisable to have amplitude limiters on the feedback paths of θ and q to protect the aircraft in the event of a hardover failure. The simulations have shown that in the event of a hardover failure the aircraft can experience a dangerously high load factor and high angle of attack. Sumarizing the results obtained, the various failure modes can be grouped as described in table 6.5

TABLE 6.5 – FAILURE MODES

	SENSOR FAILED		
	w	q	θ
PRIMARY FAILURES	SB0q_w	SB0w_q	SB0w_θ
	SB0θ_w	SB0θ_q	SB0q_θ
SECONDARY FAILURES	0w0q_w	0q0w_q	0θ0w_θ
	0w0θ_w	0q0θ_q	0θ0q_θ

Table 6.6 illustrates the maximum values of control effort and control rate effort required in the case SB0q_w, table 6.7 illustrates the case for SB0w_q and table 6.8 illustrates the case for SB0w_θ.

TABLE 6.6 – CASE SB0q_w – STEADY FLIGHT

MAXIMUM CONTROL EFFORT REQUIRED

sensor failure mode	η_{min} (deg)	η_{max} (deg)	$\dot{\eta}_{min}$ (deg/s)	$\dot{\eta}_{max}$ (deg/s)	threshold delay time (sec) TDH
α_{max}	-7.2	3.2	-78	46	0.10
α_{min}	-3.3	6.8	-44	76	
α_{max}	-15	9.0	-78	100	0.30
α_{min}	-9	15	-100	77	

TABLE 6.7 – CASE SB0w_q – STEADY FLIGHT

MAXIMUM CONTROL EFFORT REQUIRED

sensor failure mode	η_{min} (deg)	η_{max} (deg)	$\dot{\eta}_{min}$ (deg/s)	$\dot{\eta}_{max}$ (deg/s)	threshold delay time (sec) TDH
q_{max}	-13	9	-100	162	0.10
q_{min}	-32	9	-290	162	
zero	-12	0	-66	38	

TABLE 6.8 – CASE SB0w_θ – TDH = 0.10 sec

MAXIMUM CONTROL EFFORT REQUIRED

sensor failure mode	η_{min} (deg)	η_{max} (deg)	$\dot{\eta}_{min}$ (deg/s)	$\dot{\eta}_{max}$ (deg/s)	flight condition considered
θ_{max}	-22	44	-277	500	steady state trimmed flight
θ_{min}	-46	22	-500	324	
θ_{max}	-27	31	-250	432	manoeuvering flight
θ_{min}	-61	22	-583	324	
zero	-14	0	-72	32	

(A) PRIMARY FAILURES

A comparison of SB0q_w with SB0θ_w shows that they are practically identical with respect to control effort, control rate effort, angle of attack, load factor, pitch rate, pitch attitude, altitude and forward speed transient responses. They differ only with respect to dropback criterion performance, as previously seen in chapter 5 where CL_0B_q and CL_0B_θ are compared with CL_SB, and observer performance. Similarly comparison of SB0w_q with SB0θ_q and SB0w_θ and SB0q_θ leads to broadly similar conclusions.

(B) SECONDARY FAILURES

A comparison of 0w0q_w with 0w0θ_w again shows identical results, similarly when 0q0w_q is compared with 0q0θ_q and when 0θ0w_θ is compared with 0θ0q_θ.

(C) PRIMARY AND SECONDARY FAILURES

A comparison of SBOq_w, SBOθ_w, OwOq_w and Ow0θ_w leads to the same conclusion as when SBOq_w is compared with SBOθ_w as noted in (A) above. So these four cases demonstrate similar aircraft response during the failure transients, except with respect to dropback criterion performance, a feature which depends on the particular control law, and observer performance, which also depends on the particular observer design. The same conclusion can be drawn when SBOw_q, SBOθ_q, OqOw_q and Oq0θ_q are compared, and also when SBOw_θ, SBOq_θ, OθOw_θ and OθOq_θ are compared. So, from a comparison of the simulation results it was concluded that in order to continue the studies of failure conditions it is only necessary to take into account the cases SBOq_w, SBOw_q and SBOw_θ. These three cases are representative of the transient conditions following the failure of each sensor, that is, these three cases are alone sufficient to represent the aircraft subject to the failure conditions studied.

Referring to dropback characteristics, the following was observed,

(i) CL_OB_w has a tendency to give an excessive overshoot, dropback attitude around -6.9°.
(ii) CL_OB_q and CL_OB_θ have a good response with respect to dropback characteristics, giving a reasonable dropback attitude, 1.2° for CL_OB_q and -1.7° for CL_OB_θ.

It is important to note that the above performances are obtained following failure conditions and so they are not the same as those obtained without failure conditions. From these observations it is concluded that in the event of a primary failure, the implementation of CL_OB_q or CL_OB_θ must have preference over the choice of CL_OB_w. A comparison of the observer response shows:

(i) Relative to estimates of u (forward speed), better estimates of u are obtained with CL_OB_q and CL_OB_θ.
(ii) Relative to estimates of w (normal velocity), control laws,

CL_OB_q and CL_OB_θ give the same accuracy.

(iii) Relative to estimates of q (pitch rate) , CL_OB_θ is better than CL_OB_w.

(iv) Relative to estimates of θ (pitch attitude), CL_OB_q is better than CL_OB_w.

Concerning the u estimates, it is also important to note that even in the steady state flight cases, there is always an error in the u estimate with any of the designed observers. This fact shows that these observers are not appropriate for use with a control law that requires the use of a u estimate in a feedback path. Comparing the primary failure cases: SB0q_w, SB0q_θ, SB0θ_q and SB0θ_w with those of secondary failures: 0w0q_w, 0θ0q_θ, 0q0θ_q and 0w0θ_w, the u estimates are better than those obtained following the secondary cases. The estimates of w, q and θ are without error following any of the steady state failure cases.

The following performance characteristics were also observed during the simulation studies ;

(i) Following a steady-state failure condition the demand for high control effort and control rate effort increases with the following order of sensor signal failures w, q and θ.

(ii) In the case of a failure during a pilot input, when any of the sensors fails to zero, there is no significant difference in the control effort or control rate effort required.

(iii) The failure of the q sensor or the θ sensor is followed by saturation of control and control rate when the failure is of the hardover type, irrespective of the initial state of the aircraft.

(iv) The length of the threshold detection time delay has a much more critical effect following the failures of q or θ sensors.

(v) When a sensor is failed to zero the influence of the threshold detection time delay is pratically insignificant.

(vi) A failure of the w sensor does not influence the altitude response of the aircraft significantly compared with the other sensor failures.

(vii) The θ sensor failure leads to the greatest deterioration of the flying qualities of the aircraft, followed by the q sensor failure and the w sensor failure in order of deterioration.

Consequently it is concluded that it would be advisable to include some safety device, such as a limiter, on the feedback paths of q and θ. The main problem identified was the saturation of control rate effort, a feature also identified in McRuer-Johnston-Myers[71]. This problem occurs with both designs, optimal and pole-placement and can probably be minimized by designing the control law by optimal control methods but with a modified performance index, as suggested by Lewis-Stevens[18]. In order to design the amplitude limiter for each feedback path, it is only necessary to perform a study of the following conditions:

(i) SBOq_w in hardover failure
(ii) SBOw_q in hardover failure
(iii) SBOw_θ in hardover failure

Finally, if the control laws are to be reconfigured following failures then the switching logic should select the control laws in the order presented in figure 6.14.

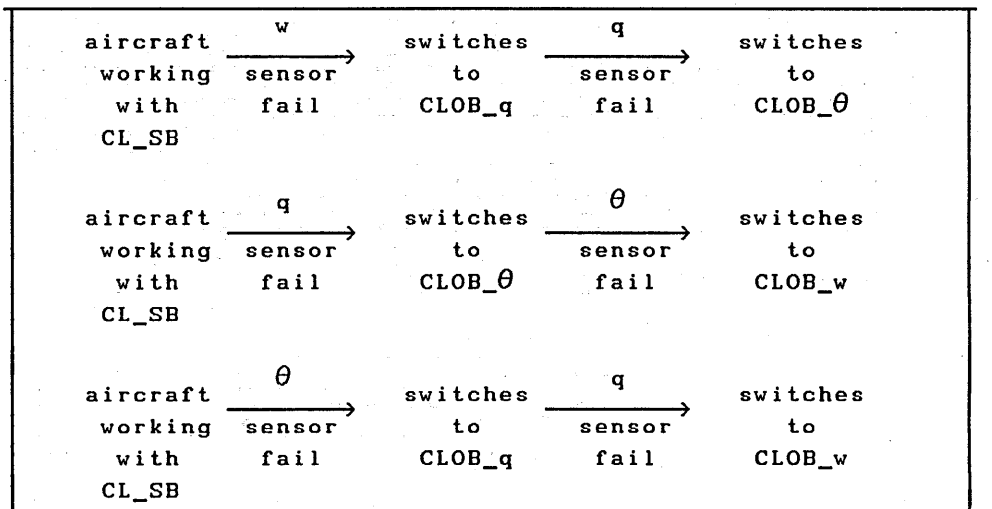

figure 6.14 - suggested order of reconfiguration in the event of sensor failures

The order suggested in figure 6.14 is capable of closely maintaining the original flying qualities of the designed sensor based control law. Note that CL_OB_w is only implemented in the case of a double failure, this is a result of the analysis performed here as well as in chapter 5 which shows that CL_OB_w offers the worst performance compared to CL_OB_q and CL_OB_θ.

7 COMPARATIVE FLIGHT CONTROL SYSTEM PERFORMANCE ANALYSIS

7.1 THE REGULATOR CHARACTERISTICS

7.1.1 INTRODUCTION

The Gibson dropback criterion is concerned with the tracking performance of the control law, that is, the ability of the aircraft to track a reference input. It is also interesting to evaluate the ability of the flight control system to restore the states if these are perturbed. That aspect is commonly assessed in the aeronautical industry by simulating an alpha release, that is, simulating the aircraft response for an initial perturbation in angle of attack, for the longitudinal case, and a beta release, that is simulating the aircraft response for an initial perturbation in sideslip. As the problem considered is the longitudinal case, an alpha release will be used to assess the regulator performance of the designed control laws. The alpha perturbation used was a release at $t = 0$ from an initial condition of $\alpha = 5^{\circ}$, and so an equivalent initial perturbation in w was introduced in the equations of motion, that is, the simulation is performed with $w(0) \neq 0$.

7.1.2 THE SENSOR BASED CONTROL LAW CL_SB

The study was performed for both designs, the pole placement control law design and the optimal control law design. The comparison of both designs shows that the optimal control law design restores the perturbed state w to zero faster than the pole placement control law design. It was also noticed that the optimal control law design presents a smoother response in pitch rate and in pitch attitude compared with the pole placement control law design. In figure 7.1 there is a time history comparison for both designs at flight condition 6 for the same perturbation.

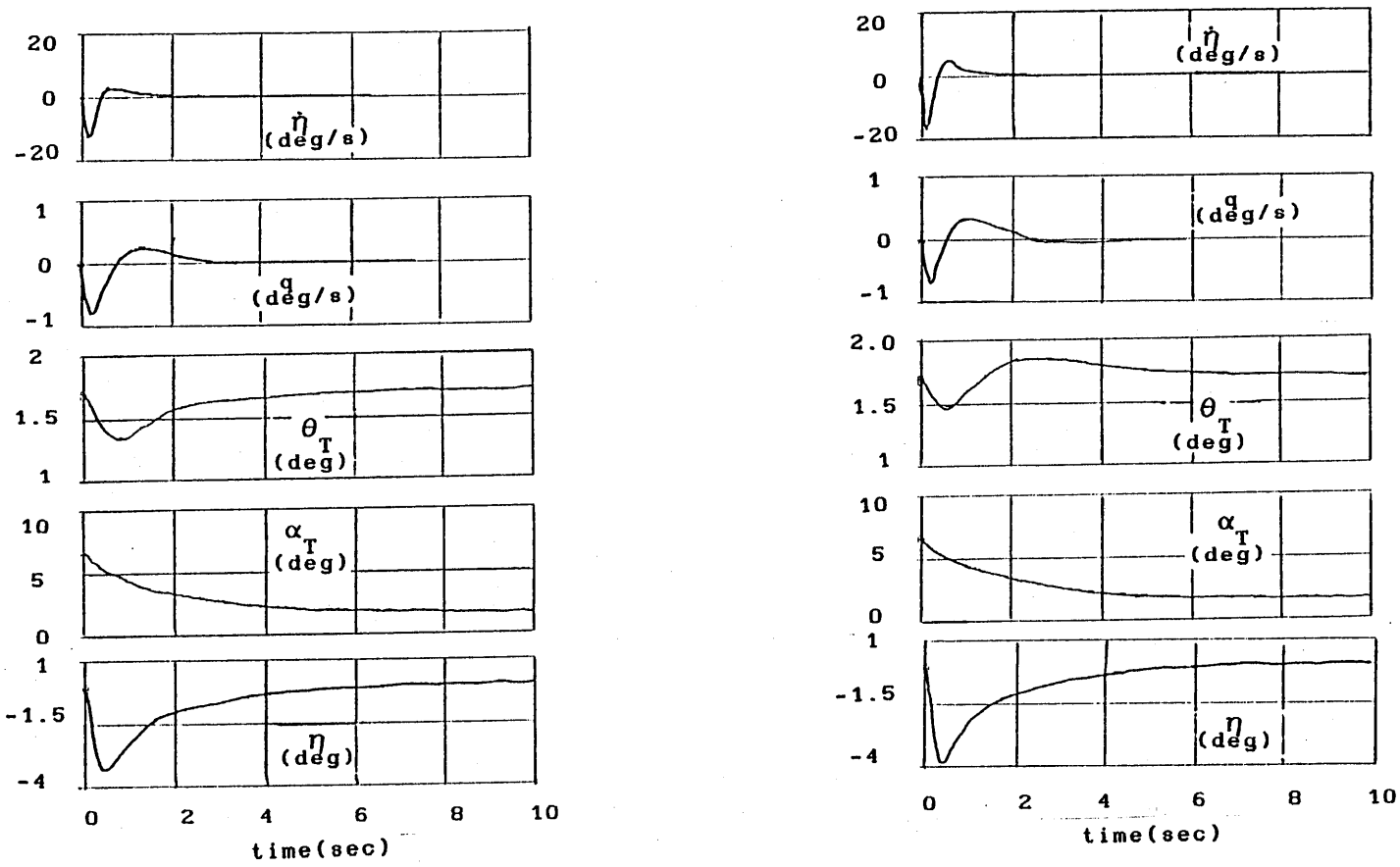

figure 7.1 - time histories following an initial alpha perturbation of 5° for the aircraft with optimal control law design and with pole placement control law design at 20000 ft mach 0.70

In table 7.1 the control effort and control rate effort obtained for each control law design is presented. It has been noticed that the pole placement control law design requires more control rate effort and also more control effort. This was expected since the magnitude of the feedback gains of the pole placement control law design are higher than the magnitude of the feedback gains of the optimal control law design.

TABLE 7.1

CONTROL EFFORT AND CONTROL RATE EFFORT COMPARISON

FC #	POLE PLACEMENT		OPTIMAL CONTROL	
	η_{min} (deg)	$\dot{\eta}_{min}$ (deg/sec)	η_{min} (deg)	$\dot{\eta}_{min}$ (deg/sec)
3	-3.2	-14.4	-3.3	-13.3
6	-3.9	-17.8	-3.4	-13.4
9	-4.9	-21.3	-3.6	-13.3
13	-5.5	-26.8	-3.7	-15.6
17	-3.9	-17.8	-3.6	-14.2

7.1.3 THE OBSERVER BASED CONTROL LAW CL_OB_w

The same simulations were performed for control law CL_OB_w designed by both methods, pole placement and optimal control, and the findings are summarized as follows,

(i) In this case the pitch attitude response, θ , takes more time to return to zero compared with the case of CL_SB. This happens with both designs, pole placement and optimal control.

(ii) The regulation of w is the same as obtained with CL_SB for both designs, pole placement and optimal control.

(iii) The pitch rate, q, response is different with both designs, that is, the transient response is different. However, in both designs the pitch rate returns to zero. These transients explain the finding (i).

(iv) The control effort and control rate effort obtained with CL_OB_w are lower than the corresponding efforts obtained with CL_SB.

(v) With respect to the estimates of u, q and θ, it is quite clear that these estimates are not very precise. This is the explanation for the findings mentioned above. The estimates are not very precise due to the observer, which in this case, has a pair of complex poles located very close to the s-plane origin (that pair of complex poles corresponds with the transmission zero of the open loop tranfer function w/η).

In table 7.2 the control effort and control rate effort obtained with each control law design are shown, and in figure 7.2 the time histories obtained for flight condition 6 with the optimal control law design are shown.

TABLE 7.2

CONTROL EFFORT AND CONTROL RATE EFFORT COMPARISON

FC #	POLE PLACEMENT		OPTIMAL CONTROL	
	η_{min} (deg)	$\dot{\eta}_{min}$ (deg/sec)	η_{min} (deg)	$\dot{\eta}_{min}$ (deg/sec)
3	-2.7	-12.8	-2.6	-10.9
6	-3.4	-15.5	-2.8	-10.5
9	-4.2	-18.9	-3.0	-12.0
13	-5.4	-25.4	-3.3	-13.3
17	-3.4	-15.0	-2.9	-11.7

As noticed the regulation characteristics presented by CL_OB_w are little different from those of the CL_SB. The disadvantage here is that the pitch attitude, θ , takes longer to return to zero than it does with CL_SB. On the other hand, there is the advantage of lower control effort and control rate effort.

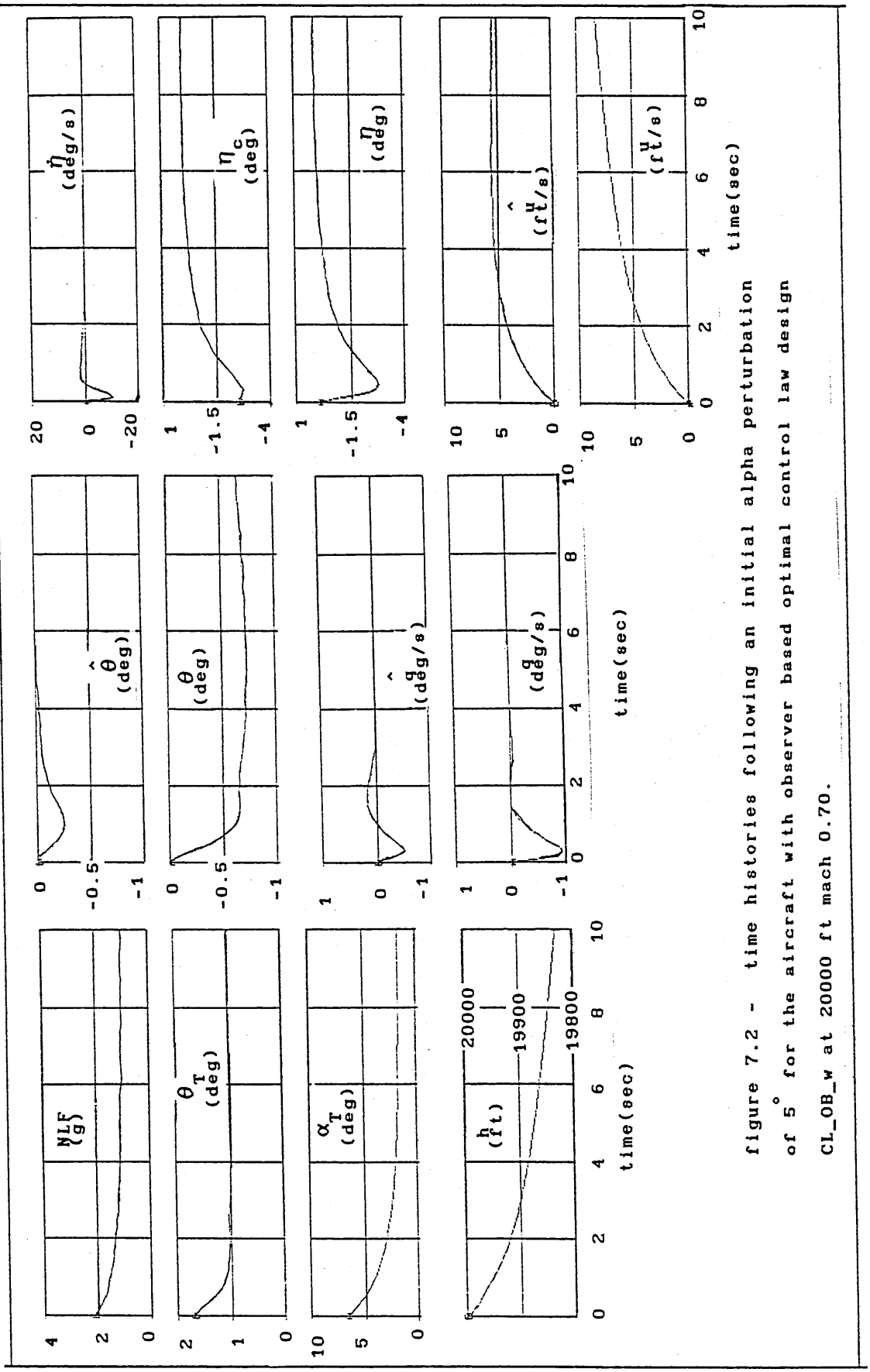

figure 7.2 - time histories following an initial alpha perturbation of 5° for the aircraft with observer based optimal control law design CL_OB_w at 20000 ft mach 0.70.

7.1.4 THE OBSERVER BASED CONTROL LAW CL_OB_q

The same alpha release simulation was performed with CL_OB_q with both designs, pole placement and optimal control. Here the time histories obtained replicate the performance obtained with CL_SB. This fact can be attributed to the fact that as can be seen on figure 7.3, the estimates of u, w and θ are very precise. In table 7.3 the control effort and control rate effort obtained in this case are presented and in figure 7.3 the time histories obtained with optimal control law design at flight condition 6 are shown.

TABLE 7.3

CONTROL EFFORT AND CONTROL RATE EFFORT COMPARISON

FC #	POLE PLACEMENT		OPTIMAL CONTROL	
	η_{min} (deg)	$\dot{\eta}_{min}$ (deg/sec)	η_{min} (deg)	$\dot{\eta}_{min}$ (deg/sec)
3	-3.2	-14.4	-3.2	-13.3
6	-3.8	-17.2	-3.3	-13.3
9	-4.9	-21.3	-3.5	-13.8
13	-5.5	-26.1	-3.7	-15.5
17	-4.0	-17.8	-3.6	-13.8

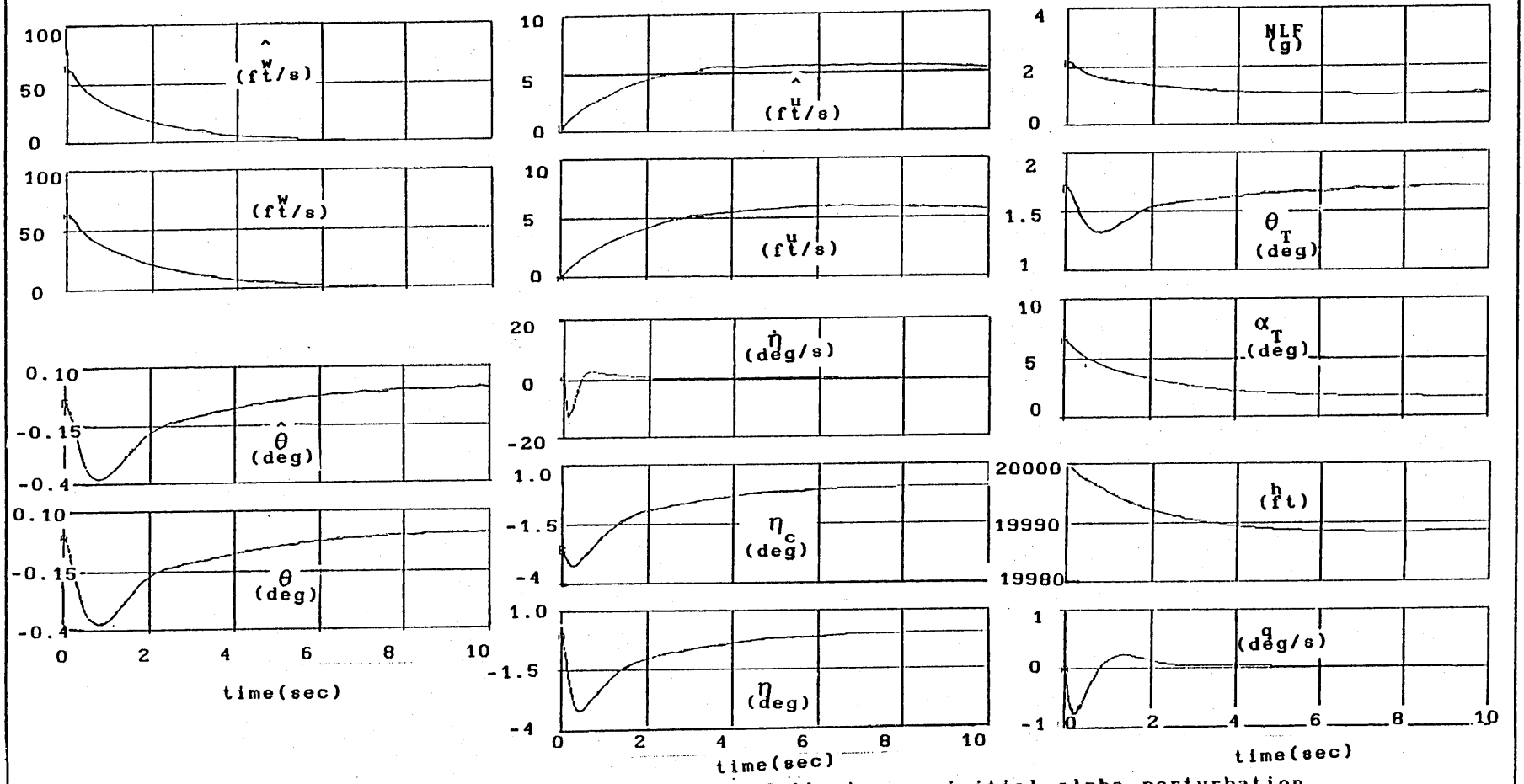

figure 7.3 - time histories following an initial alpha perturbation of 5° for the aircraft with observer based optimal control law design CL_OB_q at 20000 ft mach 0.70.

7.1.5 THE OBSERVER BASED CONTROL LAW CL_OB_θ

The same alpha release simulation was performed with CL_OB_θ with both designs, pole placement and optimal control, and again, as in the case of CL_OB_q, the time histories are very similar to those obtained with CL_SB. Certainly this is due to the fact that the observer estimates are very precise. In table 7.4 the control effort and control rate effort obtained with this control law are presented and in figure 7.4 the time histories obtained with the optimal control law design at flight condition 6 are shown.

TABLE 7.4

CONTROL EFFORT AND CONTROL RATE EFFORT COMPARISON

FC #	POLE PLACEMENT		OPTIMAL CONTROL	
	η_{min} (deg)	$\dot{\eta}_{min}$ (deg/sec)	η_{min} (deg)	$\dot{\eta}_{min}$ (deg/sec)
3	-3.1	-14.4	-3.2	-13.9
6	-3.8	-17.8	-3.3	-13.3
9	-4.9	-21.3	-3.5	-14.4

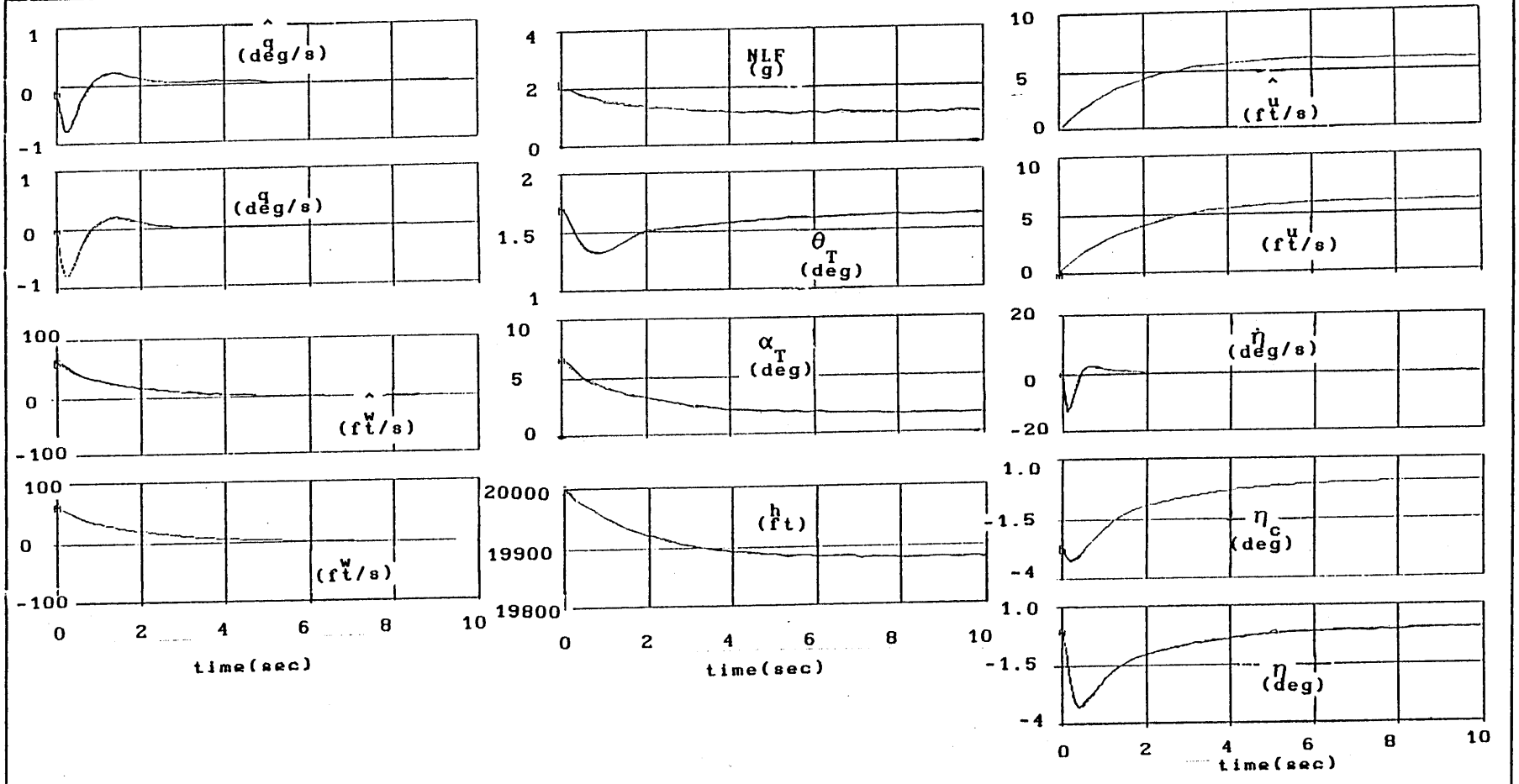

figure 7.4 - time histories following an initial alpha perturbation of 5° for the aircraft with observer based optimal control law design CL_OB_θ at 20000 ft mach 0.70.

7.1.6 INTERIM CONCLUSIONS

From the studies carried out it can be concluded that both control law designs are quite good with respect to regulator performance. The optimal control law design has a little better performance since it restores the disturbed state (w) to its initial condition faster than the pole placement control law design. Also, there is an advantage with the optimal control law design with respect to control effort and control rate effort. In conclusion, the only control law that does not give an acceptable performance is CL_OB_w, due to the responses of pitch rate (q) and pitch attitude (θ) being a little different from those of CL_SB. This can be corrected by designing the observer of CL_OB_w by the same method used to design the observer of CL_OB_q and CL_OB_θ as stated before. So, in the event of a sensor failure, the same order of reconfiguration suggested in chapter 6 showed be applied. It is also interesting to perform the same study with an initial perturbation in pitch attitude, θ , or in the forward velocity u. That is, the same simulations firstly with $\theta(0) \neq 0$ and secondly with $u(o) \neq 0$ in order to assess the regulator performance when such perturbations are included.

7.2 EVALUATION OF THE CONTROL LAWS WITH THE FULL NON-LINEAR MODEL OF THE AIRCRAFT

7.2.1 INTRODUCTION

It is now interesting to review the performance of both control law designs, pole placement and optimal control, working with a non-linear aircraft model. The sensor based and the observer based control laws are investigated in order to give an indication of the behaviour of the augmented aircraft with each control law design. In this analysis only flight conditions 3, 6 and 9 were used and the study was performed by simulation only. During the simulation the gains of the control laws and the gains of the observers were maintained fixed.

The actuator used was actuator no.2 ,described in chapter 3, and the lead pre-filter used was discussed in chapter 4, for both control law designs. In figure 5.3 the control law structure used in the simulations is shown for the case of CL_SB, with the exception that " aircraft dynamics " , now imply the non-linear aircraft dynamics. The pilot input considered is shown in figure 5.4., in order to allow comparison with the results obtained with the linear aircraft model.

7.2.2 EQUATIONS OF THE NON-LINEAR AIRCRAFT MODEL

The non-linear model used in the simulations was a six degree of freedom aircraft model, the equations were obtained from Roskam[72], Mclean[73] and Heffley[11]. This model includes aerodynamic coefficients which vary during the simulation as functions of Mach number, altitude and angle of attack. So at each integration step the aerodynamic coefficients are updated. The equations comprising this model are the following,

$$\dot{u} = r V_T - q W_T - g \sin(\theta_T) + X_0/m + X^*_u u + X_w w + X_q q + X_{\delta e} \delta_e \quad (7.1)$$

$$\dot{v} = p W_T - r U_T + g \cos(\theta_T)\sin(\phi) + Y_0/m + Y_v v + Y_r r + Y_p p + Y^*_{\delta a} \delta_a + Y^*_{\delta r} \delta_r \quad (7.2)$$

$$\dot{w} = (q U_T - p V_T)/(1 - Z_{\dot{w}}) + [g \cos(\theta_T)\sin(\phi)]/(1 - Z_{\dot{w}}) + Z_0/(1 - Z_{\dot{w}}) + [Z^*_u u + Z_w w + Z_q q + Z_{\delta e} \delta e]/(1 - Z_{\dot{w}}) \quad (7.3)$$

$$\dot{p} = (L'_\beta v)/ U_1 + L'_r r + L'_p p + k_5 p q - k_6 q r + L'_{\delta a} \delta a + L'_{\delta r} \delta r \quad (7.4)$$

$$\dot{q} = (I_x - I_z)p\ r/I_y - I_{xz}(p^2 - r^2)/I_y + M_u^* u + M_w w +$$

$$M_{\dot{w}} \dot{w} + M_q q + M_{\delta e}\delta e \qquad (7.5)$$

$$\dot{r} = (N'_\beta v)/ U_1 + N'_r r + N'_p p - k_3 q r + k_4 p q +$$

$$N'_{\delta a}\delta a + N'_{\delta r}\delta r \qquad (7.6)$$

$$\dot{\phi} = p + [q \sin(\phi) + r \cos(\phi)] \tg(\theta_T) \qquad (7.7)$$

$$\dot{\psi} = [q \sin(\phi) + r \cos(\phi)]/ \cos(\theta_T) \qquad (7.8)$$

$$\dot{\theta} = q \cos(\phi) - r \sin(\phi) \qquad (7.9)$$

The auxiliary equations also used are as follows,

$$U_T = U_0 + u \qquad (7.10)$$

$$V_T = V_0 + v \qquad (7.11)$$

$$W_T = W_0 + w \qquad (7.12)$$

$$\alpha_T = \tg^{-1}(W_T / U_T) \qquad (7.13)$$

$$\theta_T = \theta + \theta_0 \qquad (7.14)$$

$$U_1 = \sqrt{U_T^2 + V_T^2 + W_T^2} \qquad (7.15)$$

$$\dot{\beta} = \dot{v} / U_1 \qquad (7.16)$$

$$\dot{\alpha} = \dot{w} / U_T \qquad (7.17)$$

$$X_0 = \mathcal{W} \sin(\theta_0) \qquad (7.18)$$

$$Y_0 = -\mathcal{W} \cos(\theta_0) \sin(\phi_0) \qquad (7.19)$$

$$Z_0 = -\mathcal{W} \cos(\theta_0) \cos(\phi_0) \qquad (7.20)$$

$$\dot{h} = U_T \sin(\theta_T) - V_T \sin(\phi) \cos(\theta_T) - W_T \cos(\phi) \cos(\theta_T) \qquad (7.21)$$

$$Mach = U_1 / V_{sound} \tag{7.22}$$

The inertia constants used in these equations are:

$$k_{lat} = 1 / [\, 1 - I_{xz}^2 / (I_x I_z) \,] \tag{7.23}$$

$$k_1 = I_{xz} / I_z \tag{7.24}$$

$$k_2 = I_{xz} / I_x \tag{7.25}$$

$$k_3 = k_1 k_{lat} [1 + (I_z - I_y)/ I_x \,] \tag{7.26}$$

$$k_4 = k_{lat} [\, k_7 - (I_y - I_x)/ I_z \,) \tag{7.27}$$

$$k_5 = k_2 k_{lat} [1 - (I_y - I_x)/ I_z) \tag{7.28}$$

$$k_6 = k_{lat} [\, k_7 + (I_z - I_y)/ I_x \,] \tag{7.29}$$

$$k_7 = I_{xz}^2 / (\, I_x I_z) \tag{7.30}$$

The aerodynamic derivatives are all defined in Heffley[11], and the complete model is described on the report by Oliva and Cook[12], which also contains a comparison of the linear model and the non-linear model responses for the same input. The linear model is also described briefly in appendix A. However, for completeness it is repeated here. So the equations used in the linear model are simply given by,

$$\dot{u} = X_u^* u + X_w w + X_q q - W_0 q - g \cos(\theta_0)\, \theta + X_{\delta e}\, \delta e \tag{7.31}$$

$$\dot{w} = [Z_u^* /(1-Z_{\dot{w}}) \,] u + [\, Z_w /(1-Z_{\dot{w}}) \,] w + [(Z_q + U_0)/(1-Z_{\dot{w}})] q +$$

$$- [g \sin(\theta_0)/(1-Z_{\dot{w}})] \theta + [\, Z_{\delta e}/(1-Z_{\dot{w}}) \,] \delta e \tag{7.32}$$

$$\dot{q} = M_u^* u + [M_{\dot{w}} Z_u^*/(1-Z_{\dot{w}})] u + M_w w + [M_{\dot{w}} Z_w /(1-Z_{\dot{w}})] w +$$

$$M_q q + [\, M_{\dot{w}} (Z_q + U_0)/(1-Z_{\dot{w}}) \,] q - [M_{\dot{w}}\, g \sin(\theta_0)/(1-Z_{\dot{w}})] \theta +$$

$$M_{\delta e} \delta e + [M_{\dot{w}} Z_{\delta e}/(1-Z_{\dot{w}}) \,] \delta e \tag{7.33}$$

$$\dot{\theta} = q \tag{7.34}$$

Although only a comparison between the control law designs working with the linear model and with the non-linear model with respect to the dropback criterion have been performed, the non-linear model is also useful for other analysis. For example, to evaluate performance with an initial bank angle (ϕ_0) or an initial sideslip angle (β_0) or, with a pilot manoeuver not only with elevator but also with rudder or ailerons. The model is also usefull for evaluating the performance of the observers working with the non-linear model, and for studying the effects of gain scheduling. A study of a steady turn or other steady manoeuver may also be performed with the help of this model in order to assess the performance of the designed control laws under these conditions. The main non-linear feature of the simulation is the fact that the aerodynamic coefficients are not maintained fixed during the simulation, that is, they vary with time, angle of attack, altitude and Mach number. Another non-linear aspect of the model is that small angle approximations, for example, $\sin\theta \simeq \theta$ have not been used. The non-linear model also includes cross coupled inertial terms, which are not very relevant in the case of a civil aircraft. The simulations were performed for zero initial conditions, that is, $u(0) = 0$, $w(0) = 0$ $v(0) = 0$, $p(0) = 0$, $q(0) = 0$, $r(0) = 0$, $\phi(0) = 0$, $\psi(0) = 0$ and $\theta(0) = 0$.

7.2.3 THE SENSOR BASED CONTROL LAW CL_SB

The time histories obtained from the simulations performed with CL_SB are showed in figure 7.5 for the pole placement control law design and in figure 7.6 for the optimal control law design. The time histories showed in figure 7.6 can be compared with those showed in figure 5.5 obtained with the aircraft linear model. From the simulations the following may be noted with respect to the same study with the linear model:

(i) The control effort is practically unchanged.

(ii) The same occurs for the control rate effort.

(iii) The peak pitch rate q_m is also unchanged.

(iv) The steady state pitch rate q_{ss} obtained with the non-linear model is lower than it was with the linear model, which means that possibly, an adjustment of K_{ε_q} is necessary in order to guarantee that the control law continues to work well with the non linear model and to recover the same steady state pitch rate response.

(v) The general tendency of the control law working with the non linear model is to give a lower pitch attitude dropback than with the linear model, which is a consequence of (iv) above.

(vi) The peak angle of attack obtained with the non linear-model is lower than it was with the linear model, about 3° lower.

(vii) The altitude and the load factor responses are unchanged.

It was therefore necessary to repeat the same study with gain scheduling in order to assess if it is required to adjust K_{ε_q} or not, since the simulations were performed with fixed gains.

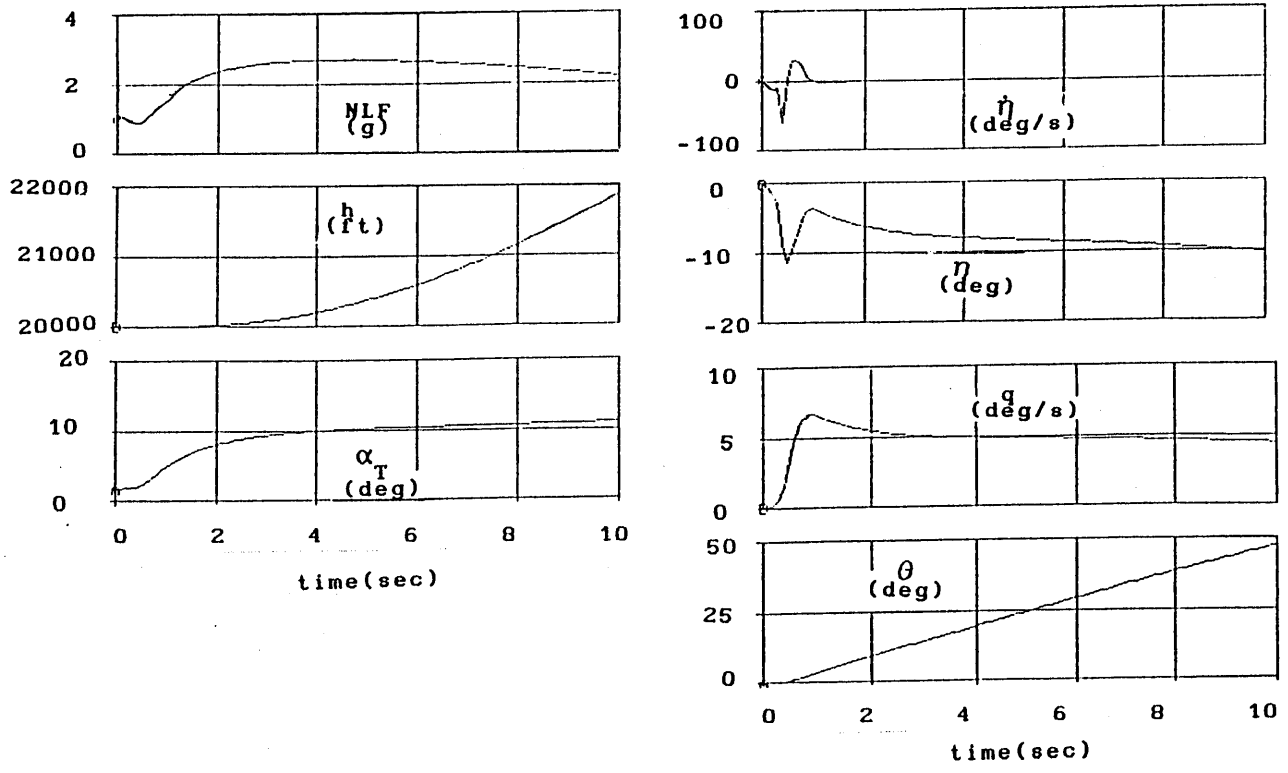

figure 7.5 - time histories obtained with the aircraft working with the sensor based pole placement control law design and full non linear aircraft model at 20000 ft mach 0.70.

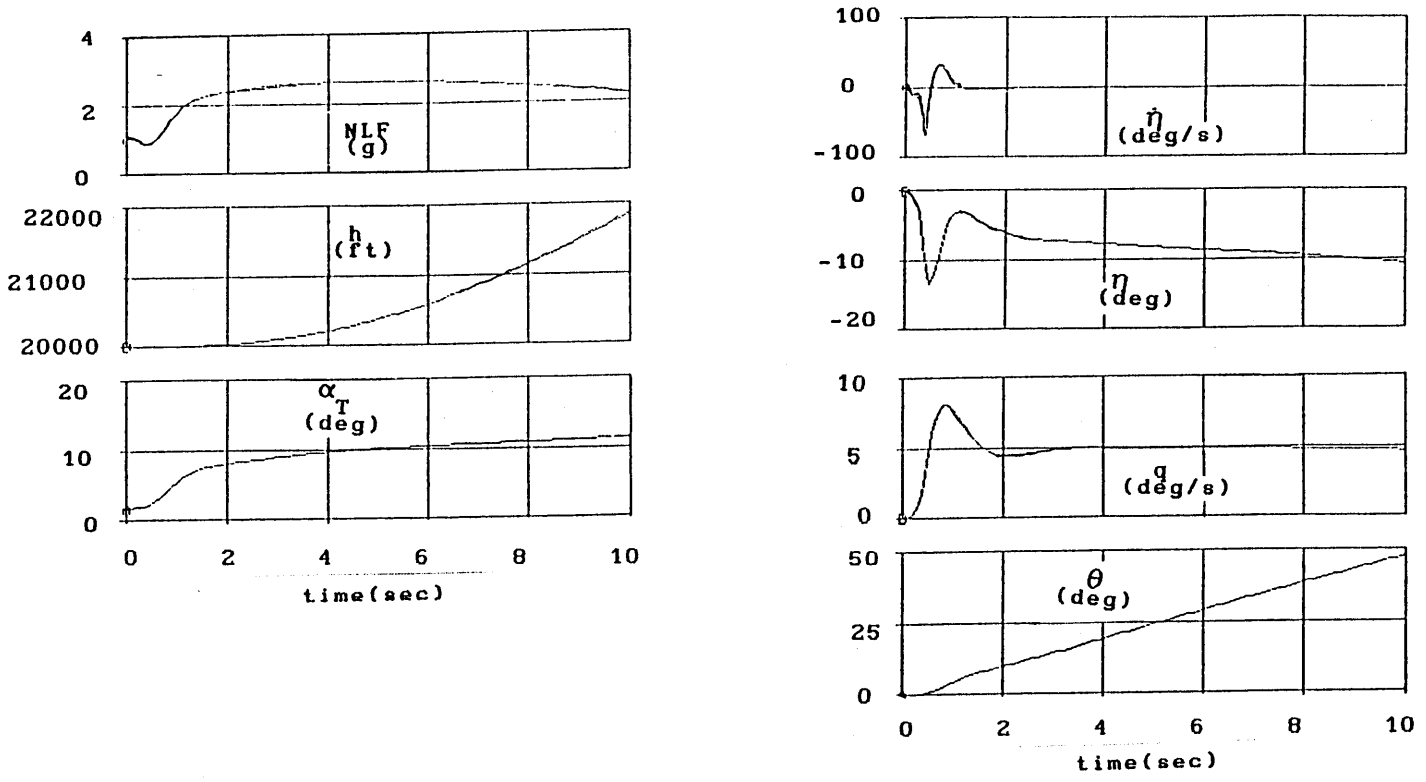

figure 7.6 - time histories obtained with the aircraft working with the sensor based optimal control law design and full non linear aircraft model at 20000 ft mach 0.70.

7.2.4 THE OBSERVER BASED CONTROL LAW CL_OB_w

Figure 5.7 shows the control law implementation for this case, again, the only change is that " aircraft dynamics " imply the non-linear aircraft dynamics. The results obtained are compared with those obtained with the linear model. In this case not only the performance of the control law is evaluated but also the observer performance. In figure 7.7 the time histories obtained with the pole placement control law design are shown and in figure 7.8 those obtained with the optimal control law design are plotted. The time histories of figure 7.8 can be compared with those showed in figure 5.8 obtained with the aircraft linear model. The observations derived from the simulations are summarized as:

(i) The control effort is unchanged with respect to the linear model, as in the, CL_SB case previously.

(ii) The same occurs to the control rate effort.

(iii) The attitude dropback characteristics are much better with the non-linear model due to the fact that the steady state pitch rate is greater here, than it is with the linear model.

(iv) The maximum pitch rate q_m is practically unchanged.

(v) The normal load factor, angle of attack and altitude are also practically unchanged.

(vi) The observer performance is better with respect to θ estimate, than it was in the linear case. However, at some flight conditions the u estimate was deteriorated compared with the linear model.

In conclusion here the performance is better than it was with the linear model, but it is necessary to assess if this is true when the system works with gain scheduling.

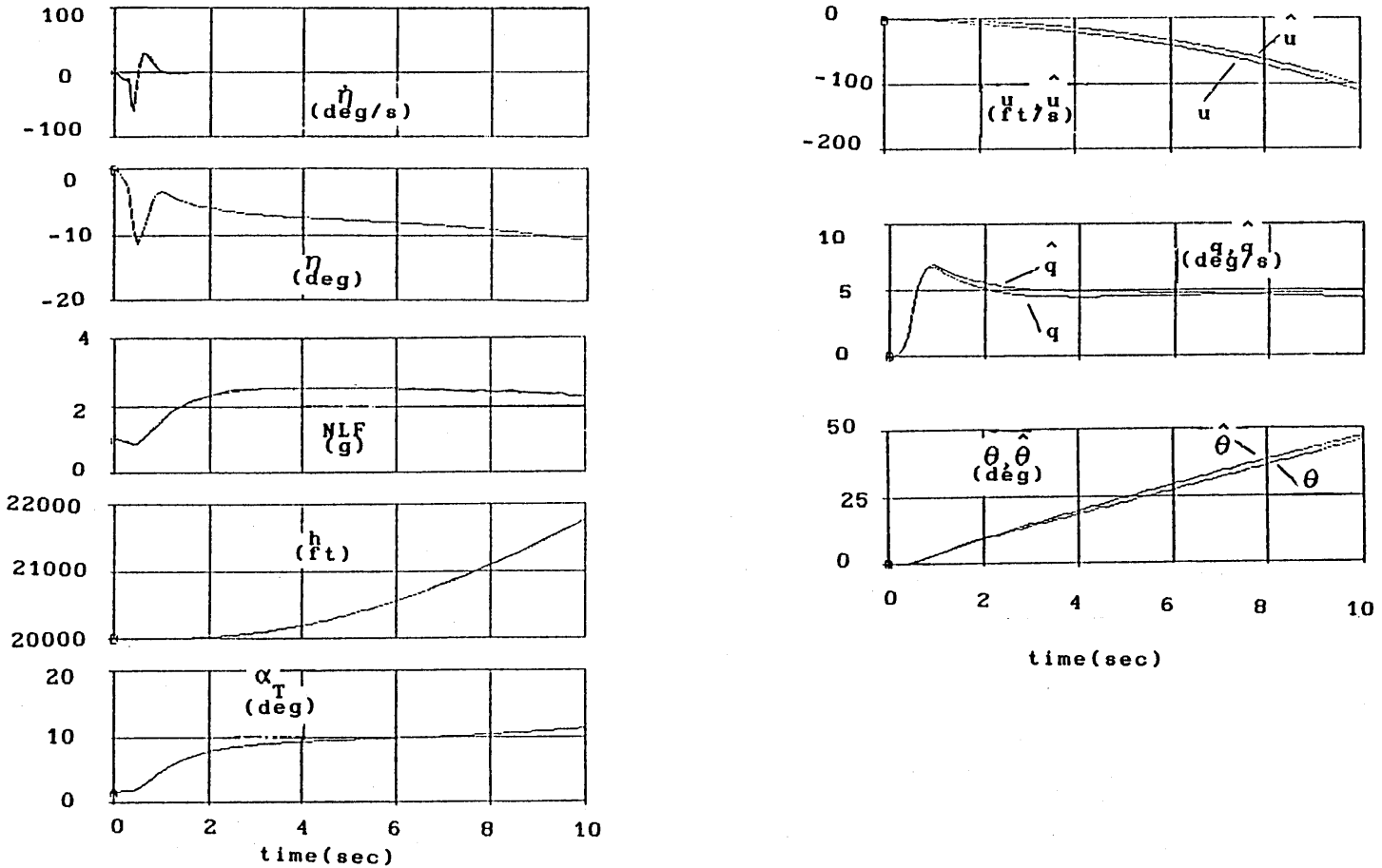

figure 7.7 - time histories obtained with the aircraft working with the observer based pole placement control law design , CL_OB_w, and full non linear aircraft model at 20000 ft mach 0.70.

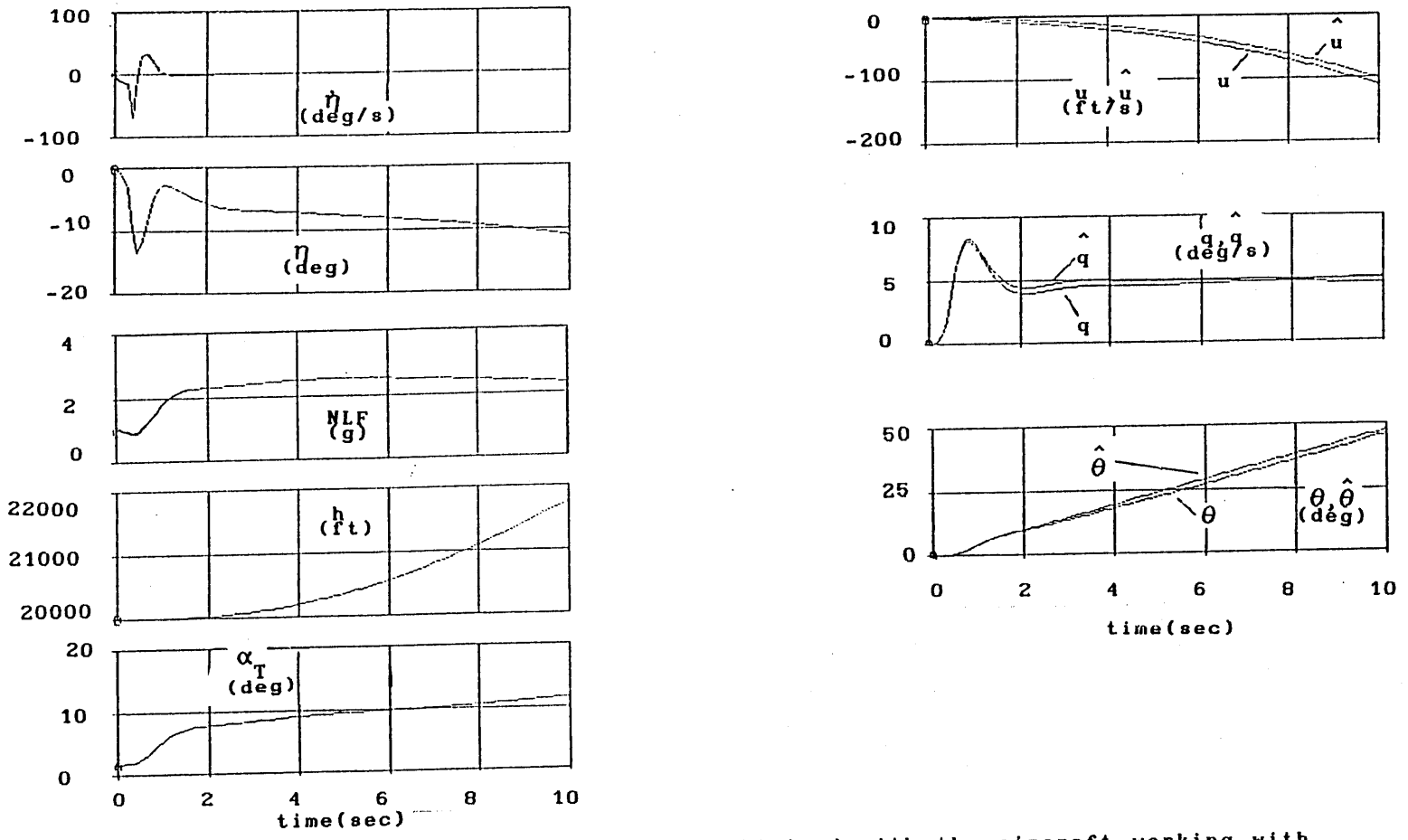

figure 7.8 - time histories obtained with the aircraft working with the observer based optimal control law design , CL_OB_w, and full non linear aircraft model at 20000 ft mach 0.70.

7.2.5 THE OBSERVER BASED CONTROL LAW CL_OB_q

The control law structure used is shown in figure 5.10, again " aircraft dynamics ", implies the non-linear aircraft dynamics. In figure 7.9 the time histories obtained with the optimal control law design are shown. The results showed in figure 7.9 can be compared with those showed in figure 5.11 obtained with the aircraft linear model. From the study performed with CL_OB_q the following observations were noted:

(i) The control effort is unchanged compared with the linear model.

(ii) The same occurs to the control rate effort

(iii) With both control law designs, pole placement or optimal control, the attitude dropback characteristic is worse than that obtained with the linear aircraft model.

(iv) The steady state pitch rate is only changed at flight condition 9

(v) The maximum pitch rate is practically unchanged

(vi) The observer estimate now is worse than it was with the linear model.

(vii) The angle of attack obtained is about 2° lower than it was with the linear model.

(viii) Here the altitude response and load factor have suffered a small change compared with the linear model.

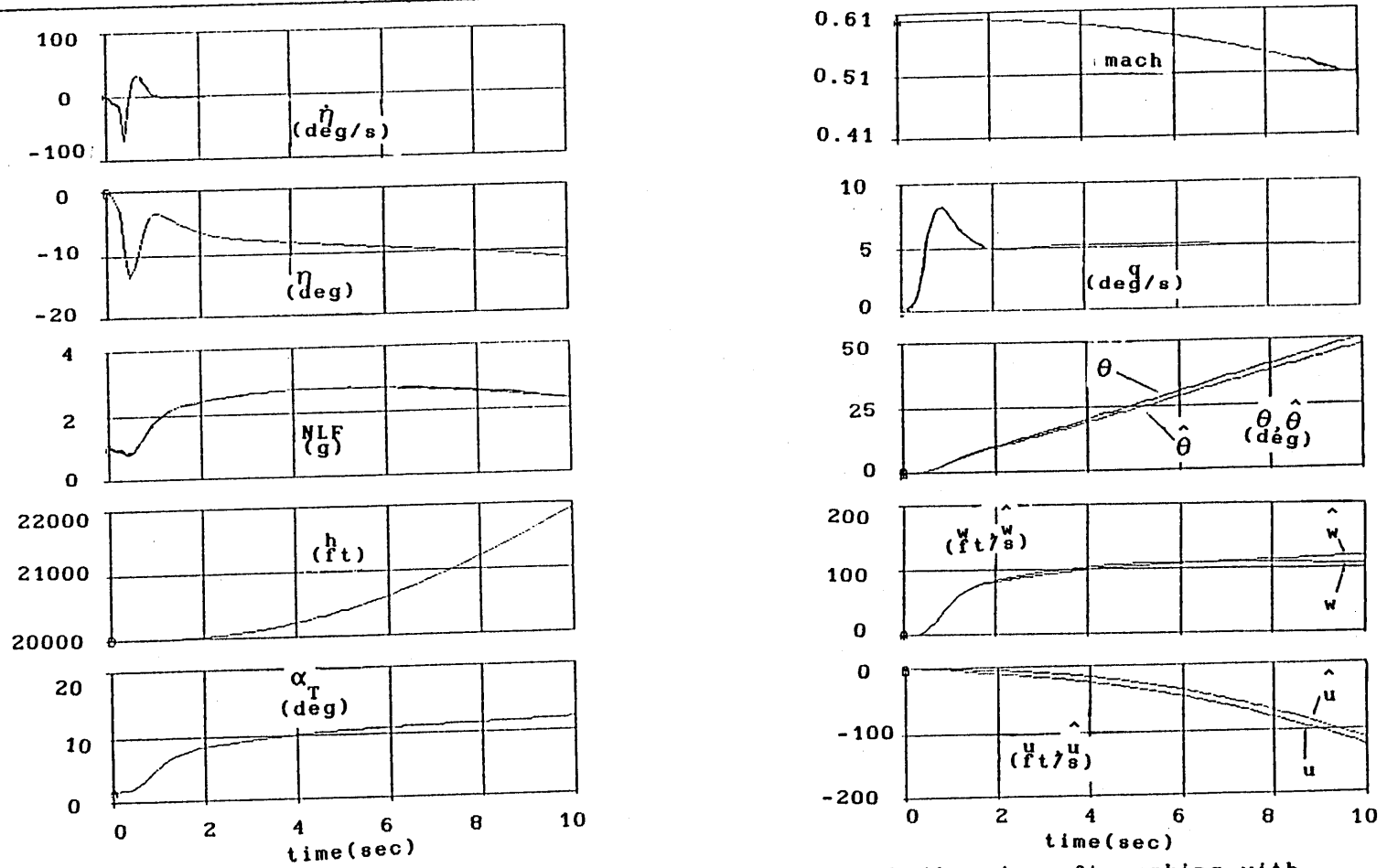

figure 7.9 - time histories obtained with the aircraft working with the observer based optimal control law design , CL_OB_q, and full non linear aircraft model at 20000 ft mach 0.70.

7.2.6 THE OBSERVER BASED CONTROL LAW CL_OB_θ

The implementation used is showed on figure 5.13, again using the non-linear aircraft dynamics. Figure 7.10 shows the time histories obtained with the optimal control law design. The time histories showed in figure 7.10 can be compared with those showed in figure 5.14 obtained with the aircraft linear model. From the results of this study the following can be summarized,

(i) Again the control effort is unchanged compared with the linear model.

(ii) The same is observed for the control rate effort

(iii) The attitude-dropback characteristics are now worse than those obtained with the linear aircraft model. However, here the deterioration is not so bad as in the case of CL_OB_q.

(iv) The steady state pitch rate is lower than it was in the linear case.

(v) The maximum pitch rate (q_m) is practically unchanged.

(vi) The normal load factor and the altitude is practically unchanged.

(vii) The angle of attack obtained is in general 2° lower than that obtained with the linear model.

(viii) The observer performance, with respect to u, w and q estimates, is worse than that obtained with the linear model.

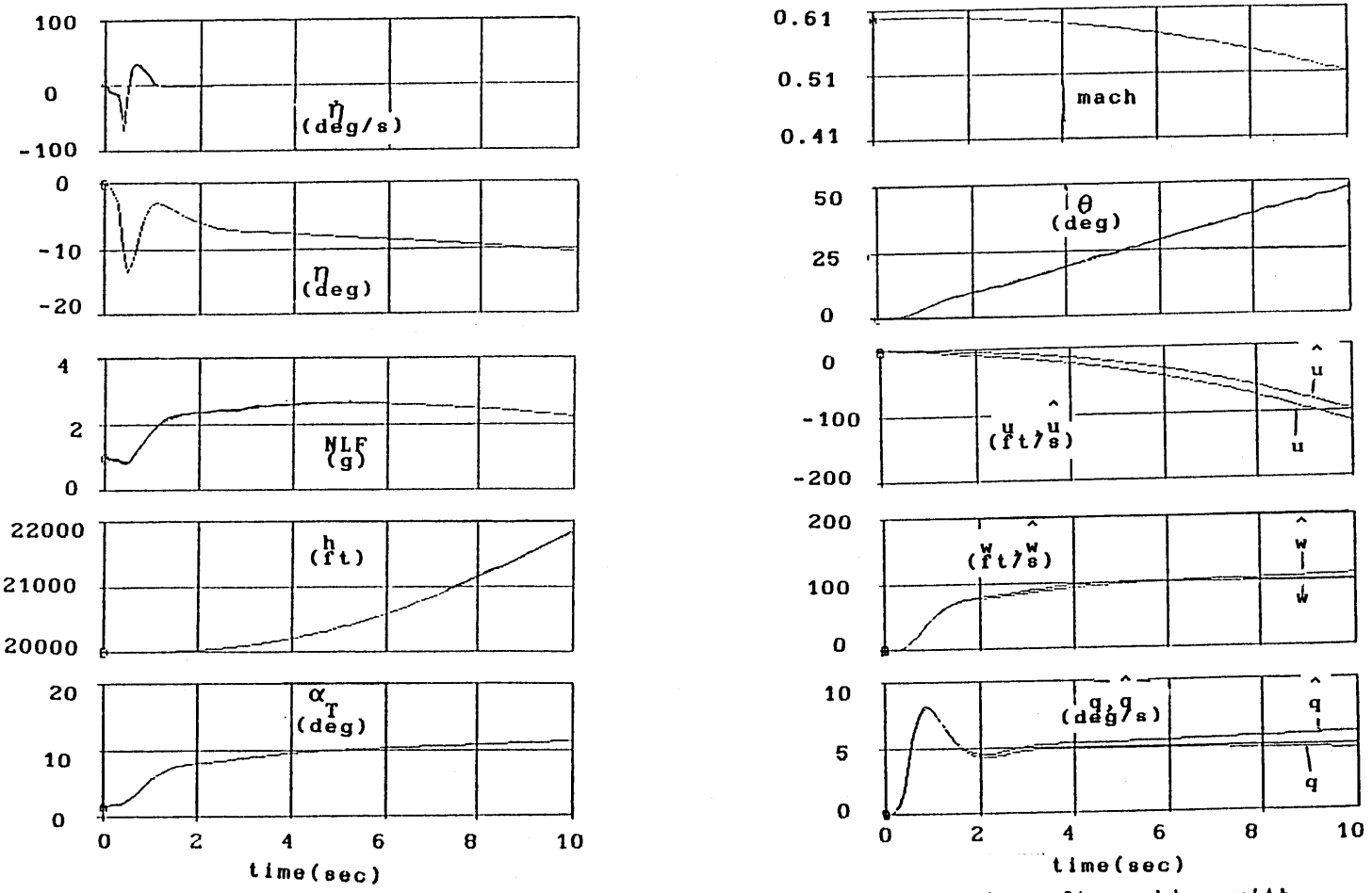

figure 7.10 - time histories obtained with the aircraft working with the observer based optimal control law design , CL_OB_θ, and full non linear aircraft model at 20000 ft mach 0.70.

7.3 INTERIM CONCLUSIONS

The results have shown that control law CL_OB_q would probably require adjustment in order to obtain good regulation of the attitude dropback characteristic, CL_OB_θ will also require some adjustment, and finally, CL_OB_w will practically not require adjustment. However, this is only a preliminary result, since the simulations have been performed with fixed gains, and during these simulation it was noticed that the altitude varied by as much as 2000 ft in 10 seconds and the Mach number varied by about 0.12 in 10 seconds. So it would be necessary to repeat the study with gain scheduling, for both the control law gains and the observer gains, in order to aquire a more realistic assessment of likely performance. Then a decision could be made on wheter the adjustments are really necessary or not. In general it was noticed that the transient characteristics are unchanged due to the fact that in the transient response the angle of attack, Mach number and altitude are practically the same as in the linear model, and so the control effort, control rate effort and maximum pitch rate are not changed because they occur at the begining of the aircraft response by the other way, the attitude dropback, steady state pitch rate, steady state angle of attack and all steady state parameters are changed due to its occurence at the final time of the simulation. In general it has been noticed that the transient characteristics are basicaly the same as obtained with the aircraft linear model, and the steady state characteristics have changed a little bit, this can be explained by the above mentioned facts about Mach number variation as also altitude and angle of attack.

8 ALTITUDE HOLD AUTOPILOT DESIGN

8.1 INTRODUCTION

One of the pilot's many tasks is to hold a specific altitude. As an aid to keeping aircraft from colliding, those aircraft on an easterly path are required to be on an odd multiple of 1000 ft, while those on a westerly path are required to be on an even multiple of 1000 ft. It is therefore of some concern to the pilot that the altitude be held to within a few hundred feet. A well trained attentive pilot can easily accomplish this task to within ± 50 ft, and this kind of tolerance is what the air traffic controllers expect pilots to maintain. Since this task requires the pilot to be fairly diligent, sophisticated aircraft often have an altitude hold autopilot to perform the task. This system is fundamentally different from the stability augmentation system designed in the previous chapters of this work in that its role is to replace the pilot for certain periods of time, while the previous stability augmentation system role is to help the pilot fly. Dynamic specifications, therefore, need not be such that pilots like the aircraft's "feel" ; instead, the design should provide the kind of ride that pilots and passengers like. So the damping ratio should be in the vicinity of 0.50, but, for a smooth ride, the natural frequency should be lower than the short period natural frequency. In this chapter the autopilot will be designed by an optimal control method, that is, designed specifically by the LQR method to work with the augmented aircraft, incorporating the inner loop control laws designed in the previous chapters.

8.2 THE DESIGN METHOD

In order to design the autopilot it is necessary to include the height equation in the model, which is written as,

$$\dot{h} = -w + U_0 \theta \qquad (8.1)$$

In this case the system must track a reference altitude, designated h_{ref}. By the same procedure as used in the design of the inner loop, it is possible to define an altitude error,

$$\dot{\varepsilon}_h = h - h_{ref} \tag{8.2}$$

Considering now the aircraft represented by the state equation,

$$\dot{x} = A\,x + B\,\eta \tag{8.3}$$

where x is simply $x^T = [\,u\ w\ q\ \theta\,]$ (8.4)

and the A and B matrices are given in appendix A. So equation 8.1 can be written as,

$$\dot{h} = [\,0\ \ -1\ \ 0\ \ U_0\,]\,x \tag{8.5}$$

As the design is for the augmented aircraft, the feedback gains of either stability augmentation control law, optimal or pole placement, are written as,

$$G = [\,0\ \ K_w\ \ K_q\ \ K_{\varepsilon_q}\,] \tag{8.6}$$

Considering the inner loop control law implemented as in figure 6.4 the augmented aircraft is represented by the state equation,

$$\dot{x} = (A - BG)\,x + B\,\eta_{AP} \tag{8.7}$$

Where η_{AP} is the control input to the elevator required by the autopilot. With this in mind the complete system can be represented as follows,

$$\dot{x}_{AP} = A_{AP}\,x_{AP} + B_{AP}\,\eta_{AP} + E\,h_{ref} \tag{8.8}$$

where, $$x_{AP}^T = [\,x\ \ h\ \varepsilon_h\,] = [\,u\ w\ q\ \theta\ h\ \varepsilon_h\,] \tag{8.9}$$

$$B_{AP}^T = [\,B\ \ 0\ 0\,] \tag{8.10}$$

$$E^T = [\,0\ 0\ 0\ 0\ 0\ -1\,] \tag{8.11}$$

and,

$$A_{AP} = \begin{bmatrix} (A - B G) & 0 & 0 \\ [0 \ -1 \ 0 \ U_0] & 0 & 0 \\ [0 \ 0 \ 0 \ 0] & 1 & 0 \end{bmatrix} \tag{8.12}$$

Thus, this model includes the height equation and the error equation. Using the LQR theory described in chapter two, as given, for example, in Friedland[13] and the other references concerned with optimal control, a performance index similar to that used in chapter 3 will be taken,

$$V_{AP} = \int_0^{\infty} (x_{AP}^T Q x_{AP} + \eta_{AP}^T R \eta_{AP}) \, dt \tag{8.13}$$

In this case Q is a matrix (6 x 6) and R is a scalar. The same design philosophy, as applied in chapter 3 for the inner loop optimal control law design will be used here, that is, only the state ε_h will be weighted in the state weight matrix Q of (8.13). Then Q will be taken as a diagonal matrix with zeros in the diagonal, except the element q_{66} which is designated $q_{66} = \rho$ and R will be taken as unity , that is, R = 1. Again, as in the previous design, the parameter ρ was found by a parametric search until a reasonable control demand and altitude response was obtained. The autopilot control law is,

$$\eta_{AP} = - G_{AP} x_{AP} \tag{8.15}$$

where G_{AP} is given by the solution of the LQR problem. With the help of MATLAB, given A_{AP}, B_{AP}, Q and R ,the feedback gain matrix is easily found,

$$G_{AP} = [G_u \ G_w \ G_q \ G_\theta \ G_h \ G_{\varepsilon_h}] \tag{8.16}$$

As a reasonable control demand is desired the design should not give high feedback gains since high gains would require higher control demand and higher control rate demand.

As a guideline, for a step input in h_{ref} the altitude should reach the required h_{ref} in 20 to 30 seconds. A parametric study was performed by varying ρ in the state weight matrix until a reasonable h response was obtained as well as a reasonable control effort. This study was performed by the method given in Friedland[13], that is, by the choosing ρ, obtaining the feedback gains, obtaining the time response of h to a unit step in h_{ref}, and checking to see if the control effort and control rate effort are acceptable or not. With few calculations the control law is easily obtained. The design can be compared with the design described by Powell[7] for the same aircraft, which is also an optimal control design. The difference that Powell's design uses proportional feedback only, that is, there is no integral feedback of the error as used in this design. In figure 8.1 the augmented aircraft considered in the design is shown, and in figure 8.2 the autopilot with the augmented aircraft is shown.

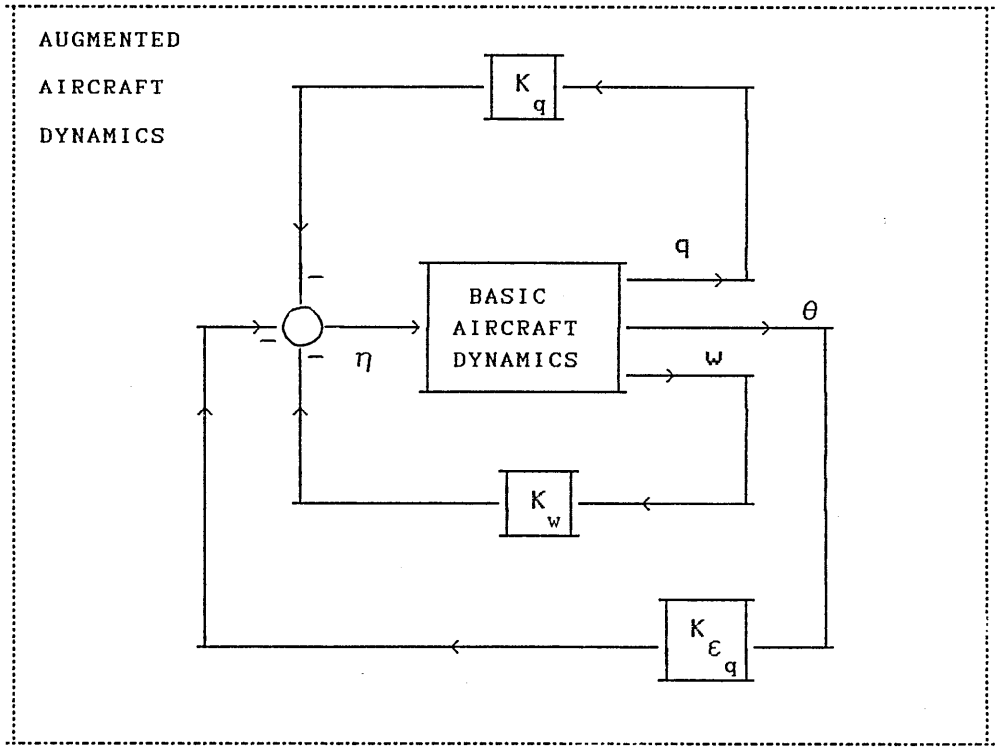

figure 8.1 - augmented aircraft dynamics used in the autopilot design

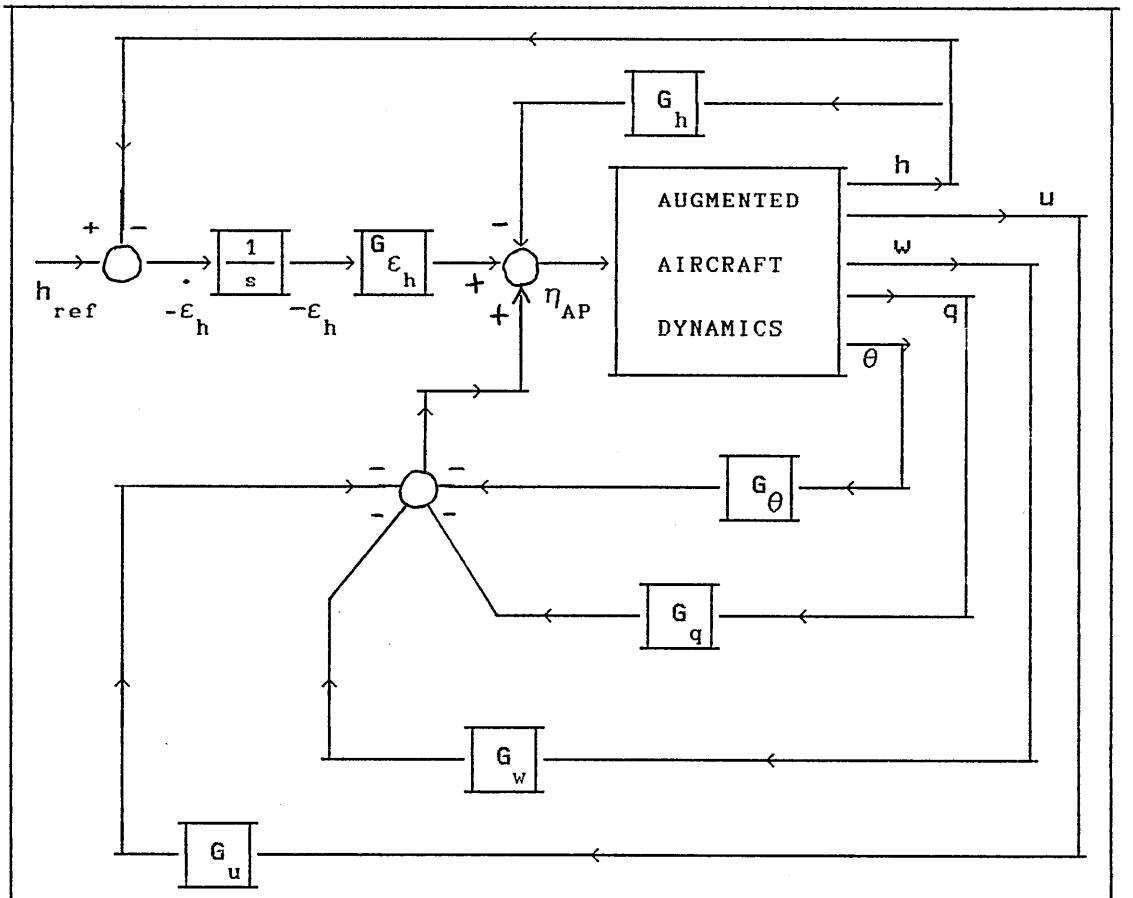

figure 8.2 - representan of the augmented aircraft from figure 8.1 and auilot control law.

It is important to appreciate that the augmented aircraft was not assessed with respect to the dropback criterion or CAP when the autopilot was engaged. It is clear that the autopilot design requires changed feedback gains on w, q and θ. However, as MIL-F-8785C and the Gibson dropback criterion are applicable to the piloted flight phases only a comparison of the gain values is not relevant in this case. In other words, when the autopilot is engaged there is no pilot input, since the autopilot replaces the pilot. It is clear that the autopilot was designed to work with the augmented aircraft as if the augmented aircraft was a new aircraft. When the pilot is manoeuvering the aircraft the autopilot is not engaged. Another comment about the design is necessary, that is, as stated by Friedland one can think that the objective is to minimize 8.13, however this is not the true objective. Equation 8.13 is used as a tool to design the autopilot

control law. In this way the parametric study performed with both inner loop control laws and for flight cases 3, 6, 9, 13 and 17 has determined a suitable ρ as

$$\rho = 1 \times 10^{-8}$$

and this was the ρ choosen in this design. It is necessary to say that other values were also found that gave acceptable responses. However, higher feedback gains were required, so in order to have lower feedback gains the above value for ρ was used.

8.3 AUTOPILOT ANALYSIS

8.3.1 THE AUTOPILOT GAINS

The autopilot design performed as described gave the gains presented in table 8.1 for the inner loop designed by pole placement and in table 8.2 for the inner loop designed by optimal control.

TABLE 8.1 - autopilot gains for the pole placement inner loop design

FC	G_u (s/ft)	G_w (s/ft)	G_q sec	G_θ rad	G_h ft^{-1}	G_{ε_h} $ft^{-1}s^{-1}$
3	-0.0004	0.0008	-0.1554	-0.9035	-0.0009	-0.0001
6	-0.0005	0.0010	-0.1924	-1.1973	-0.0008	-0.0001
9	-0.0008	0.0021	-0.2441	-2.2985	-0.0011	-0.0001
13	-0.0012	0.0012	-0.2672	-1.0220	-0.0010	-0.0001
17	-0.0007	0.0015	-0.2450	-1.6260	-0.0009	-0.0001

TABLE 8.2 - autopilot gains for the optimal control law inner loop design

FC	G_u (s/ft)	G_w (s/ft)	G_q sec	G_θ rad	G_h ft^{-1}	G_{ε_h} $ft^{-1}s^{-1}$
3	-0.0006	0.0009	-0.1356	-1.0124	-0.0010	-0.0001
6	-0.0008	0.0014	-0.1510	-1.3830	-0.0010	-0.0001
9	-0.0009	0.0023	-0.2441	-2.3253	-0.0011	-0.0001
13	-0.0020	0.0019	-0.2154	-1.3089	-0.0013	-0.0001
17	-0.0011	0.0019	-0.1978	-1.7929	-0.0011	-0.0001

It is interesting to note that the design performed by Powell[7],which is based only on proportional feedback acting in u, w, q, θ and h, gave gains G_q and G_θ of much larger magnitude than the corresponding values obtained here. Obviously an autopilot with only five feedback variables has the advantage that it only requires five feedback gains, whereas six gains are required in the present design. However, it can be seen in both tables, 8.1 and 8.2, that the feedback gain G_{ε_h} is constant for all flight cases, and so it is not necessary to be scheduled. From both tables it would appear to bepossible to use a constant G_u , G_w and G_h and so only G_q and G_θ are required to be scheduled as function of flight condition. The time responses of both designs are also compared, and it is seen that they are very similar, the response obtained by Powell is shown in figure 8.3. Perhaps it is useful again to quote Friedland's word about the design method:

" A suitable approach for the designer would be to solve for the gain matrices G that result from a range of weighting matrices Q and R, and calculate (or simulate) the corresponding closed-loop response. The gain matrix G that produces the response closest to meeting the design objectives is the ultimate selection. "

So this was the way in which this autopilot design was performed, the method is the same as that used in chapter 3 to design the optimal control law for the inner loop. At this point it is also interesting

to note that the approach adopted would also permit the design of a feedforward loop working on the input h_{ref} if desired. So an interesting exercise would be to design the autopilot in three different ways, that is the structure adopted in Powell, the structure adopted here and finally a structure that also includes a feedforward loop.

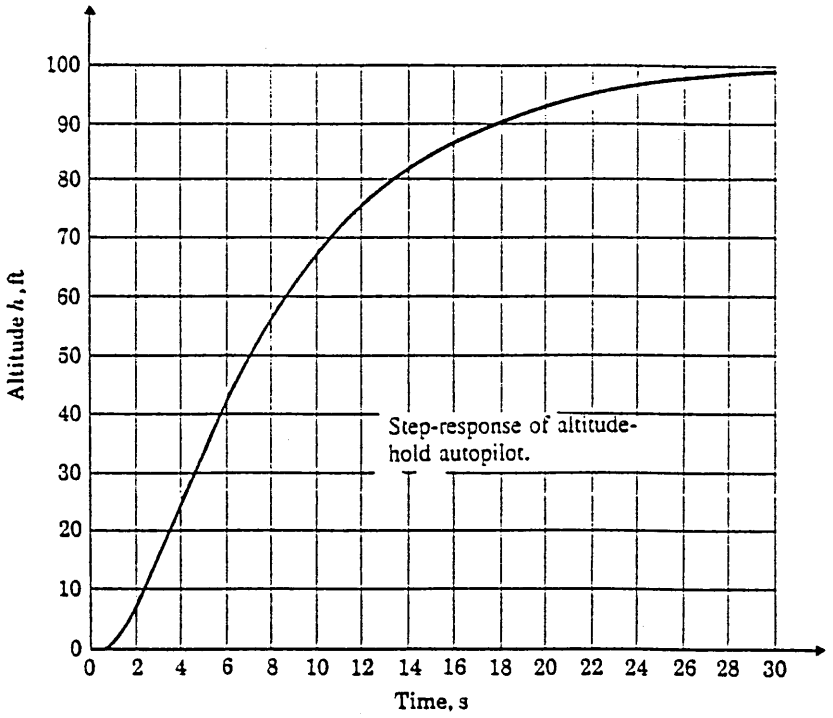

figre 8.3 - time response of the autopilot designed in Powell for the B-747 at 20000 ft mach 0.80

8.3.2 THE EFFECT OF THE ACTUATOR

This autopilot design was performed without the inclusion of the actuator dynamics. In order to investigate if the actuator has some influence on the performance, the actuator model was included. Thus, the state equation for the actuator may be written as before,

$$\dot{x}_A = A_A x_A + B_A \eta_c \qquad (8.17)$$

with

$$x_A^T = [\ \eta \quad v_\eta\ ] \qquad (8.18)$$

Thus the autopilot feedback gain vector becomes,

$$G_{AP} = [\ G_u \quad G_w \quad G_q \quad G_\theta \quad 0 \quad 0 \quad G_h \quad G_{\varepsilon_h}\ ] \tag{8.19}$$

and the autopilot control law may be written as

$$\eta_c = -G_{AP}\ [\ u \quad w \quad q \quad \theta \quad \eta \quad v_\eta \quad h \quad \varepsilon_h\ ] \tag{8.20}$$

The closed loop model is then given by,

$$\dot{x} = A\,x + E\,h_{ref} \tag{8.21}$$

$$\text{with,} \quad x^T = [\ u \quad w \quad q \quad \theta \quad \eta \quad v_\eta \quad h \quad \varepsilon_h\ ] \tag{8.22}$$

with,

$$A = \begin{bmatrix} A & [\ B \quad Z41\ ] & Z41 & Z41 \\ -B_A GAP & A_A & -B_A G_h & -B_A G_{\varepsilon_h} \\ [0 \ -1 \ 0 \ U_0] & Z12 & 0 & 0 \\ Z14 & Z12 & 1 & 0 \end{bmatrix} \tag{8.23}$$

$$E = [\ 0 \quad 0 \quad 0 \quad 0 \quad 0 \quad 0 \quad 0 \quad -1\ ] \tag{8.24}$$

and GAP given by,

$$GAP = [\ G_u \quad (K_w + G_w) \quad (K_q + G_q) \quad (K_{\varepsilon_q} + G_\theta)\ ] \tag{8.24.a}$$

with this model is possible to see that the actuator influence is completely neglible on the autopilot performance.

8.3.3 THE FREQUENCY RESPONSE AND TIME RESPONSE

In figure 8.4 and 8.5 the autopilot frequency responses are shown for both inner loop control laws respectively, that is, pole placement and optimal control, for flight condition 6. In figure 8.6 the autopilot time response for a step input in h_{ref} is shown and can be compared with figure 8.3 which shows the same response for the design performed by Powell[7] for practically the same flight case. From the results it can be seen that, in general, the pole placement inner loop design has a marginally greater bandwidth than the optimal inner loop control law design. The optimal inner loop control law design in general has a greater gain margin than the pole placement design. The results have also shown that, in general, the pole placement inner loop control law design has a faster response than the optimal inner loop control law design. In figure 8.7 the control effort for both designs is compared for the same step input in h_{ref}, and in figure 8.8 the control rate effort for both designs is compared for the same input, all for flight case 6. It can be seen that the pole placement control inner loop control law design requires more control effort than the optimal inner loop control law design. However, as shown the control effort in both cases is very low. In figure 8.9 the time histories obtained by simulating the autopilot with optimal inner loop control law design are shown for a step input in h_{ref}, for the same flight case, clearly the responses are very smooth, and the load factor varies by about $\pm$ 0.1 g, which means a very comfortable condition in terms of ride quality.

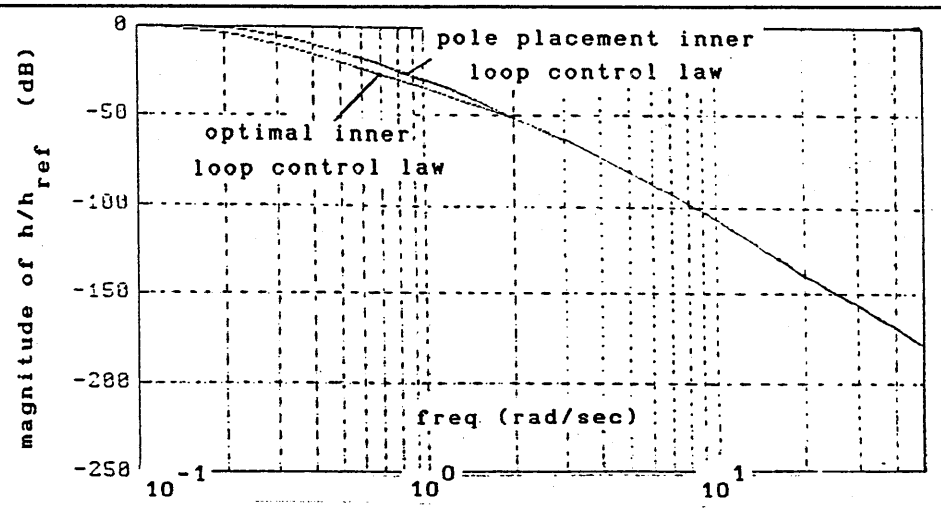

figure 8.4 - altitude frequency response of the autopilot at 20000 ft mach 0.70

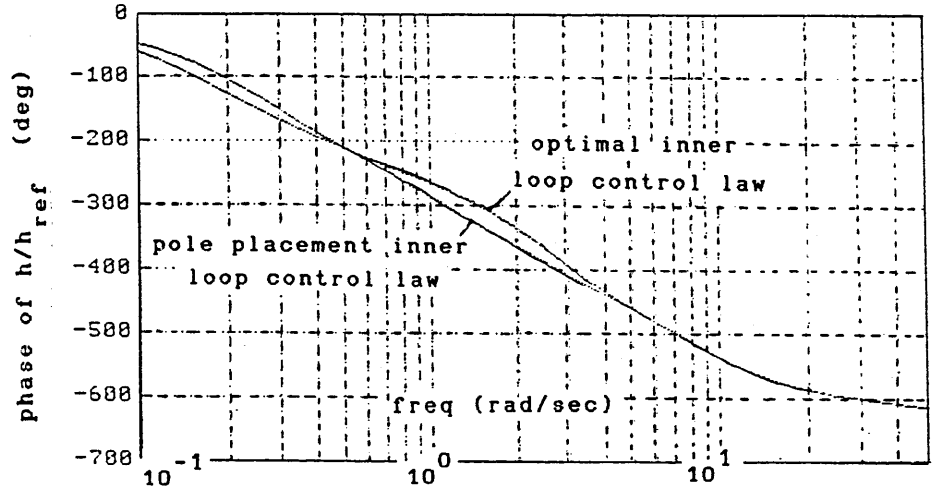

figure 8.5 - altitude frequency response of the autopilot at 20000 ft mach 0.70

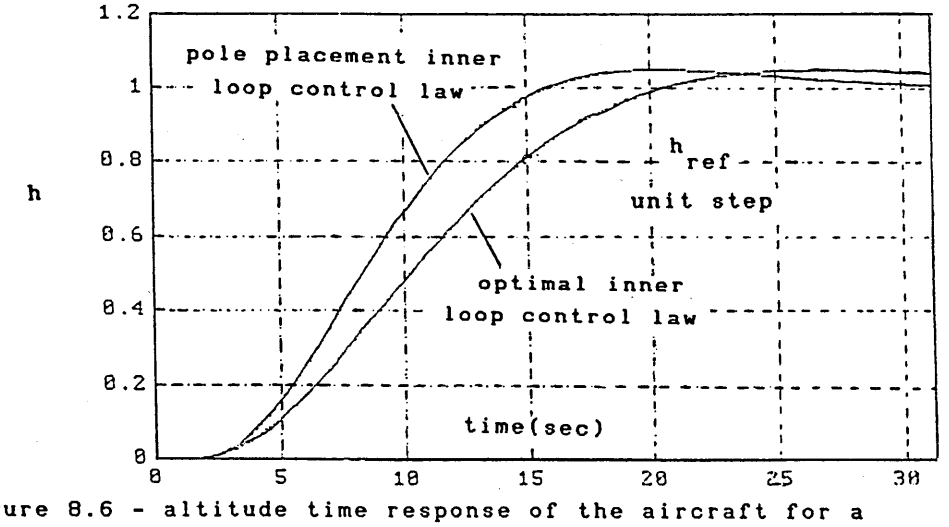

figure 8.6 - altitude time response of the aircraft for a reference step input at 20000 ft mach 0.70

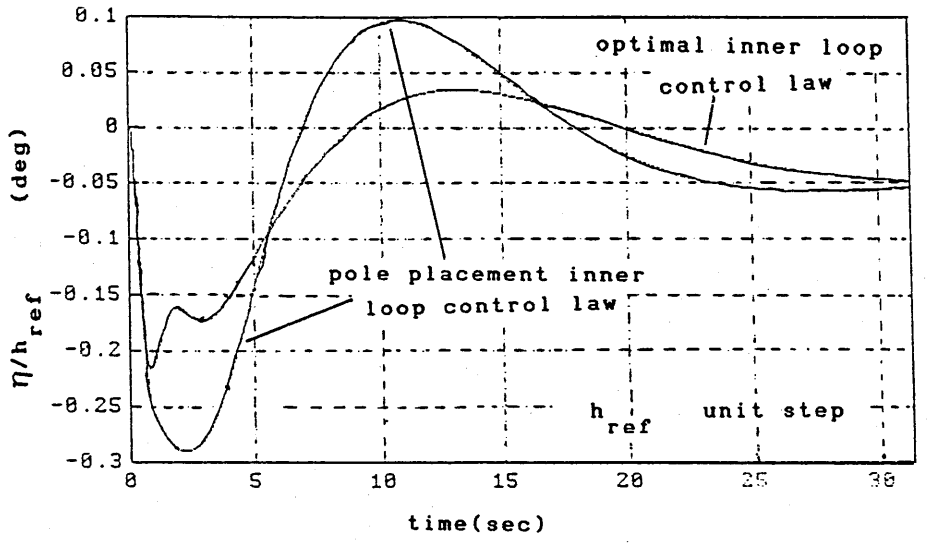

figure 8.7 - control effort response of the autopilot for a step reference input in h_{ref} at 20000 ft mach 0.70

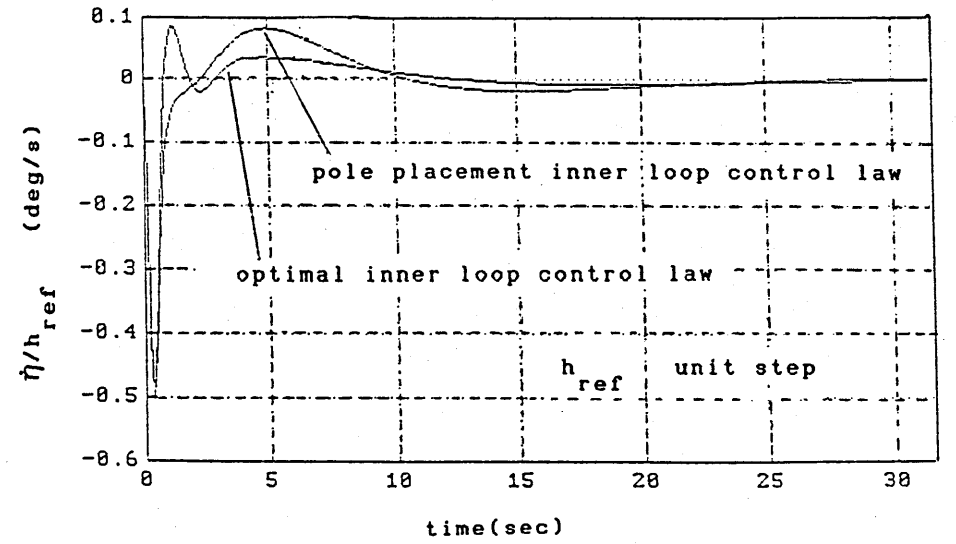

figure 8.8 - control rate effort response of the autopilot for a step reference input in h_{ref} at 20000 ft mach 0.70

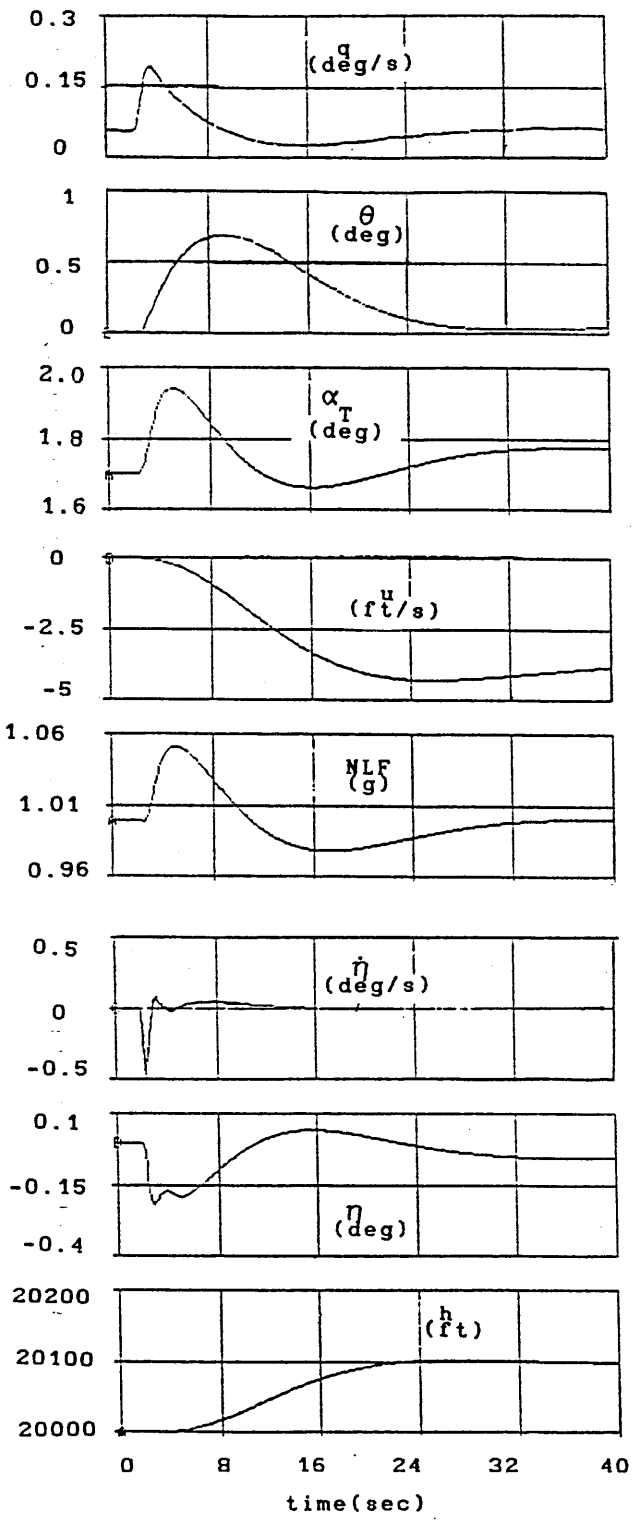

figure 8.9 - time histories of the aircraft with optimal inner loop control law and autopilot at 20000 ft mach 0.70 with a step input of 100 ft in h_{ref}

8.4 INTERIM CONCLUSIONS

From the design study it can be concluded that the autopilot responds quite well in terms of passenger ride quality, as determined from the figures and analysis. However, it was necessary to simulate the autopilot working with the non-linear aircraft model in order to obtain a better evaluation of the performance. It was also necessary to assess the regulator performance of the autopilot, as already done with the inner loop control laws, to ensure that following a disturbance, the h response does not exceed $\pm$ 50 ft. A good feature of the design is the lower gains obtained, and as a consequence the lower control effort and control rate effort required. A study with only G_θ and G_q scheduled, the other gains remaining fixed was considered useful in order to verify if such simplification is acceptable. Also, it was necessary to establish the limiting value of h_{ref} that can be applied without compromising the performance.

8.5 THE AUTOPILOT WORKING WITH THE INNER LOOP OBSERVER BASED CONTROL LAWS

8.5.1 INTRODUCTION

It is clear that in the event of a sensor failure the sensor based control law would no longer be available and so an observer based control law would be working in the aircraft. It is necessary to verify if the autopilot can function correctly with an observer based control law, so in the event of a sensor failure not only does the inner loop have a degree of redundancy but also the autopilot.

8.5.2 THE MATHEMATICAL MODEL

Here the description of the mathematical model used to study the autopilot working with the observer based control laws, CL_OB_w, CL_OB_q and CL_OB_θ are described as follows,

To represent the aircraft working with the observer based control laws the following equations are useful,

$$\dot{x}_1 = A_{11}x_1 + A_{12}x_2 + [B_1\ 0]\,x_A \tag{8.25}$$

$$\dot{x}_2 = A_{21}x_1 + A_{22}x_2 + [B_2\ 0]\,x_A \tag{8.26}$$

where ,

in the case of CL_OB_w : $x_1 = w$ (8.27)

$$x_2^T = [\ u \quad q \quad \theta\ ] \tag{8.28}$$

in the case of CL_OB_q : $x_1 = q$ (8.29)

$$x_2^T = [\ u \quad w \quad \theta\ ] \tag{8.30}$$

in the case of CL_OB_θ : $x_1 = \theta$ (8.31)

$$x_2^T = [\ u \quad w \quad q\ ] \tag{8.32}$$

The actuator is given by,

$$\dot{x}_A = A_A x_A + B_A \eta_c \tag{8.33}$$

$$x_A^T = [\ \eta \quad v_\eta\ ] \tag{8.34}$$

The height equation is,

$$\dot{h} = [\ 0 \quad -1 \quad 0 \quad U_0\ ]\,x = GW_1\,x_1 + GW_2\,x_2 \tag{8.35}$$

where ;

in the case of CL_OB_w : $GW_1 = -1$ (8.36)

$$GW_2 = [\ 0 \quad 0 \quad U_0\ ] \tag{8.37}$$

in the case of CL_OB_q : $GW_1 = 0$ (8.38)

$$GW_2 = [\ 0\ -1\ \ U_0\ ] \tag{8.39}$$

in the case of CL_OB_θ : $GW_1 = U_0$ (8.40)

$$GW_2 = [\ 0\ -1\ \ 0\ ] \tag{8.41}$$

The autopilot height error equation is given by,

$$\dot{\varepsilon}_h = h - h_{ref} \tag{8.42}$$

The observer is given by,

$$\dot{z} = F z + \bar{G} x_1 + [H\ \ 0]\, x_A \tag{8.43}$$

where ;

in the case of CL_OB_w : $\hat{x}_2 = L x_1 + z$ (8.44)

$$\hat{x}_2^T = [\ \hat{u}\ \ \hat{q}\ \ \hat{\theta}\ ] \tag{8.45}$$

in the case of CL_OB_q : $\hat{x}_2 = M x_1 + N z$ (8.46)

$$\hat{x}_2^T = [\ \hat{u}\ \ \hat{w}\ \ \hat{\theta}\ ] \tag{8.47}$$

in the case of CL_OB_θ : $\hat{x}_2 = M x_1 + N z$ (8.48)

$$\hat{x}_2^T = [\ \hat{u}\ \ \hat{w}\ \ \hat{q}\ ] \tag{8.49}$$

The gains of the inner loop control law are given by,

$$G = [\ 0\ \ K_w\ \ K_q\ \ K_{\varepsilon_q}\ ] \tag{8.50}$$

and so,

in the case of CL_OB_w $G_1 = K_w$ (8.51)

$$G_2 = [0 \quad K_q \quad K_{\varepsilon_q}] \tag{8.52}$$

in the case of CL_OB_q $G_1 = K_q$ (8.53)

$$G_2 = [0 \quad K_w \quad K_{\varepsilon_q}] \tag{8.54}$$

in the case of CL_OB_θ $G_1 = K_{\varepsilon_q}$ (8.55)

$$G_2 = [0 \quad K_w \quad K_q] \tag{8.56}$$

The gains of the autopilot are,

$$G_{AP} = [G_u \quad G_w \quad G_q \quad G_\theta \quad G_h \quad G_{\varepsilon_h}] \tag{8.57}$$

and so,

in the case of CL_OB_w $G_{AP_1} = G_w$ (8.58)

$$G_{AP_2} = [G_u \quad G_q \quad G_\theta] \tag{8.59}$$

in the case of CL_OB_q $G_{AP_1} = G_q$ (8.60)

$$G_{AP_2} = [G_u \quad G_w \quad G_\theta] \tag{8.61}$$

in the case of CL_OB_θ $G_{AP_1} = G_\theta$ (8.62)

$$G_{AP_2} = [G_u \quad G_w \quad G_q] \tag{8.63}$$

with these definitions the full control law can be expressed as,

i case CL_OB_w

$$\eta_c = -G_A x_1 - (G_2 + G_{AP_2}) z - G_h h - G_{\varepsilon_h} \varepsilon_h \tag{8.64}$$

$$\text{where, } G_A = (G_1 + G_{AP_1}) + (G_2 + G_{AP_2}) L \tag{8.65}$$

ii case CL_OB_q and CL_OB_θ

$$\eta_c = -G_A x_1 - (G_2 + G_{AP_2}) N z - G_h h - G_{\varepsilon_h} \varepsilon_h \tag{8.66}$$

$$\text{where, } G_A = (G_1 + G_{AP_1}) + (G_2 + G_{AP_2}) M \tag{8.67}$$

Thus the closed loop model for CL_OB_w, CL_OB_q and CL_OB_θ can be represented by,

$$\dot{x} = A x + B u \tag{8.68}$$

with,

$$x^T = [\, x_1 \;\; x_2 \;\; x_A \;\; h \;\; \varepsilon_h \;\; z \,] \tag{8.69}$$

$$B^T = [\, 0 \;\; Z31 \;\; Z21 \;\; 0 \;\; -1 \;\; Z31 \,] \tag{8.70}$$

$$u = h_{ref} \tag{8.71}$$

in the case of CL_OB_w ,

$$A = \begin{bmatrix} A_{11} & A_{12} & [B_1\ 0] & 0 & 0 & Z13 \\ A_{21} & A_{22} & [B_2\ Z31] & Z31 & Z31 & Z31 \\ -B_A G_A & Z23 & A_A & -B_A G_h & -B_A G_{\varepsilon_h} & -B_A(G_2+G_{AP_2}) \\ GW_1 & GW_2 & Z12 & 0 & 0 & Z13 \\ 0 & Z13 & Z12 & 1 & 0 & Z13 \\ \bar{G} & 0 & [H\ Z31] & Z31 & Z31 & F \end{bmatrix} \tag{8.72}$$

in the case of CL_OB_q and CL_OB_θ ,

$$A = \begin{bmatrix} A_{11} & A_{12} & [B_1\ 0] & 0 & 0 & Z13 \\ A_{21} & A_{22} & [B_2\ Z31] & Z31 & Z31 & Z31 \\ -B_A G_A & Z23 & A_A & -B_A G_h & -B_A G_{\varepsilon_h} & -B_A(G_2+G_{AP_2})N \\ GW_1 & GW_2 & Z12 & 0 & 0 & Z13 \\ 0 & Z13 & Z12 & 1 & 0 & Z13 \\ \bar{G} & 0 & [H\ Z31] & Z31 & Z31 & F \end{bmatrix} \quad (8.73)$$

8.5.3 THE RESULTS OBTAINED WITH CONTROL LAW CL_OB_w

A comparison between the responses obtained with the baseline system control law CL_SB with autopilot and CL_OB_w with autopilot show excellent agreement. In figure 8.10 and 8.11 the frequency response obtained for flight case 6 is shown, and can be compared with figure 8.4 and 8.5 respectively showing a very good match between designs. In figure 8.12 the altitude time response for a reference step input is shown with CL_OB_w and can be compared with figure 8.6, again showing a very good match between both designs. The fact that the responses match exactly confirms the special properties of the Doyle-Stein observer and allow the same redundancy provided for the inner loop control laws to be extended to the autopilot. Here a comment is in order; as seen before, the Doyle-Stein observer designed for the inner loop control laws does not offer a very precise estimate of u, forward velocity. However, this does not have a significant influence due to the fact that the autopilot gains that depend on u are very small. In figure 8.13 the ACSL simulation performed with CL_OB_w and autopilot is shown for flight case 6, for the aircraft with optimal inner loop control law. A comparison with figure 8.7 confirms the perfect match between both sets of responses.

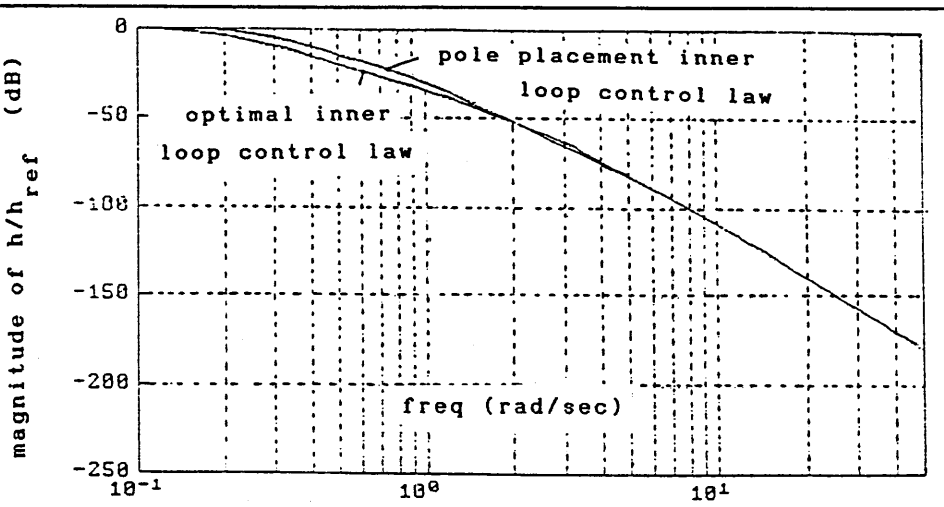

figure 8.10- altitude frequency response of the autopilot at 20000 ft mach 0.70 with inner loop control law CL_OB_w

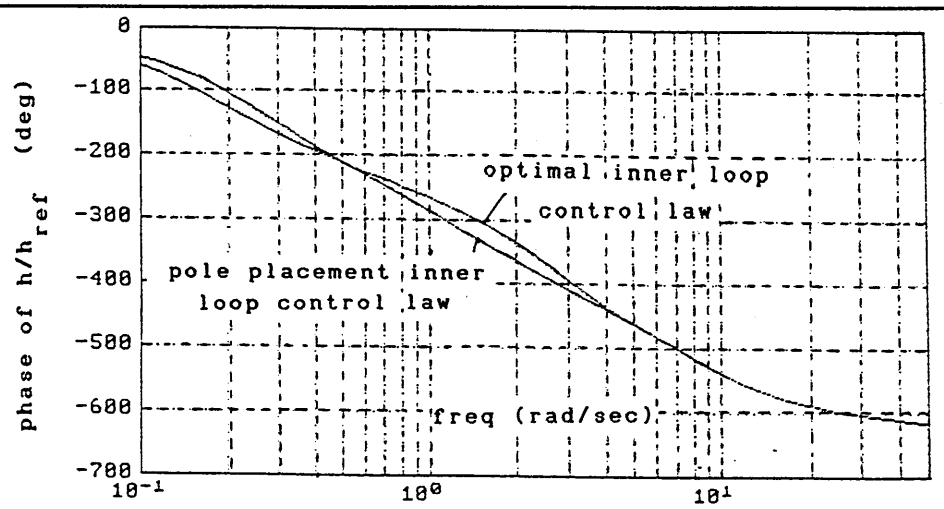

figure 8.11- altitude frequency response of the autopilot at 20000 ft mach 0.70 with inner loop control law CL_OB _w

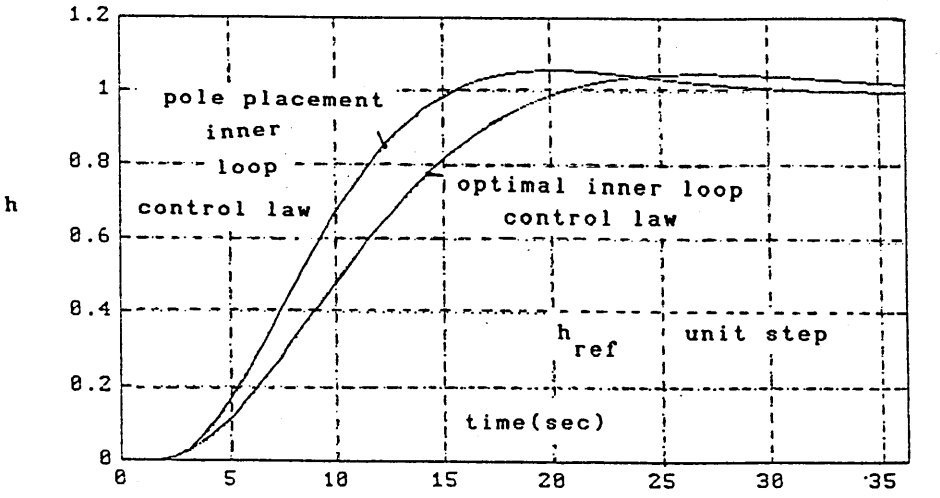

figure 8.12- altitude time response of the aircraft for unit step h_{ref} input at 20000 ft mach 0.70 with inner control law CL_OB_w

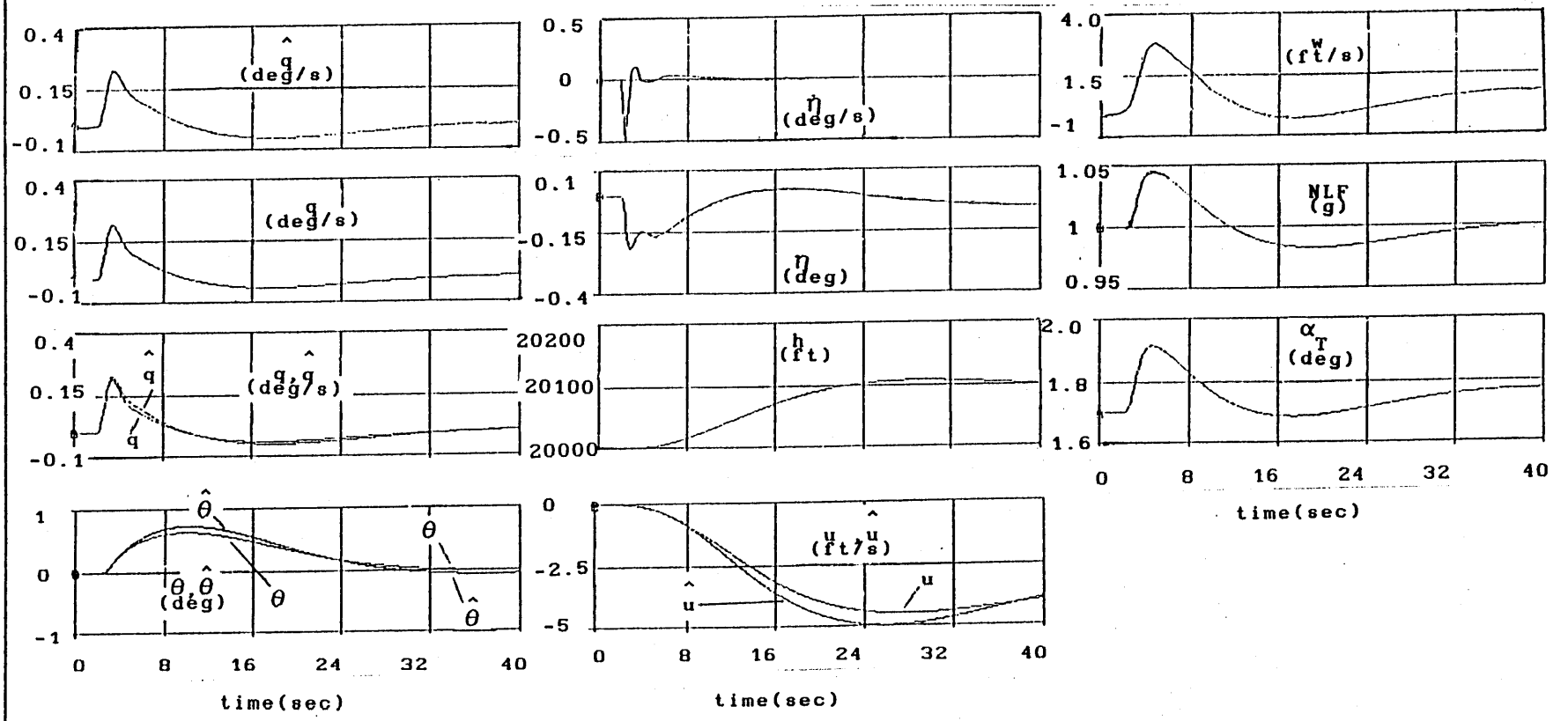

figure 8.13 - time histories of the aircraft with optimal inner loop control law CL_OB_w and autopilot at 20000 ft mach 0.70 with a step input of 100 ft

8.5.4 THE RESULTS OBTAINED WITH CONTROL LAW CL_OB_q

In figures 8.14 and 8.15 the altitude frequency response obtained with the autopilot working with the CL_OB_q inner loop control law is shown, and can be compared with figures 8.4 and 8.5 respectively. Again a very good agreement between both is apparent. In figure 8.16 the altitude time response for a step of h_{ref} is shown and can be compared with figure 8.6, showing a very good match between both. The ACSL simulations obtained for flight case 6, with inner loop control law CL_OB_q designed by optimal control are in figure 8.17, and can be compared with figure 8.7, with a very good similarity between both. In conclusion it is clear that the autopilot works satisfactorily with CL_OB_q. It can be seen that the u estimates are better here than with CL_OB_w, as already expected from the inner loop analysis.

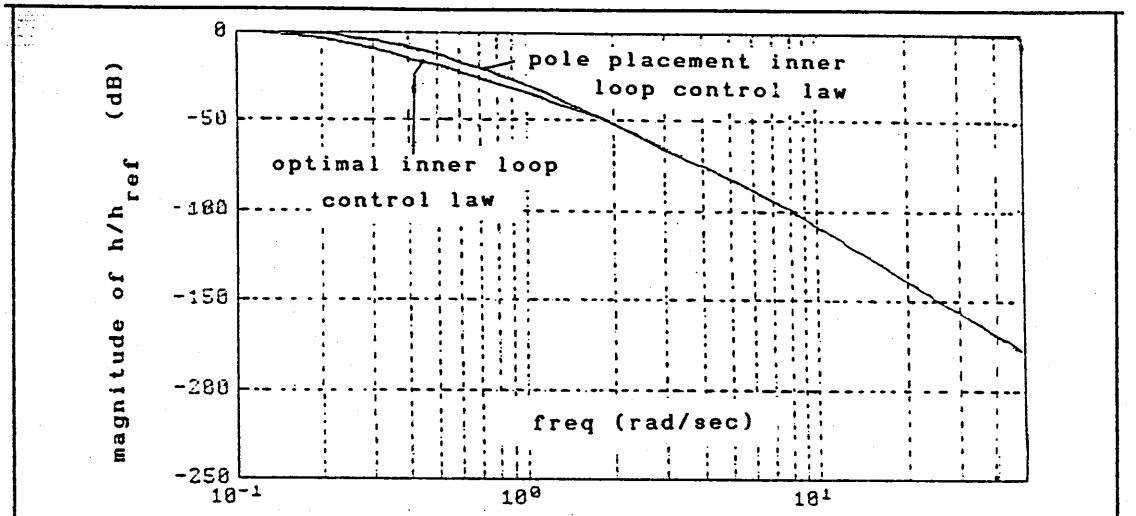

figure 8.14- altitude frequency response of the autopilot at 20000 ft mach 0.70 with inner loop control law CL_OB_q

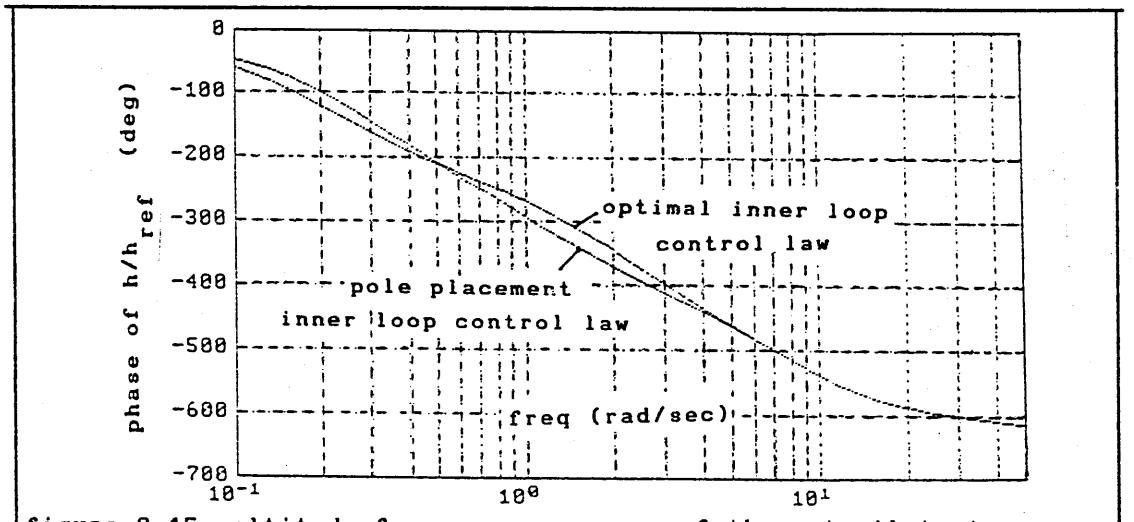

figure 8.15- altitude frequency response of the autopilot at 20000 ft mach 0.70 with inner loop control law CL_OB_q

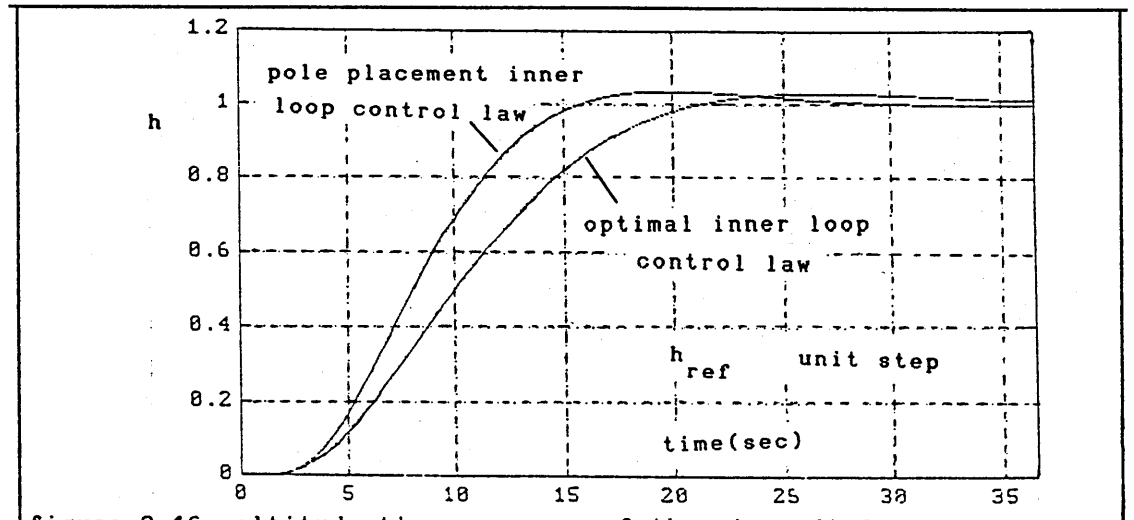

figure 8.16- altitude time response of the aircraft for a unit step h_{ref} input at 20000 ft mach 0.7 with inner loop control law CL_OB_q

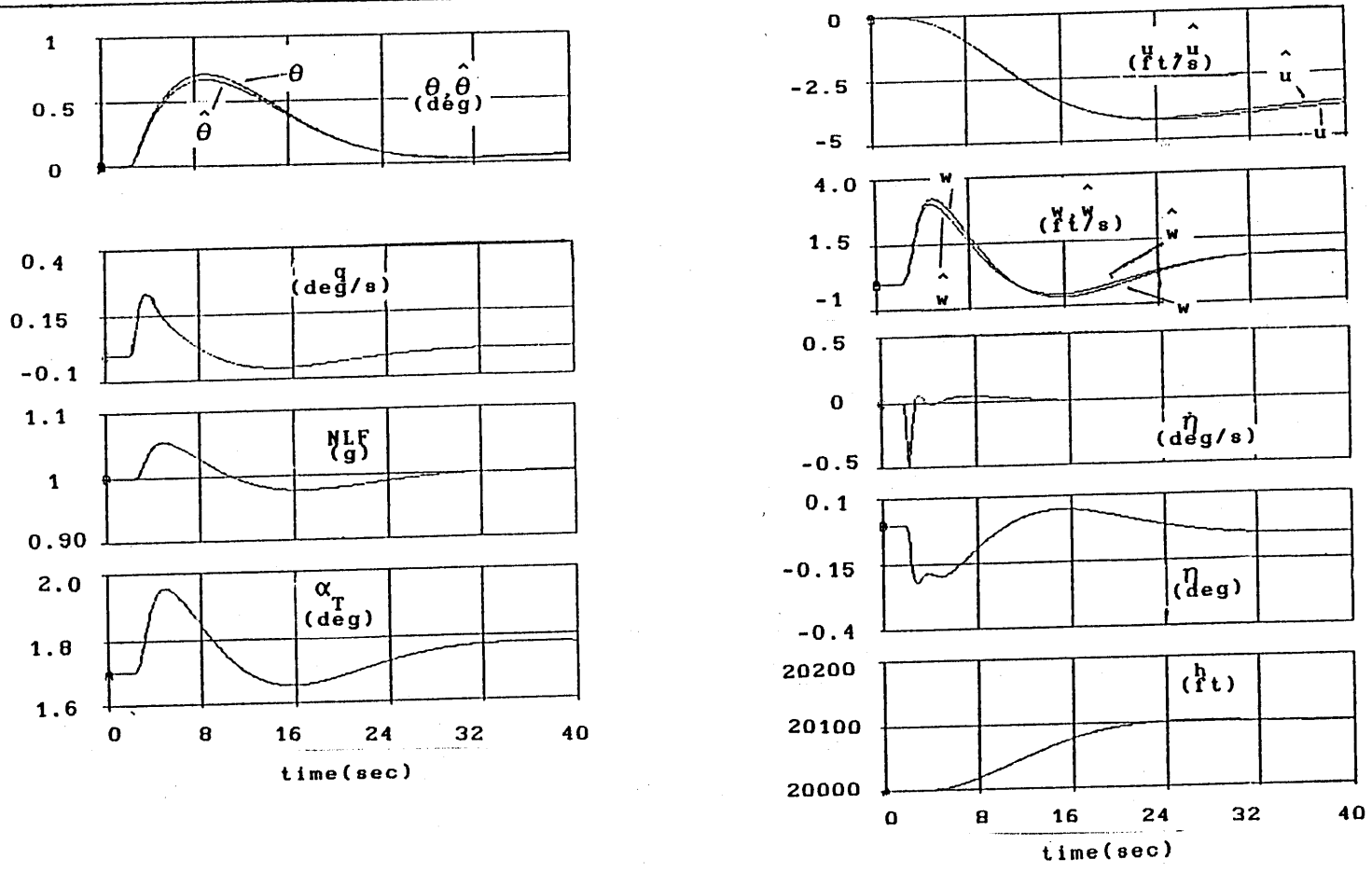

figure 8.17 - time histories of the aircraft with optimal inner loop control law CL_OB_q and autopilot at 20000 ft mach 0.70 with a step input of 100 ft

8.5.5 THE RESULTS OBTAINED WITH CONTROL LAW CL_OB_θ

Here again a comparison of the results with the baseline control law has shown a very good agreement. In figure 8.18 and 8.19 the altitude frequency response obtained with the autopilot working with the CL_OB_θ inner loop control law is shown which can be compared with figures 8.4 and 8.5 respectively. Again a very good agreement between both is evident. In figure 8.20 the altitude time response for a step of h_{ref} is shown and can be compared with figure 8.6, again showing a very good match between both. The ACSL simulations obtained for flight case 6, with inner loop control law CL_OB_θ designed by optimal control are in figure 8.21, and can be compared with figure 8.7, indicating a perfect match between both. In conclusion it is clear that the autopilot works with CL_OB_θ quite satisfactorily.

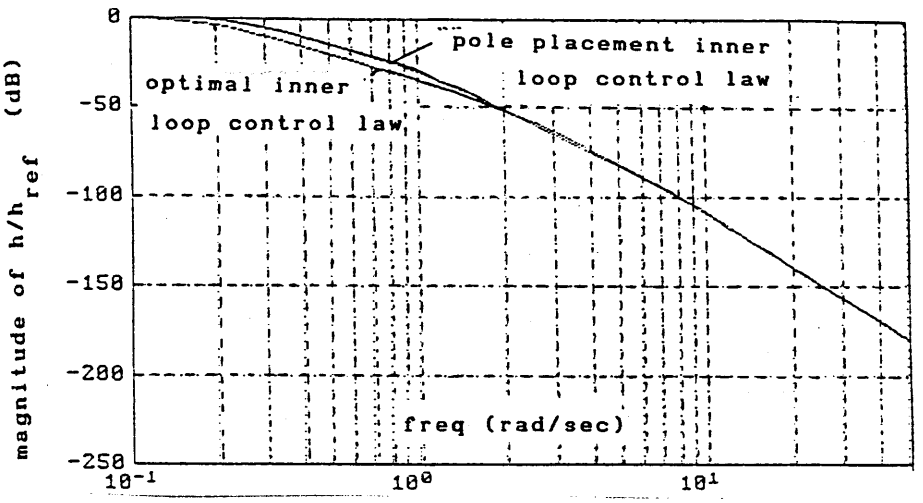

figure 8.18- altitude frequency response of the autopilot at 20000 ft mach 0.70 with inner loop CL_OB_θ

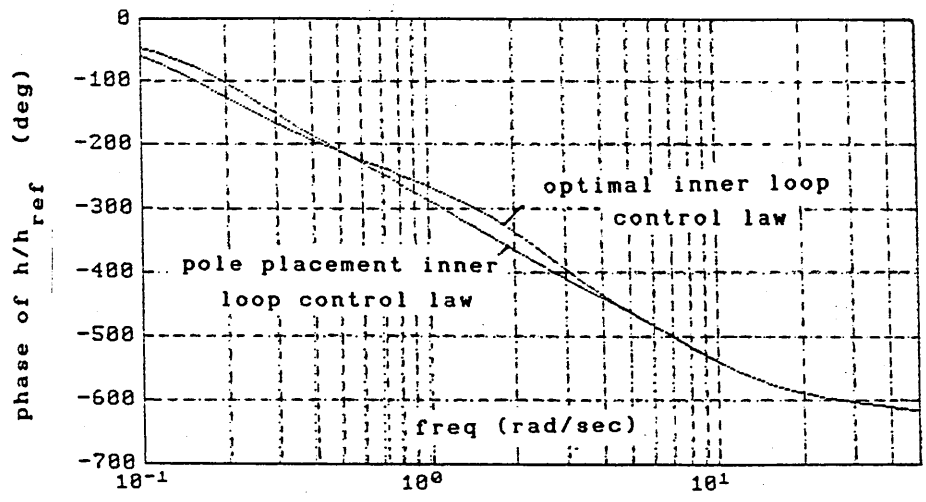

figure 8.19- altitude frequency response of the autopilot at 20000 ft mach 0.70 with inner loop CL_OB_θ

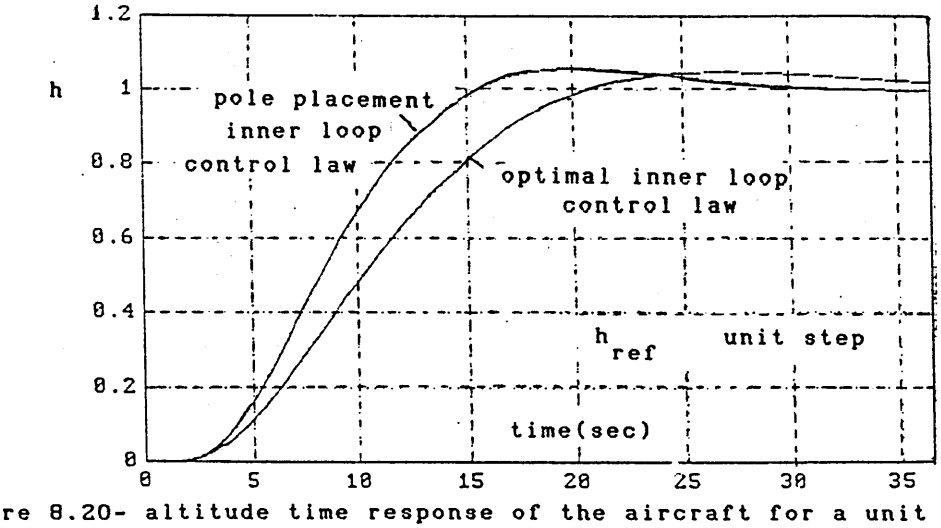

figure 8.20- altitude time response of the aircraft for a unit step h_{ref} input at 20000 ft mach 0.7 with inner loop control law CL_OB_θ

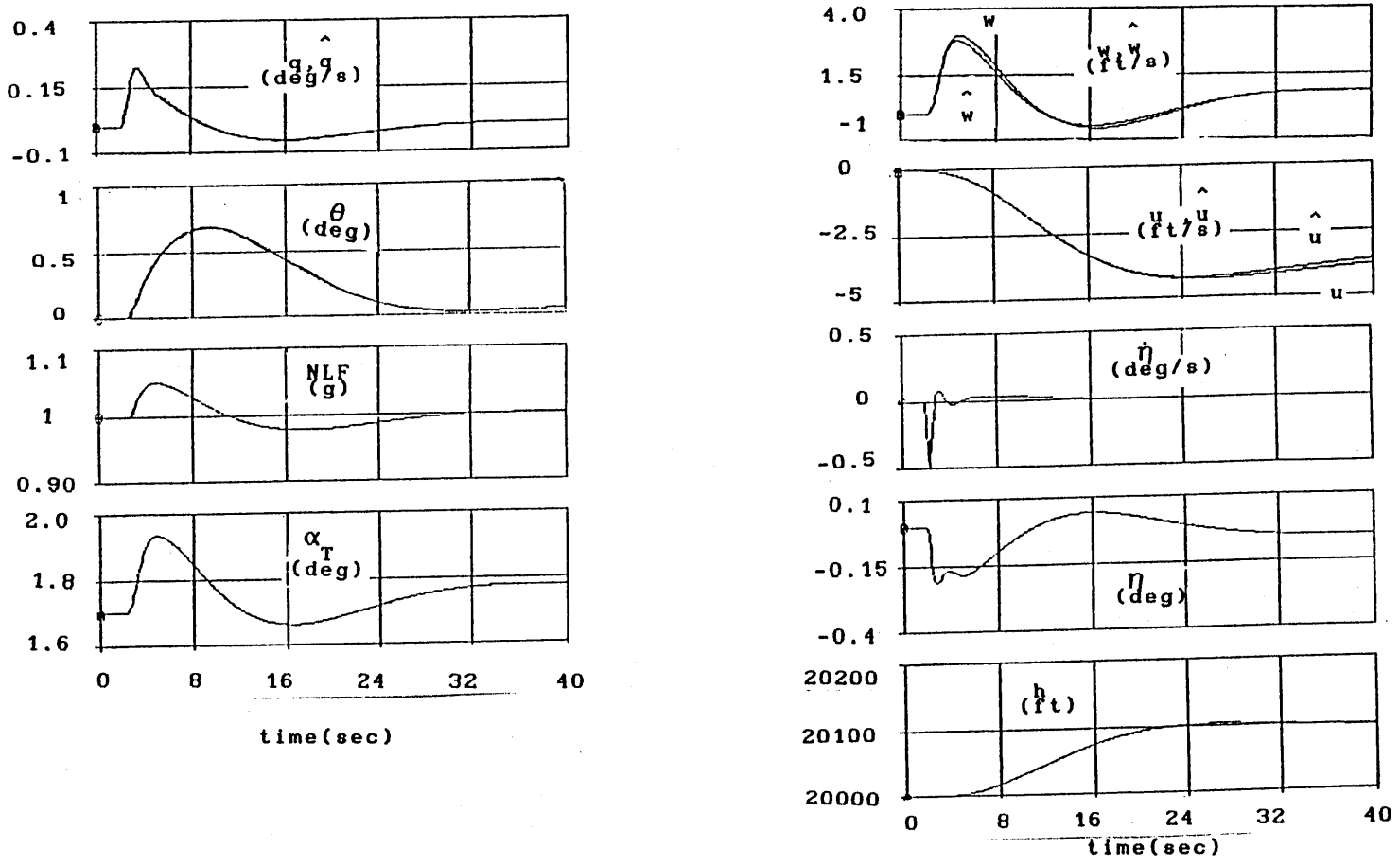

figure 8.21 - time histories of the aircraft with optimal inner loop control law CL_OB_θ and autopilot at 20000 ft mach 0.70 with a α step input of 100 ft

9. CONCLUSIONS AND OBSERVATIONS.

9.1 CONCLUSIONS

(i) The optimal control law design is much easier to adjust than the pole-placement control law design. This was also the case when the actuator model, the phugoid model, or even when the lead pre filter was added to the system. In all these cases the optimal design was very friendly and easy to accept new changes.

(ii) The magnitude of the feedforward gain obtained by the optimal control design method is greater than the magnitude of the feedforward gain of the pole-placement design method. A greater feedforward gain causes greater control rate effort and control effort. This was due to the methods by which each gain was obtained.

(iii) The optimal control law design is always more robust than the pole-placement control law design with respect to stability requirements. The reason for this is that in the design process the optimal control method does not introduce so many changes as the pole placement method. That is, it achieves a better balance with respect to closed loop pole locations ,control effort and in meeting the design criteria.

(iv) The pole-placement control law design is more robust than the optimal control law design with respect to the Gibson attitude dropback criterion when additional dynamics are included in the loop.

(v) The pole-placement control law design always has a greater phase and gain margin than the optimal control law design.

(vi) The method used to design the observer of control laws CL_OB_q and CL_OB_θ, leads to an observer with a better performance than the observer of control law CL_OB_w.

(vii) With respect to aircraft parameter variations, the optimal control law design is more robust than the pole-placement control law design. When both control laws were designed, the aircraft MATLAB model was used however, when both control laws were simulated the ACSL aircraft model was used, and in this case the optimal designs maintained better performance compared with the pole placement designs.

(viii) The control laws CL_OB_q and CL_OB_θ have better overall performance than control law CL_OB_w. This can be attributed to the method used in the observer designed for each control law. The complex poles of the observer used in CL_OB_w are very close to the origin of the s-plane, so the observer has much more influence on the system dynamics than the observers used in CL_OB_q and CL_OB_θ.

(ix) The baseline control law CL_SB implemented with sensors for angle of attack α, pitch-rate q, and pitch-attitude θ is more robust, and is also safer than control law CL_SB implemented with sensors of angle of attack α, and pitch-rate q only.

(x) The optimal control law design is more robust with respect to feedback gain variations and feedback path failures.

(xi) The order of control law reconfiguration in the event of a sensor failure should be, CL_OB_q, CL_OB_θ and finally CL_OB_w. This is the order that guarantees the best maintenance of flying qualities and stability characteristics.

(xii) Gain scheduling is easier to implement with the optimal control law design than it is with the pole-placement control law design. Obviously, the fact that K_{ε_q} is constant for all flight cases in the optimal design simplifies the requirement.

(xiii) The control law implemented with w, q and θ sensors and designed by the optimal control method is the best option since it is the one that offers the best performance and safety, and it accepts changes very easily.

(xiv) It appears that the optimal control method is advisable to design this kind of flight control system, since the approach followed in the design by the pole placement method has not worked so well as expected. The idea of closed loop pole allocation presented in chapter 3 does not offer the same transparency as the optimal control design method offers. In addition, when designing the control law, not just one set of the pair of weighting matrices (Q and R) are able to meet the criteria, but various sets of (Q, R) and so it is a more flexible method.

9.2 SUGGESTIONS FOR FURTHER WORK

(i) It is necessary to design control law CL_OB_w by the same method as used for CL_OB_q and CL_OB_θ in order that a meaningful comparison of the control laws may be made.

(ii) It is essential to study the behaviour of the control laws with the non-linear model of the aircraft and with fully scheduled gains in the control law and the observer.

(iii) It is interesting to study the allocation of poles of the observer in control laws CL_OB_q and CL_OB_θ, that is the approximation -0.01 in CL_OB_q and -4 in CL_OB_θ.

(iv) It is necessary to study the effects of control rate saturation and control displacement saturation, this can be done by simulation as described in Lewis-Stevens[18], and the use of limiters in the feedback paths, or as a better option try a new design, based on a performance index that weights the control rate , control displacement and also gain magnitude, as presented in Lewis-Stevens[18].

(v) It may be interesting to design an observer based control law with a full order Doyle-Stein observer instead of the reduced order form used in this study.

9.3 CLOSING COMMENTS

In conclusion the designed control laws have been assessed with respect to various criteria. However, a better study should be performed evaluating the performance of the control laws with the gains of the control laws and observers, schedulled with flight condition together with the non-linear aircraft model. After this a final evaluation can be conducted by the implementation of the control laws in a simulator and assessing the augmented aircraft with a pilot in the loop. The optimal control method only introduces the necessary changes in order that the augmented aircraft meets the criteria. Alternatively, the pole placement method introduced unecessary changes, this was particularly visible when both methods were assessed with respect to the Gibson phase rate criterion. Unless the designer has a very strong " feel " of where to locate the closed loop poles, it is preferable to design the flight control system by the optimal control method. This is specially so with respect to the integrator pole in the control law system. A final comment is in order about the Doyle-Stein observer. If the system has right half plane zeros the procedure may still work, as described in Maciejowski[74], particularly if the zeros lie beyond the operating bandwidth of the system as finally designed. This comment is relevant because in the case of the aircraft lateral-directional model there may be right half plane zeros and, as mentioned by Maciejowski, the procedure may also be applied in such cases.

10 REFERENCES

[1] Gibson, J.C.
Piloted handling qualities design criteria for high order flight control systems. - AGARD-CP-333 - april - 1982

[2] Gibson, J.C.
Handling qualities for unstable combat aircraft.
Proc. 15th Congress of ICAS - september - 1986

[3] Blagg, J.
The application of contemporary dynamic handling criteria to advanced fly-by-wire civil aircraft. - MSc Thesis - Cranfield Institute of Technology - College of Aeronautics - 1991

[4] MIL-F-8785C
Flying qualities of piloted airplanes.
DoD, United States Government - 1980

[5] Rynaski, E.G.
Flight control synthesis using robust output observers.
Proc. AIAA, Guidance and Control Conference. - San Diego - CA - august - 1982 - pp 825-831

[6] Doyle, J.C. and Stein, G.
Robustness with observers. - IEEE Transactions on Automatic control. - vol. AC-24, no.4, august 1979, pp 607-611.

[7] Powell, J.D - Franklin, G.F - Emami-Naeini , A.
Feedback Control of Dynamic Systems, second edition, Addison-Wesley Publishing Co. , 1991.

[8] CODAS II
Control System Design and Simulation.
Golten and Verwer Partners - 1989.

[9] MATLAB
The Mathworks, Inc. 21 Eliot street. - South Natick, MA 01760.

[10] Mitchell, E. and Gauthier.
Advanced Continuous Simulation Language.
Mitchell and Gauthier Associates, 1981, Concord, Mass. 01742.

[11] Heffley, R.K. and Jewell, W.F.
Aircraft Handling Qualities Data. NASA CR-2144, 1972.

[12] Oliva, A.P. and Cook, M.V.
A Simulation of the Boeing B-747 aircraft. College of Aeronautics report no.9202 - Cranfield Institute of Technology, 1992.

[13] Friedland, B.
Control System Design. An Introduction to state-space methods. McGraw-Hill Book Co. 1986.

[14] Chi-Tsong Chen
Linear System Theory and Design. CBS College Publishing, Holt , Rinehart and Winston, 1984.

[15] Patton, R.J. and Burrows ,S.P.
Robust Low Norm Output Feedback Design for Flight Control Systems. - AIAA-90-3505-CP - pp 1711-1719 - 1990

[16] Shapiro, E.Y. - Fredricks, D.A - Rooney, R.H. - Barmish, B.R.
Pole placement with output feedback. - J.Guidance and control vol.4, no.4, jul-aug 1981, pp 441-442.

[17] Anderson, B.D.O. and Moore, J.B.
Optimal Control - Linear Quadratic Methods - Prentice Hall Int.Ed. 1989.

[18] Stevens, B.L. and Lewis, F.L.
Aircraft Control and Simulation. John Wiley and sons, Inc, 1992

[19] Lewis, F.L.
Optimal Control. John Wiley and sons, Inc, 1986.

[20] Monahemi, M.M - Barlow, J.B. - O'Leary, D.P.
Design of Reduced-Order Observers with Precise Loop Transfer Recovery. - J.Guidance, Control, and Dynamics. vol.15, No.6 , nov-dec 1992, pp 1320-1326.

[21] Phillips, C.L. - Wilson, R.F. - Graf, E. - Starks. S.A.
Observers as Noise Filters in an Automatic Aircraft Landing System. J.Guidance.- vol. 6 - no.2 - mar-apr 1983 - pp 119-120.

[22] Sobel, K.M. and Banda, S.S.
Design of a Modalized Observer with Eigenvalue Sensitivity Reduction. - J.Guidance - vol.12 - no.5 - sep-oct 1989 - pp 762-764.

[23] Shapiro, E.Y. -Chung, J.C. - Andry, A.N.
Modalized Observers. - IEEE Transactions on Automatic Control vol. AC-29, no.7, july 1984. pp 669-672.

[24] Panossian, H.V.
Reduced-order observers applied to state and parameter estimation of hydromechanical servoactuators. - J.Guidance - vol.9 - no.2 - mar-apr 1986 - pp 249-251.

[25] Zak, S.H. and Walcott, B.L.
State observation of nonlinear uncertain dynamical systems. IEEE Transactions on Automatic Control, vol.AC-32, no.2, feb-1987, pp 166-170.

[26] Bossi, J.A. and Bryson, A.E.
Disturbance estimation for a STOL transport during landing. J.Guidance - vol.5 - no.3 - may-june 1982 - pp 258-262.

[27] Levin, V. and Kreindler, E.
Use of disturbance estimator for disturbance suppression. IEEE Transactions on Automatic Control, oct 1976 - pp 776-778.

[28] Stefani, R.T.
Observer steady-state errors induced by errors in realization. IEEE Transactions on Automatic Control, april 1976. pp 280-282

[29] Wang, S. - Davidson, E.J and Dorato, P.
Observing the states of systems with unmeasurable disturbances. IEEE Transactions on Automatic Control, oct-1975, pp 716-717.

[30] Yang, F. and Wilde, R.W.
Observers for linear systems with unknown inputs. IEEE Transactions on Automatic Control, vol.33, no.7 , july 1988, pp 677-681.

[31] Tsui, C.
A new algorithm for the design of multifunctional observers. IEEE Transactions on Automatic Control, vol.AC-30, no.1, jan 1985 - pp 89-93.

[32] Tsui, C.
Comparison of two state observer design algorithms. IEEE Transactions on Automatic Control. vol.AC-30, no.12. dec-1985. pp 1238-1240.

[33] Carrol ,R.L. and Shafai, B.
Minimal-order observer designs for linear time-varying multivariable systems. - IEEE Transactions on Automatic Control - vol.AC-31, no.8, aug-1986, pp 757-761.

[34] Lee, T.N. and Nguyen, C.
Design of a state estimator for a class of time-varying multivariable systems. - IEEE Transactions on Automatic Control - vol.AC-30, no.2, feb-1985, pp 179-182.

[35] Blight, J.D. - Gangsaas, D. - Richardson, T.M.
Control law synthesis for an airplane with relaxed static stability. - J.Guidance, vol.9, no.5 - sep-oct 1986 - pp 546-554.

[36] Gangsaas, D. - Bruce,K.R. - Blight, J.D. - Uy Loi Ly
Application of modern synthesis to aircraft control:Three case studies. - IEEE Transactions on Automatic Control, vol. AC-31, no.11, nov-1986, pp 995-1014.

[37] Yu, W. and Sobel, K.
Robust eigenstructure assignment with structured state space uncertainty. - J.Guidance, vol.14, no.3, may-june 1991, pp 621-628.

[38] McRuer, D. and Graham, D.
Eighty years of flight control : Triumphs and pitfalls of the systems approach. - J.Guidance and Control, vol.4, no.4, july-aug 1981, pp 353-362.

[39] Ashkenas, I.L.
Twenty-five years of handling qualities research. J.Aircraft - vol.21, no.5, may-1984, pp 289-301.

[40] Phillips, W.H.
Flying qualities from early airplanes to the space shuttle. J.Guidance, vol.12, no.4, jul-aug 1989, pp 449-459.

[41] Harper, R.P. and Cooper, G.E.
Handling qualities and pilot evaluation. J.Guidance, vol.9, no.5, sep-oct 1986, pp 515-529.

[42] Stengel, R.F.
A unifying framework for longitudinal flying qualities criteria. J.Guidance, vol.6, no.2, mar-apr 1983, pp 84-90.

[43] Mooij, H.A. and van Gool, M.F.C.
Handling qualities of transports with advanced flight control systems. AGARD-CP-333, april 1982, pp 7-1 to 7-15.

[44] Govindaraj, K.S. and Rynaski, E.G.
Design criteria for optimal flight control systems.
J.Guidance and Control. vol.3, no.4, jul-aug 1980, pp 376-378.

[45] Pope, R.E. and Cunningham, T.B.
Advanced flight control design techniques and handling quality requirements. AGARD-CP-333, april 1982, pp 21-1 to 21-13.

[46] Stevens, B.L. - Lewis, F.L. - Al-Sunni, F.
Aircraft flight controls design using output feedback.
J.Guidance, vol.15, no.1, jan-feb 1992, pp 238-246.

[47] Franklin, S.N and Ackermann , J.
Robust flight control: A design example.
J.Guidance and Control, vol.4, no.6, nov-dec 1981, pp 597-605.

[48] Horowitz, I. - Gobulev, B. - Kopelman , T.
Flight control design based on nonlinear model with uncertain parameters. - J.Guidance and Control, vol.3, no.2, mar-apr 1980, pp 113-118.

[49] Ashkenazi, A. and Bryson , A.E.
Control logic for parameter insensitivity and disturbance attenuation. J.Guidance, vol.5, no.4, jul-aug 1982, pp 383-388.

[50] Schaechter, D.B.
Closed-loop control performance sensitivity to parameter variations. - J.Guidance, vol.6, no.5, sep-oct 1983, pp 399-402

[51] Yanushevsky, R.T.
Approach to robust control systems design. J. Guidance, vol.14 no.1, jan-feb 1991, pp 218-220.

[52] Okada, T. - Kihara , M - Ikeda , M.
Robust control system design synthesis with observers.
J.Guidance, vol.13, no.2, mar-apr 1990, pp 337-342.

[53] Chalk, C.R.
Flying qualities of pitch-rate command/attitude hold control systems for landing. - J.Guidance, vol.9, no.5, sep-oct 1986, pp 541-545.

[54] Mitchell, D.G. and Hoh, R.H.
Low-order approaches to high-order systems: Problems and promises. - J. Guidance, vol.5, no.5, sep-oct 1982, pp 482-489.

[55] Bischoff, D.E.
The definition of short-period flying qualities characteristics via equivalent systems. - J. Aircraft, vol.20, no.6, june 1983, pp 494-499.

[56] Schafer, M.F.
Low-order equivalent models of highly augmented aircraft determined from flight data. - J.Guidance , vol.5, no.4, sep-oct 1982, pp 504-511.

[57] Harvey, C.H. and Stein , G.
Quadratic weights for asymptotic regulator properties.
IEEE Transactions on Automatic Control, vol.AC-23, no.3, june 1978 , pp 378-387.

[58] Roskam , J.
Evolution of airplane stability and control: A designer's viewpoint. - J.Guidance, vol.14, no.3, may-jun 1991, pp 481-491.

[59] D'Azzo, J. and Houpis, C.H.
Linear Control System Analysis and Design : Conventional and Modern. Third Edition. McGraw Hill Book Co., 1988.

[60] Brogan, W.L.
Modern Control Theory, Second edition, Prentice-Hall, Inc. 1985.

[61] Madiwale, A.N. and Willians, D.E.
Some extensions of loop transfer recovery. Proc.American Control Conference, Boston, MA, june 1985, pp 790-795.

[62] Cook, M.V.
Unpublished lecture notes for Flight Control Systems - Cranfield Institute of Technology - College of Aeronautics - january 1992

[63] Athans, M.
On the design of PID controllers using optimal linear regulator theory. Automatica, vol.no.7, 1971, pp 643-647.

[64] Parker, K.T.
Design of proportional integral derivative controllers by the use of the optimal regulator theory. Proc. IEE, vol.119, no.7, pp 911-914, july 1972.

[65] D'Sousa, A. F.
Design of Control Systems. Prentice Hall Int, 1988.

[66] Hess, R.A. and Kalteis , R.M.
Technique for predicting longitudinal pilot induced oscillations. J.Guidance, vol.14, no.1, jan-feb 1991, pp 198-204 .

[67] Powers, B.G.
An adaptive stick-gain to reduce PIO tendencies. J.Guidance, vol.5, no.2, march-apr 1982, pp 138-142.

[68] Kuo, B.C.
Automatic Control Systems. Fifth edition, Prentice-Hall International, 1987.

[69] Miron, D.B.
Design of Feedback Control Systems
Harcourt Brace Jovanovich, Publishers, 1989.

[70] Nelson, R.C.
Flight Stability and Automatic Control.
McGraw Hill Book Company, Inc., 1989.

[71] McRuer, D. , Johnston , D. and Myers, T.
A perspective on superaugmented flight control: Advantages and problems. J. Guidance, vol.9, no.5, sep-oct 1986, pp 530-540.

[72] Roskam , J.
Airplane Flight Dynamics. Kansas, Roskam Publishing, 1979.

[73] McLean, D.
Automatic Flight Control Systems.
Prentice Hall Int, 1990.

[74] Maciejowski , J.M.
Multivariable Feedback Design
Addison-Wesley Publishing Company - 1989

APPENDIX A

AIRCRAFT MATHEMATICAL MODEL

AND FLIGHT CONDITIONS USED IN THE WORK

The flight conditions used in this work are identified in table A-1. It can be seen that in general only flight cases 3, 6, 9, 13 and 17 have been used throughout the wole work, with occasional mention of cases 1, 5, 8, 12 and 16 in chapter 3.

TABLE A-1 IDENTIFICATION OF THE FLIGHT CASES

FC #	Altitude (ft)	Mach number	FC #	Altitude (ft)	Mach number
1	1000	0.30	10	40000	0.85
2	1000	0.50	11	40000	0.90
3	1000	0.60	12	10000	0.30
4	1000	0.70	13	10000	0.40
5	20000	0.50	14	10000	0.50
6	20000	0.70	15	10000	0.70
7	20000	0.80	16	30000	0.50
8	40000	0.70	17	30000	0.70
9	40000	0.80	18	30000	0.90

The aircraft model was obtained directly from Heffley[11] and for the longitudinal model is given by the state space equation,

$$\dot{x}_{LM} = A_{LM}\, x_{LM} + B_{LM}\, \eta \qquad (a.1)$$

with,

$$x_{LM}^{T} = [\, u \;\; w \;\; q \;\; \theta \,] \qquad (a.2)$$

$$A_{LM} = \begin{bmatrix} a_{11} & a_{12} & a_{13} & a_{14} \\ a_{21} & a_{22} & a_{23} & a_{24} \\ a_{31} & a_{32} & a_{33} & a_{34} \\ a_{41} & a_{42} & a_{43} & a_{44} \end{bmatrix} \qquad (a.3)$$

$$B_{LM}^{T} = [\, b_{11} \quad b_{21} \quad b_{31} \quad b_{41} \,] \qquad (a.4)$$

The reduced order short period model is represented by,

$$\dot{x}_{RO} = A_{RO}\, x_{RO} + B_{RO}\, \eta \qquad (a.5)$$

with,

$$x_{RO}^{T} = [\, w \quad q \,] \qquad (a.6)$$

$$A_{RO} = \begin{bmatrix} a_{22} & a_{23} \\ a_{32} & a_{33} \end{bmatrix} \qquad (a.7)$$

$$B_{RO}^{T} = [\, b_{21} \quad b_{31} \,] \qquad (a.8)$$

with the coefficients a_{ij} and b_{ij} given by :

$$a_{11} = X_u^* \qquad a_{24} = \frac{-g \sin\theta_0}{1 - Z_{\dot{w}}}$$

$$a_{12} = X_w$$

$$a_{13} = X_q - W_0 \qquad a_{31} = \frac{M_u^* + M_w Z_u^*}{1 - Z_{\dot{w}}}$$

$$a_{14} = -g \cos \theta_0$$

$$a_{21} = \frac{Z_u^*}{1 - Z_{\dot{w}}}$$

$$a_{22} = \frac{Z_w}{1 - Z_{\dot{w}}}$$

$$a_{23} = \frac{(Z_q + U_0)}{1 - Z_{\dot{w}}}$$

$$a_{41} = 0$$

$$a_{42} = 0$$

$$a_{43} = 1$$

$$a_{44} = 0$$

$$a_{32} = \frac{M_w + Z_w M_{\dot{w}}}{1 - Z_{\dot{w}}}$$

$$a_{33} = \frac{M_q + M_{\dot{w}} (Z_q + U_0)}{1 - Z_{\dot{w}}}$$

$$a_{34} = \frac{-M_w g \sin \theta_0}{1 - Z_{\dot{w}}}$$

$$b_{11} = 0$$

$$b_{21} = \frac{Z_\eta}{1 - Z_{\dot{w}}}$$

$$b_{31} = \frac{M_\eta + (M_{\dot{w}} Z_\eta)}{1 - Z_{\dot{w}}}$$

$$b_{41} = 0$$

The aerodynamic stability derivatives used are referred to body-axes, and the definition of each derivative is contained in Heffley[11] and in Oliva-Cook[12]. The A and B matrices of the aircraft for flight conditions 3, 6, 9, 13 and 17, are also listed in this appendix in table A-2 and A-3, for the MATLAB aircraft model and for the ACSL aircraft model. In table A-4 the parameter $T_{\theta 2}$ is listed for the flight cases presented in this work. In table A-5 the trim angle of attack and steady state velocity are listed for flight cases 3, 6, 9, 13 and 17. In table A-6 the coefficients of the state matrix and the coefficients of the control matrix are listed for flight cases 1, 5, 8, 12 and 16, as used in the MATLAB aircraft model.

TABLE A-2 - COEFFICIENTS OF THE STATE MATRIX

FC		3	6	9	13	17
a_{11}	MATLAB	-0.00820	-0.00480	-0.00410	-0.00570	-0.00350
	ACSL	-0.00729	-0.00424	-0.00364	-0.00504	-0.00313
a_{12}	MATLAB	0.06270	0.05960	0.05160	0.10750	0.04800
	ACSL	0.05557	0.05282	0.04570	0.09520	0.04250
a_{13}	MATLAB	-7.68850	-21.5287	-60.510	-64.8000	-55.2200
	ACSL	-7.68850	-21.5287	-60.516	-64.8059	-55.2260
a_{14}	MATLAB	-32.1900	-32.1258	-32.100	-31.8300	-32.0900
	ACSL	-32.1979	-32.1858	-32.100	-31.8339	-32.0980
a_{21}	MATLAB	-0.14620	-0.12430	-0.0881	-0.12660	-0.11400
	ACSL	-0.12900	-0.10988	-0.0779	-0.11182	-0.10137
a_{22}	MATLAB	-1.03600	-0.66600	-0.3703	-0.58960	-0.48000
	ACSL	-0.91510	-0.58940	-0.3278	-0.52093	-0.42570
a_{23}	MATLAB	684.96	732.769	768.50	431.290	696.700
	ACSL	682.37	731.315	767.82	430.062	695.787
a_{24}	MATLAB	-0.38310	-0.9717	-2.5450	-4.96300	-2.584
	ACSL	-0.38173	-0.9697	-2.5428	-4.94921	-2.581
a_{31}	MATLAB	-0.00010	0.00010	0.0	0.0004	0.000100
	ACSL	-0.00005	0.00007	-0.00003	0.0004	0.000064
a_{32}	MATLAB	-0.00230	-0.00180	-0.00110	-0.00190	-0.00140
	ACSL	-0.00227	-0.00177	-0.00104	-0.00183	-0.00137
a_{33}	MATLAB	-1.00950	-0.70700	-0.44340	-0.55220	-0.50600
	ACSL	-0.98457	-0.68980	-0.43267	-0.53870	-0.49430
a_{34}	MATLAB	0.00010	0.00020	0.00030	0.00080	0.00030
	ACSL	0.00008	0.00016	0.00028	0.00077	0.00032

TABLE A-3 COEFFICIENTS OF THE CONTROL MATRIX

FC		3	6	9	13	17
b_{11}	MATLAB	0.39370	0.97830	1.63890	2.52000	1.91800
	ACSL	0.34880	0.86670	1.45190	2.23260	1.69958
b_{21}	MATLAB	-35.3270	-33.5437	-20.9800	-16.9800	-24.4000
	ACSL	-31.1799	-29.6590	-18.5760	-15.0039	-21.5880
b_{31}	MATLAB	-1.99140	-1.91730	-1.21000	-0.97300	-1.41900
	ACSL	-1.94418	-1.87160	-1.18123	-0.94980	-1.38570

TABLE A-4 $T_{\theta 2}$ PARAMETER

FC #	$T_{\theta 2}$	FC #	$T_{\theta 2}$
3	1.00	1	1.72
6	1.58	5	2.13
9	2.85	8	3.09
13	1.79	12	2.16
17	2.33	16	2.65

TABLE A-5 TRIM ANGLE OF ATTACK AND STEADY STATE VELOCITY

FC #	V_e (ft/sec)	α_0 (deg)
3	667.6	0.66
6	725.8	1.70
9	771.5	4.50
13	430.1	8.70
17	696.3	4.60

TABLE A-6

COEFFICIENTS OF THE STATE MATRIX AND CONTROL MATRIX

FC	1	5	8	12	16
a_{11}	-0.00930	-0.00180	0.00030	0.00230	0.01190
a_{12}	0.14730	0.09040	0.03920	0.12710	-0.01040
a_{13}	-54.5650	-61.3750	-86.9237	-83.0980	-85.4900
a_{14}	-31.7600	-31.9700	-31.9300	-31.1170	-31.7200
a_{21}	-0.15330	-0.08320	-0.09350	-0.14610	-0.11300
a_{22}	-0.61770	-0.49810	-0.34150	-0.48920	-0.39700
a_{23}	334.69	518.540	668.719	314.250	490.450
a_{24}	-5.43800	-3.8800	-4.1796	-8.47840	-5.600
a_{31}	0.00050	0.0003	0.0001	0.00050	0.0002
a_{32}	-0.00200	-0.00170	-0.00100	-0.00150	-0.00120
a_{33}	-0.56760	-0.49400	-0.35380	-0.42210	-0.34900
a_{34}	0.00120	0.00050	0.00040	0.00120	0.00060
b_{11}	2.13140	2.27670	2.22680	2.58900	2.43200
b_{21}	-13.290	-19.4415	-17.286	-9.971	-14.119
b_{31}	-0.7582	-1.105	-1.0229	-0.591	-0.842

APPENDIX B

DERIVATION OF GIBSON ATTITUDE DROPBACK EQUATION

In this appendix the Gibson attitude dropback equation used in chapter 3, equation (3.14), obtained from Cook[62] is explained. In order to obtain an equation for attitude dropback, DB, in terms of the aircraft state description the following analysis is useful. The Laplace transform of the aircraft state equations may be written as,

$$s\,x(s) = A\,x(s) + b\,\eta(s) \tag{b.1}$$

$$q(s) = c'\,x(s) \tag{b.2}$$

Where the output matrix c' defines the single output variable q(s). Eliminating x(s) from these equations enables pitch rate output to be defined in terms of the elevator angle input.

$$q(s) = c'\,(sI - A)^{-1}\,b\,\eta(s) \tag{b.3}$$

The steady state value of pitch rate response q_{ss} to a unit step input is given by writing $\eta(s) = 1/s$ and applying the final value theorem to equation (b.3), Thus

$$q(t) = \lim_{t \to \infty} (s\,q(s)) = \lim_{s \to 0} [c'(sI-A)^{-1}b] \tag{b.4}$$

$$q_{ss} = q(t) = -c'A^{-1}b \tag{b.5}$$

Dropback may be defined from the typical steady state pitch attitude response, shown on figure (b.1), to a unit elevator angle input.

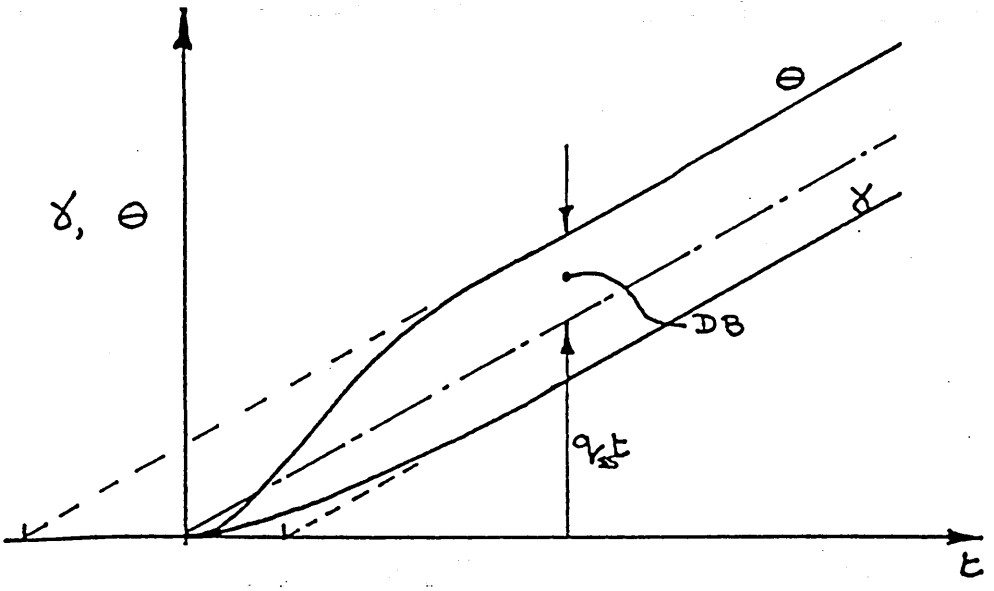

figure b.1 - Typical pitch attitude and flight path angle responses to a unit step elevator angle input

Given the state equations:

$$\dot{x}(t) = Ax(t) + b\eta(t) \tag{b.6}$$

$$q(t) = c' x(t) \tag{b.7}$$

the pitch rate response is given by,

$$q(t) = c'e^{A(t-t_0)} x(t_0) + c'\int_{t_0}^{t} \phi(t-\tau)b\eta(\tau)d\tau \tag{b.8}$$

Making the appropriate substitution for the transition matrix $\phi(t-t_0)$

$$q(t) = c'e^{A(t-t_0)} x(t_0) + c'\int_{t_0}^{t} e^{A(t-\tau)} b\eta(\tau)d\tau \tag{b.9}$$

Now, A, c' and b are constant, for a unit step input, $\eta(t) = 1$, and taking $t_0 = 0$, equation (b.9) may be written as,

$$q(t) = c'e^{At} x(0) + c'\int_{t_0}^{t} e^{A(t-\tau)} bd\tau \tag{b.10}$$

$$q(t) = c'e^{At} x(0) + c' e^{At} \left[\frac{-1}{A} e^{-A\tau} \right]_0^t b \qquad (b.11)$$

$$q(t) = c'e^{At} x(0) + c'A^{-1}[e^{At} - I] b \qquad (b.12)$$

Assuming zero initial conditions such that $x(0) = 0$, then,

$$q(t) = c'A^{-1}[e^{At} - I] b = c'A^{-1} e^{At} b - c'A^{-1}b \qquad (b.13)$$

Substituting for $c'A^{-1}b$ from equation (b.5)

$$q(t) = c'A^{-1}e^{At}b + q_{ss} \qquad (b.14)$$

Integrating equation (b.14) gives pitch attitude response to a unit step elevator input, thus,

$$\theta(t) = \int_0^t q(\tau)d\tau = \int_0^t [c'A^{-1} e^{A\tau} b + q_{ss}] d\tau \qquad (b.15)$$

$$\theta(t) = c' A^{-2}[e^{A\tau} - I]b + q_{ss}t \qquad (b.16)$$

The steady state pitch attitude response may be obtained by letting $t \to \infty$ and noting that,

$$\lim_{t\to\infty} e^{At} = 0 \qquad (b.17)$$

Provided that A describes an assymptotically stable matrix. Thus,

$$\theta_{ss} = -c' A^{-2} b + q_{ss} t \qquad (b.18)$$

The pitch attitude response described by equation (b.18) is shown on figure (b.2), and it is clear that dropback is defined by,

$$DB = -c' A^{-2} b \qquad (b.19)$$

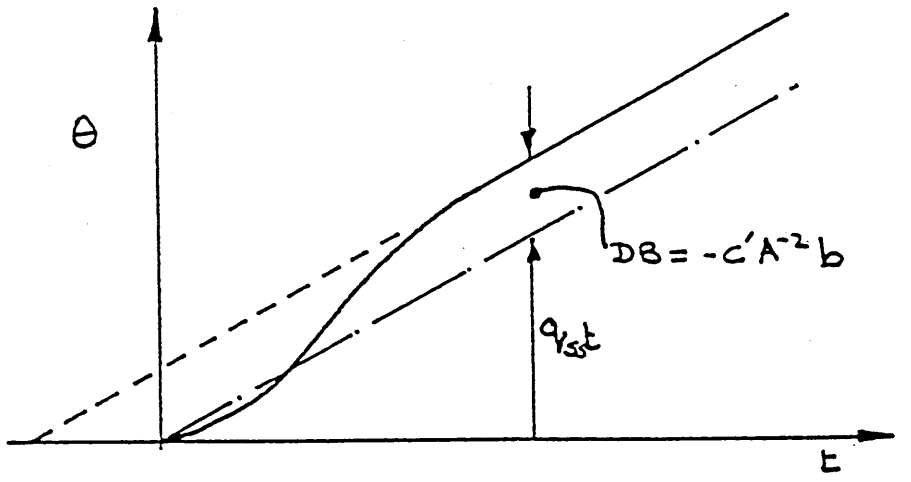

figure b.2 - steady state pitch attitude response

Now using the aircraft model based on the reduced order pitch rate response transfer function,

$$\frac{q(s)}{\eta(s)} = \frac{K_q (1 + T_{\theta 2} s)}{(s^2 + 2\zeta_{sp} \omega_{sp} s + \omega_{sp}^2)} \qquad (b.20)$$

and using the methods for system realisation the state space description of the aircraft may be defined in controllable companion form with state, input and output matrices as follows,

$$A = \begin{bmatrix} 0 & 1 \\ -\omega_{sp}^2 & -2\zeta_{sp}\omega_{sp} \end{bmatrix} \qquad (b.21)$$

$$b = \begin{bmatrix} 0 \\ \\ 1 \end{bmatrix} \qquad \text{(b.22)}$$

$$c' = \begin{bmatrix} K_q & K_q T_{\theta 2} \end{bmatrix} \qquad \text{(b.23)}$$

Using (b.21), (b.22) and (b.23) into (b.19) it is obtained ;

$$\frac{DB}{q_{ss}} = T_{\theta 2} - \frac{2\,\zeta_{sp}}{\omega_{sp}} \qquad \text{(b.24)}$$

Which is equation (3.14) used in the design of the pole placement control law design.

APPENDIX C

RESPONSE TRANSFER FUNCTIONS OF THE BASIC AIRCRAFT

In this appendix the poles and the transmission zeros of the following response transfer functions of the basic aircraft are listed;

$$w/\eta \quad , \quad q/\eta \quad \text{and} \quad \theta/\eta$$

which were obtained from the complete model :

$$\dot{x} = A\,x + B\,\eta$$

with, $x^T = [\,u \;\; w \;\; q \;\; \theta\,]$

as described in appendix A.

FC # 3 –	1000 ft – MACH 0.60
POLES	$-1.02 \pm i\,1.25$, $-0.0049 \pm i\,0.0580$
T.Z. of w/η	$-0.0046 \pm i0.0814$, -39.62
T.Z. of q/η	-0.9859 , -0.0175 , 0.0
T.Z. of θ/η	-0.9859 , -0.0175 , ∞

FC # 6 –	20000 ft – MACH 0.70
POLES	$-0.68 \pm i\,1.15$, $-0.0028 \pm i\,0.0700$
T.Z. of w/η	$-0.0035 \pm i\,0.0735$, -42.59
T.Z. of q/η	-0.6226 , -0.0167 , 0.0
T.Z. of θ/η	-0.6226 , -0.0167 , ∞

FC # 9 – 40000 ft – MACH 0.80			
POLES	$-0.40 \pm i\ 0.90$	, $-0.0032 \pm i\ 0.0516$	
T.Z. of w/η	$-0.0038 \pm i0.0590$	, -44.76	
T.Z. of q/η	-0.3380	, -0.0173 ,	0.0
T.Z. of θ/η	-0.3380	, -0.0173 ,	∞

FC # 13 – 10000 ft – MACH 0.40			
POLES	$-0.56 \pm i\ 0.91$	, $-0.0061 \pm i\ 0.1158$	
T.Z. of w/η	$-0.0065 \pm i0.0978$	, -25.27	
T.Z. of q/η	-0.5308	, -0.0307 ,	0.0
T.Z. of θ/η	-0.5308	, -0.0307 ,	∞

FC # 17 – 30000 ft – MACH 0.70			
POLES	$-0.49 \pm i\ 0.98$	, $-0.0036 \pm i\ 0.0709$	
T.Z. of w/η	$-0.0044 \pm i0.0722$	, -41.00	
T.Z. of q/η	-0.4439	, -0.0155 ,	0.0
T.Z. of θ/η	-0.4439	, -0.0155 ,	∞

APPENDIX D

PARAMETERS OF THE OBSERVER WHEN THE OUTPUT IS w

In this appendix the parameters for the Doyle-Stein observer when the output is normal velocity, y = w, are listed. The observer equations used in this case are,

$$\dot{z} = F\, z + \bar{G}\, y + H\, \eta$$

$$\hat{x}_2 = L\, y + z$$

As known, in this case H = 0 at all flight conditions, so it is only necessary to list F, $\bar{G}$ and L. Here, these matrices are given for flight conditions 3, 6, 9, 13 and 17.

$$L_3 = \begin{bmatrix} -0.0111 \\ 0.0564 \\ 0.0 \end{bmatrix} \quad L_6 = \begin{bmatrix} -0.0292 \\ 0.0572 \\ 0.0 \end{bmatrix} \quad L_9 = \begin{bmatrix} -0.0781 \\ 0.0577 \\ 0.0 \end{bmatrix}$$

$$L_{13} = \begin{bmatrix} -0.1484 \\ 0.0573 \\ 0.0 \end{bmatrix} \quad L_{17} = \begin{bmatrix} -0.0786 \\ 0.0582 \\ 0.0 \end{bmatrix}$$

$$\bar{G}_3 = \begin{bmatrix} 0.0482 \\ -2.1774 \\ 0.0564 \end{bmatrix} \quad \bar{G}_6 = \begin{bmatrix} 0.0314 \\ -2.3984 \\ 0.0572 \end{bmatrix} \quad \bar{G}_9 = \begin{bmatrix} -0.0040 \\ -2.5619 \\ 0.0577 \end{bmatrix}$$

$$\bar{G}_{13} = \begin{bmatrix} -0.0218 \\ -1.4171 \\ 0.0573 \end{bmatrix} \quad \bar{G}_{17} = \begin{bmatrix} -0.0152 \\ -2.3597 \\ 0.0582 \end{bmatrix}$$

$$F_3 = \begin{bmatrix} -0.0099 & -0.055 & -32.19 \\ 0.0082 & -39.62 & 0.0217 \\ 0.0 & 1.0 & 0.0 \end{bmatrix}$$

$$F_6 = \begin{bmatrix} -0.0084 & -0.1575 & -32.21 \\ 0.0072 & -45.59 & 0.0557 \\ 0.0 & 1.0 & 0.0 \end{bmatrix}$$

$$F_9 = \begin{bmatrix} -0.0110 & -0.4769 & -32.29 \\ 0.0050 & -44.76 & 0.1471 \\ 0.0 & 1.0 & 0.0 \end{bmatrix}$$

$$F_{13} = \begin{bmatrix} -0.0245 & -0.7923 & -32.56 \\ 0.0077 & -25.26 & 0.2852 \\ 0.00 & 1.0 & 0.0 \end{bmatrix}$$

$$F_{17} = \begin{bmatrix} -0.0125 & -0.4548 & -32.29 \\ 0.0067 & -41.02 & 0.1506 \\ 0.0 & 1.0 & 0.0 \end{bmatrix}$$

APPENDIX E

PARAMETERS OF THE OBSERVER WHEN THE OUTPUT IS q

In this appendix the parameters for the Doyle-Stein observer when the output is pitch rate, that is, $y = q$, are listed. The observer equations used in this case are,

$$\dot{z} = F\, z + \bar{G}\, y + H\, \eta$$

$$\hat{x}_2 = M\, y + N\, z$$

In this case a constant $\bar{G}$ was used in the design at all flight conditions, i.e. $\bar{G}^T=[\ 1\ 1\ 1\ ]$, and so it is necessary to give F, H, M and N only. Here, these matrices are listed for flight conditions 3, 6, 9, 13 and 17.

$$H_3 = \begin{bmatrix} 0.0 \\ 0.0001 \\ -0.0163 \end{bmatrix} \quad H_6 = \begin{bmatrix} 0.0 \\ 0.0 \\ -0.0088 \end{bmatrix} \quad H_9 = \begin{bmatrix} 0.0 \\ 0.0 \\ -0.011 \end{bmatrix}$$

$$H_{13} = \begin{bmatrix} 0.0 \\ 0.0 \\ -0.0069 \end{bmatrix} \quad H_{17} = \begin{bmatrix} 0.0 \\ 0.0 \\ -0.0055 \end{bmatrix}$$

$$M_3 = \begin{bmatrix} 35.4 \\ 12.6 \\ -0.019 \end{bmatrix} \quad M_6 = \begin{bmatrix} 22.6 \\ 12.9 \\ -0.01 \end{bmatrix} \quad M_9 = \begin{bmatrix} 42.1 \\ 6.68 \\ -0.02 \end{bmatrix}$$

$$M_{13} = \begin{bmatrix} 9.2 \\ 14.7 \\ -0.01 \end{bmatrix} \quad M_{17} = \begin{bmatrix} 22.6 \\ 11.2 \\ -0.01 \end{bmatrix}$$

$$N_3 = \begin{bmatrix} 4482 & -102.6 & -4349 \\ -658.5 & 704.5 & 633.8 \\ -1.4 & 0.03 & 2.3 \end{bmatrix}$$

$$N_6 = \begin{bmatrix} 5114 & -123.5 & -4995 \\ -1021 & 766 & 985 \\ -1.6 & 0.02 & 2.5 \end{bmatrix}$$

$$N_9 = \begin{bmatrix} 4983 & -238 & -4785 \\ 1255 & 847 & 1173 \\ -1.5 & 0.06 & 2.5 \end{bmatrix}$$

$$N_{13} = \begin{bmatrix} 17255 & -110.6 & -1672 \\ -426 & 467 & 388 \\ -0.5 & 0.02 & 1.5 \end{bmatrix}$$

$$N_{17} = \begin{bmatrix} -6255 & -132.8 & -6165 \\ -1588 & 742 & 1540 \\ -1.9 & 0.02 & 2.9 \end{bmatrix}$$

The F matrices here, as already known, are all diagonal, and so they are the following,

$$F_3 = \begin{bmatrix} -0.0175 & 0.0 & 0.0 \\ 0.0 & -0.9859 & 0.0 \\ 0.0 & 0.0 & -0.01 \end{bmatrix}$$

$$F_6 = \begin{bmatrix} -0.0167 & 0.0 & 0.0 \\ 0.0 & -0.6226 & 0.0 \\ 0.0 & 0.0 & -0.01 \end{bmatrix}$$

$$F_9 = \begin{bmatrix} -0.0173 & 0.0 & 0.0 \\ 0.0 & -0.3386 & 0.0 \\ 0.0 & 0.0 & -0.01 \end{bmatrix}$$

$$F_{13} = \begin{bmatrix} -0.0307 & 0.0 & 0.0 \\ 0.0 & -0.5308 & 0.0 \\ 0.0 & 0.0 & -0.01 \end{bmatrix}$$

$$F_{17} = \begin{bmatrix} -0.0155 & 0.0 & 0.0 \\ 0.0 & -0.4439 & 0.0 \\ 0.0 & 0.0 & -0.01 \end{bmatrix}$$

APPENDIX F

PARAMETERS OF THE OBSERVER WHEN THE OUTPUT IS θ

In this appendix the parameters for the Doyle-Stein observer when the output is pitch attitude, $y = \theta$, are listed. The observer equations used in this case are,

$$\dot{z} = F\, z + \bar{G}\, y + H\, \eta$$

$$\hat{x}_2 = M\, y + N\, z$$

In this case a constant $\bar{G}$ was used at all flight conditions, i.e. $\bar{G}^T = [\ 1 \quad 1 \quad 1\ ]$, and so it is necessary to give F, H, M and N only. Here, these matrices are given for flight conditions 3, 6, 9, 13 and 17.

$$H_3 = \begin{bmatrix} -0.0001 \\ -0.0008 \\ 0.1433 \end{bmatrix} \quad H_6 = \begin{bmatrix} 0.0001 \\ -0.0020 \\ 0.1312 \end{bmatrix} \quad H_9 = \begin{bmatrix} -0.0001 \\ -0.0019 \\ 0.0804 \end{bmatrix}$$

$$H_{13} = \begin{bmatrix} 0.0 \\ 0.0005 \\ 0.0665 \end{bmatrix} \quad H_{17} = \begin{bmatrix} 0.0001 \\ 0.0005 \\ 0.0947 \end{bmatrix}$$

$$M_3 = \begin{bmatrix} -7.31 \\ 737.62 \\ 2.95 \end{bmatrix} \quad M_6 = \begin{bmatrix} -22.37 \\ 791 \\ 3.26 \end{bmatrix} \quad M_9 = \begin{bmatrix} -64.8 \\ 831.5 \\ 3.53 \end{bmatrix}$$

$$M_{13} = \begin{bmatrix} -73.35 \\ 491.2 \\ 3.41 \end{bmatrix} \quad M_{17} = \begin{bmatrix} -59.8 \\ 757.3 \\ 3.46 \end{bmatrix}$$

$$N_3 = \begin{bmatrix} 43.62 & -33.2 & 2.58 \\ -676.9 & 4.88 & 246.7 \\ 0.522 & -0.002 & -13.9 \end{bmatrix}$$

$$N_6 = \begin{bmatrix} 44.6 & -33.74 & 6.91 \\ -466.6 & 6.79 & -255.4 \\ 0.25 & -0.0038 & -14.6 \end{bmatrix}$$

$$N_9 = \begin{bmatrix} 41.5 & -34.8 & 19.6 \\ -275.9 & 9.07 & -260.9 \\ 0.081 & -0.0022 & -15.05 \end{bmatrix}$$

$$N_{13} = \begin{bmatrix} 47.55 & -35.1 & 38.1 \\ -243.2 & 8.8 & -255.4 \\ 0.1383 & -0.0079 & -14.62 \end{bmatrix}$$

$$N_{17} = \begin{bmatrix} 33.64 & -33.5 & 20.38 \\ -320.9 & 8.71 & -257.38 \\ 0.1279 & -0.0036 & -14.98 \end{bmatrix}$$

The F matrices here, as already known, are all diagonal, and so,

$$F_3 = \begin{bmatrix} -0.9859 & 0.0 & 0.0 \\ 0.0 & -0.0175 & 0.0 \\ 0.0 & 0.0 & -4.0 \end{bmatrix}$$

$$F_6 = \begin{bmatrix} -0.6226 & 0.0 & 0.0 \\ 0.0 & -0.0167 & 0.0 \\ 0.0 & 0.0 & -4.0 \end{bmatrix}$$

$$F_9 = \begin{bmatrix} -0.3386 & 0.0 & 0.0 \\ 0.0 & -0.0173 & 0.0 \\ 0.0 & 0.0 & -4.0 \end{bmatrix}$$

$$F_{13} = \begin{bmatrix} -0.5308 & 0.0 & 0.0 \\ 0.0 & -0.0307 & 0.0 \\ 0.0 & 0.0 & -4.0 \end{bmatrix}$$

$$F_{17} = \begin{bmatrix} -0.4439 & 0.0 & 0.0 \\ 0.0 & -0.0155 & 0.0 \\ 0.0 & 0.0 & -4.0 \end{bmatrix}$$